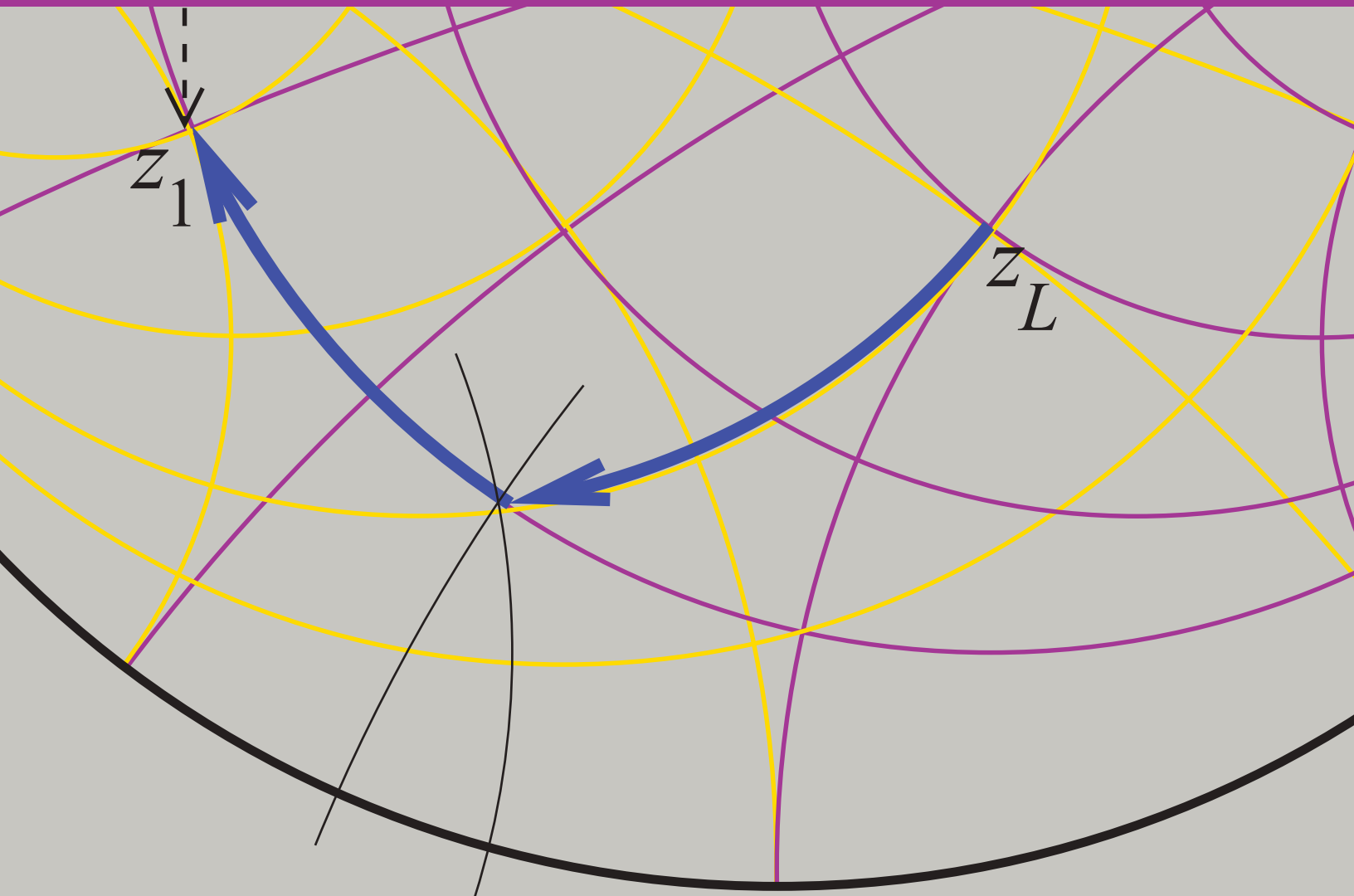


Volume 3

MICROWAVE AND RF DESIGN NETWORKS



Michael Steer

Third Edition

Microwave and RF Design *Networks*

Volume 3

Third Edition

Michael Steer

Microwave and RF Design *Networks*

Volume 3

Third Edition

Michael Steer

Copyright © 2019 by M.B. Steer

Citation: Steer, Michael. *Microwave and RF Design: Networks*. Volume 3. (Third Edition), NC State University, 2019. doi: <https://doi.org/10.5149/9781469656953> Steer

This work is licensed under a Creative Commons Attribution-NonCommercial 4.0 International license (CC BY-NC 4.0). To view a copy of the license, visit <http://creativecommons.org/licenses>.

ISBN 978-1-4696-5694-6 (paperback)
ISBN 978-1-4696-5695-3 (open access ebook)

Published by NC State University

NC STATE UNIVERSITY

Distributed by the University of North Carolina Press
www.uncpress.org

Printing: 1

To

Alison

Preface

The book series *Microwave and RF Design* is a comprehensive treatment of radio frequency (RF) and microwave design with a modern “systems-first” approach. A strong emphasis on design permeates the series with extensive case studies and design examples. Design is oriented towards cellular communications and microstrip design so that lessons learned can be applied to real-world design tasks. The books in the Microwave and RF Design series are:

- Microwave and RF Design: Radio Systems, Volume 1
- Microwave and RF Design: Transmission Lines, Volume 2
- Microwave and RF Design: Networks, Volume 3
- Microwave and RF Design: Modules, Volume 4
- Microwave and RF Design: Amplifiers and Oscillators, Volume 5

The length and format of each is suitable for automatic printing and binding.

Rationale

The central philosophy behind this series’s popular approach is that the student or practicing engineer will develop a full appreciation for RF and microwave engineering and gain the practical skills to perform system-level design decisions. Now more than ever companies need engineers with an ingrained appreciation of systems and armed with the skills to make system decisions. One of the greatest challenges facing RF and microwave engineering is the increasing level of abstraction needed to create innovative microwave and RF systems. This book series is organized in such a way that the reader comes to understand the impact that system-level decisions have on component and subsystem design. At the same time, the capabilities of technologies, components, and subsystems impact system design. The book series is meticulously crafted to intertwine these themes.

Audience

The book series was originally developed for three courses at North Carolina State University. One is a final-year undergraduate class, another an introductory graduate class, and the third an advanced graduate class. Books in the series are used as supplementary texts in two other classes. There are extensive case studies, examples, and end of chapter problems ranging from straight-forward to in-depth problems requiring hours to solve. A companion book, *Fundamentals of Microwave and RF Design*, is more suitable for an undergraduate class yet there is a direct linkage between the material in this book and the series which can then be used as a career-long reference text. I believe it is completely understandable for senior-level students where a microwave/RF engineering course is offered. The book series is a comprehensive RF and microwave text and reference, with detailed index, appendices, and cross-references throughout. Practicing engineers will find the book series a valuable systems primer, a refresher as needed, and a

reference tool in the field. Additionally, it can serve as a valuable, accessible resource for those outside RF circuit engineering who need to understand how they can work with RF hardware engineers.

Organization

This book is a volume in a five volume series on RF and microwave design. The first volume in the series, *Microwave and RF Design: Radio Systems*, addresses radio systems mainly following the evolution of cellular radio. A central aspect of microwave engineering is distributed effects considered in the second volume of this book series, *Microwave and RF Design: Transmission Lines*. Here transmission lines are treated as supporting forward- and backward-traveling voltage and current waves and these are related to electromagnetic effects. The third volume, *Microwave and RF Design: Networks*, covers microwave network theory which is the theory that describes power flow and can be used with transmission line effects. Topics covered in *Microwave and RF Design: Modules*, focus on designing microwave circuits and systems using modules introducing a large number of different modules. Modules is just another term for a network but the implication is that it is packaged and often available off-the-shelf. Other topics that are important in system design using modules are considered including noise, distortion, and dynamic range. Most microwave and RF designers construct systems using modules developed by other engineers who specialize in developing the modules. Examples are filter and amplifier modules which once designed can be used in many different systems. Much of microwave design is about maximizing dynamic range, minimizing noise, and minimizing DC power consumption. The fifth volume in this series, *Microwave and RF Design: Amplifiers and Oscillators*, considers amplifier and oscillator design and develops the skills required to develop modules.

Volume 1: Microwave and RF Design: Radio Systems

The first book of the series covers RF systems. It describes system concepts and provides comprehensive knowledge of RF and microwave systems. The emphasis is on understanding how systems are crafted from many different technologies and concepts. The reader gains valuable insight into how different technologies can be traded off in meeting system requirements. I do not believe this systems presentation is available anywhere else in such a compact form.

Volume 2: Microwave and RF Design: Transmission Lines

This book begins with a chapter on transmission line theory and introduces the concepts of forward- and backward-traveling waves. Many examples are included of advanced techniques for analyzing and designing transmission line networks. This is followed by a chapter on planar transmission lines with microstrip lines primarily used in design examples. Design examples illustrate some of the less quantifiable design decisions that must be made. The next chapter describes frequency-dependent transmission line effects and describes the design choices that must be taken to avoid multimoding. The final chapter in this volume addresses coupled-lines. It is shown how to design coupled-line networks that exploit this distributed effect to realize novel circuit functionality and how to design networks that minimize negative effects. The modern treatment of transmission lines in this volume emphasizes planar circuit design and the practical aspects of designing

around unwanted effects. Detailed design of a directional coupler is used to illustrate the use of coupled lines. Network equivalents of coupled lines are introduced as fundamental building blocks that are used later in the synthesis of coupled-line filters. The text, examples, and problems introduce the often hidden design requirements of designing to mitigate parasitic effects and unwanted modes of operation.

Volume 3: Microwave and RF Design: Networks

Volume 3 focuses on microwave networks with descriptions based on S parameters and $ABCD$ matrices, and the representation of reflection and transmission information on polar plots called Smith charts. Microwave measurement and calibration technology are examined. A sampling of the wide variety of microwave elements based on transmission lines is presented. It is shown how many of these have lumped-element equivalents and how lumped elements and transmission lines can be combined as a compromise between the high performance of transmission line structures and the compactness of lumped elements. This volume concludes with an in-depth treatment of matching for maximum power transfer. Both lumped-element and distributed-element matching are presented.

Volume 4: Microwave and RF Design: Modules

Volume 4 focuses on the design of systems based on microwave modules. The book considers the wide variety of RF modules including amplifiers, local oscillators, switches, circulators, isolators, phase detectors, frequency multipliers and dividers, phase-locked loops, and direct digital synthesizers. The use of modules has become increasingly important in RF and microwave engineering. A wide variety of passive and active modules are available and high-performance systems can be realized cost effectively and with stellar performance by using off-the-shelf modules interconnected using planar transmission lines. Module vendors are encouraged by the market to develop competitive modules that can be used in a wide variety of applications. The great majority of RF and microwave engineers either develop modules or use modules to realize RF systems. Systems must also be concerned with noise and distortion, including distortion that originates in supposedly linear elements. Something as simple as a termination can produce distortion called passive intermodulation distortion. Design techniques are presented for designing cascaded systems while managing noise and distortion. Filters are also modules and general filter theory is covered and the design of parallel coupled line filters is presented in detail. Filter design is presented as a mixture of art and science. This mix, and the thought processes involved, are emphasized through the design of a filter integrated throughout this chapter.

Volume 5: Microwave and RF Design: Amplifiers and Oscillators

The fifth volume presents the design of amplifiers and oscillators in a way that enables state-of-the-art designs to be developed. Detailed strategies for amplifiers and voltage-controlled oscillators are presented. Design of competitive microwave amplifiers and oscillators are particularly challenging as many trade-offs are required in design, and the design decisions cannot be reduced to a formulaic flow. Very detailed case studies are presented and while some may seem quite complicated, they parallel the level of sophistication required to develop competitive designs.

Case Studies

A key feature of this book series is the use of real world case studies of leading edge designs. Some of the case studies are designs done in my research group to demonstrate design techniques resulting in leading performance. The case studies and the persons responsible for helping to develop them are as follows.

1. Software defined radio transmitter.
2. High dynamic range down converter design. This case study was developed with Alan Victor.
3. Design of a third-order Chebyshev combline filter. This case study was developed with Wael Fathelbab.
4. Design of a bandstop filter. This case study was developed with Wael Fathelbab.
5. Tunable Resonator with a varactor diode stack. This case study was developed with Alan Victor.
6. Analysis of a 15 GHz Receiver. This case study was developed with Alan Victor.
7. Transceiver Architecture. This case study was developed with Alan Victor.
8. Narrowband linear amplifier design. This case study was developed with Dane Collins and National Instruments Corporation.
9. Wideband Amplifier Design. This case study was developed with Dane Collins and National Instruments Corporation.
10. Distributed biasing of differential amplifiers. This case study was developed with Wael Fathelbab.
11. Analysis of a distributed amplifier. This case study was developed with Ratan Bhatia, Jason Gerber, Tony Kwan, and Rowan Gilmore.
12. Design of a WiMAX power amplifier. This case study was developed with Dane Collins and National Instruments Corporation.
13. Reflection oscillator. This case study was developed with Dane Collins and National Instruments Corporation.
14. Design of a C-Band VCO. This case study was developed with Alan Victor.
15. Oscillator phase noise analysis. This case study was developed with Dane Collins and National Instruments Corporation.

Many of these case studies are available as captioned YouTube videos and qualified instructors can request higher resolution videos from the author.

Course Structures

Based on the adoption of the first and second editions at universities, several different university courses have been developed using various parts of what was originally one very large book. The book supports teaching two or three classes with courses varying by the selection of volumes and chapters. A standard microwave class following the format of earlier microwave texts can be taught using the second and third volumes. Such a course will benefit from the strong practical design flavor and modern treatment of measurement technology, Smith charts, and matching networks. Transmission line propagation and design is presented in the context of microstrip technology providing an immediately useful skill. The subtleties of multimoding are also presented in the context of microstrip lines. In such

a class the first volume on microwave systems can be assigned for self-learning.

Another approach is to teach a course that focuses on transmission line effects including parallel coupled-line filters and module design. Such a class would focus on Volumes 2, 3 and 4. A filter design course would focus on using Volume 4 on module design. A course on amplifier and oscillator design would use Volume 5. This course is supported by a large number of case studies that present design concepts that would otherwise be difficult to put into the flow of the textbook.

Another option suited to an undergraduate or introductory graduate class is to teach a class that enables engineers to develop RF and microwave systems. This class uses portions of Volumes 2, 3 and 4. This class then omits detailed filter, amplifier, and oscillator design.

The fundamental philosophy behind the book series is that the broader impact of the material should be presented first. Systems should be discussed up front and not left as an afterthought for the final chapter of a textbook, the last lecture of the semester, or the last course of a curriculum.

The book series is written so that all electrical engineers can gain an appreciation of RF and microwave hardware engineering. The body of the text can be covered without strong reliance on this electromagnetic theory, but it is there for those who desire it for teaching or reader review. The book is rich with detailed information and also serves as a technical reference.

The Systems Engineer

Systems are developed beginning with fuzzy requirements for components and subsystems. Just as system requirements provide impetus to develop new base technologies, the development of new technologies provides new capabilities that drive innovation and new systems. The new capabilities may arise from developments made in support of other systems. Sometimes serendipity leads to the new capabilities. Creating innovative microwave and RF systems that address market needs or provide for new opportunities is the most exciting challenge in RF design. The engineers who can conceptualize and architect new RF systems are in great demand. This book began as an effort to train RF systems engineers and as an RF systems resource for practicing engineers. Many RF systems engineers began their careers when systems were simple. Today, appreciating a system requires higher levels of abstraction than in the past, but it also requires detailed knowledge or the ability to access detailed knowledge and expertise. So what makes a systems engineer? There is not a simple answer, but many partial answers. We know that system engineers have great technical confidence and broad appreciation for technologies. They are both broad in their knowledge of a large swath of technologies and also deep in knowledge of a few areas, sometimes called the “T” model. One book or course will not make a systems engineer. It is clear that there must be a diverse set of experiences. This book series fulfills the role of fostering both high-level abstraction of RF engineering and also detailed design skills to realize effective RF and microwave modules. My hope is that this book will provide the necessary background for the next generation of RF systems engineers by stressing system principles immediately, followed by core RF technologies. Core technologies are thereby covered within the context of the systems in which they are used.

Supplementary Materials

Supplementary materials available to qualified instructors adopting the book include PowerPoint slides and solutions to the end-of-chapter problems. Requests should be directed to the author. Access to downloads of the books, additional material and YouTube videos of many case studies are available at <https://www.lib.ncsu.edu/do/open-education>

Acknowledgments

Writing this book has been a large task and I am indebted to the many people who helped along the way. First I want to thank the more than 1200 electrical engineering graduate students who used drafts and the first two editions at NC State. I thank the many instructors and students who have provided feedback. I particularly thank Dr. Wael Fathelbab, a filter expert, who co-wrote an early version of the filter chapter. Professor Andreas Cangellaris helped in developing the early structure of the book. Many people have reviewed the book and provided suggestions. I thank input on the structure of the manuscript: Professors Mark Wharton and Nuno Carvalho of Universidade de Aveiro, Professors Ed Delp and Saul Gelfand of Purdue University, Professor Lynn Carpenter of Pennsylvania State University, Professor Grant Ellis of the Universiti Teknologi Petronas, Professor Islam Eshrah of Cairo University, Professor Mohammad Essaadi and Dr. Otman Aghzout of Abdelmalek Essaadi Univeristy, Professor Jianguo Ma of Guangdong University of Technology, Dr. Jayesh Nath of Apple, Mr. Sony Rowland of the U.S. Navy, and Dr. Jonathan Wilkerson of Lawrence Livermore National Laboratories, Dr. Josh Wetherington of Vadum, Dr. Glen Garner of Vadum, and Mr. Justin Lowry who graduated from North Carolina State University.

Many people helped in producing this book. In the first edition I was assisted by Ms. Claire Sideri, Ms. Susan Manning, and Mr. Robert Lawless who assisted in layout and production. The publisher, task master, and chief coordinator, Mr. Dudley Kay, provided focus and tremendous assistance in developing the first and second editions of the book, collecting feedback from many instructors and reviewers. I thank the Institution of Engineering and Technology, who acquired the original publisher, for returning the copyright to me. This open access book was facilitated by John McLeod and Samuel Dalzell of the University of North Carolina Press, and by Micah Vandergrift and William Cross of NC State University Libraries. The open access ebooks are host by NC State University Libraries.

The book was produced using LaTeX and open access fonts, line art was drawn using xfig and inkscape, and images were edited in gimp. So thanks to the many volunteers who developed these packages.

My family, Mary, Cormac, Fiona, and Killian, gracefully put up with my absence for innumerable nights and weekends, many more than I could have ever imagined. I truly thank them. I also thank my academic sponsor, Dr. Ross Lampe, Jr., whose support of the university and its mission enabled me to pursue high risk and high reward endeavors including this book.

Michael Steer
North Carolina State University
Raleigh, North Carolina
mbs@ncsu.edu

List of Trademarks

3GPP® is a registered trademark of the European Telecommunications Standards Institute.

802® is a registered trademark of the Institute of Electrical & Electronics Engineers .

APC-7® is a registered trademark of Amphenol Corporation.

AT&T® is a registered trademark of AT&T Intellectual Property II, L.P.

AWR® is a registered trademark of National Instruments Corporation.

AWRDE® is a trademark of National Instruments Corporation.

Bluetooth® is a registered trademark of the Bluetooth Special Interest Group.

GSM® is a registered trademark of the GSM MOU Association.

Mathcad® is a registered trademark of Parametric Technology Corporation.

MATLAB® is a registered trademark of The MathWorks, Inc.

NEC® is a registered trademark of NEC Corporation.

OFDMA® is a registered trademark of Runcom Technologies Ltd.

Qualcomm® is a registered trademark of Qualcomm Inc.

Teflon® is a registered trademark of E. I. du Pont de Nemours.

RFMD® is a registered trademark of RF Micro Devices, Inc.

SONNET® is a trademark of Sonnet Corporation.

Smith is a registered trademark of the Institute of Electrical and Electronics Engineers.

Touchstone® is a registered trademark of Agilent Corporation.

WiFi® is a registered trademark of the Wi-Fi Alliance.

WiMAX® is a registered trademark of the WiMAX Forum.

All other trademarks are the properties of their respective owners.

Contents

Preface	v
1 Introduction to RF and Microwave Networks	1
1.1 Introduction to Microwave Networks	1
1.2 Book Outline	2
1.3 References	3
2 Microwave Network Analysis	5
2.1 Introduction	5
2.2 Two-Port Networks	6
2.2.1 Reciprocity, Symmetry, Passivity, and Linearity	6
2.2.2 Parameters Based on Total Voltage and Current	7
2.2.3 Series Connection of Two-Port Networks	10
2.2.4 Parallel Connection of Two-Port Networks	11
2.2.5 Series-Parallel Connection of Two-Port Networks	11
2.2.6 <i>ABCD</i> Matrix Characterization of Two-Port Networks	12
2.3 Scattering Parameters	14
2.3.1 Reflection Coefficient	14
2.3.2 Reflection Coefficient with Complex Reference Impedance	15
2.3.3 Two-Port <i>S</i> Parameters	16
2.3.4 Input Reflection Coefficient of a Terminated Two-Port Network	18
2.3.5 Evaluation of the Scattering Parameters of an Element	19
2.3.6 Properties of a Two-Port in Terms of <i>S</i> Parameters	21
2.3.7 Scattering Transfer or <i>T</i> Parameters	21
2.4 Generalized Scattering Parameters	22
2.4.1 The <i>N</i> -Port Network	22
2.4.2 Power Waves	23
2.4.3 Scattering Parameters in Terms of <i>a</i> and <i>b</i> waves	25
2.4.4 Normalized and Generalized <i>S</i> Parameters	26
2.4.5 Change of Reference Impedance	26
2.4.6 Passivity in Terms of Scattering Parameters	27
2.4.7 Impedance Matrix Representation	28
2.4.8 Admittance Matrix Representation	29
2.5 Scattering Parameter Matrices of Common Two-Ports	30
2.6 <i>T</i> or Chain Scattering Parameters of Cascaded Two-Port Networks	31
2.6.1 Terminated Two-Port Network	35
2.7 Scattering Parameter Two-Port Relationships	35
2.7.1 Change in Reference Plane	35
2.7.2 Conversion Between <i>S</i> and <i>ABCD</i> Parameters	36
2.8 Return Loss, Substitution Loss, and Insertion Loss	37
2.8.1 Return Loss	37
2.8.2 Substitution Loss and Insertion Loss	38

2.8.3	Measurement of Insertion Loss	39
2.8.4	Minimum Transducer Loss, Intrinsic Attenuation . . .	41
2.9	Scattering Parameters and Directional Couplers	42
2.10	Summary	43
2.11	References	44
2.12	Exercises	44
2.12.1	Exercises by Section	47
2.12.2	Answers to Selected Exercises	48
3	Graphical Network Analysis	49
3.1	Introduction	49
3.2	Signal Flow Graph	49
3.2.1	SFG Representation of Mathematical Relations	50
3.2.2	SFG Representation of Scattering Parameters	50
3.2.3	Simplification and Reduction of SFGs	50
3.2.4	SFG Model of a Source	54
3.2.5	Mason's Rule	56
3.2.6	Summary	57
3.3	Polar Representations of Scattering Parameters	57
3.3.1	Shift of Reference Planes as a S Parameter Rotation . .	58
3.3.2	Polar Plot of Reflection Coefficient	58
3.3.3	Summary	59
3.4	Smith Chart	60
3.4.1	Impedance Smith Chart	61
3.4.2	Admittance Smith Chart	64
3.4.3	Combined Smith Chart	65
3.4.4	Smith Chart Manipulations	70
3.4.5	An Alternative Admittance Chart	76
3.4.6	Expanded Smith Chart	76
3.4.7	Summary	76
3.5	Transmission Lines and Smith Charts	77
3.5.1	Bilinear Transform	77
3.5.2	Reference Impedance Change as a Bilinear Transform	78
3.5.3	Reflection Coefficient Locus	80
3.5.4	Summary	81
3.6	Summary	81
3.7	References	82
3.8	Exercises	82
3.8.1	Exercises by Section	87
3.8.2	Answers to Selected Exercises	87
4	Microwave Measurements	89
4.1	Introduction	89
4.2	Measurement of Scattering Parameters	89
4.2.1	Vector Network Analyzer	89
4.3	Calibration	93
4.3.1	One-Port Calibration	94
4.3.2	De-Embedding	96
4.3.3	Two-Port Calibration	96
4.3.4	Transmission Line-Based Calibration Schemes	99
4.3.5	Through-Line Calibration	100

4.3.6	Two-Tier Calibration	105
4.4	Extraction of Transmission Line Parameters	107
4.4.1	Summary	109
4.5	Determining Z_0 of a Line from the Smith Chart	109
4.6	Summary	110
4.7	References	110
4.8	Exercises	112
4.8.1	Exercises by Section	113
4.8.2	Answers to Selected Exercises	113
5	Passive Components	115
5.1	Introduction	115
5.2	Q Factor	115
5.2.1	Definition	116
5.2.2	Q of Lumped Elements	117
5.2.3	Loaded Q Factor	118
5.2.4	Summary of the Properties of Q	118
5.3	Integrated Lumped Elements	118
5.3.1	On-Chip Capacitors	119
5.3.2	Planar Inductors	120
5.4	Surface-Mount Components	121
5.5	Terminations and Attenuators	122
5.5.1	Terminations	122
5.5.2	Attenuators	124
5.6	Transmission Line Stubs and Discontinuities	127
5.6.1	Open	127
5.6.2	Discontinuities	128
5.6.3	Impedance Transformer	129
5.6.4	Planar Radial Stub	129
5.6.5	Stub Transformations	130
5.7	Resonators	131
5.7.1	Dielectric Resonators	132
5.8	Magnetic Transformer	132
5.8.1	Properties of a Magnetic Transformer	133
5.9	Hybrids	135
5.9.1	Quadrature Hybrid	136
5.9.2	180° Hybrid	136
5.9.3	Magnetic Transformer Hybrid	137
5.10	Baluns	139
5.10.1	Marchand Balun	140
5.11	Combiners and Dividers	141
5.11.1	Wilkinson Combiner and Divider	141
5.11.2	Chireix Combiner	143
5.12	Transmission Line Transformer	143
5.12.1	Transmission Line Transformer as a Balun	145
5.12.2	4:1 Impedance Transformer at High Frequencies	145
5.12.3	4:1 Impedance Transformer at Low Frequencies	147
5.12.4	Hybrid Transformer Used as a Combiner	148
5.12.5	Hybrid Transformer Used as a Power Splitter	149
5.12.6	Broadband Hybrid Combiner	149
5.13	Transmission Line-Based Hybrids	150

5.13.1	Branch-Line Hybrids Based on Transmission Lines . . .	150
5.13.2	Lumped-Element Hybrids	152
5.14	Summary	153
5.15	References	154
5.16	Exercises	155
5.16.1	Exercises by Section	157
5.16.2	Answers to Selected Exercises	157
6	Impedance Matching	159
6.1	Introduction	159
6.2	Matching Networks	159
6.2.1	Matching for Zero Reflection or for Maximum Power Transfer	160
6.2.2	Types of Matching Networks	160
6.2.3	Summary	162
6.3	Impedance Transforming Networks	162
6.3.1	The Ideal Transformer	162
6.3.2	A Series Reactive Element	162
6.3.3	A Parallel Reactive Element	164
6.4	The L Matching Network	164
6.4.1	Design Equations for $R_S < R_L$	166
6.4.2	L Network Design for $R_S > R_L$	167
6.5	Dealing with Complex Sources and Loads	168
6.5.1	Matching	168
6.6	Multielement Matching	171
6.6.1	Design Concept for Manipulating Bandwidth	171
6.6.2	Three-Element Matching Networks	172
6.6.3	The Pi Network	174
6.6.4	Matching Network Q Revisited	176
6.6.5	The T Network	177
6.6.6	Broadband (Low Q) Matching	177
6.7	Impedance Matching Using Smith Charts	179
6.7.1	Two-Element Matching	179
6.8	Distributed Matching	183
6.8.1	Stub Matching	185
6.8.2	Hybrid Lumped-Distributed Matching	187
6.9	Matching Options Using the Smith Chart	187
6.9.1	Locating the Design Points	187
6.9.2	Design Options	189
6.9.3	Design 1, Hybrid Design	189
6.9.4	Design 1 with an Open-Circuited Stub	192
6.9.5	Design 2, Lumped-Element Design	193
6.9.6	Design 3, Single Line Matching	195
6.9.7	Summary	196
6.10	Summary	197
6.11	References	198
6.12	Exercises	198
6.12.1	Exercises by Section	204
6.12.2	Answers to Selected Exercises	204
7	Broadband Matching	205

7.1	Introduction	205
7.2	Fano-Bode Limits	206
7.3	Constant Q Circles	207
7.4	Stepped-Impedance Transmission Line Transformer	209
7.4.1	Quarter-Wave Transformer using Geometric Means	209
7.4.2	Design Based on the Theory of Small Reflections	210
7.4.3	Maximally Flat Stepped Impedance Transformer	211
7.4.4	Stepped Impedance Transformer With Chebyshev Response	213
7.4.5	Stepped Impedance Transformer Design	216
7.4.6	Summary	216
7.5	Tapered Matching Transformers	217
7.5.1	Small Reflection Theory and Tapered Lines	217
7.5.2	Linear taper	218
7.5.3	Exponential taper	218
7.5.4	Klopfenstein taper	219
7.5.5	Simplified Klopfenstein taper	220
7.5.6	Comparison of Transmission Line Impedance Transformers	222
7.5.7	Summary	225
7.6	Matching a Series RC load	225
7.6.1	Summary	228
7.6.2	Matching using Cascaded Transmission Lines and Constant Q Circles	229
7.7	Broadband Matching to Reactive Loads	231
7.7.1	Broadband Matching to a Series RC Load	231
7.7.2	Summary	234
7.8	Summary	234
7.9	References	235
7.10	Exercises	235
7.10.1	Exercises by Section	236
7.10.2	Answers to Selected Exercises	236
	Index	237

Introduction to RF and Microwave Networks

1.1	Introduction to Microwave Networks	1
1.2	Book Outline	2
1.3	References	3

1.1 Introduction to Microwave Networks

At microwave frequencies a ground plane cannot always be defined as circuits are large enough that a “ground” in one part of a circuit is not the same as a “ground” in another spatially separated part of the circuit. If they were the same “ground” then charges would need to be able to instantaneously redistribute and this is not possible because of the finite speed of causality (that is, the speed of light). One of the consequences of this is that voltage and current occur as forward- and backward-traveling voltage and current waves on transmission lines, or in microwave networks as incident and reflected voltage and current waves at interfaces between different parts of a circuit. At any point the sum of the forward-traveling (or incident) voltage wave and the backward-traveling (or reflected) voltage wave is the total voltage used with low-frequency circuits. A similar description applies to currents. A voltage wave directly relates to the movement of power or what are called power waves. Because of this, the conventional circuit parameters, the y and z parameters defined when there is a single ground, prove to be inadequate to describe signals in microwave circuits. Scattering parameters, or S parameters, are the most convenient network parameters to use with microwave circuits as they neatly describe the properties of traveling waves of voltage and current. A further attribute is that the S parameters relate directly to power flow.

In the early days of electrical engineering all circuits were called networks. That usage remains with microwave circuits but it is more commonly used with circuits that operate at microwave frequencies but only the external terminals are presented and internal details often hidden. The use of the network term also conveys a subtle reminder that there is not necessarily a universal ground. S parameters are defined even when there is not a universal ground.

Most RF and microwave design is concerned with the movement of signal power and minimizing noise power to maintain a high signal-to-noise ratio in a circuit. This maximizes the performance of communication, radar and

sensor systems. Thus maximizing power transfer is critical and the design technique that does this is called matching.

1.2 Book Outline

Chapter 2 presents microwave network analysis and in particular S parameters and other parameters that are useful in design. One of the characteristics of a microwave designer is that they work very well with graphical information about a network. The visual display is the fastest way to convey information to the human brain. A human recognizes patterns very well so it is not surprising that microwave design methods have evolved to make extensive use of graphical means of representing network information, and of design strategies that are based on graphical manipulations. Graphical methods for representing the description of microwave networks are considered in the third chapter of this book, Chapter 3, entitled Graphical Network Analysis. The all important Smith chart is described here. Working knowledge of S parameters and of Smith charts are the two biggest 'barriers to entry' to microwave design. They are the two main topics that must be understood and absorbed before one can become a competent microwave designer or even converse with other engineers about microwave designs. There is no simpler way to describe the intended or actual performance of a microwave circuit design.

The fourth chapter, Chapter 4, discusses microwave measurements and how information about a network can be interpreted from the graphical display of measured information or from a design solution sketched out on a Smith chart. The Smith chart is the microwave engineer's 'back-of-the-envelope' sketch pad.

Chapter 5 introduces many novel microwave elements and these rarely have an analog below microwave frequencies. These circuit elements exploit distributed effects, i.e. transmission line effects. Sometimes there are a few low frequency analogs but these were developed by first conceiving the microwave element and then replacing transmission lines by their approximate LC equivalent circuits. This chapter introduces transmission line stubs, hybrids (which are four-port circuits that route signal power), baluns (which interface balanced and unbalanced circuits), and power combiners and dividers.

The final two chapters in this book, Chapter 6 on impedance matching, i.e. matching for maximum power transfer, and Chapter 7 on broadband matching are concerned with the design of impedance matching networks, with managing the bandwidth of these networks, and with describing the performance of microwave circuit elements.

This book is the third volume in a series on microwave and RF design. The first volume in the series addresses radio systems [1] mainly following the evolution of cellular radio. A central aspect of microwave engineering is distributed effects considered in the second volume of his book series [2]. Here the transmission lines are treated as supporting forward- and backward-traveling voltage and current waves and these are related to electromagnetic effects. The fourth volume [3] focuses on designing microwave circuits and systems using modules introducing a large number of different modules. Modules is just another term for a network but the implication is that it is packaged and often available off-the-

shelf. Other topics in this chapter that are important in system design using modules are considered including metrics for describing noise, distortion, and dynamic range. Most microwave and RF designers construct systems using modules developed by other engineers who specialize in developing the modules. Examples are filter and amplifier chip modules which once designed can be used in many different systems. Much of microwave design is about maximizing dynamic range, minimizing noise, and minimizing DC power consumption. The fifth volume in this series [4] considers amplifier and oscillator design and develops the skills required to develop modules.

The books in the Microwave and RF Design series are:

- Microwave and RF Design: Radio Systems
- Microwave and RF Design: Transmission Lines
- Microwave and RF Design: Networks
- Microwave and RF Design: Modules
- Microwave and RF Design: Amplifiers and Oscillators

1.3 References

- | | |
|--|--|
| [1] M. Steer, <i>Microwave and RF Design, Radio Systems</i> , 3rd ed. North Carolina State University, 2019. | [3] —, <i>Microwave and RF Design, Modules</i> , 3rd ed. North Carolina State University, 2019. |
| [2] —, <i>Microwave and RF Design, Transmission Lines</i> , 3rd ed. North Carolina State University, 2019. | [4] —, <i>Microwave and RF Design, Amplifiers and Oscillators</i> , 3rd ed. North Carolina State University, 2019. |

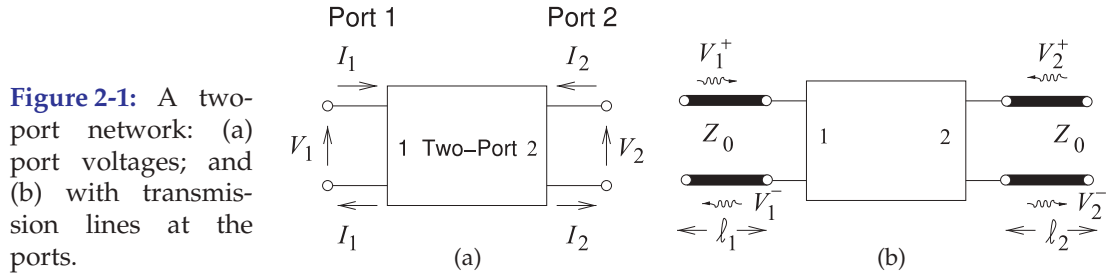
Microwave Network Analysis

2.1	Introduction	5
2.2	Two-Port Networks	6
2.3	Scattering Parameters	14
2.4	Generalized Scattering Parameters	22
2.5	Scattering Parameter Matrices of Common Two-Ports	30
2.6	T or Chain Scattering Parameters of Cascaded Two-Ports	31
2.7	Scattering Parameter Two-Port Relationships	35
2.8	Return Loss and Insertion Loss	37
2.9	Scattering Parameters and Coupled Lines	42
2.10	Summary	43
2.11	References	44
2.12	Exercises	44

2.1 Introduction

Analog circuits at frequencies up to a few tens of megahertz are characterized by admittances, impedances, voltages, and currents. Above these frequencies it is not possible to measure voltage, current, or impedance directly. One reason for this is that measurement equipment is separated from the device by lengths of transmission line that are electrically long (i.e., at least an appreciable fraction of a wavelength long). It is better to use quantities such as voltage reflection and transmission coefficients that can be quite readily measured and are related to power flow. As well, in RF and microwave circuit design the power of signals and of noise is always of interest. Thus there is a predisposition to focus on measurement parameters that are related to the reflection and transmission of power.

Scattering parameters, S parameters, embody the effects of reflection and transmission. As will be seen, it is easy to convert these to more familiar network parameters such as admittance and impedance parameters. In this chapter S parameters will be defined and related to impedance and admittance parameters, then it will be demonstrated that the use of S parameters helps in the design and interpretation of RF circuits. S parameters have become the most important parameters for RF and microwave engineers and many design methodologies have been developed around them.



This chapter presents microwave circuit theory which is based on the representation of distributed structures that are too large to be considered to be dimensionless, by lumped element circuits. The origins of microwave circuit theory were in the 1940s, 1950s and 1960s [1–3] with extensions for networks with lossy transmission lines [4, 5].

2.2 Two-Port Networks

Many of the techniques employed in analyzing circuits require that the voltage at each terminal of a circuit be referenced to a common point such as ground. In microwave circuits it is generally difficult to do this. Recall that with transmission lines it is not possible to establish a common ground point. However, with transmission lines (and circuit elements that utilize distributed effects) it was seen that for each signal current there is a signal return current. Thus at radio frequencies, and for circuits that are distributed, ports are used, as shown in Figure 2-1(a), which define the voltages and currents for what is known as a two-port network, or just two-port.¹ The network in Figure 2-1(a) has four terminals and two ports. A port voltage is defined as the voltage difference between a pair of terminals with one of the terminals in the pair becoming the reference terminal. The current entering the network at the top terminal of Port 1 is I_1 and there is an equal current leaving the reference terminal. This arrangement clearly makes sense when transmission lines are attached to Ports 1 and 2, as in Figure 2-1(b). With transmission lines at Ports 1 and 2 there will be traveling-wave voltages, and at the ports the traveling-wave components add to give the total port voltage. In dealing with nondistributed circuits it is preferable to use the total port voltages and currents— V_1 , I_1 , V_2 , and I_2 , shown in Figure 2-1(a). However, with distributed elements it is preferable to deal with traveling voltages and currents— V_1^+ , V_1^- , V_2^+ , and V_2^- , shown in Figure 2-1(b). RF and microwave design necessarily requires switching between the two forms.

2.2.1 Reciprocity, Symmetry, Passivity, and Linearity

Reciprocity, symmetry, passivity, and linearity are fundamental properties of networks. A network is linear if the response (voltages and currents) is linearly dependent on the drive level, and superposition also applies. So if the two-port shown in Figure 2-1(a) is linear, the currents I_1 and I_2 are linear functions of V_1 and V_2 . An example of a linear network would be one with resistors and capacitors. A network with a diode would be an example of a nonlinear network.

¹ Even when the term “two-port” is used on its own, the hyphen is used, as it is referring to a two-port network.

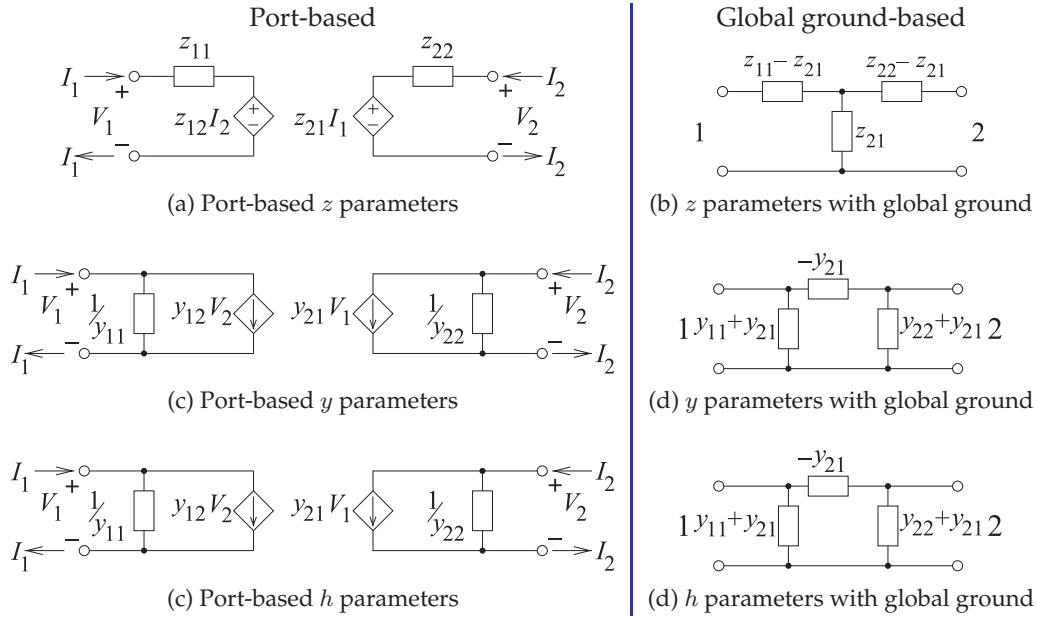


Figure 2-2: The z -, y -, and h - parameter equivalent circuits for port-based and global ground representations. The immittances are shown as impedances.

A passive network has no internal sources of power and so a network with an embedded battery is not a passive network. A symmetrical two-port has the same characteristics at each of the ports. An example of a symmetrical network is a transmission line with a uniform cross section.

A reciprocal two-port has a response at Port 2 from an excitation at Port 1 that is the same as the response at Port 1 to the same excitation at Port 2. As an example, consider the two-port in Figure 2-1(a) with $V_2 = 0$. If the network is reciprocal, then the ratio I_2/V_1 with $V_2 = 0$ will be the same as the ratio I_1/V_2 with $V_1 = 0$. Most networks with resistors, capacitors, and transmission lines, for example, are reciprocal. A transistor amplifier is not reciprocal, as gain, analogous to the ratio V_2/V_1 , is in just one direction (or unidirectional).

2.2.2 Parameters Based on Total Voltage and Current

Here port-based impedance (z), admittance (y), and hybrid (h) parameters will be described. These are similar to the more conventional z , y , and h parameters defined with respect to a common or global ground. The contrasting circuit representations of the parameters are shown in Figure 2-2.

Impedance parameters

First, port-based impedance parameters will be considered based on total port voltages and currents as defined for the two-port in Figure 2-1. These parameters are also referred to as port impedance parameters or just impedance parameters when the context is understood to be ports.

Port-based impedance parameters, or z parameters, are defined as

Figure 2-3: Circuit equivalence of the z and y parameters for a reciprocal network (in (b) the elements are admittances).

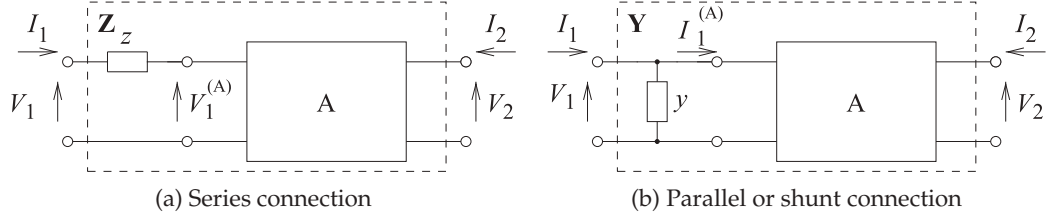
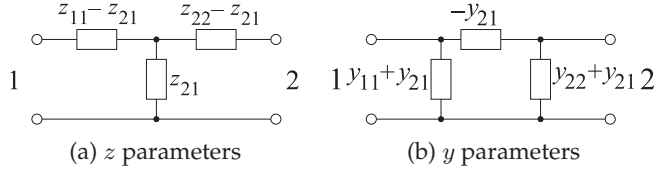


Figure 2-4: Connection of a two-terminal element to a two-port.

$$V_1 = z_{11}I_1 + z_{12}I_2 \quad (2.1) \quad V_2 = z_{21}I_1 + z_{22}I_2, \quad (2.2)$$

$$\text{or in matrix form as} \quad \mathbf{V} = \mathbf{Z}\mathbf{I}. \quad (2.3)$$

The double subscript on a parameter is ordered so that the first refers to the output and the second refers to the input, so z_{ij} relates the voltage output at Port i to the current input at Port j . If the network is reciprocal, then $z_{12} = z_{21}$, but this simple type of relationship does not apply to all network parameters. The reciprocal circuit equivalence of the z parameters is shown in Figure 2-3(a). It will be seen that the z parameters are convenient parameters to use when an element is in series with one of the ports, as then the operation required in developing the z parameters of the larger network is just addition.

Figure 2-4(a) shows the series connection of a two-terminal element with a two-port designated as network A. The z parameters of network A are

$$\mathbf{Z}_A = \begin{bmatrix} z_{11}^{(A)} & z_{12}^{(A)} \\ z_{21}^{(A)} & z_{22}^{(A)} \end{bmatrix}, \quad (2.4)$$

$$\text{so that } V_1^{(A)} = z_{11}^{(A)}I_1 + z_{12}^{(A)}I_2 \quad (2.5) \quad V_2 = z_{21}^{(A)}I_1 + z_{22}^{(A)}I_2. \quad (2.6)$$

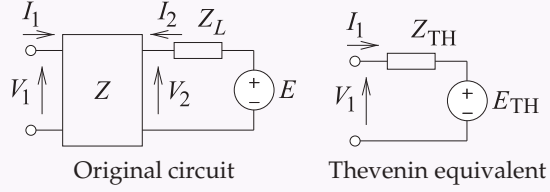
$$\text{Now } V_1 = zI_1 + V_1^{(A)} = zI_1 + z_{11}^{(A)}I_1 + z_{12}^{(A)}I_2, \quad (2.7)$$

so the z parameters of the whole network can be written as

$$\mathbf{Z} = \begin{bmatrix} z & 0 \\ 0 & 0 \end{bmatrix} + \mathbf{Z}_A. \quad (2.8)$$

EXAMPLE 2.1**Thevenin equivalent of a source with a two-port**

What is the Thevenin equivalent circuit of the source-terminated two-port network on the right.

**Solution:**

From the original circuit

$$V_1 = Z_{11}I_1 + Z_{12}I_2 \quad (2.9)$$

$$V_2 = Z_{21}I_1 + Z_{22}I_2 \quad (2.10)$$

$$V_2 = E - I_2Z_L \quad (2.11)$$

Substituting Equation (2.11) in Equation (2.10)

$$E = Z_{21}I_1 + (Z_{22} + Z_L)I_2 \quad (2.12)$$

Multiplying Equation (2.9) by $(Z_{22} + Z_L)$ and

Equation (2.12) by Z_{12}

$$(Z_{22} + Z_L)V_1 = (Z_{22} + Z_L)Z_{11}I_1 + (Z_{22} + Z_L)Z_{12}I_2 \quad (2.13)$$

$$Z_{12}E = Z_{12}Z_{21}I_1 + Z_{12}(Z_{22} + Z_L)I_2 \quad (2.14)$$

Subtracting Equation (2.14) from Equation (2.13)

$$(Z_{22} + Z_L)V_1 - Z_{12}E = [(Z_{22} + Z_L)Z_{11} - Z_{12}Z_{21}]I_1$$

$$V_1 = \frac{Z_{12}E}{Z_{22} + Z_L} + \left(Z_{11} - \frac{Z_{12}Z_{21}}{Z_{22} + Z_L} \right) I_1 \quad (2.15)$$

For the Thevenin equivalent circuit $V_1 = E_{TH} + I_1Z_{TH}$ and so

$$Z_{TH} = \left(Z_{11} - \frac{Z_{12}Z_{21}}{Z_{22} + Z_L} \right) \quad \text{and} \quad E_{TH} = \frac{Z_{12}E}{Z_{22} + Z_L} \quad (2.16)$$

Admittance parameters

When an element is in shunt with a two-port, port-based admittance parameters, or y parameters, are the most convenient to use. These are defined as

$$I_1 = y_{11}V_1 + y_{12}V_2 \quad (2.17) \quad I_2 = y_{21}V_1 + y_{22}V_2, \quad (2.18)$$

$$\text{or in matrix form as} \quad \mathbf{I} = \mathbf{YV}. \quad (2.19)$$

Now, for reciprocity, $y_{12} = y_{21}$ and the circuit equivalence of the y parameters is shown in Figure 2-3(b). Consider the shunt connection of an element shown in Figure 2-4(b) where the y parameters of network A are

$$\mathbf{Y}_A = \begin{bmatrix} y_{11}^{(A)} & y_{12}^{(A)} \\ y_{21}^{(A)} & y_{22}^{(A)} \end{bmatrix} = \mathbf{Z}_A^{-1}. \quad (2.20)$$

The port voltages and currents are related as follows

$$I_1^{(A)} = y_{11}^{(A)}V_1 + y_{12}^{(A)}V_2 \quad \text{and} \quad I_2 = y_{21}^{(A)}V_1 + y_{22}^{(A)}V_2 \quad (2.21)$$

$$I_1 = yV_1 + I_1^{(A)} = (y + y_{11}^{(A)})V_1 + y_{12}^{(A)}V_2. \quad (2.22)$$

Thus the y parameters of the whole network are

$$\mathbf{Y} = \begin{bmatrix} y & 0 \\ 0 & 0 \end{bmatrix} + \mathbf{Y}_A. \quad (2.23)$$

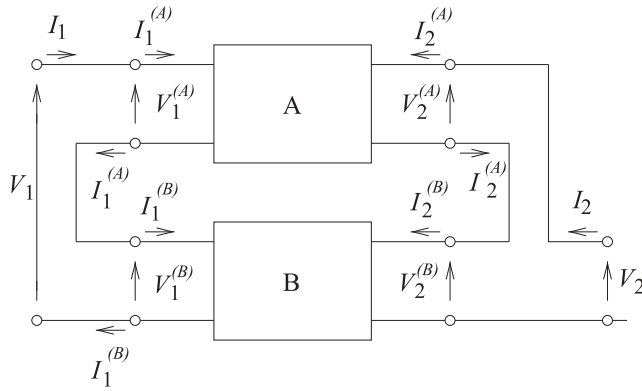


Figure 2-5: Series connection of two two-port networks.

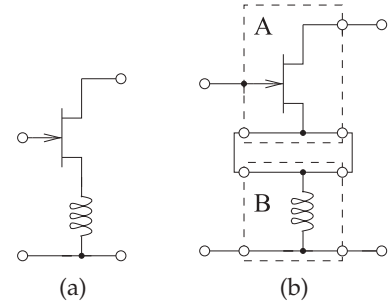


Figure 2-6: Example of a series connection of two two-port networks: (a) an amplifier; and (b) its components represented as two-port networks.

Hybrid parameters

Sometimes it is more convenient to use hybrid parameters, or h parameters, defined by

$$V_1 = h_{11}I_1 + h_{12}V_2 \quad \text{and} \quad I_2 = h_{21}I_1 + h_{22}V_2, \quad (2.24)$$

or in matrix form as

$$\begin{bmatrix} V_1 \\ I_2 \end{bmatrix} = \mathbf{H} \begin{bmatrix} I_1 \\ V_2 \end{bmatrix}. \quad (2.25)$$

These parameters are convenient to use with transistor circuits, as they describe a voltage-controlled current source that is a simple model of a transistor.

The choice of which network parameters to use depends on convenience, but as will be seen throughout this text, some parameters naturally describe a particular characteristic desired in a design. For example, with Port 1 being the input port of an amplifier and Port 2 being the output port, h_{21} describes the current gain of the amplifier.

2.2.3 Series Connection of Two-Port Networks

A series connection of two two-ports is shown in Figure 2-5. An example of when the series connection occurs is shown in Figure 2-6, which is the schematic of a transistor amplifier configuration with an inductor in the source leg. The transistor and the inductor can each be represented as two-ports so that the circuit of Figure 2-6(a) is the series connection of two two-ports, as shown in Figure 2-6(b). In the following, two-port parameters of the complete circuit are developed using the two-port parameter descriptions of the component two-ports. The procedure with any interconnection is to write down the relationships between the voltages and currents of the constituent networks. Which network parameters to use requires identification of the arithmetic path requiring the fewest operations.

Simple algebra relates the various total voltage and current parameters. From Figure 2-5,

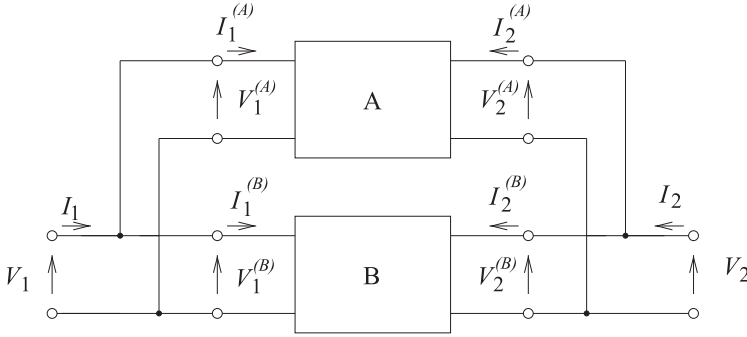


Figure 2-7: Parallel connection of two-port networks.

$$I_1^{(A)} = I_1^{(B)} = I_1, \quad I_2^{(A)} = I_2^{(B)} = I_2, \quad V_1 = V_1^{(A)} + V_1^{(B)}, \quad V_2 = V_2^{(A)} + V_2^{(B)},$$

which in matrix form becomes

$$\begin{bmatrix} V_1^{(A)} \\ V_2^{(A)} \end{bmatrix} = \begin{bmatrix} z_{11}^{(A)} & z_{12}^{(A)} \\ z_{21}^{(A)} & z_{22}^{(A)} \end{bmatrix} \begin{bmatrix} I_1^{(A)} \\ I_2^{(A)} \end{bmatrix}; \quad \begin{bmatrix} V_1^{(B)} \\ V_2^{(B)} \end{bmatrix} = \begin{bmatrix} z_{11}^{(B)} & z_{12}^{(B)} \\ z_{21}^{(B)} & z_{22}^{(B)} \end{bmatrix} \begin{bmatrix} I_1^{(B)} \\ I_2^{(B)} \end{bmatrix} \quad (2.26)$$

or

$$\begin{bmatrix} V_1 \\ V_2 \end{bmatrix} = (\mathbf{Z}^A + \mathbf{Z}^B) \begin{bmatrix} I_1 \\ I_2 \end{bmatrix}. \quad (2.27)$$

Thus the impedance matrix of the series connection of two-ports is

$$\mathbf{Z} = \mathbf{Z}_A + \mathbf{Z}_B. \quad (2.28)$$

2.2.4 Parallel Connection of Two-Port Networks

Admittance parameters are most conveniently combined to obtain the overall parameters of the two-port parallel connection of Figure 2-7. The total voltage and current are related by

$$V_1^{(A)} = V_1^{(B)} = V_1 \quad (2.29) \quad I_1 = I_1^{(A)} + I_1^{(B)} \quad (2.31)$$

$$V_2^{(A)} = V_2^{(B)} = V_2 \quad (2.30) \quad I_2 = I_2^{(A)} + I_2^{(B)} \quad (2.32)$$

and

$$\begin{bmatrix} I_1^{(A)} \\ I_2^{(A)} \end{bmatrix} = \begin{bmatrix} y_{11}^{(A)} & y_{12}^{(A)} \\ y_{21}^{(A)} & y_{22}^{(A)} \end{bmatrix} \begin{bmatrix} V_1^{(A)} \\ V_2^{(A)} \end{bmatrix} \quad (2.33)$$

$$\begin{bmatrix} I_1^{(B)} \\ I_2^{(B)} \end{bmatrix} = \begin{bmatrix} y_{11}^{(B)} & y_{12}^{(B)} \\ y_{21}^{(B)} & y_{22}^{(B)} \end{bmatrix} \begin{bmatrix} V_1^{(B)} \\ V_2^{(B)} \end{bmatrix}. \quad (2.34)$$

So the overall y parameter relation is

$$\begin{bmatrix} I_1 \\ I_2 \end{bmatrix} = (\mathbf{Y}_A + \mathbf{Y}_B) \begin{bmatrix} V_1 \\ V_2 \end{bmatrix}. \quad (2.35)$$

Figure 2-8 is an example of subcircuits that can be represented as two-ports that are then connected in parallel.

2.2.5 Series-Parallel Connection of Two-Port Networks

A similar approach to that in the preceding subsection is followed in developing the overall network parameters of the series-parallel connection of

Figure 2-8: Example of the parallel connection of two two-ports: (a) a feedback amplifier; and (b) its components represented as two-port networks A and B.

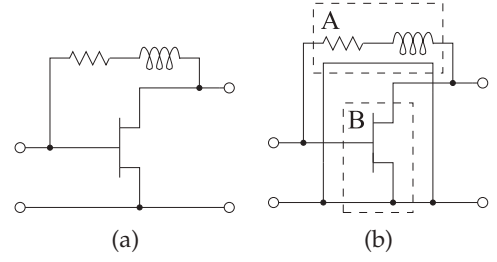


Figure 2-9: Series-parallel connection of two-ports.

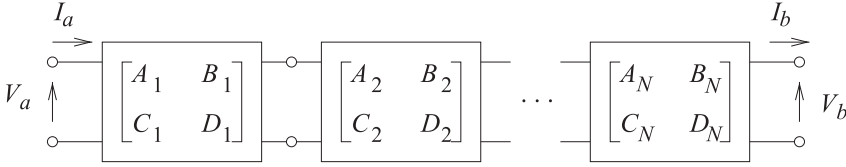
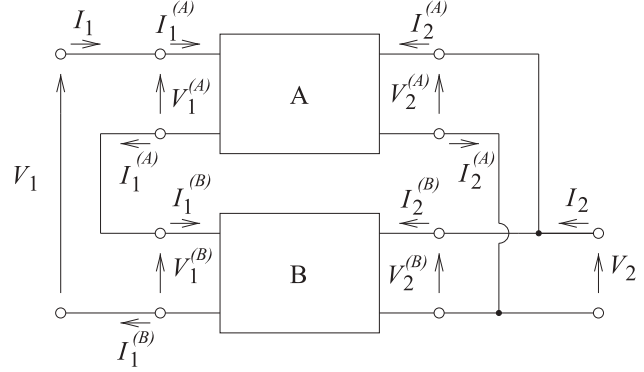


Figure 2-10: Cascade of two-port networks.

two-ports shown in Figure 2-9. Now,

$$I_1^{(A)} = I_1^{(B)} = I_1 \quad (2.36)$$

$$V_2^{(A)} = V_2^{(B)} = V_2 \quad (2.37)$$

$$V_1 = V_1^{(A)} + V_1^{(B)} \quad (2.38)$$

$$I_2 = I_2^{(A)} + I_2^{(B)}, \quad (2.39)$$

and so, using hybrid parameters,

$$\begin{bmatrix} V_1^{(A)} \\ I_2^{(A)} \end{bmatrix} = \begin{bmatrix} h_{11}^{(A)} & h_{12}^{(A)} \\ h_{21}^{(A)} & h_{22}^{(A)} \end{bmatrix} \begin{bmatrix} I_1^{(A)} \\ V_2^{(A)} \end{bmatrix} \quad (2.40)$$

$$\begin{bmatrix} V_1^{(B)} \\ I_2^{(B)} \end{bmatrix} = \begin{bmatrix} h_{11}^{(B)} & h_{12}^{(B)} \\ h_{21}^{(B)} & h_{22}^{(B)} \end{bmatrix} \begin{bmatrix} I_1^{(B)} \\ V_2^{(B)} \end{bmatrix}. \quad (2.41)$$

Putting this in compact form:

$$\begin{bmatrix} V_1 \\ I_2 \end{bmatrix} = (\mathbf{H}_A + \mathbf{H}_B) \begin{bmatrix} I_1 \\ V_2 \end{bmatrix}. \quad (2.42)$$

2.2.6 ABCD Matrix Characterization of Two-Port Networks

ABCD parameters are the best parameters to use when cascading two-ports, as in Figure 2-10, and total voltage and current relationships are required. First, consider Figure 2-11, which puts the voltages and currents

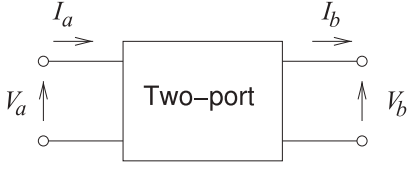


Figure 2-11: Two-port network with cascadable voltage and current definitions.

in cascadable form with the input variables in terms of the output variables:

$$\begin{bmatrix} V_a \\ I_a \end{bmatrix} = \begin{bmatrix} A & B \\ C & D \end{bmatrix} \begin{bmatrix} V_b \\ I_b \end{bmatrix}. \quad (2.43)$$

The reciprocity relationship of the $ABCD$ parameters is not as simple as for the z and y parameters. To see this, first express $ABCD$ parameters in terms of z parameters. Note that the current at Port 2 is in the opposite direction to the usual definition of the two-port current shown in Figure 2-1(a). So

$$V_a = V_1 \quad (2.44) \quad V_b = V_2 \quad (2.47)$$

$$I_a = I_1 \quad (2.45) \quad I_b = -I_2 \quad (2.48)$$

$$V_a = z_{11}I_a - z_{12}I_b \quad (2.46) \quad V_b = z_{21}I_a - z_{22}I_b. \quad (2.49)$$

From Equation (2.49),
$$I_a = \frac{z_{22}}{z_{21}}I_b + \frac{1}{z_{21}}V_b, \quad (2.50)$$

and substituting this into Equation (2.46) yields

$$V_a = \frac{z_{11}}{z_{21}}V_b + \left(z_{11}\frac{z_{22}}{z_{21}} - z_{12} \right) I_b. \quad (2.51)$$

Comparing Equations (2.50) and (2.51) to Equation (2.43) leads to

$$\begin{aligned} A &= z_{11}/z_{21} & B &= \Delta_z/z_{21} \\ C &= 1/z_{21} & D &= z_{22}/z_{21}, \end{aligned} \quad (2.52)$$

where
$$\Delta_z = z_{11}z_{22} - z_{12}z_{21}. \quad (2.53)$$

Rearranging,

$$\begin{aligned} z_{11} &= A/C & z_{12} &= (AD - BC)/C \\ z_{21} &= 1/C & z_{22} &= D/C. \end{aligned} \quad (2.54)$$

Now the reciprocity condition in terms of $ABCD$ parameters can be determined. For z parameters, $z_{12} = z_{21}$ for reciprocity; that is, from Equation (2.54), for a reciprocal network,

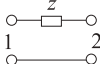
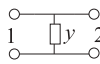

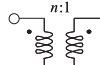
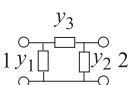
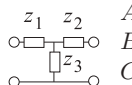


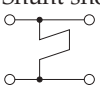
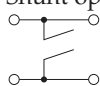
$$\frac{AD - BC}{C} = \frac{1}{C} \quad \text{and} \quad AD - BC = 1. \quad (2.55)$$

Thus for a two-port network to be reciprocal, $AD - BC = 1$. The utility of these parameters is that the $ABCD$ matrix of the cascade connection of N two-ports in Figure 2-10 is equal to the product of the $ABCD$ matrices of the individual two-ports:

$$\begin{bmatrix} A & B \\ C & D \end{bmatrix} = \begin{bmatrix} A_1 & B_1 \\ C_1 & D_1 \end{bmatrix} \begin{bmatrix} A_2 & B_2 \\ C_2 & D_2 \end{bmatrix} \cdots \begin{bmatrix} A_N & B_N \\ C_N & D_N \end{bmatrix}. \quad (2.56)$$

See Table 2-1 for the $ABCD$ parameters of several two-port networks.

Table 2-1: $ABCD$ parameters of several two-ports. The transmission line is lossless with a propagation constant of β . ($\beta\ell$ and θ are electrical lengths of transmission lines in radians.)

<p>Series impedance, z</p>  $A = 1 \quad B = z$ $C = 0 \quad D = 1$	<p>Shunt admittance, y</p>  $A = 1 \quad B = 0$ $C = y \quad D = 1$
<p>Transmission line, length ℓ, $Z_0 = 1/Y_0$</p>  $A = \cos(\beta\ell) \quad B = jZ_0 \sin(\beta\ell)$ $C = jY_0 \sin(\beta\ell) \quad D = \cos(\beta\ell)$	<p>Transformer, ratio $n:1$</p>  $A = n \quad B = 0$ $C = 0 \quad D = 1/n$
<p>Pi network</p>  $A = 1 + y_2/y_3 \quad B = 1/y_3$ $C = y_1 + y_2 + y_1y_2/y_3$ $D = 1 + y_1/y_3$	<p>Tee network</p>  $A = 1 + z_1/z_3$ $B = z_1 + z_2 + z_1z_2/z_3$ $C = 1/z_3 \quad D = 1 + z_2/z_3$
<p>Series shorted stub, electrical length θ</p>  $A = 1 \quad B = jZ_0 \tan \theta$ $C = 0 \quad D = 1$	<p>Series open stub, electrical length θ</p>  $A = 1 \quad B = -jZ_0/(\tan \theta)$ $C = 0 \quad D = 1$
<p>Shunt shorted stub, electrical length θ</p>  $A = 1 \quad B = 0$ $C = -j/(Z_0 \tan \theta) \quad D = 1$	<p>Shunt open stub, electrical length θ</p>  $A = 1 \quad B = 0$ $C = j \tan \theta/Z_0 \quad D = 1$

2.3 Scattering Parameters

Direct measurement of the z , y , h , and $ABCD$ parameters requires that the ports be terminated in either short or open circuits. For active circuits, such terminations could result in undesired behavior, including oscillation or destruction. Also, at RF it is difficult to realize a good open or short. Since RF circuits are designed with close attention to maximum power transfer conditions, resistive terminations are preferred, as these are closer to the actual operating conditions. Thus the effect of measurement errors will have less impact than when parameter extraction relies on imperfect opens and shorts. The essence of scattering parameters (or S parameters²) is that they relate forward- and backward-traveling waves on a transmission line, thus S parameters are related to power flow.

The discussion of S parameters begins by considering the reflection coefficient, which is the S parameter of a one-port network.

2.3.1 Reflection Coefficient

The reflection coefficient, Γ , of a load, as in Figure 2-12, can be determined by separately measuring the forward- and backward-traveling voltages on the transmission line:

$$\Gamma(x) = \frac{V^-(x)}{V^+(x)}. \quad (2.57)$$

² For historical reasons a capital “ S ” is used when referring to S parameters. For most other network parameters, lowercase is used (e.g., z parameters for impedance parameters).

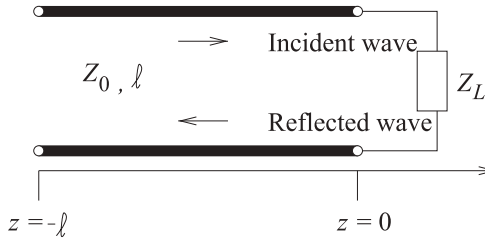


Figure 2-12: Transmission line of characteristic impedance Z_0 and length ℓ terminated in a load of impedance Z_L .

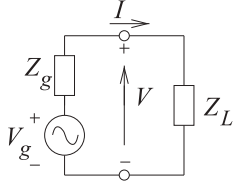


Figure 2-13: A Thevenin equivalent source with generator V_g and source impedance Z_g terminated in a load Z_L .

Γ at the load is related to the impedance Z_L by

$$\Gamma(0) = \frac{Z_L - Z_0}{Z_L + Z_0}, \quad (2.58)$$

where Z_0 is the characteristic impedance of the connecting transmission line. This can also be written as

$$\Gamma(0) = \frac{Y_0 - Y_L}{Y_0 + Y_L}, \quad (2.59)$$

where $Y_0 = 1/Z_0$ and $Y_L = 1/Z_L$.

2.3.2 Reflection Coefficient with Complex Reference Impedance

Here the reflection coefficient of Z_L in Figure 2-13 will be developed with respect to the complex reference impedance Z_g . The total voltage and current at the load are

$$V = V_g \frac{Z_L}{Z_g + Z_L} \quad (2.60) \quad \text{and} \quad I = \frac{V_g}{Z_g + Z_L}. \quad (2.61)$$

To develop the reflection coefficient, first define equivalent forward- and backward-traveling waves. This can be done by imagining that between the generator and the load there is a transmission line of characteristic impedance Z_g which has infinitesimal length. The incident voltage and current waves (V^+ , I^+) are the total voltage and current obtained when the generator is conjugately matched to the load (i.e., $Z_L = Z_g^*$). So the equations of forward-traveling voltage and current become³

$$V^+ = V_g \frac{Z_g^*}{Z_g + Z_g^*} = V_g Z_g^* 2\Re\{Z_g\} \quad (2.62) \quad I^+ = V_g \frac{1}{2\Re\{Z_g\}}. \quad (2.63)$$

Now return to considering the actual load, Z_L . The reflected voltage and current (V^- , I^-) are obtained by calculating the actual voltage and current at the source using the relationships

$$V = V^+ + V^- \quad (2.64) \quad I = I^+ + I^- \quad (2.65)$$

³ Here \Re is the real operator, which yields the real part of a complex number.

to determine the backward-traveling components. In Equations (2.64) and (2.65) the forward-traveling components are those in Equations (2.62) and (2.63). From Equation (2.62),

$$V_g = V^+ \frac{Z_g + Z_g^*}{Z_g^*}, \quad (2.66)$$

and from Equations (2.60), (2.64), and (2.66),

$$\begin{aligned} V^- &= V - V^+ = V_g \frac{Z_L}{Z_g + Z_L} - V^+ = \left[\frac{Z_g + Z_g^*}{Z_g^*} \frac{Z_L}{Z_g + Z_L} - 1 \right] V^+ \\ &= \left[\frac{Z_g Z_L + Z_g^* Z_L - Z_g^* Z_g - Z_g^* Z_L}{Z_g^* (Z_g + Z_L)} \right] V^+ \\ &= \underbrace{\left(\frac{Z_L - Z_g^*}{Z_L + Z_g} \right) \frac{Z_g}{Z_g^*}}_{\Gamma^V} V^+ = \Gamma^V V^+. \end{aligned} \quad (2.67)$$

$$\text{Similarly} \quad I^- = - \underbrace{\left(\frac{Z_L - Z_g^*}{Z_L + Z_g} \right) \frac{Z_g}{Z_g^*}}_{\Gamma^I} I^+ = \Gamma^I I^+. \quad (2.68)$$

Γ^V is the voltage reflection coefficient, which is usually denoted as just Γ , while Γ^I is the current reflection coefficient. It is clear that $\Gamma^V = 0 = \Gamma^I$ when $Z_L = Z_g^*$ and $\Gamma^V = -\Gamma^I = (Z_L - R_g)/(Z_L + R_g)$ when Z_g is purely resistive (i.e., when $Z_g = R_g$). Generally the reflection coefficients are defined using a purely resistive Z_g . This becomes the reference resistance, which is more commonly referred to as the reference impedance, Z_0 , or, if the same reference impedance is used throughout, the system impedance.

2.3.3 Two-Port S Parameters

Two-port S parameters are defined in terms of traveling waves on transmission lines with real characteristic impedance Z_0 attached to each of the ports of the network, see Figure 2-1(b):

$$V_1^- = S_{11} V_1^+ + S_{12} V_2^+ \quad (2.69) \quad V_2^- = S_{21} V_1^+ + S_{22} V_2^+, \quad (2.70)$$

where S_{ij} are the individual S parameters. In matrix form the equations above become

$$\begin{bmatrix} V_1^- \\ V_2^- \end{bmatrix} = \begin{bmatrix} S_{11} & S_{12} \\ S_{21} & S_{22} \end{bmatrix} \begin{bmatrix} V_1^+ \\ V_2^+ \end{bmatrix} = \mathbf{S} \begin{bmatrix} V_1^+ \\ V_2^+ \end{bmatrix}. \quad (2.71)$$

Individual S parameters are determined by measuring the forward- and backward-traveling waves with loads $Z_L = Z_0$ at the ports. For the output line the load cannot reflect power and so $V_2^+ = 0$, then

$$S_{11} = \left. \frac{V_1^-}{V_1^+} \right|_{V_2^+ = 0}. \quad (2.72)$$

The remaining three parameters are determined similarly and so S_{22} is found as

$$S_{22} = \left. \frac{V_2^-}{V_2^+} \right|_{V_1^+ = 0} \quad (2.73)$$

and the transmission parameter as

$$S_{21} = \left. \frac{V_2^-}{V_1^+} \right|_{V_2^+ = 0} \quad (2.74)$$

S_{21} is also called the transmission coefficient, T . In the reverse direction,

$$S_{12} = \left. \frac{V_1^-}{V_2^+} \right|_{V_1^+ = 0} \quad (2.75)$$

In the above Z_0 is referred to as the **normalization impedance** or equivalently the **reference impedance**. In some circumstances Z_{REF} is used to denote reference impedance to avoid possible confusion with a transmission line impedance that is not the same as the reference impedance. The S parameters here are also called normalized S parameters, and the S parameters are normalized to the same reference impedance at each port. Calling them **normalized S parameters** also carries the additional meaning that the S parameters are referenced to the one real impedance.

The relationships between the two-port S parameters and the common network parameters are given in Table 2-2. It is interesting to note that $S_{21}/S_{12} = z_{21}/z_{12} = y_{21}/y_{12} = h_{21}/h_{12}$. That is, the ratio of the forward to reverse parameters (at least for S , z , y , and h parameters) are the same and this ratio is one for a reciprocal device. An S parameter is a voltage ratio, so when it is expressed in decibels $S_{ij}|_{\text{dB}} = 20 \log(S_{ij})$.

A reciprocal network has $S_{12} = S_{21}$. If unit power flows into a two-port (with ports terminated in the reference impedance), a fraction, $|S_{11}|^2$, is reflected and a further fraction, $|S_{21}|^2$, is transmitted through the network.

EXAMPLE 2.2 Two-Port S Parameters

What are the S parameters of a 30 dB attenuator?

Solution:

An attenuator is shown with a system impedance of Z_0 . An ideal attenuator has no reflection at each of the two ports when the attenuator is embedded in its system impedance. Thus $\Gamma_{\text{in}} = 0 = \Gamma_{\text{out}}$. Since there is no reflection from the load or the source, this implies that $S_{11} = 0 = S_{22}$.

Since this is a 30 dB attenuator, the power delivered to the load impedance Z_0 is 30 dB below the power available from the source, thus $S_{21} = -30 \text{ dB} = 0.0316$. The attenuator is reciprocal and so $S_{12} = S_{21}$. Thus the S parameters of the attenuator are

$$\mathbf{S} = \begin{bmatrix} 0 & 0.0316 \\ 0.0316 & 0 \end{bmatrix} \quad (2.76)$$

Note that the reference impedance did not need to be known to develop the S parameters.

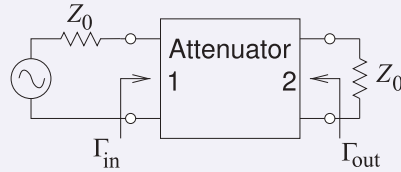
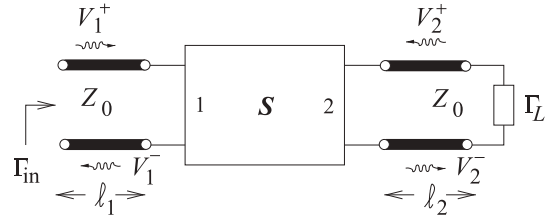


Table 2-2: Two-port S parameter conversion chart. The z , y , and h parameters are normalized to Z_0 . Z' , Y' , and H' are the actual parameters. For $ABCD$ parameter conversion see Section 2.7.2.

	S	In terms of S
z	$Z'_{11} = z_{11}Z_0$ $Z'_{12} = z_{12}Z_0$ $\delta_z = (1 + z_{11})(1 + z_{22}) - z_{12}z_{21}$ $S_{11} = [(z_{11} - 1)(z_{22} + 1) - z_{12}z_{21}]/\delta_z$ $S_{12} = 2z_{12}/\delta_z$ $S_{21} = 2z_{21}/\delta_z$ $S_{22} = [(z_{11} + 1)(z_{22} - 1) - z_{12}z_{21}]/\delta_z$	$Z'_{21} = z_{21}Z_0$ $Z'_{22} = z_{22}Z_0$ $\delta_S = (1 - S_{11})(1 - S_{22}) - S_{12}S_{21}$ $z_{11} = [(1 + S_{11})(1 - S_{22}) + S_{12}S_{21}]/\delta_S$ $z_{12} = 2S_{12}/\delta_S$ $z_{21} = 2S_{21}/\delta_S$ $z_{22} = [(1 - S_{11})(1 + S_{22}) + S_{12}S_{21}]/\delta_S$
y	$Y'_{11} = y_{11}/Z_0$ $Y'_{12} = y_{12}/Z_0$ $\delta_y = (1 + y_{11})(1 + y_{22}) - y_{12}y_{21}$ $S_{11} = [(1 - y_{11})(1 + y_{22}) + y_{12}y_{21}]/\delta_y$ $S_{12} = -2y_{12}/\delta_y$ $S_{21} = -2y_{21}/\delta_y$ $S_{22} = [(1 + y_{11})(1 - y_{22}) + y_{12}y_{21}]/\delta_y$	$Y'_{21} = y_{21}/Z_0$ $Y'_{22} = y_{22}/Z_0$ $\delta_S = (1 + S_{11})(1 + S_{22}) - S_{12}S_{21}$ $y_{11} = [(1 - S_{11})(1 + S_{22}) + S_{12}S_{21}]/\delta_S$ $y_{12} = -2S_{12}/\delta_S$ $y_{21} = -2S_{21}/\delta_S$ $y_{22} = [(1 + S_{11})(1 - S_{22}) + S_{12}S_{21}]/\delta_S$
h	$H'_{11} = h_{11}Z_0$ $H'_{12} = h_{12}$ $\delta_h = (1 + h_{11})(1 + h_{22}) - h_{12}h_{21}$ $S_{11} = [(h_{11} - 1)(h_{22} + 1) - h_{12}h_{21}]/\delta_h$ $S_{12} = 2h_{12}/\delta_h$ $S_{21} = -2h_{21}/\delta_h$ $S_{22} = [(1 + h_{11})(1 - h_{22}) + h_{12}h_{21}]/\delta_h$	$H'_{21} = h_{21}$ $H'_{22} = h_{22}/Z_0$ $\delta_S = (1 - S_{11})(1 + S_{22}) + S_{12}S_{21}$ $h_{11} = [(1 + S_{11})(1 + S_{22}) - S_{12}S_{21}]/\delta_S$ $h_{12} = 2S_{12}/\delta_S$ $h_{21} = -2S_{21}/\delta_S$ $h_{22} = [(1 - S_{11})(1 - S_{22}) - S_{12}S_{21}]/\delta_S$

Figure 2-14: A terminated two-port network with transmission lines of infinitesimal length at the ports.



2.3.4 Input Reflection Coefficient of a Terminated Two-Port Network

A two-port is shown in Figure 2-14 that is terminated at Port 2 in a load with a reflection coefficient Γ_L . The lines at each of the ports are of infinitesimal length (i.e., $\ell_1 \rightarrow 0$ and $\ell_2 \rightarrow 0$) and are used to make it easier to visualize the separation of the voltage into forward- and backward-traveling components. The aim in this section is to develop a formula for the input reflection coefficient $\Gamma_{in} = V_1^-/V_1^+$. For the circuit in Figure 2-14 three equations can be developed:

$$V_1^- = S_{11}V_1^+ + S_{12}V_2^+ \quad (2.77)$$

$$V_2^- = S_{21}V_1^+ + S_{22}V_2^+ \quad (2.78)$$

$$V_2^+ = \Gamma_L V_2^-, \quad \text{i.e.,} \quad V_2^- = V_2^+/\Gamma_L. \quad (2.79)$$

Note that V_2^- is the voltage wave that leaves the two-port but is incident on the load Γ_L . The aim here is to eliminate V_2^+ and V_2^- . Substituting Equation

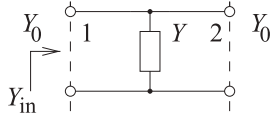


Figure 2-15: Shunt element in the form of a two-port.

(2.79) into Equation (2.78) leads to

$$V_2^+ / \Gamma_L = S_{21} V_1^+ + S_{22} V_2^+ \quad (2.80)$$

$$V_2^+ \left(\frac{1 - S_{22} \Gamma_L}{\Gamma_L} \right) = S_{21} V_1^+ \quad (2.81)$$

$$V_2^+ = \left(\frac{S_{21} \Gamma_L}{1 - S_{22} \Gamma_L} \right) V_1^+. \quad (2.82)$$

Now substituting Equation (2.82) in Equation (2.77) yields

$$V_1^- = S_{11} V_1^+ + S_{12} \left(\frac{S_{21} \Gamma_L}{1 - S_{22} \Gamma_L} \right) V_1^+ \quad (2.83)$$

and so

$$\Gamma_{in} = S_{11} + \frac{S_{12} S_{21} \Gamma_L}{1 - S_{22} \Gamma_L}. \quad (2.84)$$

2.3.5 Evaluation of the Scattering Parameters of an Element

Scattering parameters can be derived analytically for various circuit configurations and in this section the procedure is illustrated for the shunt element of Figure 2-15. The procedure to find S_{11} is to match Port 2 so that $V_2^+ = 0$, then S_{11} is the reflection coefficient at Port 1:

$$S_{11} = \frac{Y_0 - Y_{in}}{Y_0 + Y_{in}}, \quad (2.85)$$

where $Y_{in} = Y_0 + Y$, since the matched termination at Port 2 (i.e., $Y_0 = 1/Z_0$) shunts the admittance Y . Thus

$$S_{11} = \frac{Y_0 - Y_0 - Y}{2Y_0 + Y} = \frac{-Y}{2Y_0 + Y}. \quad (2.86)$$

From the symmetry of the two-port,

$$S_{22} = S_{11}. \quad (2.87)$$

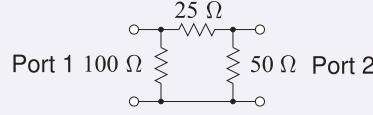
S_{21} is evaluated by determining the transmitted wave, V_2^- , with the output line matched so that again an admittance, Y_0 , is placed at Port 2 and $V_2^+ = 0$. After some algebraic manipulation,

$$S_{21} = 2Y_0 / (Y + 2Y_0) \quad (2.88)$$

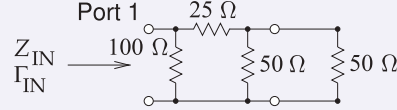
is obtained. Since this is clearly a reciprocal network, $S_{12} = S_{21}$ and all four S parameters are obtained. A similar procedure of selectively applying matched loads is used to obtain the S parameters of other networks.

EXAMPLE 2.3**Calculation of the S Parameters of a Two-Port Network**

Derive the two-port $50\ \Omega$ S parameters of the resistive circuit to the right.

**Solution:**

Calculation of S_{11} . This involves terminating Port 2 in the system reference impedance, $50\ \Omega$, and then calculating the input impedance of the augmented network. This is then converted to a reflection coefficient, which here is S_{11} . The circuit for calculation is to the right. Now



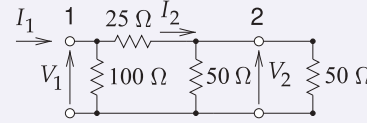
$$Z_{IN} = 100 \parallel [25 \ \$ (50 \parallel 50)] \ \Omega = 100 \parallel 50 \ \Omega = 33.33 \ \Omega, \quad (2.89)$$

where \parallel indicates the parallel-connection calculation and $\$$ indicates the series-connection calculation. Thus

$$S_{11} = \Gamma_{IN} = \frac{Z_{IN} - Z_0}{Z_{IN} + Z_0} = \frac{33.33 - 50}{33.33 + 50} = -0.2. \quad (2.90)$$

Calculation of S_{21} . This involves terminating Port 2 in the system reference impedance, $50\ \Omega$, and then calculating the forward-traveling voltage wave at Port 1 and the reverse-traveling voltage wave at Port 2. Note that the reverse-traveling voltage wave at Port 2 is leaving the two-port.

Since there is no wave reflected from the termination at Port 2, the total voltage at Port 2 is just V_2^- . The circuit for calculation is on the right.



$$V_1 = V_1^+ + V_1^- = V_1^+ (1 + S_{11}) \rightarrow V_1^+ = \frac{V_1}{1 + S_{11}} = 1.25 V_1. \quad (2.91)$$

The voltage at Port 1 is

$$V_1 = I_1 Z_{IN} = 33.33 I_1 \rightarrow V_1^+ = 1.25 \cdot 33.33 I_1 = 41.66 I_1. \quad (2.92)$$

The next step is to find an expression for I_2 :

$$V_1 = I_1 Z_{IN} = 33.33 I_1 = I_2 (25 \ \$ 50 \parallel 50) = 50 I_2. \quad (2.93)$$

Rearranging,

$$I_2 = I_1 \frac{33.33}{50} = 0.6667 I_1. \quad (2.94)$$

Now

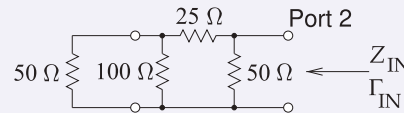
$$V_2^- = V_2 = I_2 (50 \parallel 50) = 25 I_2 = 16.67 I_1. \quad (2.95)$$

So

$$S_{21} = \frac{V_2^-}{V_1^+} = \frac{16.67}{41.66} = 0.4. \quad (2.96)$$

Calculation of S_{12} . The two-port is a reciprocal network (as are all networks with only lumped R , L , and C elements) and so $S_{12} = S_{21}$.

Calculation of S_{22} . Using a similar procedure to that used for finding S_{11} , the circuit for the calculation is on the right:



$$Z_{IN} = 50 \parallel [25 \parallel (100 \parallel 50)] \Omega = 50 \parallel (25 \parallel 33.33) = 50 \parallel 58.33 = 26.92 \Omega. \quad (2.97)$$

$$\text{Therefore} \quad S_{22} = \Gamma_{IN} = \frac{26.92 - 50}{26.92 + 50} = -0.3. \quad (2.98)$$

Collecting the individual S parameters:

$$\mathbf{S} = \begin{bmatrix} -0.2 & 0.4 \\ 0.4 & -0.3 \end{bmatrix}. \quad (2.99)$$

2.3.6 Properties of a Two-Port in Terms of S Parameters

The properties of most interest are whether the two-port network is lossless, passive, or reciprocal.

If a network is lossless, all of the power input to the network must leave the network. The power incident on Port 1 of a network is

$$P_1^+ = \left| \frac{\frac{1}{2}V_1^+}{Z_0} \right|^2 \quad (2.100)$$

and the power leaving Port 1 is

$$P_1^- = \left| \frac{\frac{1}{2}V_1^-}{Z_0} \right|^2. \quad (2.101)$$

This can be repeated for Port 2 and the factor $\frac{1}{2}/Z_0$ appears in all expressions. So cancelling this factor, the condition for the network to be lossless is

$$|S_{11}|^2 + |S_{21}|^2 = 1 \quad \text{and} \quad |S_{12}|^2 + |S_{22}|^2 = 1. \quad (2.102)$$

For a network to be passive, no more power can leave the network than enters it. So the condition for passivity is

$$|S_{11}|^2 + |S_{21}|^2 \leq 1 \quad \text{and} \quad |S_{12}|^2 + |S_{22}|^2 \leq 1. \quad (2.103)$$

Reciprocity requires that $S_{21} = S_{12}$.

2.3.7 Scattering Transfer or T Parameters

S parameters relate reflected waves to incident waves, thus mixing the quantities at the input and output ports. However, in dealing with cascaded networks it is preferable to relate the traveling waves at the input ports to the output ports. Such parameters are called the scattering transfer (or ST) parameters, which for a two-port network are defined by

$$\begin{bmatrix} V_1^- \\ V_1^+ \end{bmatrix} = \begin{bmatrix} ^ST_{11} & ^ST_{12} \\ ^ST_{21} & ^ST_{22} \end{bmatrix} \begin{bmatrix} V_2^+ \\ V_2^- \end{bmatrix}, \quad (2.104)$$

where

$$^s\mathbf{T} = \begin{bmatrix} ^ST_{11} & ^ST_{12} \\ ^ST_{21} & ^ST_{22} \end{bmatrix}. \quad (2.105)$$

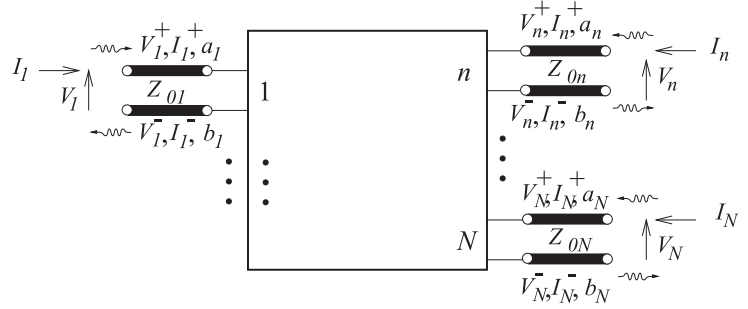


Figure 2-16: N -port network with traveling voltage and current waves.

The two-port ${}^S T$ parameters and S parameters are related by

$$\begin{bmatrix} {}^S T_{11} & {}^S T_{12} \\ {}^S T_{21} & {}^S T_{22} \end{bmatrix} = \begin{bmatrix} -(S_{11}S_{22} - S_{12}S_{21})/S_{21} & (S_{11}/S_{21}) \\ -(S_{22}/S_{21}) & (1/S_{21}) \end{bmatrix} \quad (2.106)$$

and

$$\begin{bmatrix} S_{11} & S_{12} \\ S_{21} & S_{22} \end{bmatrix} = \begin{bmatrix} {}^S T_{12} {}^S T_{22}^{-1} & ({}^S T_{11} - {}^S T_{12} {}^S T_{22}^{-1} {}^S T_{21}) \\ {}^S T_{22}^{-1} & -{}^S T_{22}^{-1} {}^S T_{21} \end{bmatrix}. \quad (2.107)$$

Very often the ${}^S T$ parameters are called T parameters, but there are at least two types of T parameters, so it is necessary to be specific. (Another form will be introduced in Section 2.6.) If networks A and B have parameters ${}^S \mathbf{T}_A$ and ${}^S \mathbf{T}_B$, then the ${}^S \mathbf{T}$ parameters of the cascaded network are

$${}^S \mathbf{T} = {}^S \mathbf{T}_A \cdot {}^S \mathbf{T}_B. \quad (2.108)$$

There are two forms of the scattering T parameters. Here the scattering transfer parameters are designated as the ${}^S T$ parameters but often T on its own is used. The other more common form are the chain scattering parameters which will be considered in Section 2.6.

2.4 Generalized Scattering Parameters

The scattering parameters up to now are known as normalized S parameters because they have the same reference impedance at each port. However the qualification ‘normalized’ is not used unless it is necessary to distinguish them from a more general form of S parameters. In this section generalized S parameters that have different reference impedances at each of the ports are considered. These are particularly useful in designing amplifiers but are also useful in measurements where the system impedance of a design may not be the same as the reference impedance of the measurement system. For example an RFIC may have a system impedance of 100 Ω , but the measurement system have a reference impedance of 50 Ω .

2.4.1 The N -Port Network

The N -port network is a generalization of a two-port, as you may have guessed. A network with many ports is shown in Figure 2-16. Again, each port consists of a pair of terminals, one of which is the reference for voltage. Each port has equal and opposite currents at the two terminals. The incident and reflected voltages at any port can be related to each other using the

voltage scattering parameter matrix relation:

$$\begin{bmatrix} V_1^- \\ V_2^- \\ \vdots \\ V_N^- \end{bmatrix} = \begin{bmatrix} S_{11} & S_{12} & \dots & S_{1N} \\ S_{21} & S_{22} & \dots & S_{2N} \\ \vdots & & \ddots & \\ S_{N1} & S_{N2} & \dots & S_{NN} \end{bmatrix} \begin{bmatrix} V_1^+ \\ V_2^+ \\ \vdots \\ V_N^+ \end{bmatrix}, \quad (2.109)$$

$$\text{or in compact form as} \quad \mathbf{V}^- = \mathbf{S}\mathbf{V}^+ \quad (2.110)$$

Notice that

$$S_{ij} = \left. \frac{V_i^-}{V_j^+} \right|_{V_k^+ = 0 \text{ for } k \neq j}. \quad (2.111)$$

In words, S_{ij} is found by driving Port j with an incident wave of voltage V_j^+ and measuring the reflected wave V_i^- at Port i , with all ports other than j terminated in a matched load. Reflection and transmission coefficients can also be defined using the above relationship, provided that the ports are terminated in matched loads:

- S_{ii} : reflection coefficient seen looking into Port i
- S_{ij} : transmission coefficient from j to i .

2.4.2 Power Waves

The S parameters used so far have the same reference impedance at each port. These can be generalized so that the reference impedances at each port can be different. These are useful if the actual system being considered has different loading conditions at the ports. Generalized S parameters, denoted here as $^G S$, are defined in terms of what are called root power waves, which in turn are defined using forward- and backward-traveling voltage waves. Consider the N -port network of Figure 2-16, where the n th port has a reference transmission line of characteristic impedance Z_{0n} , which can have infinitesimal length. The transmission line at the n th port serves to separate the forward- and backward-traveling voltage (V_n^+ and V_n^-) and current (I_n^+ and I_n^-) waves.

The reference characteristic impedance matrix \mathbf{Z}_0 is a diagonal matrix, $\mathbf{Z}_0 = \text{diag}(Z_{01} \dots Z_{0n} \dots Z_{0N})$, and the **root power waves** at the n th port, a_n and b_n , are defined by

$$a_n = V_n^+ / \sqrt{\Re\{Z_{0n}\}} \quad \text{and} \quad b_n = V_n^- / \sqrt{\Re\{Z_{0n}\}}, \quad (2.112)$$

and shown in Figure 2-17 and are often called just **power waves**. The unit of the a and b values is root power, that is, in the SI unit system, $\sqrt{\text{W}}$. In matrix form

$$\mathbf{a} = \mathbf{Z}_0^{-1/2} \mathbf{V}^+ = \mathbf{Y}_0^{1/2} \mathbf{V}^+, \quad \mathbf{b} = \mathbf{Z}_0^{-1/2} \mathbf{V}^- = \mathbf{Y}_0^{1/2} \mathbf{V}^-, \quad (2.113)$$

$$\mathbf{V}^+ = \mathbf{Z}_0^{1/2} \mathbf{a} = \mathbf{Y}_0^{-1/2} \mathbf{a}, \quad \mathbf{V}^- = \mathbf{Z}_0^{1/2} \mathbf{b} = \mathbf{Y}_0^{-1/2} \mathbf{b}, \quad (2.114)$$

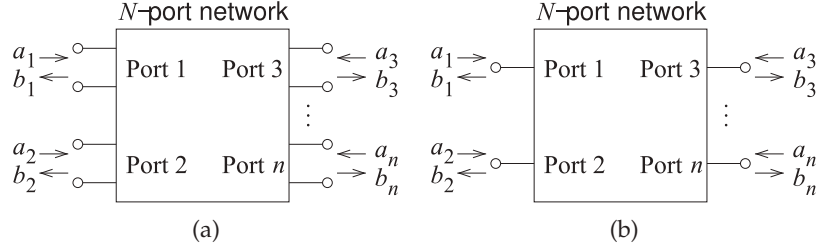
where

$$\mathbf{a} = [a_1 \dots a_n \dots a_N]^T, \quad \mathbf{b} = [b_1 \dots b_n \dots b_N]^T, \quad (2.115)$$

$$\mathbf{V}^+ = [V_1^+ \dots V_n^+ \dots V_N^+]^T, \quad \mathbf{V}^- = [V_1^- \dots V_n^- \dots V_N^-]^T, \quad (2.116)$$

Figure 2-17:

N -ports defining the a and b root power waves: (a) two-terminal ports; and (b) ports on their own.



and the characteristic admittance matrix is $\mathbf{Y}_0 = \mathbf{Z}_0^{-1}$. The power waves are interpreted as describing power flow:

$$\frac{1}{\sqrt{2}}|a_n| = \sqrt{\text{incident power at Port } n}$$

and $\frac{1}{\sqrt{2}}|b_n| = \sqrt{\text{power leaving at Port } n}.$ (2.117)

That is, for example, the incident (or available) power at Port n , referenced to Z_{0n} , is $\frac{1}{2}|a_n|^2$ and the reflected power at the port is $\frac{1}{2}|b_n|^2$. Thus the power delivered by the n th port is $\frac{1}{2}(|b_n|^2 - |a_n|^2)$.

After some manipulation it can be shown that on each reference line the power waves can be related to the total voltages and currents as

$$\mathbf{a} = \frac{\mathbf{V} + \mathbf{Z}_0 \mathbf{I}}{2\sqrt{\Re\{\mathbf{Z}_0\}}} \quad \text{and} \quad \mathbf{b} = \frac{\mathbf{V} - \mathbf{Z}_0^* \mathbf{I}}{2\sqrt{\Re\{\mathbf{Z}_0\}}}, \quad (2.118)$$

where \mathbf{V} and \mathbf{I} are vectors of total voltage and total current. Now, generalized S parameters can be formally defined as

$$\mathbf{b} = {}^G \mathbf{S} \mathbf{a}, \quad (2.119)$$

thus $\mathbf{Y}_0^{1/2} \mathbf{V}^- = {}^G \mathbf{S} \mathbf{Y}_0^{1/2} \mathbf{V}^+$, and so $\mathbf{V}^- = \mathbf{Y}_0^{-1/2} {}^G \mathbf{S} \mathbf{Y}_0^{1/2} \mathbf{V}^+$. This reduces to $\mathbf{V}^- = {}^G \mathbf{S} \mathbf{V}^+$ when all of the reference transmission lines have the same characteristic impedance. However, when the ports have different reference impedances, \mathbf{S}^V is used for voltage scattering parameters and \mathbf{S}^I for current scattering parameters, where $\mathbf{V}^- = \mathbf{S}^V \mathbf{V}^+$ and $\mathbf{I}^- = \mathbf{S}^I \mathbf{I}^+$.

The following conversion relationships can also be derived:

$$\mathbf{S}^I = \Re\{\mathbf{Z}_0\}^{-\frac{1}{2}} {}^G \mathbf{S} \Re\{\mathbf{Z}_0\}^{\frac{1}{2}} \quad (2.120)$$

$$\mathbf{S}^V = \mathbf{Z}_0 \Re\{\mathbf{Z}_0\}^{-\frac{1}{2}} {}^G \mathbf{S} \Re\{\mathbf{Z}_0\}^{\frac{1}{2}} \{\mathbf{Z}_0^*\}^{-1}, \quad (2.121)$$

where $\Re\{\mathbf{Z}_0\}^{\frac{1}{2}} = \text{diag}\{\sqrt{\Re\{Z_{01}\}}, \sqrt{\Re\{Z_{02}\}}, \dots, \sqrt{\Re\{Z_{0n}\}}\}$.

Recall that ${}^G \mathbf{S}$ is in terms of \mathbf{a} and \mathbf{b} , \mathbf{S}^I is in terms of \mathbf{I}^- and \mathbf{I}^+ , and \mathbf{S}^V is in terms of \mathbf{V}^- and \mathbf{V}^+ . When port impedances and reference resistances are real, Equations (2.120) and (2.121) assume the simpler forms

$$\mathbf{S}^I = -\mathbf{R}_0^{-\frac{1}{2}} {}^G \mathbf{S} \mathbf{R}_0^{\frac{1}{2}} = -{}^G \mathbf{S}, \quad (2.122)$$

$$\mathbf{S}^V = \mathbf{R}_0 \mathbf{R}_0^{-\frac{1}{2}} {}^G \mathbf{S} \mathbf{R}_0^{\frac{1}{2}} \mathbf{R}_0^{*-1} = \mathbf{R}_0 (\mathbf{R}_0^*)^{-1} {}^G \mathbf{S} = {}^G \mathbf{S}, \quad (2.123)$$

where $\mathbf{R}_0^{\frac{1}{2}} = \text{diag}\{\sqrt{R_{01}}, \sqrt{R_{02}}, \dots, \sqrt{R_{0n}}\}$, with R_{0n} being the reference resistance at the n th port. In addition, if the reference resistances at each port are the same, all of the various scattering parameter definitions become

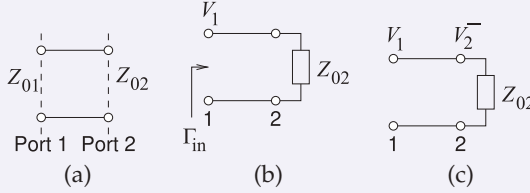
equivalent (i.e., $\mathbf{S}^V = -\mathbf{S}^I = {}^G\mathbf{S} = \mathbf{S}$), where \mathbf{S} is the normalized S parameter matrix, also called the normalized S parameter matrix.

The reciprocity condition for generalized S parameters is ${}^G S_{12} = {}^G S_{21} Z_{01}/Z_{02}$.

EXAMPLE 2.4

Generalized Scattering Parameters of a Through Connection

Develop the generalized scattering parameters of a through connection with a reference impedance Z_{01} at Port 1 and a reference impedance Z_{02} at Port 2.



Solution:

The through connection is shown in (a) and in (b) is the configuration to determine S_{11} as $V_2^+ = 0 = a_2$ since Port 2 is terminated in Z_{02} . Then

$${}^G S_{11} = \Gamma_{in} = \frac{Z_{02} - Z_{01}}{Z_{02} + Z_{01}} \quad \text{and similarly} \quad {}^G S_{22} = \frac{Z_{01} - Z_{02}}{Z_{02} + Z_{01}} = -{}^G S_{11} \quad (2.124)$$

Figure (b) is used to determine S_{21} as here $V_2^+ = 0 = a_2$

$$V_2^- = b_2 \sqrt{\Re\{Z_{02}\}} = V_1 = V_1^+ + V_1^- = V_1^+ (1 + S_{11}) = a_1 \sqrt{\Re\{Z_{01}\}}. \quad (2.125)$$

Thus,

$${}^G S_{21} = \frac{b_2}{a_1} \Big|_{a_2=0} = \frac{\sqrt{\Re\{Z_{01}\}}}{\sqrt{\Re\{Z_{02}\}}} (1 + {}^G S_{11}) \quad \text{and also} \quad {}^G S_{12} = \frac{\sqrt{\Re\{Z_{02}\}}}{\sqrt{\Re\{Z_{01}\}}} (1 + {}^G S_{22}). \quad (2.126)$$

The generalized scattering parameter matrix of the through is

$${}^G \mathbf{S} = \frac{1}{Z_{01} + Z_{02}} \begin{bmatrix} Z_{02} - Z_{01} & 2Z_{01} \sqrt{\Re\{Z_{02}\}/\Re\{Z_{01}\}} \\ 2Z_{02} \sqrt{\Re\{Z_{01}\}/\Re\{Z_{02}\}} & Z_{01} - Z_{02} \end{bmatrix} \quad (2.127)$$

$$\text{and for real } Z_{01} \text{ and } Z_{02} \quad {}^G \mathbf{S} = \frac{1}{Z_{01} + Z_{02}} \begin{bmatrix} Z_{02} - Z_{01} & 2\sqrt{Z_{01}Z_{02}} \\ 2\sqrt{Z_{01}Z_{02}} & Z_{01} - Z_{02} \end{bmatrix} \quad (2.128)$$

For normalized S parameters the reference impedances at the ports are the same, i.e. $Z_{01} = Z_0 = Z_{02}$, and the normalized S parameters of the through are (as expected)

$$\mathbf{S} = {}^N \mathbf{S} = \begin{bmatrix} 0 & 1 \\ 1 & 0 \end{bmatrix}. \quad (2.129)$$

2.4.3 Scattering Parameters in Terms of a and b waves

Previously S parameters were defined in terms of forward- and backward-traveling voltage waves, see Section 2.3.3 and Equation (2.71). That definition is adequate if only one reference impedance is used throughout. A more general form of S parameters uses the a and b root power waves. This is still valid if only one reference impedance is used but they can also be used when the ports have different reference impedances. This more general definition for a two-port network, with respect to Figure 2-18, is

$$\begin{bmatrix} b_1 \\ b_2 \end{bmatrix} = \begin{bmatrix} S_{11} & S_{12} \\ S_{21} & S_{22} \end{bmatrix} \begin{bmatrix} a_1 \\ a_2 \end{bmatrix}. \quad (2.130)$$

Even if the reference impedances at ports 1 and 2 are the different. If the reference impedance are the same and real, the usual case, the scattering

parameters are identical when used to relate traveling voltage waves as in the following:

$$\begin{bmatrix} V_1^- \\ V_2^- \end{bmatrix} = \begin{bmatrix} S_{11} & S_{12} \\ S_{21} & S_{22} \end{bmatrix} \begin{bmatrix} V_1^+ \\ V_2^+ \end{bmatrix}. \quad (2.131)$$

2.4.4 Normalized and Generalized S Parameters

S parameters measured with respect to a common reference resistance are referred to as normalized S parameters. In almost all cases, measured S parameters are normalized to 50Ω , as 50Ω cables and components are used in measurement systems. In other words, $Z_{01} = Z_{02} = \dots = Z_{0N} = R_0 (= 50 \Omega)$. Generalized S parameters can be used to simplify the design process of devices such as amplifiers. For example, it is often convenient to use the input and output impedances of an amplifier as the normalization impedances. Also, it is often desirable to be able to convert between measured S parameters (normalized to 50Ω) and generalized S parameters. Let ${}^N\mathbf{S}$ be the measured (normalized) S parameter matrix. (So ${}^N\mathbf{S}$ is the conventional S parameter matrix.) The development is tedious, but it can be shown that the generalized S parameters are

$${}^G\mathbf{S} = (\mathbf{D}^*)^{-1}({}^N\mathbf{S} - \mathbf{\Gamma}^*)(\mathbf{U} - \mathbf{\Gamma} {}^N\mathbf{S})^{-1}\mathbf{D}, \quad (2.132)$$

where \mathbf{U} is the unit matrix ($\mathbf{U} = \text{diag}(1, 1, \dots, 1)$), R_0 is the reference impedance of the normalized S parameters, ${}^N\mathbf{S}$, and \mathbf{D} is a diagonal matrix with elements

$$D_{ii} = |1 - \Gamma_i^*|^{-1}(1 - \Gamma_i)\sqrt{1 - |\Gamma_i|^2} \quad (2.133)$$

$$\Gamma_i = (Z_{0i} - R_0)(Z_{0i} + R_0)^{-1} \quad i = 1, 2, \dots, N, \quad (2.134)$$

and $\mathbf{\Gamma}$ is a diagonal matrix with elements Γ_i . Z_{0i} is the system impedance at Port i to which the generalized S parameters are to be referred.

2.4.5 Change of Reference Impedance

The result in the section above can be used to change scattering parameters referenced to a real impedance R_1 (i.e., ${}^{R1}\mathbf{S}$) to scattering parameters referenced to R_2 (i.e., ${}^{R2}\mathbf{S}$). Note that ${}^{R1}\mathbf{S}$ and ${}^{R2}\mathbf{S}$ are the conventional or normalized S parameters. The elements in Equations (2.133) and (2.134) become

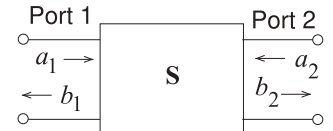
$$D_{ii} = D = |1 - \Gamma_{R2}|^{-1}(1 - \Gamma_{R2})\sqrt{1 - |\Gamma_{R2}|^2} = \sqrt{1 - |\Gamma_{R2}|^2} \quad (2.135)$$

$$\Gamma_{R2} = (R_2 - R_1)(R_2 + R_1)^{-1}, \quad (2.136)$$

and $|\Gamma_{R2}| < 1$. So Equation (2.132) becomes

$${}^{R2}\mathbf{S} = \mathbf{D}^{-1}({}^{R1}\mathbf{S} - \mathbf{\Gamma})(\mathbf{U} - \mathbf{\Gamma} {}^{R1}\mathbf{S})^{-1}\mathbf{D} = ({}^{R1}\mathbf{S} - \mathbf{\Gamma})(\mathbf{U} - \mathbf{\Gamma} {}^{R1}\mathbf{S})^{-1} \quad (2.137)$$

Figure 2-18: Definition of S parameters in terms of a and b root power waves. $a_1 = V_1^+/\Re\{\mathbf{Z}_{01}\}$, $b_1 = V_1^-/\Re\{\mathbf{Z}_{01}\}$, $a_2 = V_2^+/\Re\{\mathbf{Z}_{02}\}$, $b_2 = V_2^-/\Re\{\mathbf{Z}_{02}\}$. Incident power at Port 1 (2) is $|a_1|^2$ ($|a_2|^2$). Power leaving Port 1 (2) is $|b_1|^2$ ($|b_2|^2$)



since \mathbf{D} is a diagonal matrix with all diagonal entries the same. So for a two-port

$$\begin{aligned} {}^{R2}\mathbf{S} &= \begin{bmatrix} {}^{R2}S_{11} & {}^{R2}S_{12} \\ {}^{R2}S_{21} & {}^{R2}S_{22} \end{bmatrix} \\ &= \begin{bmatrix} {}^{R1}S_{11} - \Gamma_{R2} & {}^{R1}S_{12} \\ {}^{R1}S_{21} & {}^{R1}S_{22} - \Gamma_{R2} \end{bmatrix} \begin{bmatrix} 1 - \Gamma_{R2} {}^{R1}S_{11} & -\Gamma_{R2} {}^{R1}S_{12} \\ -\Gamma_{R2} {}^{R1}S_{21} & 1 - \Gamma_{R2} {}^{R1}S_{22} \end{bmatrix}^{-1}. \end{aligned} \quad (2.138)$$

EXAMPLE 2.5 Change of Reference Impedance

An attenuator has the $50\ \Omega$ S parameters:

$${}^{50}\mathbf{S} = \begin{bmatrix} 0 & 0.3162 \\ 0.3162 & 0 \end{bmatrix}. \quad (2.139)$$

What are the S parameters referenced to $75\ \Omega$?

Solution:

The conversion uses Equation (2.138) with $R_1 = 50\ \Omega$ and $R_2 = 75\ \Omega$.

So $\Gamma_{75} = (75 - 50)/(75 + 50) = 0.2$. Thus the S parameters referenced to $75\ \Omega$ are

$$\begin{aligned} {}^{75}\mathbf{S} &= \begin{bmatrix} {}^{50}S_{11} - \Gamma_{75} & {}^{50}S_{12} \\ {}^{50}S_{21} & {}^{50}S_{22} - \Gamma_{75} \end{bmatrix} \begin{bmatrix} 1 - \Gamma_{75} {}^{50}S_{11} & -\Gamma_{75} {}^{50}S_{12} \\ -\Gamma_{75} {}^{50}S_{21} & 1 - \Gamma_{75} {}^{50}S_{22} \end{bmatrix} \\ &= \begin{bmatrix} -0.2 & 0.3162 \\ 0.3162 & -0.2 \end{bmatrix} \begin{bmatrix} 1 & -0.2 \cdot 0.3162 \\ -0.2 \cdot 0.3162 & 1 \end{bmatrix} \\ &= \begin{bmatrix} -0.2 & 0.3162 \\ 0.3162 & -0.2 \end{bmatrix} \begin{bmatrix} 1 & 0.06324 \\ 0.06324 & 1 \end{bmatrix} = \begin{bmatrix} -0.18 & 0.3036 \\ 0.3036 & -0.18 \end{bmatrix}. \end{aligned} \quad (2.140)$$

2.4.6 Passivity in Terms of Scattering Parameters

Consider an N -port characterized by its generalized scattering matrix \mathbf{S} . The time-averaged power dissipated in the N -port is

$$P = \frac{1}{2} \sum_{i=1}^N (|\mathbf{a}_i|^2 - |\mathbf{b}_i|^2) = \frac{1}{2} (\mathbf{a}^{*T} \mathbf{a} - \mathbf{b}^{*T} \mathbf{b}), \quad (2.141)$$

and so
$$P = \frac{1}{2} \mathbf{a}^{*T} [\mathbf{U} - (\mathbf{S}^*)^T \mathbf{S}] \mathbf{a}. \quad (2.142)$$

In the above, the conjugate, \mathbf{a}^* , of the matrix \mathbf{a} is obtained from \mathbf{a} by taking the complex conjugate of each element. For a passive N -port,

$$\mathbf{U} - (\mathbf{S}^*)^T \mathbf{S} \geq 0 \quad \text{for all real } \omega, \quad (2.143)$$

This can also be written in summation form as

$$\sum_{k=1}^N S_{kj} S_{kj}^* = P_j. \quad (2.144)$$

$P_j = 1$ for all j if the network is lossless. For a network to be passive $P_j \leq 1$ for all j . By examining the S parameters it can be determined quickly

whether a network is lossless, lossy, or perhaps has gain.

$$\text{For a lossless } N\text{-port, } \mathbf{U} - \mathbf{S}^{*\text{T}}\mathbf{S} = 0. \quad (2.145)$$

Rearranging, taking the transpose of both sides and noting that $\mathbf{U}^{\text{T}} = \mathbf{U}$

$$\mathbf{S}^*\mathbf{S}^{\text{T}} = \mathbf{U}. \quad (2.146)$$

This is known as the **unitary condition**. That is, for a lossless N -port

$$\mathbf{S}^* = (\mathbf{S}^{\text{T}})^{-1}. \quad (2.147)$$

The important result here is that for a lossless network (these are the unitary conditions)

$$\sum_{k=1}^N S_{kj} S_{kj}^* = 1 \quad (2.148)$$

$$\sum_{k=1}^N S_{ki} S_{kj}^* = 0 \quad \text{for } i \text{ not equal to } j. \quad (2.149)$$

2.4.7 Impedance Matrix Representation

In this section N -port S parameters are related to N -port z parameters. The basic relationship of voltage and current at any port using impedances is

$$\begin{bmatrix} V_1 \\ V_2 \\ \vdots \\ V_N \end{bmatrix} = \begin{bmatrix} z_{11} & z_{12} & \dots & z_{1N} \\ z_{21} & z_{22} & \dots & z_{2N} \\ \vdots & & \ddots & \\ z_{N1} & z_{N2} & \dots & z_{NN} \end{bmatrix} \begin{bmatrix} I_1 \\ I_2 \\ \vdots \\ I_N \end{bmatrix}, \quad (2.150)$$

$$\text{or in compact form as } \mathbf{V} = \mathbf{Z}\mathbf{I} \quad (2.151)$$

\mathbf{Z} is reciprocal if $z_{ij} = z_{ji}$. The z parameters defined here are more formally called port-based z parameters, as the voltage and current variables are port quantities.

Relating z and S parameters begins by relating the total voltage and current at the n th terminal plane to the traveling voltage and current waves. From Figure 2-16,

$$V_n = V_n^+ + V_n^-, \quad \text{and} \quad I_n = I_n^+ - I_n^-, \quad (2.152)$$

and in vector form

$$\begin{aligned} \mathbf{V} &= \mathbf{V}^+ + \mathbf{V}^- & \mathbf{I} &= \mathbf{I}^+ + \mathbf{I}^- \\ \mathbf{V}^+ &= \mathbf{Z}_0^* \mathbf{I}^+ & \mathbf{V}^- &= -\mathbf{Z}_0 \mathbf{I}^-, \end{aligned} \quad (2.153)$$

where $\mathbf{Z}_0 = \text{diag}(Z_{01}, Z_{02}, \dots, Z_{0N})$ (and z_{0n} can be complex). After some algebraic manipulation, the following relationships are obtained:

$$\mathbf{S}^V = [\mathbf{U} + \mathbf{Z}\mathbf{Z}_0^{-1}]^{-1}[\mathbf{Z}(\mathbf{Z}_0^*)^{-1} - \mathbf{U}] \quad (2.154)$$

$$\mathbf{Z} = [\mathbf{U} + \mathbf{S}^V][\mathbf{Z}_0^{*-1} - \mathbf{Z}_0^{-1}(\mathbf{S}^V)]^{-1}. \quad (2.155)$$

Note that \mathbf{S}^V is the voltage scattering parameter matrix. These are related to the generalized scattering parameter matrix by Equation (2.123). For normalized S parameters the same real reference impedance is used at all ports ($Z_{0n} = Z_0, n = 1, \dots, N$), then Equations (2.154) and (2.155) become

$$\mathbf{S} = [\mathbf{Z} + Z_0 \mathbf{U}]^{-1} [\mathbf{Z} - Z_0 \mathbf{U}] \quad \text{and} \quad \mathbf{Z} = Z_0 [\mathbf{U} + \mathbf{S}] [\mathbf{U} - \mathbf{S}]^{-1}. \quad (2.156)$$

2.4.8 Admittance Matrix Representation

In this section, N -port S parameters are related to N -port y parameters. The currents and voltages are related as

$$\begin{bmatrix} I_1 \\ I_2 \\ \vdots \\ I_N \end{bmatrix} = \begin{bmatrix} y_{11} & y_{12} & \cdots & y_{1N} \\ y_{21} & y_{22} & \cdots & y_{2N} \\ \vdots & & \ddots & \\ y_{N1} & y_{N2} & \cdots & y_{NN} \end{bmatrix} \begin{bmatrix} V_1 \\ V_2 \\ \vdots \\ V_N \end{bmatrix}, \quad (2.157)$$

or in compact form the port-based y parameters are

$$\mathbf{I} = \mathbf{YV}. \quad (2.158)$$

Using a similar approach to that in the previous subsection, the relationship between S and y parameters can be developed. The development will be done slightly differently and this development is applicable to generalized scattering parameters. First, consider the relationship of the total port voltage $\mathbf{V} = [V_1 \dots V_n \dots V_N]^T$ and current $\mathbf{I} = [I_1 \dots I_n \dots I_N]^T$ to forward- and backward-traveling voltage and current waves:

$$\mathbf{V} = \mathbf{V}^+ + \mathbf{V}^- \quad \text{and} \quad \mathbf{I} = \mathbf{I}^+ + \mathbf{I}^-, \quad (2.159)$$

where $\mathbf{I}^+ = \mathbf{Y}_0 \mathbf{V}^+ = \mathbf{Y}_0^{1/2} \mathbf{a}$ and $\mathbf{I}^- = -\mathbf{Y}_0 \mathbf{V}^- = -\mathbf{Y}_0^{1/2} \mathbf{b}$. (Each element of \mathbf{Y}_0 , $Y_{0n} = 1/Z_{0n}$ and can be complex.) Using traveling waves, Equation (2.158) becomes

$$\mathbf{I}^+ + \mathbf{I}^- = \mathbf{Y}(\mathbf{V}^+ + \mathbf{V}^-) \quad (2.160)$$

$$\mathbf{Y}_0(\mathbf{V}^+ - \mathbf{V}^-) = \mathbf{Y}(\mathbf{V}^+ + \mathbf{V}^-) \quad (2.161)$$

$$\mathbf{Y}_0(1 - \mathbf{Y}_0^{-1/2} \mathbf{S} \mathbf{Y}_0^{1/2}) \mathbf{V}^+ = \mathbf{Y}(1 + \mathbf{Y}_0^{-1/2} \mathbf{S} \mathbf{Y}_0^{1/2}) \mathbf{V}^+, \quad (2.162)$$

and so the port y parameters in terms of the generalized scattering parameters are

$$\mathbf{Y} = \mathbf{Y}_0(1 - \mathbf{Y}_0^{-1/2} \mathbf{S} \mathbf{Y}_0^{1/2})(1 + \mathbf{Y}_0^{-1/2} \mathbf{S} \mathbf{Y}_0^{1/2})^{-1}. \quad (2.163)$$

Alternatively, Equation (2.161) can be rearranged as

$$(\mathbf{Y}_0 + \mathbf{Y}) \mathbf{V}^- = (\mathbf{Y}_0 - \mathbf{Y}) \mathbf{V}^+ \quad (2.164)$$

$$\mathbf{V}^- = (\mathbf{Y}_0 + \mathbf{Y})^{-1} (\mathbf{Y}_0 - \mathbf{Y}) \mathbf{V}^+ \quad (2.165)$$

$$\mathbf{Y}_0^{-1/2} \mathbf{b} = (\mathbf{Y}_0 + \mathbf{Y})^{-1} (\mathbf{Y}_0 - \mathbf{Y}) \mathbf{Y}_0^{-1/2} \mathbf{a}. \quad (2.166)$$

Comparing this to the definition of generalized S parameters in Equation (2.119) leads to

$${}^G \mathbf{S} = \mathbf{Y}_0^{1/2} (\mathbf{Y}_0 + \mathbf{Y})^{-1} (\mathbf{Y}_0 - \mathbf{Y}) \mathbf{Y}_0^{-1/2}. \quad (2.167)$$

Figure 2-19: An amplifier with an active device and input (M_1) and output (M_2) matching networks. The biasing arrangement is not shown, but usually this is done with the appropriate choice of matching network topology.

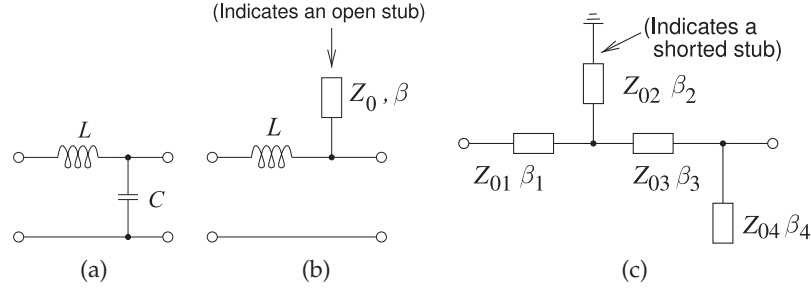
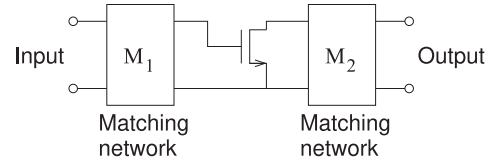


Figure 2-20: Three forms of matching networks with increasing use of transmission line sections.

For the usual case where all of the reference transmission lines have the same characteristic impedance $Z_0 = 1/Y_0$ (note $S = {}^N S$),

$$\mathbf{Y} = Y_0(\mathbf{U} - \mathbf{S})(\mathbf{U} + \mathbf{S})^{-1} \quad \text{and} \quad \mathbf{S} = (\mathbf{Y}_0 + \mathbf{Y})^{-1}(\mathbf{Y}_0 - \mathbf{Y}). \quad (2.168)$$

2.5 Scattering Parameter Matrices of Common Two-Ports

RF and microwave circuits can generally be represented as interconnected two-ports, as most RF and microwave circuit designs involve cascaded functional blocks such as amplifiers, matching networks, filters, etc.⁴ (see Figure 2-19). Thus there is great interest in various manipulations that can be performed on two-ports as well as the network parameters of common two-port circuit topologies. As an example, consider the matching networks in Figure 2-19. These are used to achieve maximum power transfer in an amplifier by acting as impedance transformers. Matching networks assume a variety of forms, as shown in Figure 2-20, and all can be viewed as two-port networks and a combination of simpler components. In this section, strategies are presented for developing the S parameters of two-ports.

Transmission Line

The traveling waves on a transmission line (Figure 2-21(a)) have a phase that depends on the electrical length, θ , of the line. The transmission line has a characteristic impedance, Z_0 , and length, ℓ , which in general is different from

⁴ This arrangement tends to maximize bandwidth, minimize losses, and maximize efficiency. Lower-frequency analog design utilizes more complex arrangements; for example, feedback high in the circuit hierarchy improves the reliability and robustness of design but comes at the cost of reduced bandwidth and lower power efficiency.

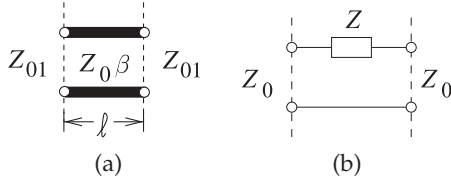


Figure 2-21: Two-ports: (a) section of transmission line; and (b) series element in the form of a two-port.

the system reference impedance, here Z_{01} . Thus

$$S_{11} = S_{22} = \frac{\Gamma(1 - e^{-2j\theta})}{1 - \Gamma^2 e^{-2j\theta}} \quad \text{and} \quad S_{21} = S_{12} = \frac{(1 - \Gamma^2)e^{-j\theta}}{1 - \Gamma^2 e^{-2j\theta}}, \quad (2.169)$$

where $\theta = \beta\ell$ and

$$\Gamma = \frac{Z_0 - Z_{01}}{Z_0 + Z_{01}}. \quad (2.170)$$

If the reference impedance is the same as the characteristic impedance of the line, i.e. $Z_{01} = Z_0$ and $\Gamma = 0$, the scattering parameters of the line are

$$\mathbf{S} = \begin{bmatrix} 0 & e^{-j\theta} \\ e^{-j\theta} & 0 \end{bmatrix}. \quad (2.171)$$

Shunt Element

The S parameters of the shunt element (Figure 2-15) were developed in Section 2.3.5. In a slightly different form these are

$$S_{11} = S_{22} = -\frac{\bar{y}}{(\bar{y} + 2)} \quad \text{and} \quad S_{12} = S_{21} = \frac{2}{(\bar{y} + 2)}, \quad (2.172)$$

where $\bar{y} = Y/Y_0$ is the admittance normalized to the system reference admittance ($Y_0 = 1/Z_0$).

Series Element

The S parameters of the series element (Figure 2-21(b)) are

$$S_{11} = S_{22} = \frac{\bar{z}}{(\bar{z} + 2)} \quad \text{and} \quad S_{12} = S_{21} = \frac{2}{(\bar{z} + 2)}, \quad (2.173)$$

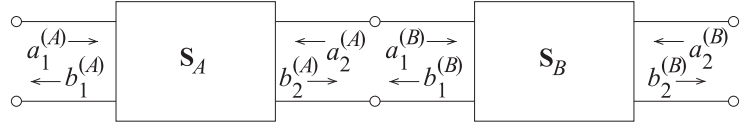
where $\bar{z} = Z/Z_0$ is the normalized impedance.

2.6 T or Chain Scattering Parameters of Cascaded Two-Port Networks

The T parameters, also known as chain scattering parameters, are a cascable form of scattering parameters. They are similar to regular S parameters and can be expressed in terms of the a and b root power waves or traveling voltage waves. Two two-port networks, A and B, in cascade are shown in Figure 2-22. Here (A) and (B) are used as superscripts to distinguish the parameters of each two-port network, but the subscripts A and B are used for matrix quantities. Since

$$a_2^{(A)} = b_1^{(B)} \quad \text{and} \quad b_2^{(A)} = a_1^{(B)}, \quad (2.174)$$

Figure 2-22: Two cascaded two-ports.



it is convenient to put the a and b parameters in cascadable form, leading to the following two-port chain matrix or T matrix representation (with respect to Figure 2-18):

$$\begin{bmatrix} a_1 \\ b_1 \end{bmatrix} = \begin{bmatrix} T_{11} & T_{12} \\ T_{21} & T_{22} \end{bmatrix} \begin{bmatrix} b_2 \\ a_2 \end{bmatrix}, \quad (2.175)$$

where the T matrix or chain scattering matrix is

$$\mathbf{T} = \begin{bmatrix} T_{11} & T_{12} \\ T_{21} & T_{22} \end{bmatrix}. \quad (2.176)$$

\mathbf{T} is very similar to the scattering transfer matrix ($^S\mathbf{T}$) of Section 2.3.7. The only difference is the ordering of the a and b components. You will come across both forms, so be careful that you understand which is being used. Both forms are used for the same function—cascading two-port networks. The relationships between \mathbf{T} and \mathbf{S} are given by

$$\mathbf{T} = \begin{bmatrix} S_{21}^{-1} & -S_{21}^{-1}S_{22} \\ S_{21}^{-1}S_{11} & S_{12} - S_{11}S_{21}^{-1}S_{22} \end{bmatrix} \quad \mathbf{S} = \begin{bmatrix} T_{21}T_{11}^{-1} & T_{22} - T_{21}T_{11}^{-1}T_{12} \\ T_{11}^{-1} & -T_{11}^{-1}T_{12} \end{bmatrix}. \quad (2.177) \quad (2.178)$$

For a two-port network, using Equations (2.174) and (2.175),

$$\begin{bmatrix} a_1^{(A)} \\ b_1^{(A)} \end{bmatrix} = \mathbf{T}_A \begin{bmatrix} b_2^{(A)} \\ a_2^{(A)} \end{bmatrix} \quad \text{and} \quad \begin{bmatrix} a_1^{(B)} \\ b_1^{(B)} \end{bmatrix} = \mathbf{T}_B \begin{bmatrix} b_2^{(B)} \\ a_2^{(B)} \end{bmatrix}, \quad (2.179)$$

thus

$$\begin{bmatrix} a_1^{(A)} \\ b_1^{(A)} \end{bmatrix} = \mathbf{T}_A \mathbf{T}_B \begin{bmatrix} b_2^{(B)} \\ a_2^{(B)} \end{bmatrix}. \quad (2.180)$$

For n cascaded two-port networks, Equation (2.180) generalizes to

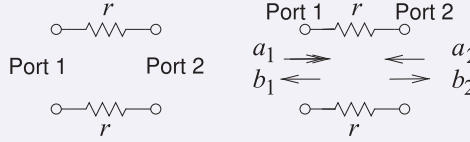
$$\begin{bmatrix} a_1^{(1)} \\ b_1^{(1)} \end{bmatrix} = \mathbf{T}_1 \mathbf{T}_2 \dots \mathbf{T}_n \begin{bmatrix} b_2^{(n)} \\ a_2^{(n)} \end{bmatrix}, \quad (2.181)$$

and so the \mathbf{T} matrix of the cascaded network is the matrix product of the \mathbf{T} matrices of the individual two-ports.

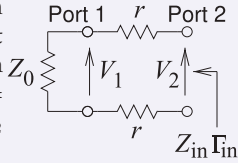
Previously, in Section 2.3.7, the scattering transfer parameters were introduced. Both the chain scattering parameters and scattering transfer parameters are referred to as T parameters. Be careful to denote which form is being used.

EXAMPLE 2.6**Development of chain scattering parameters**

Derive the T parameters of the two-port network to the right using a reference impedance Z_0 .

**Solution:**Derivation of T_{11}

Terminate Port 2 in a matched load so that $a_2 = 0$. Then Equation (2.175) becomes $a_1 = T_{11}b_2$ and $b_1 = T_{21}b_2$ so



$$\Gamma_{in} = b_1/a_1 = T_{21}/T_{11}. \quad (2.182)$$

Now $Z_{in} = 2r + Z_0$, therefore

$$\begin{aligned} \Gamma_{in} &= \frac{Z_{in} - Z_0}{Z_{in} + Z_0} \\ &= \frac{2r + Z_0 - Z_0}{2r + Z_0 + Z_0} = \frac{r}{r + Z_0}. \end{aligned}$$

Thus

$$\Gamma_{in} = \frac{T_{21}}{T_{11}} = \frac{r}{r + Z_0}. \quad (2.183)$$

The next stage is relating b_2 to a_1 and since both ports have the same reference impedance a and b can be replaced by traveling voltages

$$\begin{aligned} V_1 &= (V_1^+ + V_1^-) = V_1^+ (1 + \Gamma_{in}) \\ &= V_1^+ \frac{2r + Z_0}{r + Z_0}. \end{aligned}$$

Using voltage division (and since $V_2^+ = a_2 = 0$)

$$\begin{aligned} V_2 &= V_2^- = \frac{Z_0}{2r + Z_0} V_1 \\ &= V_1^+ \frac{Z_0}{2r + Z_0} \frac{2r + Z_0}{r + Z_0} \\ V_2^- &= V_1^+ \frac{Z_0}{r + Z_0} \\ T_{11} &= \frac{V_1^+}{V_2^-} = \frac{a_1}{b_2} = \frac{r + Z_0}{Z_0}. \end{aligned} \quad (2.184)$$

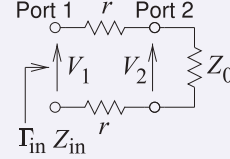
Derivation of T_{21}

Combining Equations (2.183) and (2.184)

$$T_{21} = \Gamma_{in} T_{11} = \frac{r}{r + Z_0} \frac{r + Z_0}{Z_0} = \frac{r}{Z_0} \quad (2.185)$$

Derivation of T_{22}

Terminate Port 2 in a matched load so that $a_1 = 0$. Then Equation (2.175) becomes



$$\begin{aligned} 0 &= T_{11}b_2 + T_{12}a_2 \\ \Gamma_{in} &= \frac{b_2}{a_2} = \frac{-T_{12}}{T_{11}} \rightarrow T_{12} = -T_{11}\Gamma_{in} \quad (2.186) \\ b_1 &= T_{21}b_2 + T_{22}a_2 \\ \frac{b_1}{a_2} &= T_{21} \frac{b_2}{a_2} + T_{22}. \end{aligned} \quad (2.187)$$

Now $Z_{in} = 2r + Z_0$ and so

$$\Gamma_{in} = \frac{2r + Z_0 - Z_0}{2r + Z_0 + Z_0} = \frac{r}{r + Z_0}. \quad (2.188)$$

Using voltage division

$$\begin{aligned} V_1 &= V_1^- = \frac{Z_0}{2r + Z_0} V_2 = \frac{Z_0}{2r + Z_0} V_2^+ (1 + \Gamma_{in}) \\ &= V_2^+ \frac{Z_0}{2r + Z_0} \frac{2r + Z_0}{r + Z_0} = V_2^+ \frac{Z_0}{r + Z_0} \\ \frac{V_1^-}{V_2^+} &= \frac{b_1}{a_2} = \frac{Z_0}{r + Z_0}. \end{aligned} \quad (2.189)$$

Substituting Equations (2.188) and (2.189) in Equation (2.187) and rearranging

$$T_{22} = \frac{Z_0}{r + Z_0} - T_{21} \frac{r}{r + Z_0}.$$

Combining this with Equation (2.185)

$$T_{22} = \frac{Z_0}{r + Z_0} - \frac{r}{Z_0} \frac{r}{r + Z_0} = \frac{Z_0^2 - r^2}{Z_0(r + Z_0)}. \quad (2.190)$$

Derivation of T_{12}

Combining Equations (2.184, 2.186 and 2.188)

$$T_{12} = -\frac{r + Z_0}{Z_0} \frac{r}{r + Z_0} = -\frac{r}{Z_0}. \quad (2.191)$$

Summary: The chain scattering matrix (T) parameters are given in Equations (2.184), (2.185), (2.190), and (2.191).

EXAMPLE 2.7**Cascading chain scattering parameters**

Develop the chain scattering parameters of the network to the right. Use a reference impedance $Z_{\text{REF}} = Z_0$, the characteristic impedance of the lines.

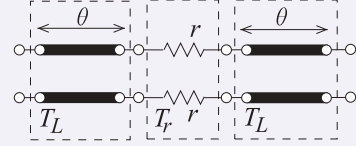
Solution:

The network comprises a transmission line of electrical length θ in cascade with a resistive network and another line of the same electrical length. From Equation (2.171) the scattering parameters of the transmission line are

$$\mathbf{S}_L = \begin{bmatrix} 0 & e^{-j\theta} \\ e^{-j\theta} & 0 \end{bmatrix}. \quad (2.192)$$

From Equation (2.177) the chain scattering matrix of the line is

$$\mathbf{T}_L = \begin{bmatrix} e^{j\theta} & 0 \\ 0 & e^{-j\theta} \end{bmatrix}. \quad (2.193)$$



From Example 2.6 the chain scattering matrix of the resistive network is

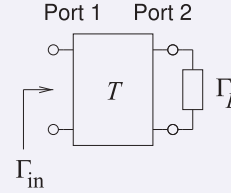
$$\mathbf{T}_r = \frac{1}{Z_0} \begin{bmatrix} gr + Z_0 & -r \\ r & (Z_0^2 - r^2)/(r + Z_0) \end{bmatrix}. \quad (2.194)$$

Yielding the chain scattering matrix of the cascade;

$$\mathbf{T}_{LrL} = \mathbf{T}_L \mathbf{T}_r \mathbf{T}_L = \frac{1}{Z_0} \begin{bmatrix} (r + Z_0)e^{2j\theta} & -r \\ r & (Z_0^2 - r^2)/(r + Z_0)e^{-2j\theta} \end{bmatrix}. \quad (2.195)$$

EXAMPLE 2.8**Input reflection coefficient of a terminated two-port.**

What is the input reflection coefficient in terms of chain scattering parameters of the terminated two-port to the right where the two-port is described by its chain scattering parameters.

**Solution:**

The chain scattering parameter relations are

$$\begin{bmatrix} a_1 \\ b_1 \end{bmatrix} = \begin{bmatrix} T_{11} & T_{12} \\ T_{21} & T_{22} \end{bmatrix} \begin{bmatrix} b_2 \\ a_2 \end{bmatrix}.$$

Expanding this matrix equation and using the substitution $a_2 = \Gamma_L b_2$

$$a_1 = T_{11}b_2 + T_{12}\Gamma_L b_2 \quad (2.196)$$

$$b_1 = T_{21}b_2 + T_{22}\Gamma_L b_2. \quad (2.197)$$

Multiplying Equation (2.196) by $(T_{21} + T_{22}\Gamma_L)$ and Equation (2.197) by $(T_{11} + T_{12}\Gamma_L)$ and then subtracting

$$(T_{21} + T_{22}\Gamma_L)a_1 = (T_{21} + T_{22}\Gamma_L)(T_{11}b_2 + T_{12}\Gamma_L b_2)$$

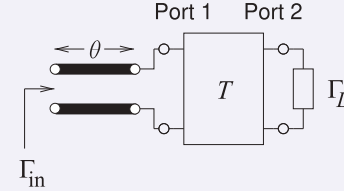
$$(T_{11} + T_{12}\Gamma_L)b_1 = (T_{11} + T_{12}\Gamma_L)(T_{21}b_2 + T_{22}\Gamma_L b_2)$$

$$(T_{21} + T_{22}\Gamma_L)a_1 = (T_{11} + T_{12}\Gamma_L)b_1.$$

Thus the input reflection coefficient is

$$\Gamma_{\text{in}} = \frac{b_1}{a_1} = \frac{T_{21} + T_{22}\Gamma_L}{T_{11} + T_{12}\Gamma_L}. \quad (2.198)$$

Now consider a transmission line of electrical length θ and characteristic impedance Z_0 (see the figure b) in cascade with the two-port.



The input reflection coefficient now is found by first determining the total chain scattering matrix of the cascade:

$$\begin{aligned} {}^T\mathbf{T} &= \mathbf{T}_L \mathbf{T} = \begin{bmatrix} e^{j\theta} & 0 \\ 0 & e^{-j\theta} \end{bmatrix} \begin{bmatrix} T_{11} & T_{12} \\ T_{21} & T_{22} \end{bmatrix} \\ &= \begin{bmatrix} T_{11}e^{j\theta} & T_{12}e^{j\theta} \\ T_{21}e^{-j\theta} & T_{22}e^{-j\theta} \end{bmatrix} \begin{bmatrix} {}^T T_{11} & {}^T T_{12} \\ {}^T T_{21} & {}^T T_{22} \end{bmatrix}. \end{aligned}$$

Thus the input reflection coefficient is now

$$\begin{aligned}\Gamma_{\text{in}} &= \frac{b_1}{a_1} = \frac{T_{21} + T_{22}\Gamma_L}{T_{11} + T_{12}\Gamma_L} \\ &= \frac{T_{21}e^{-j\theta} + T_{22}e^{-j\theta}\Gamma_L}{T_{11}e^{j\theta} + T_{12}e^{j\theta}\Gamma_L} \\ &= e^{-2j\theta} \left(\frac{T_{21} + T_{22}\Gamma_L}{T_{11} + T_{12}\Gamma_L} \right). \quad (2.199)\end{aligned}$$

If the load is now a short circuit $\Gamma_L = -1$ and the input reflection coefficient of the line and two-port cascade is

$$\Gamma_{\text{in}} = e^{-2j\theta} \left(\frac{T_{21} - T_{22}}{T_{11} - T_{12}} \right). \quad (2.200)$$

2.6.1 Terminated Two-Port Network

A two-port with Port 2 terminated in a load with reflection coefficient Γ_L is shown in Figure 2-23 and $a_2 = \Gamma_L b_2$. Substituting this in Equation (2.175) leads to

$$a_1 = (T_{11} + T_{12}\Gamma_L)b_2 \quad \text{and} \quad b_1 = (T_{21} + T_{22}\Gamma_L)b_2,$$

eliminating b_2 results in

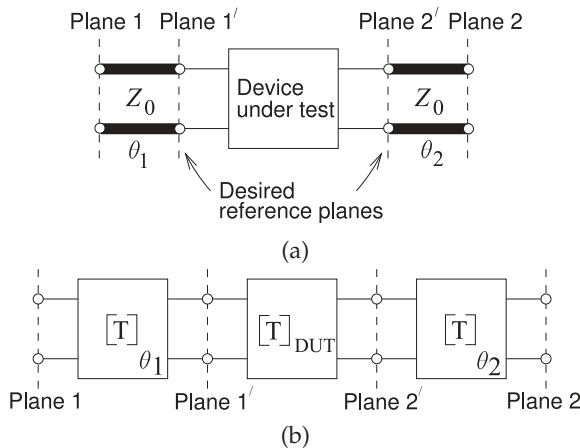
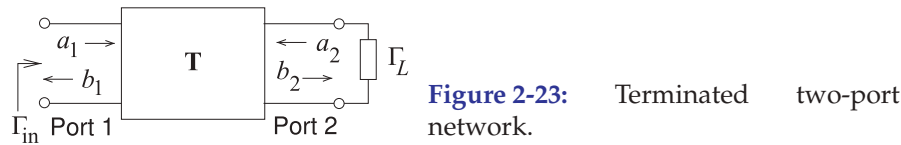
$$\Gamma_{\text{in}} = \frac{b_1}{a_1} = \frac{T_{21} + T_{22}\Gamma_L}{T_{11} + T_{12}\Gamma_L}. \quad (2.201)$$

2.7 Scattering Parameter Two-Port Relationships

2.7.1 Change in Reference Plane

It is often necessary during S parameter measurements of two-port devices to measure components at a position different from that actually desired. An example is shown in Figure 2-24(a). From direct measurement the S parameters are obtained, and thus the \mathbf{T} matrix at Planes 1 and 2. However, \mathbf{T}_{DUT} referenced to Planes 1' and 2' is required. Now,

$$\mathbf{T} = \mathbf{T}_{\theta_1} \mathbf{T}_{\text{DUT}} \mathbf{T}_{\theta_2}, \quad (2.202)$$



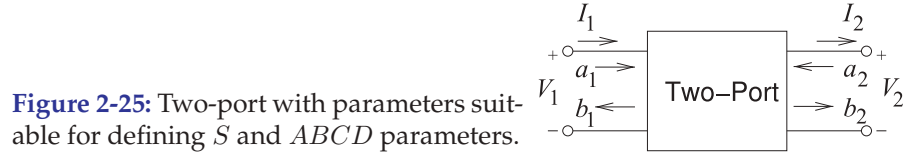


Figure 2-25: Two-port with parameters suitable for defining S and $ABCD$ parameters.

$$\text{and so} \quad \mathbf{T}_{\text{DUT}} = \mathbf{T}_{\theta_1}^{-1} \mathbf{T} \mathbf{T}_{\theta_2}^{-1}. \quad (2.203)$$

A section of line with electrical length θ and port impedances equal to its characteristic impedance has

$$\mathbf{S} = \begin{bmatrix} 0 & e^{-j\theta} \\ e^{-j\theta} & 0 \end{bmatrix} \quad (2.204) \quad \text{and} \quad \mathbf{T}_\theta = \begin{bmatrix} e^{j\theta} & 0 \\ 0 & e^{-j\theta} \end{bmatrix}. \quad (2.205)$$

Therefore Equation (2.203) becomes

$$\mathbf{T}_{\text{DUT}} = \begin{bmatrix} T_{11}e^{-j(\theta_1+\theta_2)} & T_{12}e^{-j(\theta_1-\theta_2)} \\ T_{21}e^{j(\theta_1-\theta_2)} & T_{22}e^{j(\theta_1+\theta_2)} \end{bmatrix}, \quad (2.206)$$

and then the desired S parameters of the DUT are obtained as

$$\mathbf{S}_{\text{DUT}} = \begin{bmatrix} S_{11}e^{j2\theta_1} & S_{12}e^{j(\theta_1+\theta_2)} \\ S_{21}e^{j(\theta_1+\theta_2)} & S_{22}e^{j2\theta_2} \end{bmatrix}. \quad (2.207)$$

2.7.2 Conversion Between S and $ABCD$ Parameters

Figure 2-25 can be used to relate the parameters of the two views of the network. If both ports have the same reference impedance Z_0 , then

$$\begin{bmatrix} V_1 \\ I_1 \end{bmatrix} = \begin{bmatrix} A & B \\ C & D \end{bmatrix} \begin{bmatrix} V_2 \\ I_2 \end{bmatrix} \quad \text{and} \quad \begin{bmatrix} b_1 \\ b_2 \end{bmatrix} = \begin{bmatrix} S_{11} & S_{12} \\ S_{21} & S_{22} \end{bmatrix} \begin{bmatrix} a_1 \\ a_2 \end{bmatrix}.$$

The S parameters are then expressed as

$$\begin{aligned} S_{11} &= \frac{A + B/Z_0 - CZ_0 - D}{\Delta} & S_{12} &= \frac{2(AD - BC)}{\Delta} \\ S_{21} &= \frac{2}{\Delta} & S_{22} &= \frac{-A + B/Z_0 - CZ_0 + D}{\Delta}, \end{aligned} \quad (2.208)$$

$$\text{where} \quad \Delta = A + B/Z_0 + CZ_0 + D. \quad (2.209)$$

The $ABCD$ parameters can be expressed in terms of the S parameters as

$$A = \frac{(1 + S_{11})(1 - S_{22}) + S_{12}S_{21}}{2S_{21}} \quad (2.210)$$

$$B = Z_0 \frac{(1 + S_{11})(1 + S_{22}) - S_{12}S_{21}}{2S_{21}} \quad (2.211)$$

$$C = \frac{1}{Z_0} \frac{(1 - S_{11})(1 - S_{22}) - S_{12}S_{21}}{2S_{21}} \quad (2.212)$$

$$D = \frac{(1 - S_{11})(1 + S_{22}) + S_{12}S_{21}}{2S_{21}}. \quad (2.213)$$

2.8 Return Loss, Substitution Loss, and Insertion Loss

2.8.1 Return Loss

Return loss, also known as **reflection loss**, is a measure of the fraction of power that is not delivered by a source to a load. If the power incident on a load is P_i and the power reflected by the load is P_r , then the return loss in decibels is [6, 7]

$$\text{RL}_{\text{dB}} = 10 \log \frac{P_i}{P_r}. \quad (2.214)$$

The better the load is matched to the source, the lower the reflected power and hence the higher the return loss. RL is a positive quantity if the reflected power is less than the incident power. If the load has a complex reflection coefficient ρ , then

$$\text{RL}_{\text{dB}} = 10 \log \left| \frac{1}{\rho^2} \right| = -20 \log |\rho|. \quad (2.215)$$

That is, the return loss is the negative of the input reflection coefficient expressed in decibels [8].

When generalized to a terminated two ports, the return loss is defined with respect to the input reflection coefficient of the terminated two port [9]. The two port in Figure 2-26 has the input reflection coefficient

$$\Gamma_{\text{in}} = S_{11} + \frac{\Gamma_L S_{12} S_{21}}{(1 - \Gamma_L S_{22})}, \quad (2.216)$$

where Γ_L is the reflection coefficient of the load. Thus the return loss of a terminated two-port is

$$\text{RL}_{\text{dB}} = -20 \log |\Gamma_{\text{in}}| = -20 \log \left| S_{11} + \frac{\Gamma_L S_{12} S_{21}}{(1 - \Gamma_L S_{22})} \right|. \quad (2.217)$$

If the load is matched, i.e. $Z_L = Z_0^*$ (the system reference impedance), then

$$\text{RL}_{\text{dB}} = -20 \log |S_{11}|. \quad (2.218)$$

This return loss is also called the input return loss since the reflection coefficient is calculated at Port 1. The output return loss is calculated looking into Port 2 of the two-port, where now the termination at Port 1 is just the source impedance.

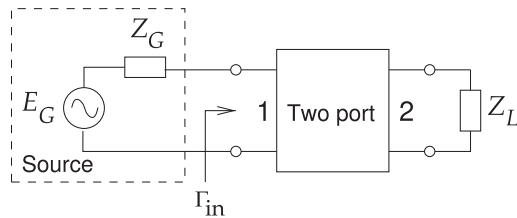


Figure 2-26: Terminated two-port used to define return loss.

2.8.2 Substitution Loss and Insertion Loss

The substitution loss is the ratio of the power, iP_L , delivered to the load by an initial two-port identified by the leading superscript ' i ', and the power delivered to the load, fP_L , with a substituted final two-port identified by the leading superscript ' f '. In terms of generalized scattering parameters with reference impedances Z_{01} at Port 1 and Z_{02} at Port 2 the substitution loss in decibels is (using the results of Example 3.2 and noting that Γ_S is referred to Z_{01} and Γ_L is referred to Z_{02})

$$L_S|_{\text{dB}} = \frac{{}^iP_L}{{}^fP_L} = 10 \log \left| \frac{{}^iS_{21} [(1 - {}^fS_{11}\Gamma_S)(1 - {}^fS_{22}\Gamma_L) - {}^fS_{12}{}^fS_{21}\Gamma_S\Gamma_L]}{{}^fS_{21} [(1 - {}^iS_{11}\Gamma_S)(1 - {}^iS_{22}\Gamma_L) - {}^iS_{12}{}^iS_{21}\Gamma_S\Gamma_L]} \right|^2. \quad (2.219)$$

Insertion loss is a special case of substitution loss with particular types of initial two-port networks. There are a number of special cases to consider.

Insertion Loss with an Ideal Adaptor

Comparing the power delivered to the load with an inserted two-port with that delivered with an ideal adaptor is the commonly accepted definition of insertion loss [10]. That is, 'insertion loss' without qualifications is the same as 'insertion loss with an ideal adaptor.' An ideal adaptor (as the initial two-port network) transforms from the Port 1 reference impedance, Z_{01} , to the Port 2 reference impedance, Z_{02} . In terms of generalized S parameters the ideal adaptor has ${}^i({}^GS_{11}) = 0 = {}^i({}^GS_{22})$ (for no reflection), ${}^i({}^GS_{12}){}^i({}^GS_{21}) = 1$ (for no loss in the adaptor and there is no phase shift), and ${}^i({}^GS_{12}) = {}^i({}^GS_{21})Z_{01}/Z_{02}$ (for reciprocity). (If $Z_{01} = Z_{02}$ this ideal adaptor is the same as a direct connection.) Insertion loss in decibels is, using Equation (2.219):

$$\text{IL}|_{\text{dB}} = 10 \log \left\{ \frac{Z_{02}}{Z_{01}} \left| \frac{[1 - {}^f({}^GS_{11})\Gamma_S][1 - {}^f({}^GS_{22})\Gamma_L] - {}^f({}^GS_{12}){}^f({}^GS_{21})\Gamma_S\Gamma_L}{{}^f({}^GS_{12})(1 - \Gamma_S\Gamma)} \right|^2 \right\} \quad (2.220)$$

Attenuation is defined as the insertion loss without source and load reflections ($\Gamma_S = 0 = \Gamma_L$) [10], and Equation (2.220) becomes

$$A|_{\text{dB}} = 10 \log \left(\frac{Z_{02}}{Z_{01}} \frac{1}{|{}^G S_{21}|^2} \right) \quad (= \text{IL}|_{\text{dB}} \text{ with } \Gamma_S = 0 = \Gamma_L). \quad (2.221)$$

where ${}^G S_{21}$ is that of the final two-port.

Insertion Loss with Direct Connection

With normalized S parameters, i.e. $Z_{01} = Z_{02}$, the insertion loss with an initial direct connection is as given in Equation (2.220). With different reference impedances at each port, the initial direct connection ' i ', from Example 2.4, ${}^i({}^GS_{11}) = (Z_{02} - Z_{01})/(Z_{02} + Z_{01})$, ${}^i({}^GS_{22}) = -{}^i({}^GS_{11})$, ${}^i({}^GS_{21}) = [1 + {}^i({}^GS_{11})] \times \sqrt{\Re\{Z_{02}\}}/\sqrt{\Re\{Z_{01}\}}$, and ${}^i({}^GS_{12}) =$

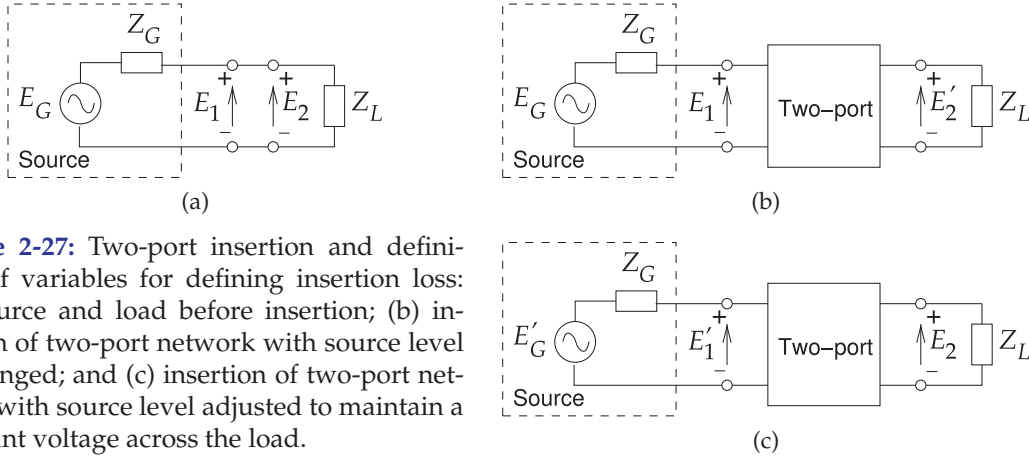


Figure 2-27: Two-port insertion and definition of variables for defining insertion loss: (a) source and load before insertion; (b) insertion of two-port network with source level unchanged; and (c) insertion of two-port network with source level adjusted to maintain a constant voltage across the load.

$[1 + i(GS_{22})] \sqrt{\Re\{Z_{01}\}} / \sqrt{\Re\{Z_{02}\}}$. These S parameters of the initial two-port network are substituted in Equation (2.219) to determine insertion loss with a direct connection.

2.8.3 Measurement of Insertion Loss

If the S parameters of a two-port network can be measured it is simple to calculate the insertion loss of the two-port. However there are situations where the S parameters cannot be measured and this includes where there is not a port connection (e.g., the air side of an antenna) and the system reference impedances differ at the two ports. In this section methods for measuring insertion loss in such difficult situations is described. If S parameter measurements are not available the insertion loss of a two-port network is defined as the ratio, in decibels, of voltages immediately beyond the point of insertion, before and after insertion [6, 11]. Referring to Figure 2-27(a and b), insertion loss is expressed in decibels as

$$IL_{dB} = 20 \log \left| \frac{E_2}{E_2'} \right|, \quad (2.222)$$

where E_2 is the voltage across the load (Z_L) before insertion of the two-port and E_2' is the voltage across the load (Z_L) after insertion of the two-port. The power delivered to the load is proportional to the square of the magnitude of the voltage across the load, so this definition is equivalent to that described in section 2.8.2 where

$$IL_{dB} = 10 \log \frac{P_L}{P_T}, \quad (2.223)$$

where P_L is the power delivered to the load before the insertion of the two-port and P_T is the power delivered to the load following insertion.

EXAMPLE 2.9**Insertion loss of a two-port in a different reference system**

A $50\ \Omega$ attenuator has an attenuation of 3 dB and a return loss of 20 dB. If the attenuator is used in a $75\ \Omega$ system what is the insertion loss of the attenuator?

Solution:

The insertion loss can be calculated using the insertion loss formula in Equation (2.219). To apply this the $50\ \Omega$ S parameters of the attenuator are needed and then the load and source reflection coefficients, Γ_L and Γ_S respectively, which will be the reflection coefficients of the $75\ \Omega$ load and source impedances referred to $50\ \Omega$. Also note that $Z_{01} = Z_{02} = 50\ \Omega$. Since there are two reference systems the leading superscripts 50 and 75 will be used to distinguish them.

Step 1. Find Γ_S and Γ_L in the $50\ \Omega$ system: $\Gamma_S = \Gamma_L = (55 - 50)/(55 + 50) = 0.2000$

Step 2. Find the S parameters in a $50\ \Omega$ system. (case 1, assume $\angle S_{11} = \angle S_{21} = 0^\circ$)

It is known that $^{50}\text{RL}_{\text{dB}} = 20\ \text{dB}$ and $^{50}\text{IL}_{\text{dB}} = 3\ \text{dB}$. Also an attenuator is symmetrical so that $^{50}S_{11} = ^{50}S_{22}$ and $^{50}S_{12} = ^{50}S_{21}$. Using Equations (2.218) and (2.221)

$$\begin{aligned} |^{50}S_{11}| &= |^{50}S_{22}| = 10^{-^{50}\text{RL}_{\text{dB}}/20} = 10^{-20/20} = 0.1000 \\ \text{and } |^{50}S_{12}| &= |^{50}S_{21}| = 10^{-^{50}\text{IL}_{\text{dB}}/20} = 10^{-3/20} = 0.7080. \end{aligned}$$

The phases of the S parameters are not known. Assume first (use the leading subscript '1') that the phases are 0° and consider alternatives later and then the S parameter matrix is

$$_1\mathbf{S} = \begin{bmatrix} ^{50}_1S_{11} & ^{50}_1S_{12} \\ ^{50}_1S_{21} & ^{50}_1S_{22} \end{bmatrix} = \begin{bmatrix} 0.1000 & 0.7080 \\ 0.7080 & 0.1000 \end{bmatrix}. \quad (2.224)$$

From Equation (2.220)

$$^{75}_1\text{IL}_{\text{dB}} = 10 \log \left[\frac{50}{50} \left| \frac{(1 - 0.1 \cdot 0.2)(1 - 0.1 \cdot 0.2) - 0.7080 \cdot 0.7080 \cdot 0.2 \cdot 0.2}{0.7080(1 - 0.2 \cdot 0.2)} \right|^2 \right] = 2.82\ \text{dB}. \quad (2.225)$$

Step 3 Four phase assumptions for S_{11} and S_{22}

Case 1	$\angle S_{11} = \angle S_{22} = 0^\circ, \angle S_{21} = \angle S_{12} = 0^\circ$	$^{75}_1\text{IL}_{\text{dB}} = 2.82\ \text{dB}$
Case 2	$\angle S_{11} = \angle S_{22} = 0^\circ, \angle S_{21} = \angle S_{12} = 180^\circ$	$^{75}_2\text{IL}_{\text{dB}} = 2.82\ \text{dB}$
Case 3	$\angle S_{11} = \angle S_{22} = 180^\circ, \angle S_{21} = \angle S_{12} = 0^\circ$	$^{75}_3\text{IL}_{\text{dB}} = 3.53\ \text{dB}$
Case 4	$\angle S_{11} = \angle S_{22} = 180^\circ, \angle S_{21} = \angle S_{12} = 180^\circ$	$^{75}_4\text{IL}_{\text{dB}} = 3.53\ \text{dB}$

Thus just knowing the return loss and insertion loss in one reference system is not enough to know the insertion loss in another system without knowing the phases of the S parameters.

EXAMPLE 2.10**Insertion loss calculation using change of reference impedance**

A $50\ \Omega$ attenuator has an attenuation of 3 dB and a return loss of 20 dB. If the attenuator is used in a $75\ \Omega$ system what is the insertion loss of the attenuator?

Solution:

This is alternative to the method used in Example 2.9. Using the S parameters of the attenuator in Equation (2.224), in a $75\ \Omega$ system the S parameters are found using Equation (2.138) and noting that $\Gamma_{75} = 0.2$ is the reflection coefficient of $75\ \Omega$ in a $50\ \Omega$ system:

$$\begin{aligned} {}^{75}\mathbf{S} &= \begin{bmatrix} {}^{75}S_{11} & {}^{75}S_{12} \\ {}^{75}S_{21} & {}^{75}S_{22} \end{bmatrix} = \begin{bmatrix} {}^{50}S_{11} - \Gamma_{75} & {}^{50}S_{12} \\ {}^{50}S_{21} & {}^{50}S_{22} - \Gamma_{75} \end{bmatrix} \begin{bmatrix} 1 - \Gamma_{75} {}^{50}S_{11} & -\Gamma_{75} {}^{50}S_{12} \\ -\Gamma_{75} {}^{50}S_{21} & 1 - \Gamma_{75} {}^{50}S_{22} \end{bmatrix}^{-1} \\ &= \begin{bmatrix} -0.1 & 0.7080 \\ 0.7080 & -0.1 \end{bmatrix} \begin{bmatrix} 0.9800 & -0.1416 \\ -0.1416 & 0.9800 \end{bmatrix}^{-1} = \begin{bmatrix} 0.002379 & 0.7227 \\ 0.7227 & 0.002379 \end{bmatrix}. \quad (2.226) \end{aligned}$$

In the $75\ \Omega$ system the load and source are matched and using Equation (2.220)

$${}^{75}_1\text{IL}_{\text{dB}} = 10 \log \frac{1}{|{}^{75}S_{21}|^2} = 10 \log \frac{1}{|0.7227|^2} = 2.82 \text{ dB}. \quad (2.227)$$

which is in agreement with the calculation in Example 2.9, see Equation (2.225).

2.8.4 Minimum Transducer Loss, Intrinsic Attenuation

Another situation often required is determining the minimum possible loss of a two-port. This is obtained with lossless two-port networks, M_1 and M_2 at the input and output of the two-port of interest, M_3 . M_1 and M_2 are adjusted to obtain the minimum possible loss of M_3 . This is not the same as designing M_1 and M_2 to obtain matching. The **minimum insertion loss**, also called the **intrinsic attenuation**, or **minimum transducer loss** in dB is [12] (the derivation is involved),

$$L_{\text{TM}}|_{\text{dB}} = 10 \log \left[\frac{Z_{02}}{Z_{01}} \frac{|1 - S_{22}\Gamma_{\text{TM}}|^2 - |(S_{12}S_{21} - S_{11}S_{22})\Gamma_{\text{TM}} + S_{11}|^2}{|S_{21}|^2(1 - |\Gamma_{\text{TM}}|^2)} \right] \quad (2.228)$$

where the S parameters are of M_3 Z_{01} and Z_{02} are the real reference impedances at ports 1 and 2 respectively, and

$$\Gamma_{\text{TM}} = \frac{B}{2A} \left(1 \pm \sqrt{1 - \frac{2|A|}{B}} \right), \quad (2.229)$$

where

$$A = S_{22} + S_{11}^* (S_{12}S_{21} - S_{11}S_{22}) \quad (2.230)$$

and

$$B = 1 - |S_{11}|^2 + |S_{22}|^2 - |S_{12}S_{21} - S_{11}S_{22}|^2. \quad (2.231)$$

The intrinsic attenuation is a useful metric when a device is being developed and has not yet been optimally matched.

Other insertion loss concepts are **comparison loss**, **mismatch loss**, and **conjugate mismatch loss**, see [10].

2.9 Scattering Parameters and Directional Couplers

Directional couplers were described in Section 5.8 of [13] but described without the use of S parameters. A directional coupler with ports defined as in Figure 2-28, and with the ports matched (so that $S_{11} = 0 = S_{22} = S_{33} = S_{44}$), has the following scattering parameter matrix:

$$\mathbf{S} = \begin{bmatrix} 0 & T & 1/C & 1/I \\ T & 0 & 1/I & 1/C \\ 1/C & 1/I & 0 & T \\ 1/I & 1/C & T & 0 \end{bmatrix}. \quad (2.232)$$

There are many types of directional couplers, and the phases of the traveling waves at the ports will not necessarily be in phase as Equation (2.232) implies. When the phase difference between traveling waves entering at Port 1 and leaving at Port 2 is 90° , Equation (2.232) becomes

$$\mathbf{S} = \begin{bmatrix} 0 & -jT & 1/C & 1/I \\ -jT & 0 & 1/I & 1/C \\ 1/C & 1/I & 0 & -jT \\ 1/I & 1/C & -jT & 0 \end{bmatrix}. \quad (2.233)$$

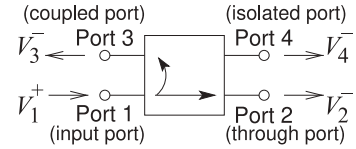


Figure 2-28: Schematic of a directional coupler.

EXAMPLE 2.11

Identifying Ports of a Directional Coupler

A directional coupler has the following S parameters:

$$\mathbf{S} = \begin{bmatrix} 0 & 0.9 & 0.001 & 0.1 \\ 0.9 & 0 & 0.1 & 0.001 \\ 0.001 & 0.1 & 0 & 0.9 \\ 0.1 & 0.001 & 0.9 & 0 \end{bmatrix}.$$

- (a) What are the through (i.e., transmission) paths? Identify two paths. That is, identify the pairs of ports at the ends of the through paths.

First note that the assignment of ports to a directional coupler is arbitrary. So the S parameters need to be considered to figure out how the ports are related. The S parameters relate the forward-traveling waves to the backward-traveling waves and this leads to the required understanding, thus

$$\begin{bmatrix} V_1^- \\ V_2^- \\ V_3^- \\ V_4^- \end{bmatrix} = \mathbf{S} \begin{bmatrix} V_1^+ \\ V_2^+ \\ V_3^+ \\ V_4^+ \end{bmatrix} = \begin{bmatrix} 0 & 0.9 & 0.001 & 0.1 \\ 0.9 & 0 & 0.1 & 0.001 \\ 0.001 & 0.1 & 0 & 0.9 \\ 0.1 & 0.001 & 0.9 & 0 \end{bmatrix} \begin{bmatrix} V_1^+ \\ V_2^+ \\ V_3^+ \\ V_4^+ \end{bmatrix}.$$

Writing the S parameters out this way makes it easier to identify the largest backward-traveling waves for each of the inputs at Ports 1, 2, 3, and 4. The backward-traveling wave will leave the directional coupler and the inputs will be forward-traveling waves. Consider Port 1, the largest backward-traveling wave is at Port 2, and so Ports 1 and 2 define one of the through paths. The other through path is between Ports 3 and 4. So the through paths are 1–2 and 3–4.

- (b) What is the coupled port for the signal entering Port 1?

The coupled port is identified by the port with the largest backward-traveling signal not including the port at the other end of the through path. For Port 1 the coupled port is Port 4.

- (c) What is the coupling factor?

$$C = \frac{V_1^+}{V_4^-} = \frac{1}{0.1} = 10 = 20 \text{ dB.}$$

- (d) What is the isolated port for the signal entering Port 1?

The isolated port is Port 3. The backward-traveling wave at this port is the smallest given an input at Port 1.

- (e) What is the isolation factor?

$$I = \frac{V_1^+}{V_3^-} = \frac{1}{0.001} = 1000 = 60 \text{ dB.}$$

- (f) What is the directivity factor?

The directivity factor indicates how much stronger the signal is at the coupled port compared to the isolated port for a signal at the input. For an input at Port 1, the directivity factor is

$$D = \frac{V_4^-}{V_3^-} = \frac{0.1}{0.001} = 100 = 40 \text{ dB.}$$

As a check $D = I/C = 1000/10 = 100$.

- (g) Draw a schematic of the directional coupler.

There are four ways to draw it depending on which port is chosen to be the input port (see Figure 2-29).

2.10 Summary

There are several network parameters used with RF and microwave circuits. Which is used depends on which makes the task of visualizing circuit operation more clear, which makes analyzing circuits more convenient, and which makes design easier.

Scattering parameters are parameters that are almost exclusively used by RF and microwave engineers. They describe power flow and traveling waves and are essential to describing distributed circuits. Much of RF and microwave engineering is concerned with managing the signal-to-noise power ratio and with power efficiency. It is therefore natural to work with parameters that directly relate to power flow. RF and microwave design is characterized by conceptual insight and it is essential to use parameters

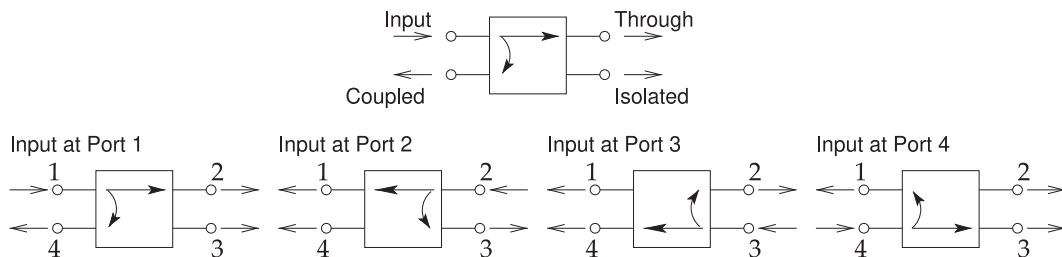


Figure 2-29: Directional coupler schematic drawn with each of the four possible input ports.

and graphical representations that are close to the physical world. Scattering parameters have very natural graphical representations, as will be seen in the next chapter.

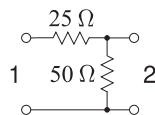
The next most important network parameters considered in this chapter are the $ABCD$ parameters. The special significance of these parameters in microwave engineering is that they can be used to relate a distributed circuit to a lumped-element circuit. Many RF designs begin as lumped-element prototypes that are eventually transformed into electrically equivalent distributed structures. This equivalence process nearly always involves $ABCD$ parameters.

2.11 References

- [1] N. Marcuvitz, *Waveguide Handbook*. McGraw-Hill, 1955.
- [2] R. Collins, *Foundations for Microwave Engineering*. McGraw Hill, 1966.
- [3] D. M. Kerns and R. W. Beatty, *Basic theory of waveguide junctions and introductory microwave network analysis*. Pergamon Press New York, 1967.
- [4] R. B. Marks and D. F. Williams, "A general waveguide circuit theory," *Journal of Research-National Institute of Standards and Technology*, vol. 97, pp. 533–533, Sep.–Oct. 1992.
- [5] D. Williams and B. Alpert, "Causality and waveguide circuit theory," *IEEE Trans. on Microwave Theory and Techniques*, vol. 49, no. 4, pp. 615–623, Apr. 2001.
- [6] "Telecommunications: Glossary of Telecommunication Terms," Federal Standard 1037C, U.S. General Services Administration Information Technology Service, Aug. 7, 1996.
- [7] T. S. Bird, "Definition and misuse of re-
- turn loss [report of the trans. editor-in-chief]," *IEEE Antennas and Propagation Magazine*, vol. 51, no. 2, pp. 166–167, Apr. 2009.
- [8] IEEE, *IEEE Standard Dictionary of Electrical and Electronic Engineering Terms*, 4th ed. IEEE Press, 1988.
- [9] T. Otoshi, "Maximum and minimum return losses from a passive two-port network terminated with a mismatched load," *IEEE Trans. on Microwave Theory and Techniques*, vol. 42, no. 5, pp. 787–792, May 1994.
- [10] R. Beatty, "Insertion loss concepts," *Proc. of the IEEE*, vol. 52, no. 6, pp. 663–671, Jun. 1964.
- [11] "MIL-STD-220C: Test method standard, method of insertion loss measurement."
- [12] R. W. Beatty, "Intrinsic attenuation," *IEEE Transactions on Microwave Theory and Techniques*, vol. 11, no. 3, pp. 179–182, 1963.
- [13] M. Steer, *Microwave and RF Design, Transmission Lines*, 3rd ed. North Carolina State University, 2019.

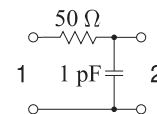
2.12 Exercises

1. A load has a reflection coefficient of $0.5 - j0.1$ in a $75\ \Omega$ reference system. What is the reflection coefficient in a $50\ \Omega$ reference system?
2. The $50\ \Omega$ S parameters of a two-port are $S_{11} = 0.5 + j0.5$, $S_{12} = 0.95 + j0.25$, $S_{21} = 0.15 - j0.05$, and $S_{22} = 0.5 - j0.5$. Port 1 is connected to a $50\ \Omega$ source with an available power of 1 W and Port 2 is terminated in $50\ \Omega$. What is the power reflected from Port 1?
3. Derive the two-port $50\ \Omega$ S parameters for the resistive circuit below.

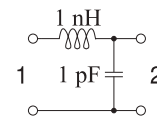


4. Derive the two-port $50\ \Omega$ S parameters at 1 GHz

for the circuit below.



5. Derive the two-port $50\ \Omega$ S parameters at 1 GHz for the circuit below.

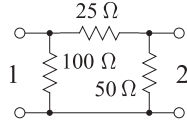


6. Derive the two-port S parameters of a shunt $25\ \Omega$ resistor in a $50\ \Omega$ reference system using the method presented in Section 2.3.5.

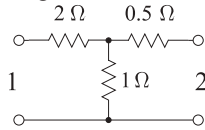
7. Derive the two-port S parameters of a series

25 Ω resistor in a 100 Ω reference system using the method presented in Section 2.3.5.

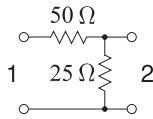
8. A two-port consists of a π resistor network as shown. Derive the scattering parameters referenced to 50 Ω using the method in Section 2.3.5.



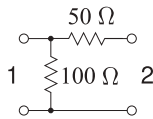
9. A two-port consists of a T resistor network as shown. Derive the scattering parameters referenced to 1 Ω using the method in 2.3.5.



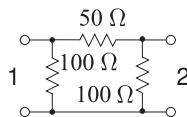
10. Derive the 50 Ω S parameters of the following.



11. Derive the 50 Ω S parameters of the following.



12. Derive the 100 Ω S parameters of the following.



13. The scattering parameters of a certain two-port are $S_{11} = 0.5 + j0.5$, $S_{12} = 0.95 + j0.25$, $S_{21} = 0.15 - j0.05$, and $S_{22} = 0.5 - j0.5$. The system reference impedance is 50 Ω .

- Is the two-port reciprocal? Explain.
- Consider that Port 1 is connected to a 50 Ω source with an available power of 1 W. What is the power delivered to a 50 Ω load placed at Port 2?
- What is the reflection coefficient of the load required for maximum power transfer at Port 2?

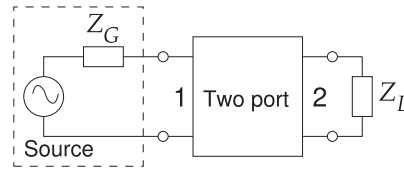
14. In characterizing a two-port, power could only be applied at Port 1. The signal reflected was measured and the signal at a 50 Ω load at Port 2 was also measured. This yielded two S parameters referenced to 50 Ω : $S_{11} = 0.3 - j0.4$ and $S_{21} = 0.5$.

- If the network is reciprocal, what is S_{12} ?

- Is the two-port lossless?

- What is the power delivered into the 50 Ω load at Port 2 when the available power at Port 1 is 0 dBm?

15. The S parameters of a two-port are $S_{11} = 0.25$, $S_{12} = 0$, $S_{21} = 1.2$, and $S_{22} = 0.5$. The system reference impedance is 50 Ω and $Z_G = 50 \Omega$. The power available from the source is 1 mW. $Z_L = 25 \Omega$.



- Is the two-port reciprocal and why?
- What is the voltage of the source?
- What is the power reflected from Port 1?
- Determine the z parameters of the two-port.
- Using z parameters, what is the power dissipated by the load at Port 2?

16. The scattering parameters of a two-port network are $S_{11} = 0.25$, $S_{21} = 2.$, $S_{21} = 0.1$, and $S_{22} = 0.5$ and the reference impedance is 50 Ω . What are the scattering transfer (T) parameters of the two-port?

17. A matched lossless transmission line has a length of one-quarter wavelength. What are the scattering parameters of the two-port?

18. Consider a two-port comprising a 100 Ω resistor connected in series between the ports.

- Write down the S parameters of the two-port using a 50 Ω reference impedance.
- From the scattering parameters derive the $ABCD$ parameters of the two-port.

19. Consider a two-port comprising a 25 Ω resistor connected in shunt.

- Write down the scattering parameters of the two-port using a 50 Ω reference impedance.
- From the scattering parameters derive the $ABCD$ parameters of the two-port.

20. What are the scattering transfer T parameters of a two port with the scattering parameters $S_{11} = 0 = S_{22}$ and $S_{12} = -j = S_{21}$?

21. The scattering parameters of a two-port amplifier referred to 50 Ω are $S_{11} = 0.5$, $S_{21} = 2$, $S_{12} = 0.1$, and $S_{22} = -0.01$. What are the generalized scattering parameters of the two-port network if the reference impedance at Port 1 is 100 Ω and at Port 2 is 10 Ω ?

22. A 50 Ω , 10 dB attenuator is inserted in a 75 Ω system. (That is, the attenuator is a two-port

- network and using a $50\ \Omega$ reference the S -parameters of the attenuator are $S_{11} = 0 = S_{22}$ and the insertion loss of the two-port in the $50\ \Omega$ system is 10 dB. Now consider the same two-port in a $75\ \Omega$ system.)
- (a) What is the transmission coefficient in the $75\ \Omega$ system?
 - (b) What is the attenuation (i.e., the insertion loss) in decibels in the $75\ \Omega$ system?
 - (c) What is the input reflection coefficient at Port 1 including the $75\ \Omega$ at Port 2?
23. A two-port has the $50\text{-}\Omega$ scattering parameters $S_{11} = 0.1$; $S_{12} = 0.9 = S_{21}$; $S_{22} = 0.2$. The $50\text{-}\Omega$ source at port 1 has an available power of 1 W. (This is the power that would be delivered to a $50\ \Omega$ termination at the source.)
 - (a) What is the power delivered to a $50\ \Omega$ load at port 2?
 - (b) What are the generalized scattering parameters with a $50\ \Omega$ reference at port 1 and a $75\ \Omega$ reference at port 2?
 - (c) Using the generalized scattering parameters, calculate the power delivered to the $50\ \Omega$ load at port 2.
 24. A two-port is matched to a source with a Thevenin impedance of $50\ \Omega$ connected at Port 1 and a load of $25\ \Omega$ at Port 2. If the two-port is represented by generalized scattering parameters, what should the normalization impedances at the ports be for $S_{11} = 0 = S_{22}$?
 25. A two-port is terminated at Port 2 in $50\ \Omega$. At Port 1 is a source with a Thevenin equivalent impedance of $75\ \Omega$. The generalized scattering parameters of the two-port are $S_{11} = 0$, $S_{21} = 2$, $S_{12} = 0.1$, and $S_{22} = 0.5$. The reference impedances are $75\ \Omega$ at Port 1 and $50\ \Omega$ at Port 2. If the Thevenin equivalent source has a peak voltage of 1 V, write down the root power waves at each port.
 26. A two-port is terminated at Port 2 in $10\ \Omega$. At Port 1 is a source with a Thevenin equivalent impedance of $100\ \Omega$. The generalized scattering parameters of the two-port are $S_{11} = 0.2$, $S_{21} = 0.5$, $S_{12} = 0.1$, and $S_{22} = 0.3$. The reference impedances are $100\ \Omega$ at Port 1 and $10\ \Omega$ at Port 2. If the Thevenin equivalent source has a peak voltage of 50 V, what are a_1 , b_1 , a_2 , and b_2 ?
 27. The scattering parameters of a two-port network are $S_{11} = 0.6$, $S_{21} = 0.8$, $S_{12} = 0.5$, and $S_{22} = 0.3$ and the reference impedance is $50\ \Omega$. At Port 1 a $50\ \Omega$ transmission line with an electrical length of 90° is connected and at Port 2 a $50\ \Omega$ transmission line with an electrical length of 180° is connected. What are the scattering parameters of the cascaded system (transmission line–original two-port–transmission line)?
 28. A connector has the scattering parameters $S_{11} = 0.05$, $S_{21} = 0.9$, $S_{12} = 0.9$, and $S_{22} = 0.04$ and the reference impedance is $50\ \Omega$. What is the return loss in dB of the connector at Port 1 in a $50\ \Omega$ system?
 29. The scattering parameters of an amplifier are $S_{11} = 0.5$, $S_{21} = 2$, $S_{12} = 0.1$, and $S_{22} = -0.2$ and the reference impedance is $50\ \Omega$. If the amplifier is terminated at Port 2 in a resistance of $25\ \Omega$, what is the return loss in dB at Port 1?
 30. A two-port network has the scattering parameters $S_{11} = -0.5$, $S_{21} = 0.9$, $S_{12} = 0.8$, and $S_{22} = 0.04$ and the reference impedance is $50\ \Omega$.
 - (a) What is the return loss in dB of the connector at Port 1 in a $50\ \Omega$ system?
 - (b) Is the two-port reciprocal and why?
 31. A two-port network has the scattering parameters $S_{11} = -0.2$, $S_{21} = 0.8$, $S_{12} = 0.7$, and $S_{22} = 0.5$ and the reference impedance is $75\ \Omega$.
 - (a) What is the return loss in dB of the connector at Port 1 in a $75\ \Omega$ system?
 - (b) Is the two-port reciprocal and why?
 32. A cable has the scattering parameters $S_{11} = 0.1$, $S_{21} = 0.7$, $S_{12} = 0.7$, and $S_{22} = 0.1$. At Port 2 is a $55\ \Omega$ load and the S parameters and reflection coefficients are referred to $50\ \Omega$.
 - (a) What is the load's reflection coefficient?
 - (b) What is the input reflection coefficient of the terminated cable?
 - (c) What is the return loss, at Port 1 and in dB, of the cable terminated in the load?
 33. A cable has the $50\ \Omega$ scattering parameters $S_{11} = 0.05$, $S_{21} = 0.5$, $S_{12} = 0.5$, and $S_{22} = 0.05$. What is the insertion loss in dB of the cable if the source at Port 1 has a $50\ \Omega$ Thevenin impedance and the termination at Port 2 is $50\ \Omega$?
 34. A 1 m long cable has the $50\ \Omega$ scattering parameters $S_{11} = 0.1$, $S_{21} = 0.7$, $S_{12} = 0.7$, and $S_{22} = 0.1$. The cable is used in a $55\ \Omega$ system.
 - (a) What is the return loss in dB of the cable in the $55\ \Omega$ system? (Hint see Section 2.3.4 and consider finding Z_{in} .)
 - (b) What is the insertion loss in dB of the cable in the $55\ \Omega$ system? Follow the procedure in Example 2.9
 - (c) What is the return loss in dB of the cable in a $50\ \Omega$ system?
 - (d) What is the insertion loss in dB of the cable in a $50\ \Omega$ system?

35. A 1 m long cable has the $50\ \Omega$ scattering parameters $S_{11} = 0.1$, $S_{21} = 0.7$, $S_{12} = 0.7$, and $S_{22} = 0.1$. The cable is used in a $55\ \Omega$ system. Follow the procedure in Example 2.10.
- What is the return loss in dB of the cable in the $55\ \Omega$ system?
 - What is the insertion loss in dB of the cable in the $55\ \Omega$ system?
36. A 10 m long cable has the $50\ \Omega$ scattering parameters $S_{11} = -0.1$, $S_{21} = 0.5$, $S_{12} = 0.5$, and $S_{22} = -0.1$. The cable is used in a $75\ \Omega$ system. Use the change of S parameter reference impedance method [Parallels Example 2.10]. Express your answers in decibels.
- What is the return loss of the cable in the $75\ \Omega$ system?
 - What is the insertion loss of the cable in the $75\ \Omega$ system?
37. A 1 m long cable has the $50\ \Omega$ scattering parameters $S_{11} = 0.05$, $S_{21} = 0.5$, $S_{12} = 0.5$, and $S_{22} = 0.05$. The Thevenin equivalent impedance of the source and terminating load impedances of the cable are $50\ \Omega$.
- What is the return loss in dB of the cable?
 - What is the insertion loss in dB of the cable?
38. A cable in a $50\ \Omega$ system has the S parameters $S_{11} = 0.1$, $S_{21} = 0.7$, $S_{12} = 0.7$, and $S_{22} = 0.1$. The available power at Port 1 is 0 dBm and at Port 2 is a $55\ \Omega$ load. Γ is reflection coefficient and a_n and b_n are the root power waves at the n th port.
- What is the load's Γ ?
 - What is a_1 (see Equation (2.117))?
 - What is b_2 ?
 - What is a_2 ?
 - What is the power, in dBm, delivered to the load?
 - What is the power, in dBm, delivered to the load if the cable is removed and replaced by a direct connection?
 - Hence what is the insertion loss, in dB, of the cable?
39. A lossy directional coupler has the following

$50\ \Omega$ S parameters:

$$S = \begin{bmatrix} 0 & -0.95j & 0.005 & 0.1 \\ -0.95j & 0 & 0.1 & 0.005 \\ 0.005 & 0.1 & 0 & -0.95j \\ 0.1 & 0.005 & -0.95j & 0 \end{bmatrix}.$$

- What are the through (transmission) paths (identify two paths)? That is, identify the pairs of ports at the ends of the through paths.
 - What is the coupling in decibels?
 - What is the isolation in decibels?
 - What is the directivity in decibels?
40. A directional coupler has the following characteristics: coupling factor $C = 20$, transmission factor 0.9, and directivity factor 25 dB. Also, the coupler is matched so that $S_{11} = 0 = S_{22} = S_{33} = S_{44}$.
- What is the isolation factor in decibels?
 - Determine the power dissipated in the directional coupler if the input power to Port 1 is 1 W.
41. A lossy directional coupler has the following $50\ \Omega$ S parameters:

$$S = \begin{bmatrix} 0 & 0.25 & -0.9j & 0.01 \\ 0.25 & 0 & 0.01 & -0.9j \\ -0.9j & 0.01 & 0 & 0.25 \\ 0.01 & -0.9j & 0.25 & 0 \end{bmatrix}.$$

- Which port is the input port (there could be more than one answer)?
 - What is the coupling in decibels?
 - What is the isolation in decibels?
 - What is the directivity factor in decibels?
 - Draw the signal flow graph of the directional coupler.
42. A directional coupler using coupled lines has a coupling factor of 3.38, a transmission factor of $-j0.955$, and infinite directivity and isolation. The input port is Port 2 and the through port is Port 2. Write down the 4×4 S parameter matrix of the coupler.

2.12.1 Exercises by Section

[†]challenging

- | | | |
|---|---|--|
| §2.3 1, 2, 3 [†] , 4 [†] , 5 [†] , 6 [†] , 7 [†] , 8 [†] , 9 [†] ,
10, 11, 12, 13 [†] , 14 [†] , 15 [†] , 16,
17 [†] , 18 [†] , 19 [†] , 20, 21, 22 [†] | §2.4 23 [†] , 24, 25 [†] , 26 [†]
§2.6 27
§2.8 28, 29, 30, 31, 32, 33, 34 [†] , 35, | 36, 37, 38
§2.9 39 [†] , 40 [†] , 41 [†] , 42 [†] |
|---|---|--|

2.12.2 *Answers to Selected Exercises*

- | | | | | | |
|---|---|-------|--------------------|-------|---------|
| 1 | $0.638 - j0.079$ | 13(d) | $50 + j100 \Omega$ | 34(b) | 2.99 dB |
| 5 | $\begin{bmatrix} .096\angle -115^\circ & .995\angle -12.6^\circ \\ .995\angle -12.6^\circ & .097\angle -91^\circ \end{bmatrix}$ | 22(c) | -0.1807 | 40(b) | 187 mW |
| 9 | $\bar{S}_{21} = 0.2222$ | 25 | $b_2 = 0.1155$ | 41(d) | 28 dB |
| | | 28 | 26 dB | | |

Graphical Network Analysis

3.1	Introduction	49
3.2	Signal Flow Graph	49
3.3	Polar Representations of Scattering Parameters	57
3.4	Smith Chart	60
3.5	Transmission Lines and Smith Charts	77
3.6	Summary	81
3.7	References	82
3.8	Exercises	82

3.1 Introduction

The network parameters that directly describe reflected and transmitted power flow in circuits are scattering (S) parameters. This chapter introduces two widely used graphical techniques for describing and solving problems using S parameters. The first graphical technique is signal flow graph analysis (SFG) and is a graphical way of representing equations and variables. Simplifying an SFG is the same as solving simultaneous equations and the equations can be kept in symbolic form. The second graphical representation is an annotated polar plot of S parameters called a Smith chart. This is one of the most powerful tools in RF and microwave engineering and is used to present measured results, to conceptualize designs, and to intuitively solve problems involving distributed networks.

3.2 Signal Flow Graph

SFGs are convenient ways to graphically represent systems of simultaneous linear equations [1, 2]. SFGs are used in many disciplines, but they are particularly useful with RF and microwave circuits.

An SFG represents a linear operation on an input. Consider the inductor shown in Figure 3-1(a), where the circuit quantities are v and i , and these are related by the impedance of the inductor sL . The SFG representation of this relation is given in Figure 3-1(b), with the operation performed written beside a directed edge. The operation here is simple, multiplying an input quantity by a scale factor. The edge is directed from the excitation node to the response node. The algebraic relationship between v and i is, in the Laplace domain,

$$v = sLi, \quad (3.1)$$

and this is exactly how the SFG of Figure 3-1(b) is interpreted. Several linear equations are represented in SFG form in Table 3-1.

3.2.1 SFG Representation of Mathematical Relations

In this section the basic rules for manipulating SFGs are presented. Think back to when you first started working with circuits. The great abstraction came about when the physical world was represented graphically as connections of circuit elements. Provided that a few simple rules were followed, the graphical representation enabled recognition of circuit topologies and the selection of appropriate solution strategies (e.g., applying the voltage divider rule). When it comes to working with S parameters and interconnections of multiport networks, SFGs serve much the same purpose. As well, SFG analysis enables the development of symbolic expressions. Only a portion of SFG theory is considered here—the aspects relevant to manipulating scattering parameter descriptions. Balabanian [3], Abrahams and Coverly [4], and Di Stefano et al. [5] provide a more detailed and general treatment.

3.2.2 SFG Representation of Scattering Parameters

Scattering parameters relate incident and reflected waves:

$$\mathbf{b} = \mathbf{S}\mathbf{a}, \quad (3.2)$$

where \mathbf{a} and \mathbf{b} are vectors and their i th elements refer to the incident and reflected waves, respectively. These relationships can be represented by SFGs. Consider the two-port in Figure 3-2(a) described by the equations

$$b_1 = S_{11}a_1 + S_{12}a_2 \quad (3.3) \quad b_2 = S_{21}a_1 + S_{22}a_2, \quad (3.4)$$

which are represented in SFG form in Figure 3-2(b).

3.2.3 Simplification and Reduction of SFGs

The power of SFG analysis is that an SFG can be formulated by building up the set of equations describing a network by connecting together the SFGs of sections. Pattern recognition can be used to identify patterns that can be

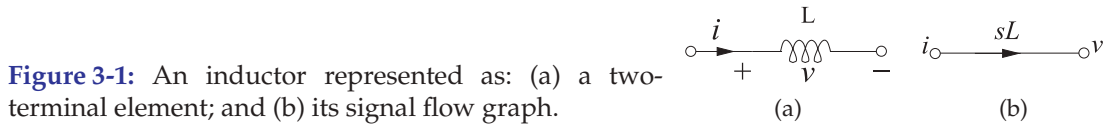


Table 3-1: Mathematical relations in the form of signal flow graphs with **edges** connecting **nodes**. Edges and nodes are used in graph theory, a superset of SFG theory. An edge is also called a **branch**.

(a)		$y = a_1x_1 + a_2x_2$
(b)		$y_1 = ax_1$ $y_2 = ax_1$
(c)		$y_1 = a_3(a_1x_1 + a_2x_2)$ $y_2 = a_4(a_1x_1 + a_2x_2)$

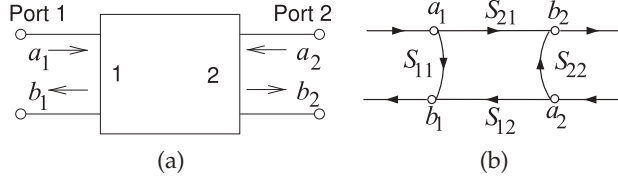


Figure 3-2: Two-port represented as (a) a two-port network with incident and reflected waves; and (b) its SFG representation.

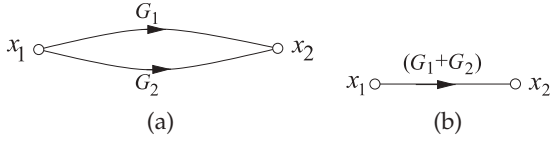


Figure 3-3: Signal flow graph representation of addition.

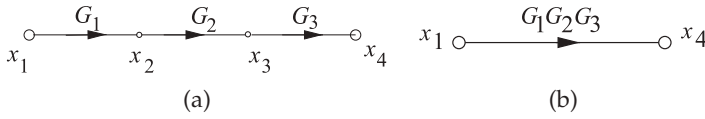


Figure 3-4: Cascade reduction of SFG: (a) three cascaded blocks; and (b) reduced form.

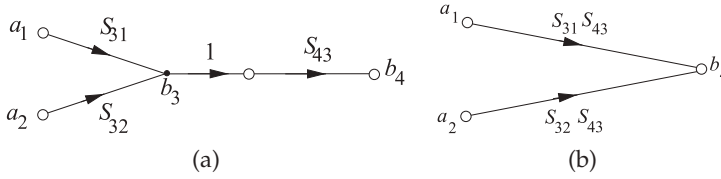


Figure 3-5: Signal flow graph simplification eliminating a variable.

reduced and simplified to arrive at a simple relationship between system input and output. Humans are extraordinarily good at pattern recognition.

Addition

Figure 3-3 depicts SFG addition. Figures 3-3(a and b) denote

$$x_2 = G_1x_1 + G_2x_1. \quad (3.5)$$

Multiplication

Consider the three cascaded blocks represented by the SFG of Figure 3-4(a). Here the output of the first block, x_2 , is described by $x_2 = G_1x_1$. Now x_2 is the input to the second block with output $x_3 = G_2x_2$, and so on. The total response is the product of the individual responses (see Figure 3-4(b)):

$$x_4 = G_1G_2G_3x_1. \quad (3.6)$$

Commutation

The rules that govern the simplification of SFGs use the fact that each graph represents a set of simultaneous equations. Consider the removal of the internal node, b_3 , in Figure 3-5(a). Here

$$b_3 = S_{31}a_1 + S_{32}a_2 \quad \text{and} \quad b_4 = S_{43}b_3. \quad (3.7)$$

Node b_3 is called a mixed node (being both input and output) and can be eliminated, so

$$b_4 = S_{31}S_{43}a_1 + S_{32}S_{43}a_2, \quad (3.8)$$

which has the SFG of Figure 3-5(b). In Figure 3-5(b) the node representing the variable b_3 has been eliminated. Thus elimination of a node corresponds to

Figure 3-6: Signal flow graphs having a self-loop: (a) original SFG; and (b) after eliminating a_2 .

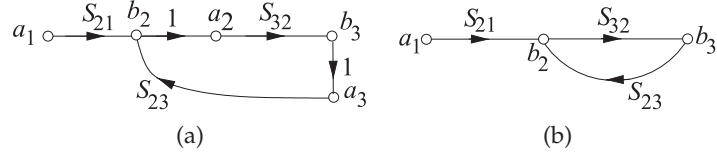


Figure 3-7: Signal flow graph of (a) a self-loop; and (b) with the loop eliminated.

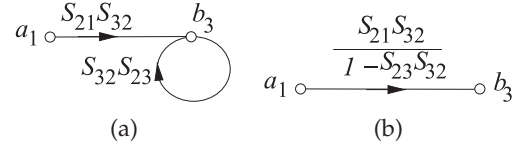
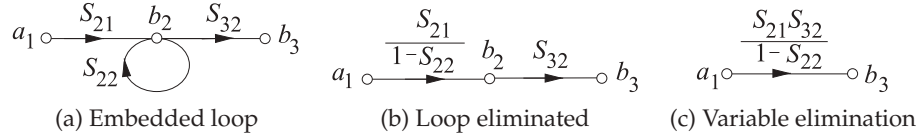


Figure 3-8: Signal flow graph with loop.



the elimination of a variable in the simultaneous. It is sufficient to recognize the SFG pattern shown in Figure 3-5(a) and replace it with the SFG of Figure 3-5(b) to achieve SFG reduction.

Self-loop

Recognizing a self-loop and eliminating it is the best example yet of pattern identification and direct application of SFG reduction strategies. Consider the SFG of Figure 3-6(a), which has a self-loop, which describes The equations for this graph are

$$b_3 = S_{32}a_2, \quad S_{23}a_2 = b_2, \quad b_2 = S_{21}a_1 + S_{23}a_3, \quad a_3 = b_3. \quad (3.9)$$

$$\text{Thus } b_3 = S_{32}S_{21}a_1 + S_{32}S_{23}b_3 \quad \text{and} \quad (1 - S_{32})b_3 = S_{32}S_{21}a_1, \quad (3.10)$$

where the variable b_2 has been eliminated. The graph of Equation (3.10) is shown in Figure 3-7(a). The loop attached to node b_3 is called a self-loop. Such loops are not particularly convenient and can be removed by writing Equation (3.10) in the form

$$b_3 = \frac{S_{21}S_{32}}{1 - S_{23}S_{32}}a_1, \quad (3.11)$$

and the SFG for this equation is shown in Figure 3-7(b). The rule for removing self-loops follows from the manner in which Figure 3-7(a) was transformed into Figure 3-7(b). As an example, Figure 3-8(a) becomes Figure 3-8(b) and this can be reduced to the SFG of Figure 3-8(c).

As a further example, consider the more difficult multiple-loop case shown in Figure 3-9(a). This may be redrawn as Figure 3-9(b). The two self-loops are added and then the graph reduces to that in Figure 3-9(c).

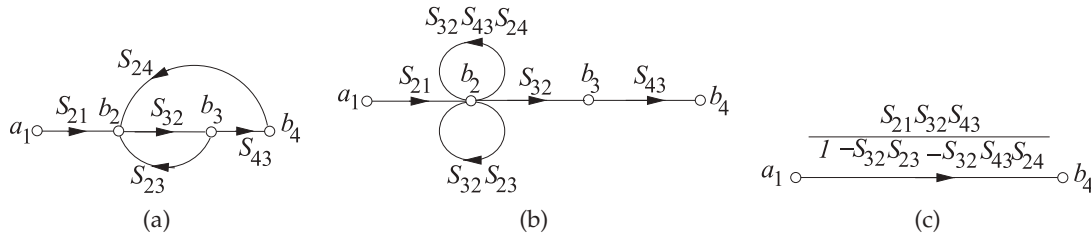


Figure 3-9: Signal flow graph with multiple loops.

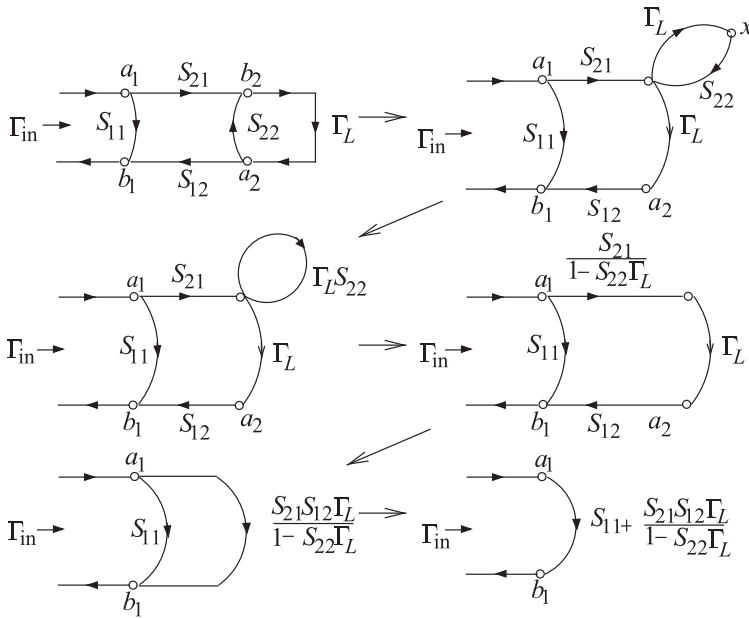


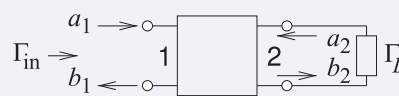
Figure 3-10: Sequence of graphical manipulations in Example 3.1 reducing a terminated two-port to a reflection only.

EXAMPLE 3.1 Signal Flow Graph

Draw the SFG of a two-port with a load (at Port 2) having a voltage reflection coefficient of Γ_L , and at Port 1 a source has a reflection coefficient of Γ_S . Using SFG analysis, derive an expression for the input reflection coefficient looking into the two-port at Port 1.

Solution:

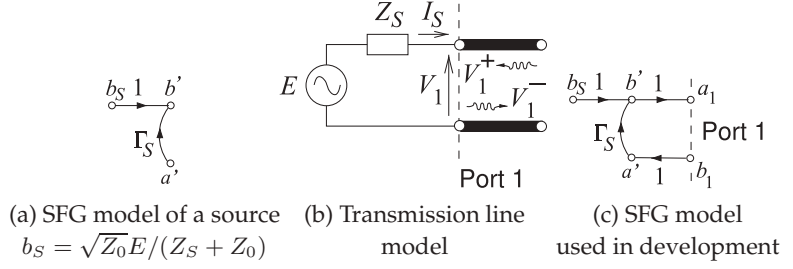
The two-port is shown to the right with the load attached. The input reflection coefficient is $\Gamma_{in} = b_1/a_1$ and the properties of the source here have no impact.



The sequence of SFG manipulations is shown in Figure 3-10 beginning with the SFG in the top left-hand corner. So the input reflection coefficient is

$$\Gamma_{in} = \frac{b_1}{a_1} = S_{11} + \frac{S_{21}S_{12}\Gamma_L}{1 - S_{22}\Gamma_L}. \quad (3.12)$$

Figure 3-11: Development of the signal flow graph model of a source. The model in (a) is for a real reference impedance Z_0 .



3.2.4 SFG Model of a Source

The SFG model, referenced to a possibly complex impedance Z_0 , of a source with a Thevenin equivalent voltage E and impedance Z_S is shown in Figure 3-11(a). In developing this model the circuit shown in Figure 3-11(b) is used where the transmission line of infinitesimal length separates the forward and backward-traveling voltage waves, V_1^+ and V_1^- for a system reference impedance of Z_0 , the characteristic impedance of the transmission line. The SFG model used with the transmission line-augmented source is shown in Figure 3-11(c). The SFG model of Figure 3-11(c) describes

$$a_1 = b_s + \Gamma_S b_1. \quad (3.13)$$

where the source reflection coefficient $\Gamma_S = (Z_S - Z_0)/(Z_S + Z_0)$. The circuit equations for Figure 3-11(b) are

$$V_1 = E - I_S Z_S = V_1^+ + V_1^- \quad \text{and} \quad I_S = \frac{V_1^+}{Z_0} - \frac{V_1^-}{Z_0}. \quad (3.14)$$

Now, the traveling wave voltages are related to the a and b root power waves as (see Equation (3.15))

$$a_1 = \frac{V_1^+}{\sqrt{\Re\{Z_0\}}} \quad \text{and} \quad b_1 = \frac{V_1^-}{\sqrt{\Re\{Z_0\}}}. \quad (3.15)$$

Then combining Equations (3.14) and (3.15) yields

$$\begin{aligned} E &= V_1^+ \frac{Z_S + Z_0}{Z_0} - V_1^- \frac{Z_S - Z_0}{Z_0} \\ \frac{Z_0}{\sqrt{\Re\{Z_0\}}} \frac{1}{Z_S + Z_0} E &= \frac{V_1^+}{\sqrt{\Re\{Z_0\}}} \left(\frac{Z_S + Z_0}{Z_S + Z_0} \right) - \frac{V_1^-}{\sqrt{\Re\{Z_0\}}} \left(\frac{Z_S - Z_0}{Z_S + Z_0} \right) \\ \frac{Z_0}{\sqrt{\Re\{Z_0\}}} \frac{1}{Z_S + Z_0} E &= a_1 - b_1 \Gamma_S. \end{aligned} \quad (3.16)$$

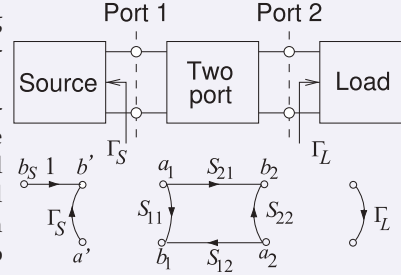
Comparing Equations (3.13) and (3.16) it is seen that

$$b_s = \frac{Z_0}{\sqrt{\Re\{Z_0\}}} \frac{1}{Z_S + Z_0} E. \quad (3.17)$$

Thus the SFG model of a source is as shown in Figure 3-11(a) where the model is shown for a real Z_0 .

EXAMPLE 3.2**Power Delivered to a Load and Substitution Loss**

This example illustrates the method for determining powers using signal flow graph analysis with generalized S parameters having reference impedances Z_{01} at Port 1 and Z_{02} at Port 2. This is then used to determine substitution loss. The substitution loss is the ratio of the power delivered to a load with an initial two-port, to the power delivered with the substituted final two-port network. The SFG elements are shown on the right with Γ_S referred to Z_{01} and Γ_L referred to Z_{02} .

**Solution:**

The SFG manipulations that determine the power delivered to the load are shown in Figure 3-12 where

$$\alpha = \frac{S_{21}}{1 - S_{22}\Gamma_L}, \quad \beta = \frac{1}{1 - \Gamma_S(S_{11} + S_{12}\Gamma_L\alpha)} \quad (3.18)$$

$$\begin{aligned} \text{and } b_2 &= b_S \alpha \beta = b_S \frac{S_{21}}{(1 - S_{22}\Gamma_L)} \frac{1}{\{1 - \Gamma_S[S_{11} + S_{12}S_{21}\Gamma_L/(1 - S_{22}\Gamma_L)]\}} \\ &= b_S \frac{S_{21}}{(1 - S_{22}\Gamma_L)} \frac{(1 - S_{22}\Gamma_L)}{[(1 - S_{22}\Gamma_L) - S_{11}\Gamma_S(1 - S_{22}\Gamma_L) + S_{12}S_{21}\Gamma_S\Gamma_L]} \\ &= b_S \frac{S_{21}}{1 - S_{22}\Gamma_L - S_{11}\Gamma_S + S_{11}S_{22}\Gamma_S\Gamma_L + S_{12}S_{21}\Gamma_S\Gamma_L} \\ &= b_S \frac{S_{21}}{(1 - S_{11}\Gamma_S)(1 - S_{22}\Gamma_L) - S_{12}S_{21}\Gamma_S\Gamma_L} \end{aligned} \quad (3.19)$$

Then the power delivered to the load is (using Equation (2.117))

$$P_L = \frac{1}{2} |b_2|^2 (1 - |\Gamma_L|^2) = \frac{\frac{1}{2} |b_S S_{21}|^2 (1 - |\Gamma_L|^2)}{|(1 - S_{11}\Gamma_S)(1 - S_{22}\Gamma_L) - S_{12}S_{21}\Gamma_S\Gamma_L|^2} \quad (3.20)$$

The **substitution loss**, L_S , is the ratio of the power delivered to the load by an initial two-port identified by the leading superscript ' i ', and the power delivered to the load with a final two port identified by the leading superscript ' f '. In decibels

$$L_S|_{\text{dB}} = 10 \log \left| \frac{i P_L}{f P_L} \right| = 10 \log \left| \frac{i S_{21}}{f S_{21}} \frac{[(1 - f S_{11}\Gamma_S)(1 - f S_{22}\Gamma_L) - f S_{12}^f S_{21}\Gamma_S\Gamma_L]}{[(1 - i S_{11}\Gamma_S)(1 - i S_{22}\Gamma_L) - i S_{12}^i S_{21}\Gamma_S\Gamma_L]} \right|^2 \quad (3.21)$$

Substitution loss is used in deriving formulas for insertion loss, see Section 2.8.2.

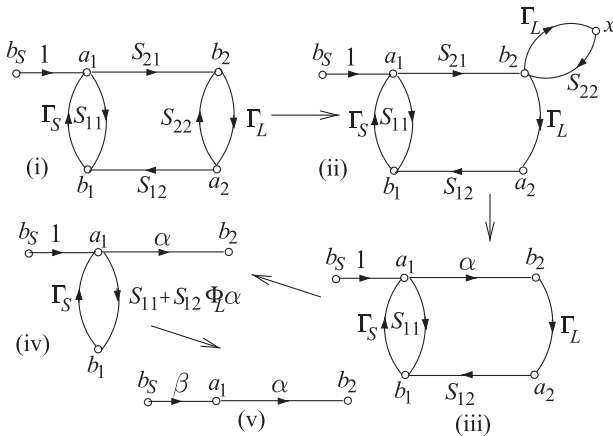


Figure 3-12: SFG manipulations in developing the power delivered to a load with a two-port network between source and load.

3.2.5 Mason's Rule

Mason's rule is a general procedure for reducing SFGs with multiple loops and is a systematic procedure for the reduction of SFGs to a single branch. Mason [6] derived the formula with the aim of developing a general method for the computer analysis of electrical circuits. First, a number of topology definitions must be introduced.

A path begins at one node and traverses a number of successive edges in the direction of the arrows to arrive at the final node or sink. In SFG analysis, a path is a forward path, as the successive edges are traversed in the direction of the arrows. An open path encounters the same node only once, and a closed path (or a loop) ends on the same node at which it is started. The product of the transmittances of all edges in a loop is called the loop transmittance. Two paths, open or closed, are said to be non-touching paths if they have no nodes in common. Similarly, disjoint loops are loops that have no nodes in common.

Mason's rule:

If T represents the overall graph transfer function and T_k represents the transfer function of the k th forward path from source to sink, then

$$T = \frac{1}{\lambda} \sum_k T_k \lambda_k, \quad (3.22)$$

where λ is the determinant of the matrix of coefficients of the equations represented by the SFG (usually called the determinant of the graph) and λ_k is the determinant of that part of the graph (subgraph) that does not touch the k th forward path. The determinant is given by

$$\lambda = 1 - \sum_j P_{j1} + \sum_j P_{j2} - \sum_j P_{j3} + \dots, \quad (3.23)$$

where the first summation in Equation (3.23) is the sum of the loop transfer functions of all the loops in the graph. In the second summation, the products of the transfer functions of all pairs of non-touching loops are added. In the third summation, the products of the transfer functions of disjoint loops taken three at a time are added, and so on. Mason's rule can be quite difficult to apply, but any problem that Mason's rule can solve can also be solved using multiple applications of SFG manipulations described previously.

EXAMPLE 3.3

Application of Mason's Rule

Use Mason's rule to reduce the SFG shown in Figure 3-13(a). Here, input node a_1 is the excitation and the output node b_4 is the response. The transmittance T is equal to b_4/a_1 .

Solution:

First, consider the determinant of the flow graph. Since all the loops have at least one node in common, the expression for the determinant reduces to

$$\lambda = 1 - \sum_j P_{j1}. \quad (3.24)$$

There are three loops identified in Figure 3-13(b) with transmittances $A = S_{21}S_{32}S_{13}$, $B = S_{32}S_{43}S_{24}$, and $C = S_{21}S_{32}S_{43}S_{14}$. Thus the sum of the loop transmittances is

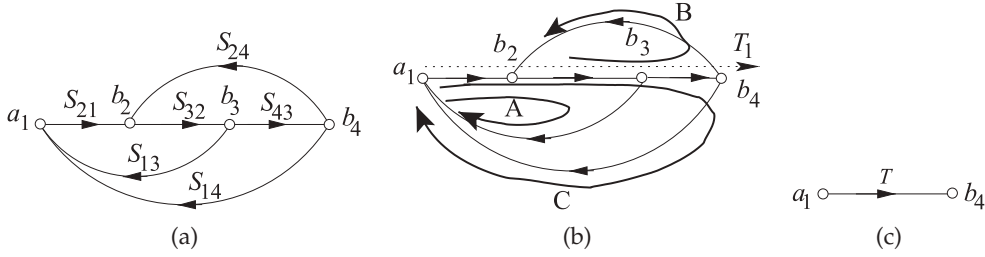


Figure 3-13: Signal flow graph used in Example 3.3 applying Mason's rule: (a) SFG; (b) annotation identifying loops and through-path; and (c) final reduction.

$$\sum_j P_{j1} = S_{21}S_{32}S_{13} + S_{32}S_{43}S_{24} + S_{21}S_{32}S_{43}S_{14} \quad (3.25)$$

and the determinant is given by

$$\lambda = 1 - S_{21}S_{32}S_{13} - S_{32}S_{43}S_{24} - S_{21}S_{32}S_{43}S_{14}. \quad (3.26)$$

This rule works well with the human ability to recognize patterns, in this case loops. There is only one forward path, identified in Figure 3-13(b), from source a_1 to sink b_4 , given by

$$T_1 = S_{21}S_{32}S_{43}. \quad (3.27)$$

Since all the loops of the graph have nodes that touch T_1 , then $\lambda_1 = 1$ and

$$\sum_k T_k \lambda_k = T_1 \lambda_1 = S_{21}S_{32}S_{43}. \quad (3.28)$$

$$\text{Thus } \frac{b_4}{a_1} = T = \frac{S_{21}S_{32}S_{43}}{1 - S_{21}S_{32}S_{13} - S_{32}S_{43}S_{24} - S_{21}S_{32}S_{43}S_{14}}. \quad (3.29)$$

This can be represented by a single edge from a_1 to b_4 as shown in Figure 3-13(c).

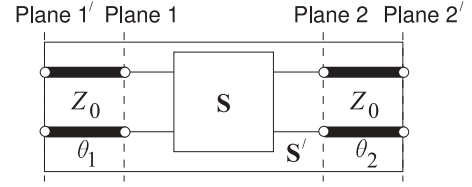
3.2.6 Summary

SFG reduction can be used with numerical values but the real power comes from the ability to develop symbolic expressions. In RF and Microwave engineering these expressions nearly always involve scattering parameters but they can be used with any sets of equations. Design is best undertaken by developing symbolic solutions as these enable optimization to be performed and insights gained as to the significance of parameters.

3.3 Polar Representations of Scattering Parameters

Scattering parameters are most naturally represented in polar form with the square of the magnitude relating to power flow. In this section a greater rationale for representing S parameters on a polar plot is presented and this serves as the basis for a more complicated representation of S parameters on a Smith chart to be described in the next section.

Figure 3-14: A two-port with scattering parameter matrix \mathbf{S} augmented by lines at each port with the line at Port n having the reference characteristic impedance at that port, i.e. Z_{0n} and with electrical length (in radians) of θ_n . The scattering parameter matrix of the augmented two-port is \mathbf{S}' .



3.3.1 Shift of Reference Planes as a S Parameter Rotation

A polar plot is a natural way to present S parameters graphically. In general S parameters are referenced to different characteristic impedances Z_{0n} at each port. Adding additional lengths of the lines at each port rotates the S parameters. Consider the two-port in Figure 3-14. Here the original two-port with scattering parameter matrix \mathbf{S} is augmented by lines at each port with each having a characteristic impedance equal to the reference impedance. The S parameter matrix of the augmented two-port, \mathbf{S}' , are the same as the original S parameter matrix but phase-shifted. That is

$$\mathbf{S}' = \begin{bmatrix} S'_{11} & S'_{12} \\ S'_{21} & S'_{22} \end{bmatrix} = \begin{bmatrix} S_{11}e^{-j2\theta_1} & S_{12}e^{-j(\theta_1+\theta_2)} \\ S_{21}e^{-j(\theta_1+\theta_2)} & S_{22}e^{-j2\theta_2} \end{bmatrix}. \quad (3.30)$$

The shift in reference planes simply rotates the S parameters. This is one of the main reasons why S parameters are commonly plotted on a polar plot.

3.3.2 Polar Plot of Reflection Coefficient

The polar plot of reflection coefficient is simply the polar plot of a complex number. Figure 3-15 is used in plotting reflection coefficients and is a polar plot that has a radius of one. So a reflection coefficient with a magnitude of one is on the unit circle. The center of the polar plot is zero so the reflection coefficient of a matched load, which is zero, is plotted at the center of the circle. Plotting a reflection coefficient on the polar plot enables convenient interpretation of the properties of a reflection. The graph has additional notation that enables easy plotting of an S parameter on the graph. Conversely, the magnitude and phase of an S parameter can be easily read from the graph. The horizontal label going from 0 to 1 is used in determining magnitude. The notation arranged on the outer perimeter of the polar plot is used to read off angle information. Notice the additional notation "ANGLE OF REFLECTION COEFFICIENT IN DEGREES" and the scale relates to the actual angle of the polar plot. Verify that the 90° point is just where one would expect it to be.

Figure 3-16 annotates the polar plot of reflection coefficient with real and imaginary axes and shows the location of the short circuit and open circuit points. Note that the reflection coefficient of an inductive impedance is in the top half of the polar plot while the reflection coefficient of a capacitive impedance is in the bottom half of the polar plot.

The nomograph shown in Figure 3-17 aids in interpretation of polar reflection coefficient plots. The nomograph relates the reflection coefficient (RFL. COEFFICIENT), ρ (ρ was originally used instead of Γ and is still used with the Smith chart); the return loss (RTN. LOSS) (in decibels); and the standing wave ratio (SWR); and the standing wave ratio (in decibels) as $20 \log(\text{SWR})$. When printed together with the reflection coefficient polar plot (Figures 3-15 and 3-17 combined) the nomograph is scaled properly, but

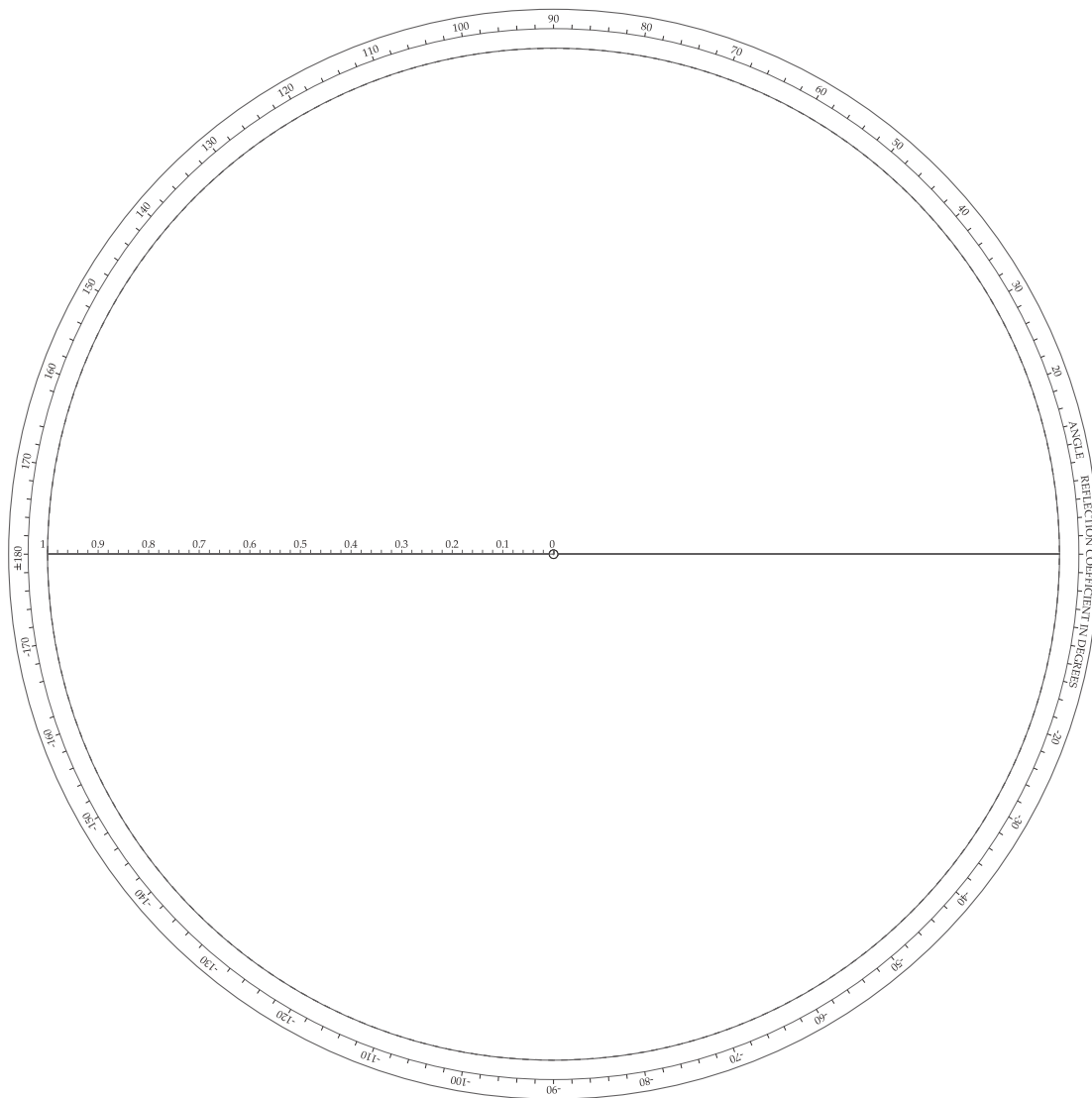


Figure 3-15: Polar chart for plotting reflection coefficient and transmission coefficient.

it is expanded here so that it can be read more easily. So with the aid of a compass with one point on the zero point of the polar plot and the other at the reflection coefficient (as plotted on the polar plot), the magnitude of the reflection coefficient is captured. The compass can then be brought down to the nomograph to read ρ , the return loss, and VSWR directly.

3.3.3 Summary

This section introduced the plotting of reflection coefficients as a complex number on a polar plot. The use of angle and magnitude scales make it easy to plot a complex number in magnitude-angle form but it is also easy to plot or read-off the complex number in real-imaginary form. Nomographs also enable return loss and SWR to be developed without calculation. The

Figure 3-16: Annotated polar plot of reflection coefficient with real, \Re , and imaginary, \Im , axes. The short circuit $\Gamma = -1$ and open circuit $\Gamma = +1$ are indicated. The reflection coefficient is referenced to a reference impedance Z_{REF} . Thus an impedance Z_L has the reflection coefficient $\Gamma = (Z_L - Z_{REF})/(Z_L + Z_{REF})$. An interesting observation is that the angle of Γ when Z_L is inductive, i.e. has a positive reactance, has a positive angle between 0° and 180° and so Γ is in the top half of the polar plot. Similarly the angle of Γ when Z_L is capacitive, i.e. has a negative reactance, has a negative angle between 0° and -180° and so Γ is in the bottom half of the polar plot.

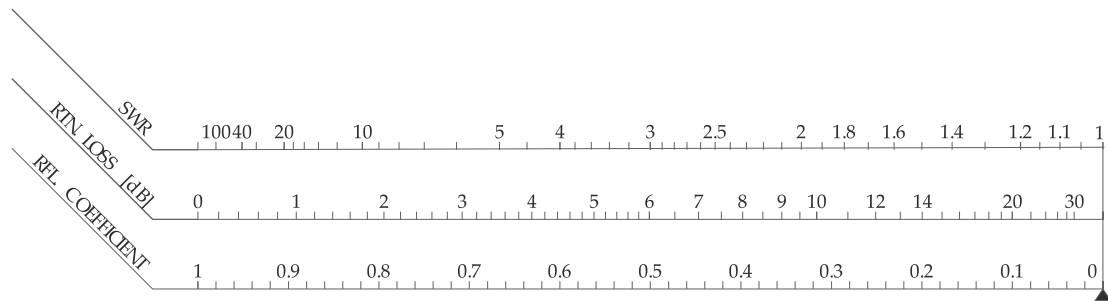
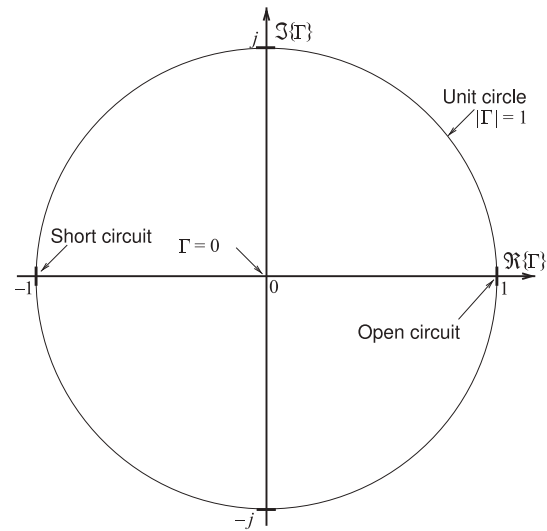


Figure 3-17: Nomograph relating the reflection coefficient (RFL. COEFFICIENT), ρ ; the return loss (RTN. LOSS) (in decibels); and the standing wave ratio (SWR).

transmission coefficient can be plotted on the same polar plot, i.e. Figure 3-15, as the polar plot is the representation of a complex number.

3.4 Smith Chart

The Smith chart is a powerful graphical tool used in the design of microwave circuits. Mastering the Smith chart is essential to entering the world of RF and microwave circuit design as all practitioners use this as if it is well understood by others. It takes effort to master but fundamentally it is quite simple combining a polar plot used for plotting S parameters directly, curves that enable normalized impedances and admittances to be plotted directly, and scales that enable electrical lengths in terms of wavelengths and degrees to be read off. The chart has many numbers printed in quite small font and with signs dropped as there is not room.

The Smith chart was invented by Phillip Smith and presented in close to its current form in 1937, see [7–10]. Once nomographs and graphical calculators were common engineering tools mainly because of limited computing resources. Only a few have survived in electrical engineering usage, with Smith charts being overwhelmingly the most important.

This section first presents the impedance Smith chart and then the admittance Smith chart before introducing a combined Smith chart which is the form needed in design. The Smith chart presents a large amount of information in a confined space and interpretation, such as applying appropriate signs, is required to extract values. The Smith chart is a 'back-of-the-envelope' tool that designers use to sketch out designs.

3.4.1 Impedance Smith Chart

The reflection coefficient, Γ , is related to a load, Z_L , by

$$\Gamma = \frac{Z_L - Z_{\text{REF}}}{Z_L + Z_{\text{REF}}}, \quad (3.31)$$

where Z_{REF} is the system reference impedance. With normalized load impedance $z_l = r + jx = Z_L/Z_{\text{REF}}$, this becomes

$$\Gamma = \frac{r + jx - 1}{r + jx + 1}. \quad (3.32)$$

Commonly in network design reactive elements are added either in shunt or in series to an existing network. If a reactive element is added in series then the input reactance, x , is changed while the input resistance, r , is held constant. So superimposing the loci of Γ (on the S parameter polar plot) with fixed values of r , but varying values of x (x varying from $-\infty$ to ∞), proves useful, as will be seen. Another loci of Γ with fixed values of x and varying values of r (r varying from 0 to ∞) is also useful. The combination of the reflection/transmission polar plots, the nomographs, and the r and x loci is called the impedance Smith chart, see Figure 3-18. This is still a polar plot of reflection coefficient and the arcs and circles of constant resistance enable easy conversion between reflection coefficient and impedance.

The full impedance Smith chart shown in Figure 3-18 is daunting so discussion will begin with the less dense form of the impedance Smith chart shown in Figure 3-19(a) which is annotated in Figure 3-19(b). Referring to Figure 3-19(b), the unit circle corresponds to a reflection coefficient magnitude of one and hence a pure reactance. Note that there are lines of constant resistance and arcs of constant reactance. All points in the top half of the Smith chart have positive reactances and so all reflection coefficient points plotted in the top half of the Smith chart indicate inductive impedances. All points in the bottom half of the Smith chart have negative reactances and so all reflection coefficient points plotted in the bottom half of the Smith chart indicate capacitive impedances. The horizontal line across the middle of the Smith chart indicates pure resistance.

A point on the unit circle indicate that the resistance of the point is zero, while a reflection coefficient point inside the unit circle indicates a finite positive resistance.

One big difference between the less dense form of the impedance Smith chart, Figure 3-19(a), and the full impedance Smith chart of Figure 3-18 is that the signs of the reactances are missing in the full impedance Smith chart. This is simply because there is not enough room and the user must add the appropriate sign when reading the chart. Thus it is essential that the user keep the annotations in Figure 3-19(b) in mind. Yet another factor that makes it difficult to develop essential Smith chart skills.

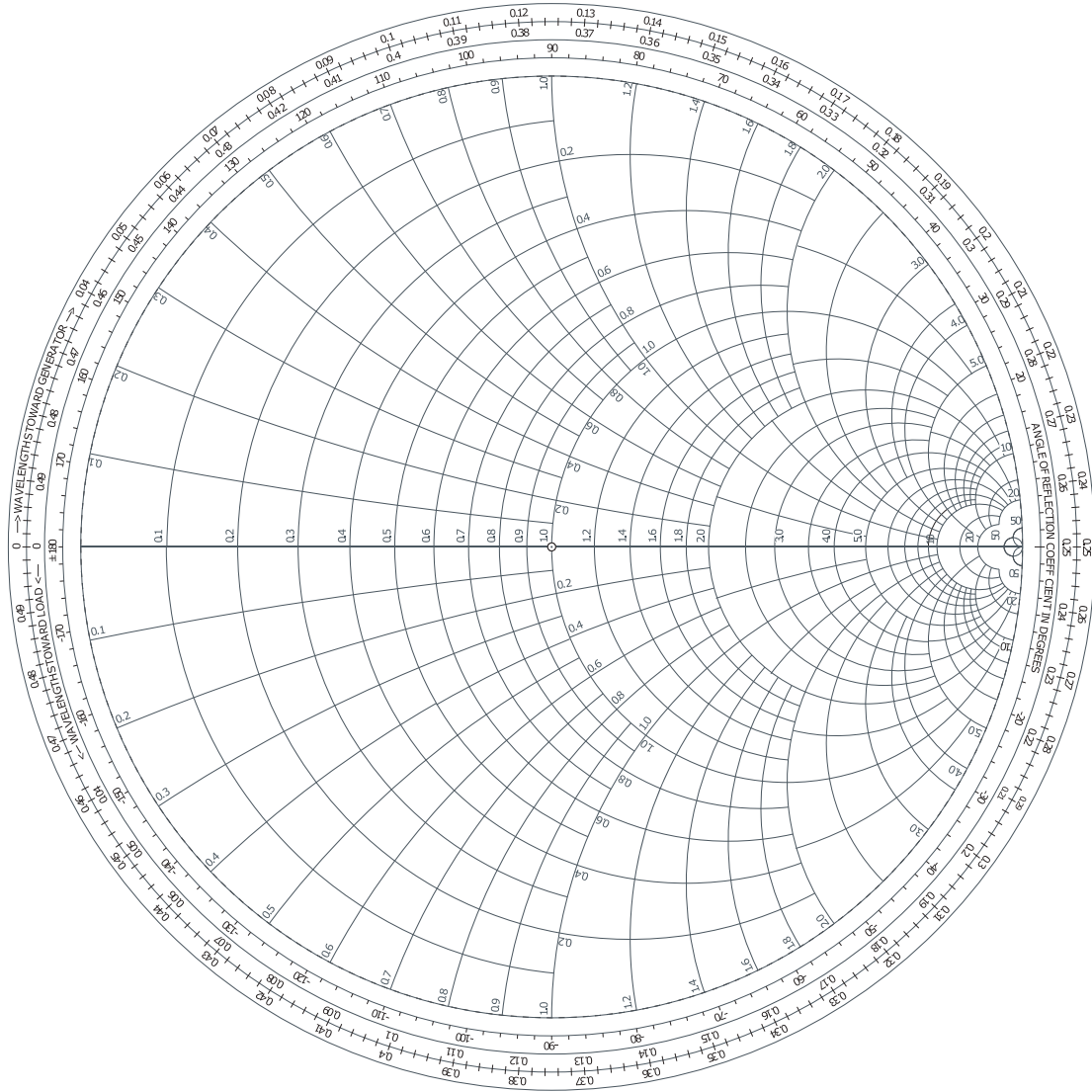


Figure 3-18: Impedance Smith chart. Also called a normalized Smith chart since resistances and reactances have been normalized to the system reference impedance Z_{REF} : $z = Z/Z_{\text{REF}}$.

A point plotted on the Smith chart represents a complex number A . The magnitude of A is obtained by measuring the distance from the origin of the polar plot (the same as the origin of the Smith chart in the center of the unit circle) to point A , say using a ruler, and comparing that to the measurement of the radius of the unit circle which corresponds to a complex number with a magnitude of 1. The angle in degrees of the complex number A is read from the innermost circular scale. The technique used is to draw a straight line from the origin through point A out to the circular scale.

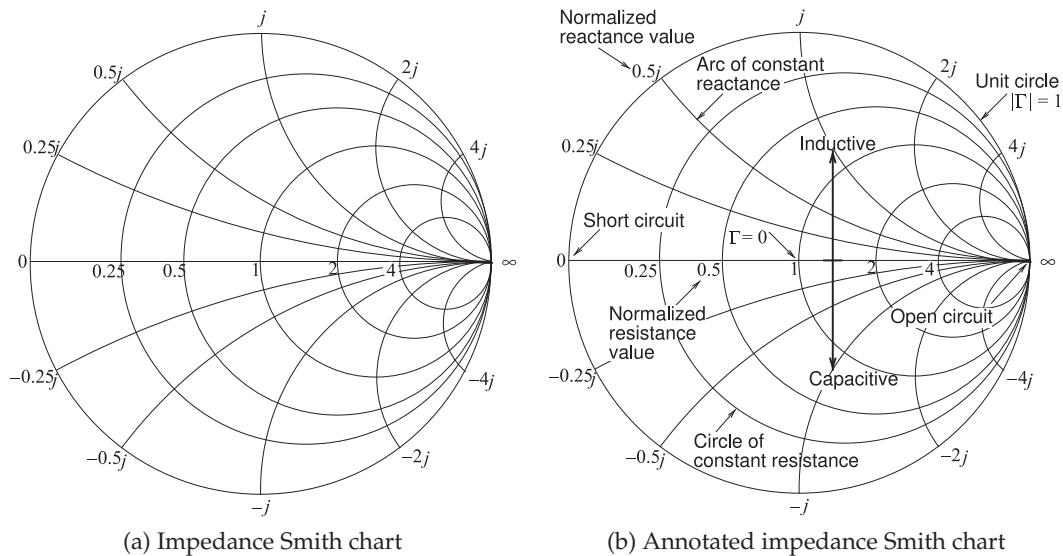


Figure 3-19: Normalized impedance Smith charts.

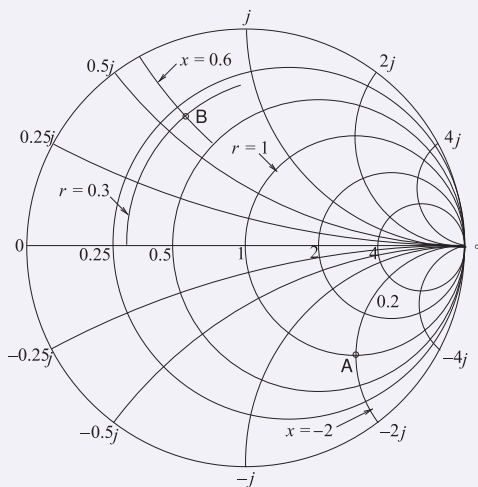
EXAMPLE 3.4 Impedance Plotting

Plot the normalized impedances $z_A = 1 - 2j$ and $z_B = 0.3 + 0.6j$ on an impedance Smith chart.

Solution:

The impedance $z_A = 1 - 2j$ is plotted as Point A to the right. To plot this, first identify the circle of constant normalized resistance $r = 1$, and then identify the arc of constant normalized reactance $x = -2$. The intersection of the circle and arc locates z_A at point A. The reader is encouraged to do this with the full impedance Smith chart as shown in Figure 3-18. Recall that signs of reactances are missing on the full chart. As an exercise read off the reflection coefficient (the answer is $0.5 - j0.5 = 0.707 \angle -45^\circ$).

The impedance $z_B = 0.3 + 0.6j$ is plotted as Point B which is at the intersection of the circle $r = 0.3$ and the arc $x = +0.6$. Interpolation is required to identify the required circle and arc. The reader should do this with the full impedance Smith chart. As an exercise read off the reflection coefficient (the answer is $-0.268 + j0.585 = 0.644 \angle 115^\circ$).



EXAMPLE 3.5**Impedance Synthesis**

Use a length of terminated transmission line to realize an impedance of $Z_{in} = j140 \Omega$.

Solution:

The impedance to be synthesized is reactive so the termination must also be lossless. The simplest termination is either a short circuit or an open circuit. Both cases will be considered. Choose a transmission line with a characteristic impedance, Z_0 , of 100Ω so that the desired normalized input impedance is $j140 \Omega / Z_0 = 1.4j$, plotted as point B in Figure 3-20.

First, the short-circuit case. In Figure 3-20, consider the path AB. The termination is a short circuit and the impedance of this load is Point A with a reference length of $\ell_A = 0 \lambda$ (from the outermost circular scale). The corresponding reflection coefficient reference angle from the scale is $\theta_A = 180^\circ$ (from the innermost circular scale labeled 'WAVELENGTHS TOWARDS THE GENERATOR' which is the same as 'wavelengths away from the load'). As the line length increases, the input impedance of the terminated line follows the clockwise path to Point B where the normalized input impedance is $j1.4$. (To verify your understanding that the locus of the reflection coefficient rotates in the clockwise direction, i.e. increasingly negative angle, as the line length increases see Section 2.3.3 of [11].) At Point B the reference line length $\ell_B = 0.1515 \lambda$ and the corresponding reflection coefficient reference angle from the scale is $\theta_B = 71.2^\circ$. The reflection coefficient angle and length in terms of wavelengths were read directly off the Smith chart and care needs to be taken that the right sign and correct scale are used. A good strategy is to correlate the scales with the easily remembered properties at the open-circuit and short-circuit points. Here the line length is

$$\ell = \ell_B - \ell_A = 0.1515\lambda - 0\lambda = 0.1515\lambda, \quad (3.33)$$

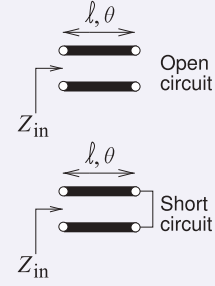
and the electrical length is half of the difference in the reflection coefficient angles,

$$\theta = \frac{1}{2} |\theta_B - \theta_A| = \frac{1}{2} |71.2^\circ - 180^\circ| = 54.4^\circ, \quad (3.34)$$

corresponding to a length of $(54.4^\circ / 360^\circ)\lambda = 0.1511\lambda$ (the discrepancy with the previously determine line length of 0.1515λ is small). This is as close as could be expected from using the scales. So the length of the stub with a short-circuit termination is 0.1515λ .

For the open-circuited stub, the path begins at the infinite impedance point $\Gamma = +1$ and rotates clockwise to Point A (this is a 90° or 0.25λ rotation) before continuing on to Point B. For the open-circuited stub,

$$\ell = 0.1515\lambda + 0.25\lambda = 0.4015\lambda. \quad (3.35)$$

**3.4.2 Admittance Smith Chart**

The admittance Smith chart has loci for discrete constant susceptances ranging from $-\infty$ to ∞ , and for discrete constant conductance ranging from 0 to ∞ , see Figure 3-21. A less dense form is shown in Figure 3-22(a). This chart looks like the flipped version of the impedance Smith chart but it is the same polar plot of a reflection coefficient so that the positions of the open and short circuit remain the same as do the capacitive and inductive halves of the Smith chart. In the full version of the admittance Smith chart, Figure 3-21, signs have been dropped as there is not room for them. Thus interpreting admittances from the chart requires that the user separately determine the signs of susceptances. The less dense version, Figure 3-22(a), retains the signs making it easier to follow some of the discussions and examples. It is important that the user readily understand the annotations on the less dense form of the Smith chart, see Figure 3-22(b).

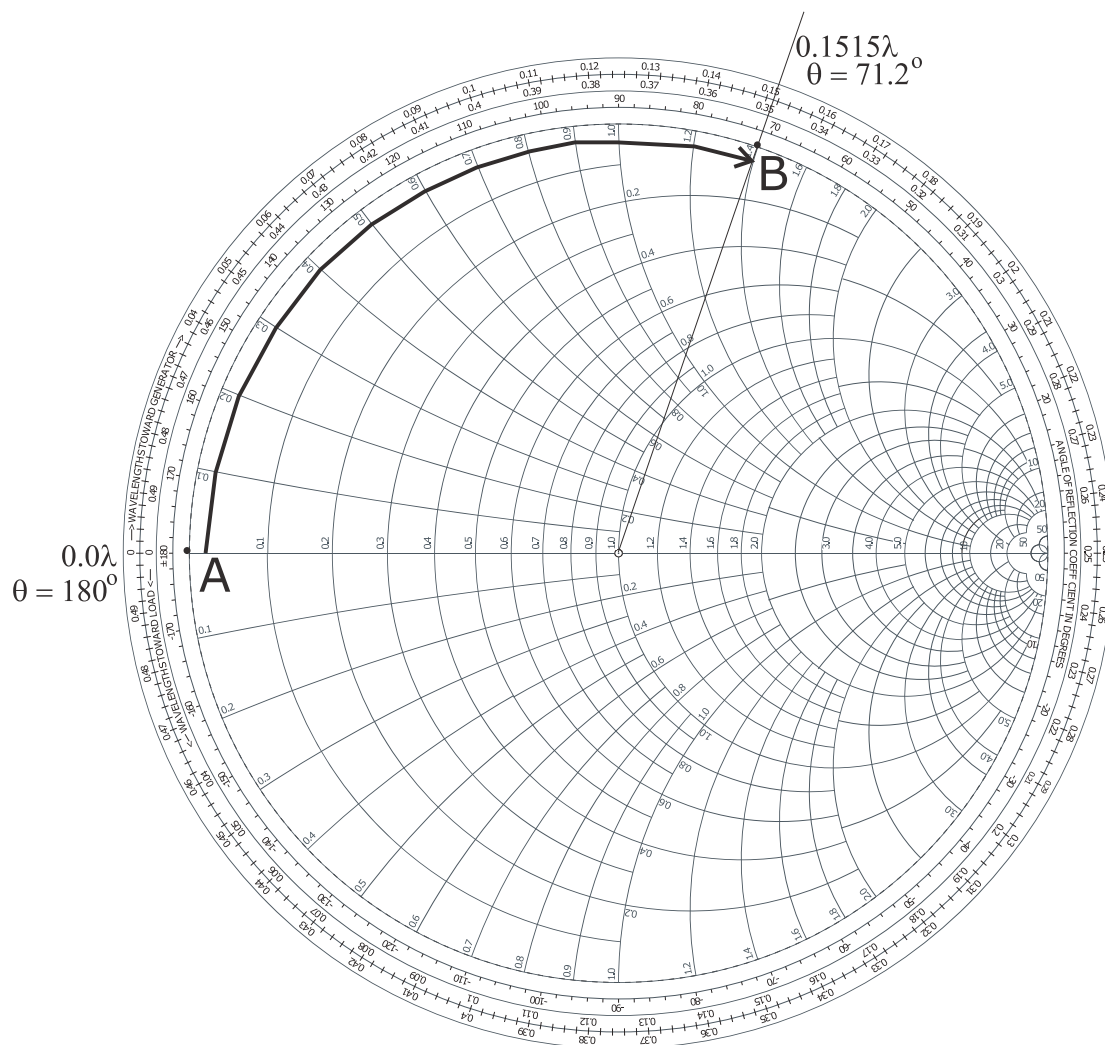


Figure 3-20: Design of a short-circuit stub with a normalized input impedance of $j1.4$. The path AB is actually on the unit circle but has been displaced here to avoid covering numbers. The electrical length in wavelengths has been read from the outermost circular scale, and the angle, θ , in degrees refers to the angle of the polar plot (and is twice the electrical length).

3.4.3 Combined Smith Chart

The combination of the reflection/transmission polar plots, nomographs, and the impedance and admittance Smith chart leads to the combined Smith chart (see Figure 3-23). This color Smith chart is the preferred version for use in design and the separate impedance and admittance versions of the Smith chart are rarely used. The combined Smith chart is rich with information and care is required to identify the lines that correspond to admittances (specifically lines of constant normalized conductance and constant normalized susceptances), and the lines that correspond to impedances (constant normalized resistances and constant normalized

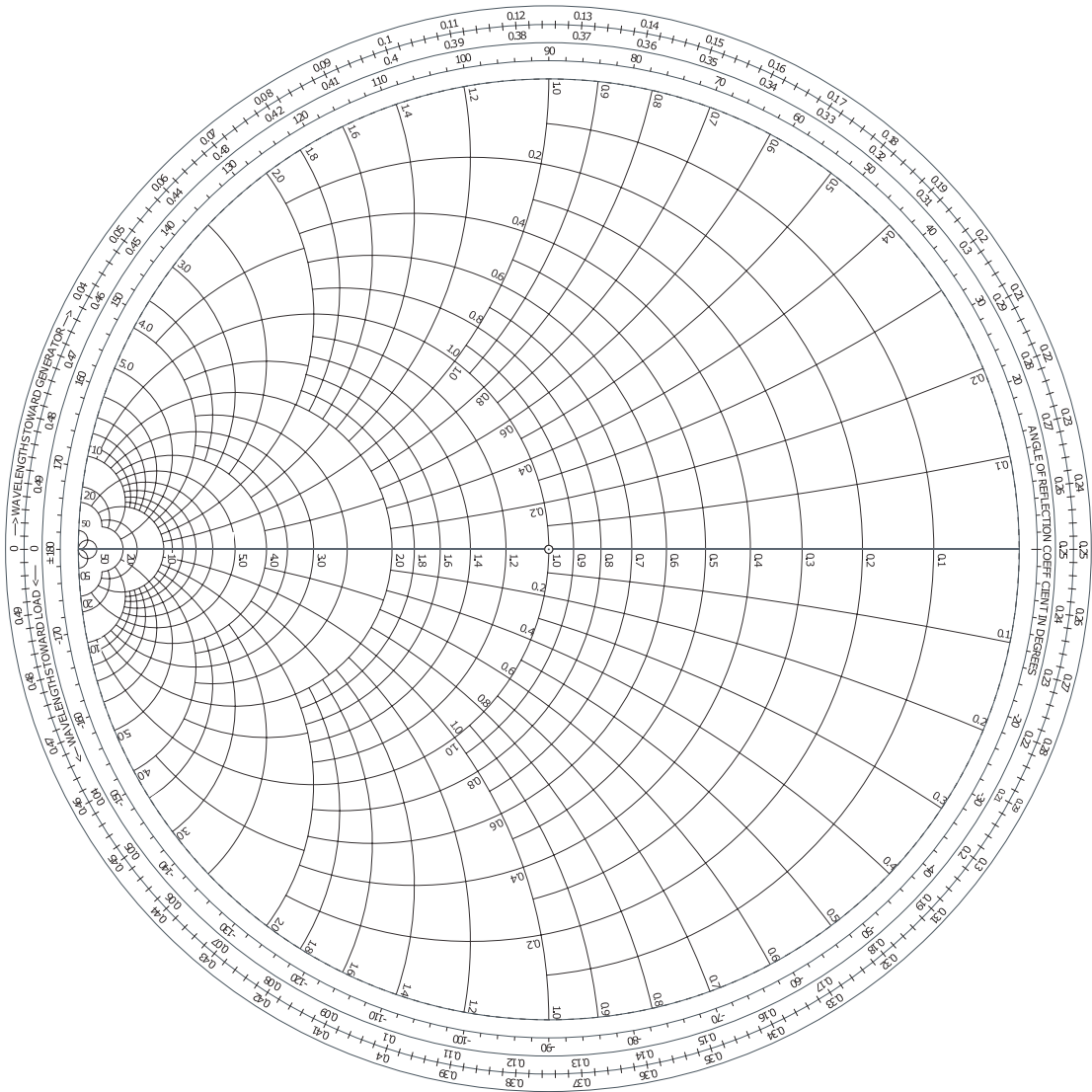


Figure 3-21: Admittance Smith chart.

reactances). The signs of the reactances and susceptance are missing and left to the user to add them depending on whether a reflection coefficient point is capacitive (in the lower half of the Smith chart and hence susceptances are positive and reactances are negative) or whether a point is inductive (in the upper half of the Smith chart and hence susceptances are negative and reactances are positive). A less dense version of the combined Smith chart, with the addition of signs, is shown in Figure 3-24(a).

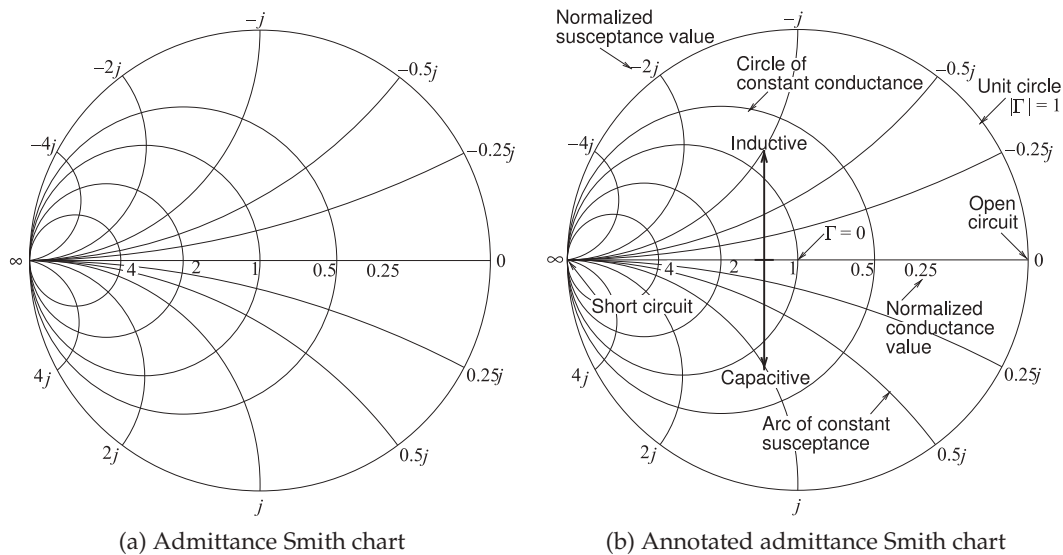


Figure 3-22: Normalized admittance Smith chart.

EXAMPLE 3.6 Impedance to Admittance Conversion

Use a Smith chart to convert the impedance $z = 1 - 2j$ to an admittance.

Solution:

The impedance $z = 1 - 2j$ is plotted as Point A in Figure 3-24(b). To read the admittance from the chart, the lines of constant conductance and constant susceptance must be interpolated from the arcs and circles provided. The interpolations are shown in the figure, indicating a conductance of 0.2 and a susceptance of $0.4j$. Thus

$$y = 0.2 + 0.4j.$$

(This agrees with the calculation: $y = 1/z = 1/(1 - 2j) = 0.2 + 0.4j$.)

Adding Reactance and Susceptance

A good amount of microwave design, such as designing a matching network for maximum power transfer, involves beginning with a load impedance plotted on a Smith chart and inserting series and shunt reactances, and transmission lines, to transform the impedance to another value. The preferred view of the design process is that of a reflection coefficient that gradually evolves from one value to another. That is, in the case of a series reactance, the effect is that of a reflection coefficient gradually changing as the reactances increase from zero to its actual value. The path traced out by the gradually evolving reflection coefficient value is called a locus. The loci of common circuit elements added to various loads are shown in Figure 3-25. For each locus the load is at the start of the arrow with the value of the element increasing from zero to its actual final value at the arrow head.

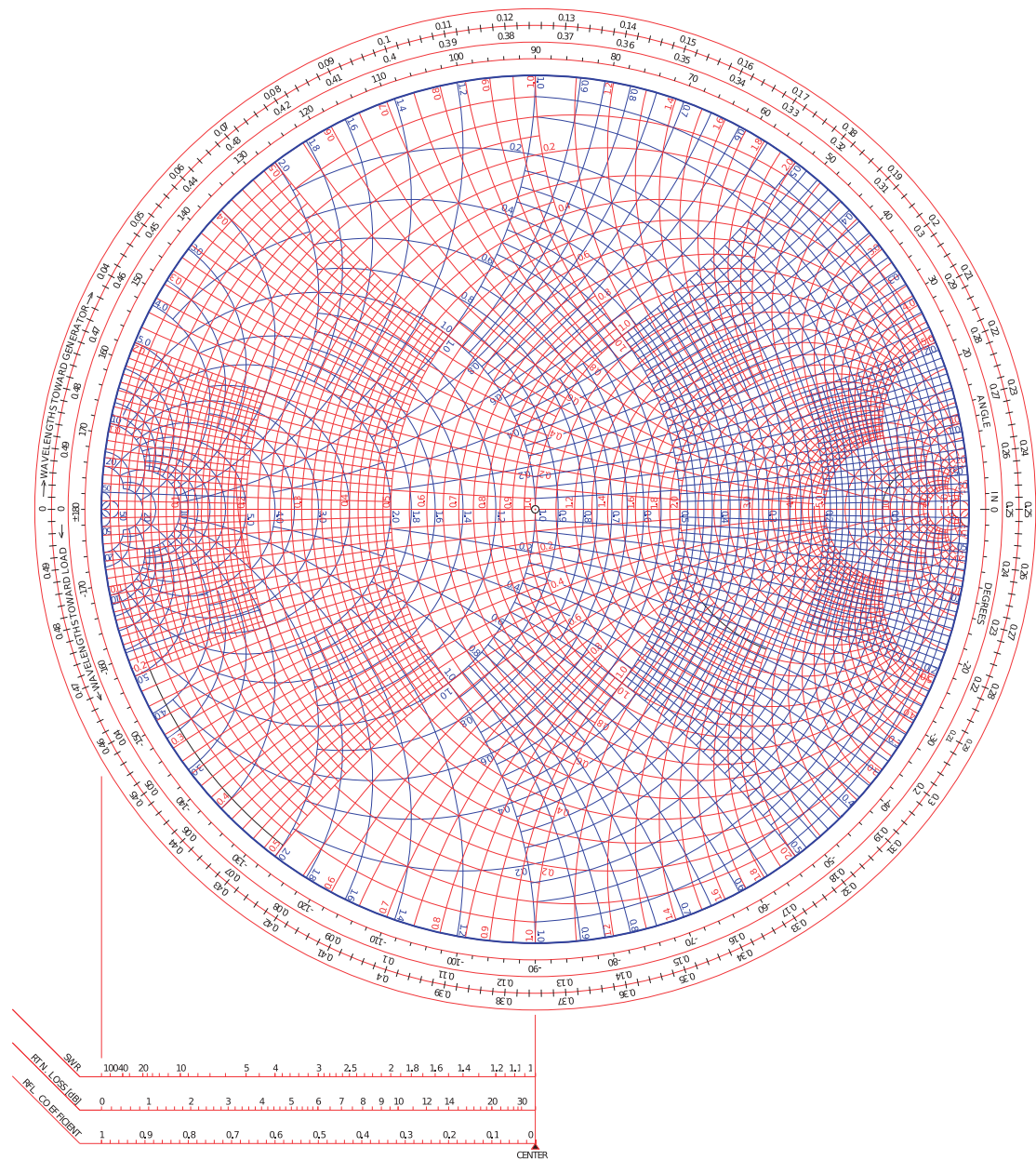


Figure 3-23: Normalized combined Smith chart combining impedance and admittance Smith charts.

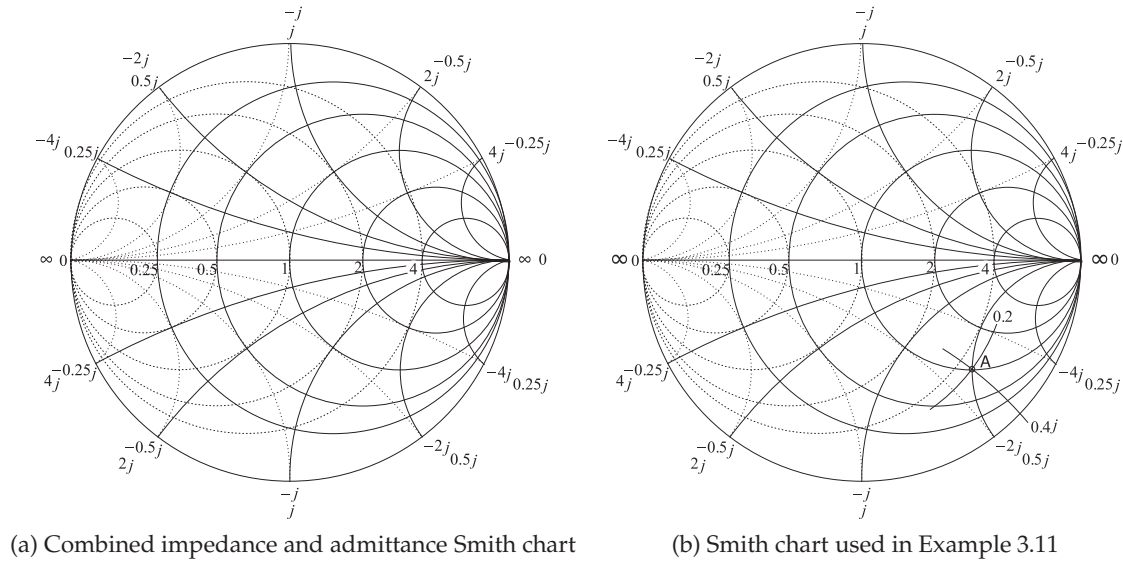


Figure 3-24: Combined impedance and admittance Smith chart.

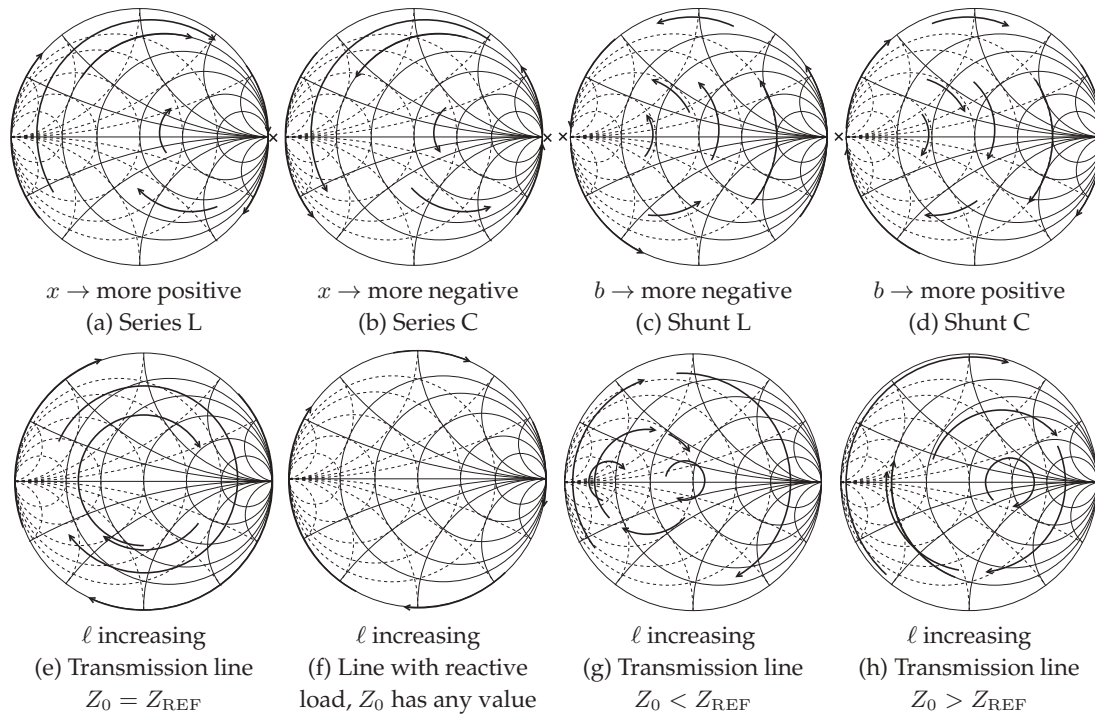


Figure 3-25: Reflection coefficient locus of a load augmented by elements as indicated. The original load is at the start of the arrowed arc. In (a) and (b) the locus is with respect to increasing $|x|$ (normalized reactance magnitude), in (c) and (d) the locus is with respect to increasing $|b|$ (normalized susceptance magnitude), and in (e)–(h) with respect to increasing length ℓ . In (e)–(h) the loci are parts of circles centered on the $x = 0$ line. x indicates that the locus cannot cross infinity (open circuit for (a) and (b), short circuit for (c) and (d)).

3.4.4 Smith Chart Manipulations

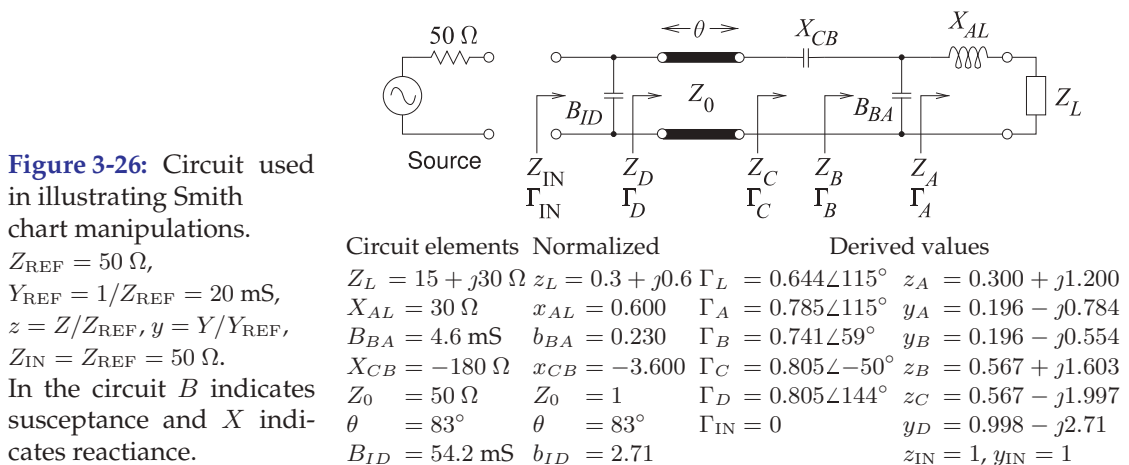
Microwave design often proceeds by taking a known load and transforming it into another impedance, perhaps for maximum power transfer. Smith charts are used to show these manipulations. In design the manipulations required are not known up front and the Smith chart enables identification of those required. Except for particular situations, lossless elements such as reactances and transmission lines are used. The few situations where resistances are introduced include introducing stability in oscillators and amplifiers, and deliberately reduce signals levels. Most of the time introducing resistances unnecessarily increases noise and reduces signal levels thus reducing critical signal-to-noise ratios.

The circuit in Figure 3-26 will be used to illustrate the representation of manipulations on a Smith chart. The most common view is to consider that the Smith chart is a plot of the reflection coefficient at various stages in the circuit, i.e., Γ_A , Γ_B , Γ_C , Γ_D , and Γ_{IN} . Additionally the load, Z_L , is plotted and reactances, susceptances, or transmission lines transform the reflection coefficient from one stage to the next. Yet another concept is the idea that the effect of an element is regarded as gradually increasing from a negligible value up to the final actual value and in so doing tracing out a locus which ends in an arrow head. This is the approach nearly all RF and microwave engineers use. The manipulations corresponding to the circuit are illustrated in Figure 3-27. The individual steps are identified in Figure 3-28. The first few steps are confined to the top half of the Smith chart which is repeated on a larger scale in Figure 3-29 for the first three steps.

Step 1 L, a, b, c, d, e, f

The first step is to plot the load Z_L on a Smith chart and this is the Point L in Figures 3-27–3-29. The reference impedance Z_{REF} is chosen to be $50\ \Omega$, the same as the characteristic impedance of the transmission line in the circuit. The Smith chart is now known as a $50\text{-}\Omega$ Smith chart. This is a common choice because then the locus of reflection coefficient variation introduced by the line will be a circle centered at the origin of the Smith chart. To plot L derive the normalized load impedance $z_L = Z_L/Z_{REF} = 0.3 + j0.6$ (future numerical values are given in Figure 3-26).

To plot z_L the normalized resistance circle for 0.3 and the normalized



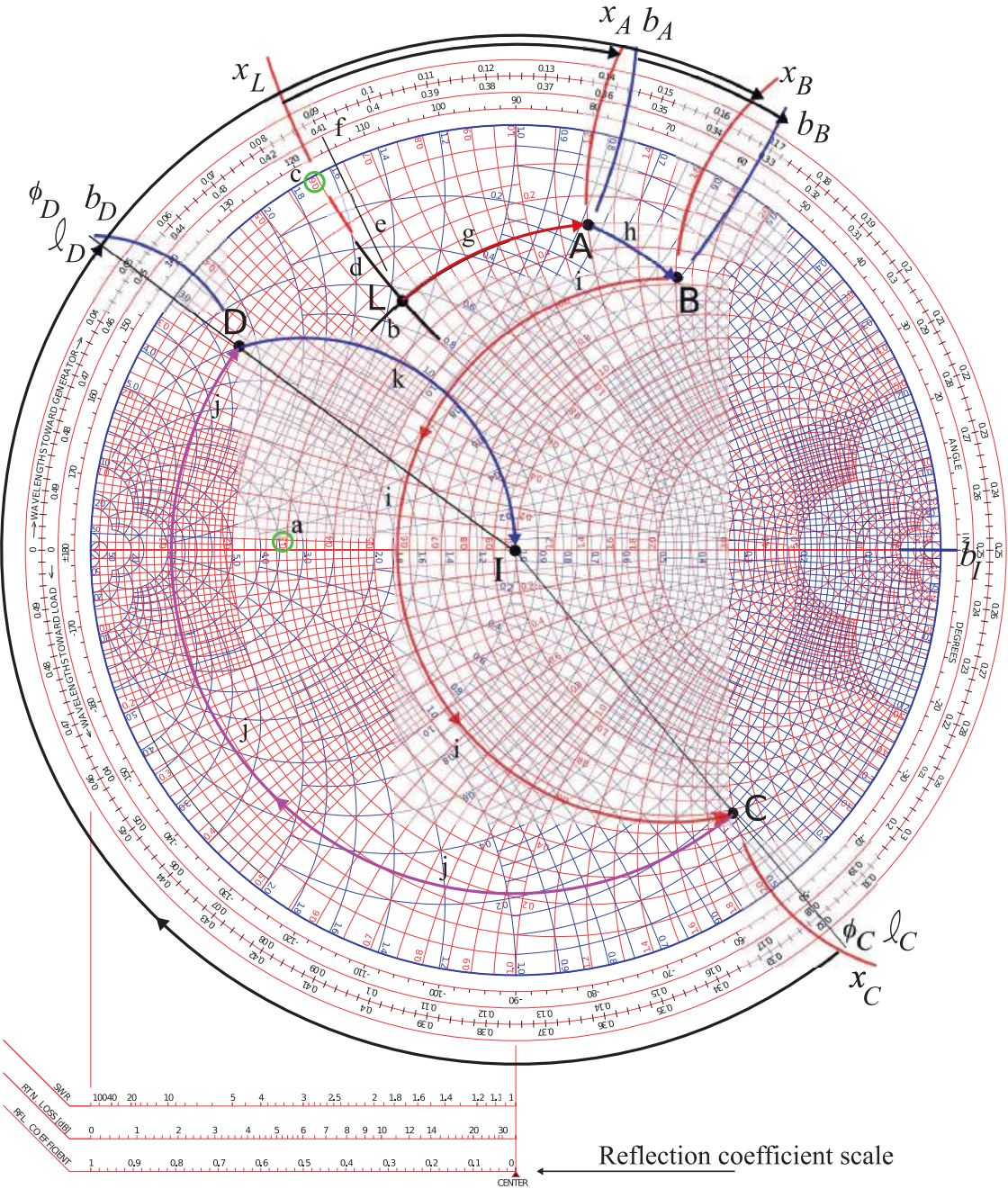


Figure 3-27: Smith chart manipulations corresponding to the circuit in Figure 3-26 with circuit elements added one at a time beginning with the load impedance at Point L.

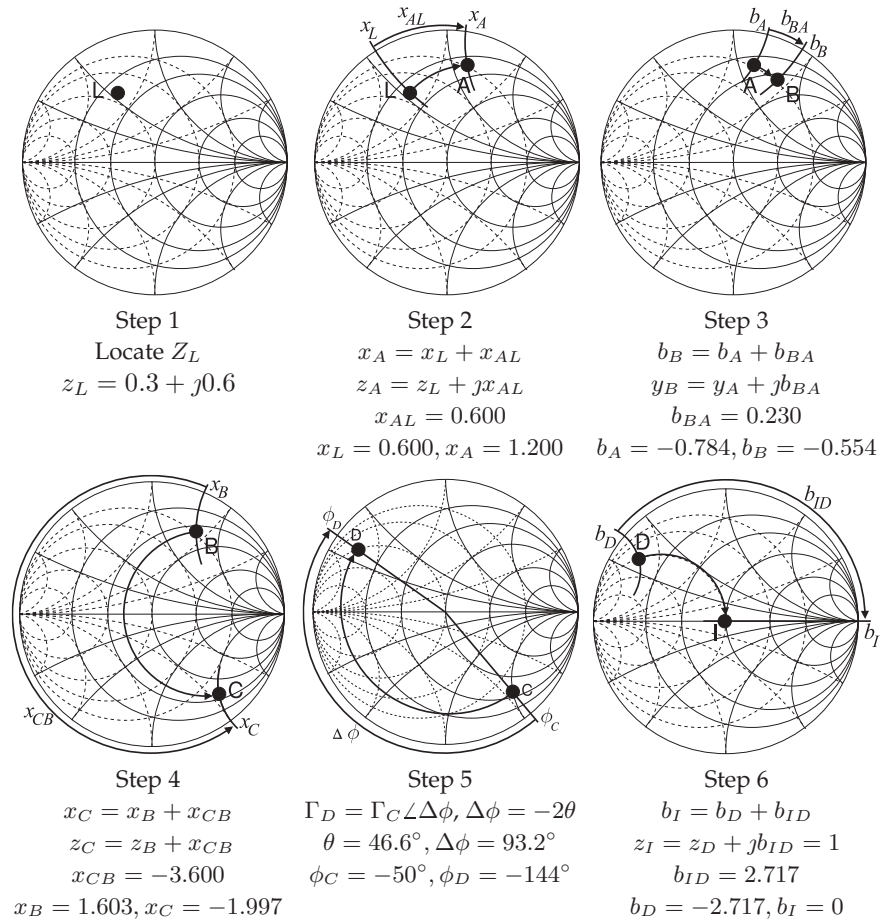


Figure 3-28: Steps in the Smith chart manipulations shown in Figures 3-27 and 3-29.

reactance arc for +0.3 must be located. The resistance circle is identified from the scale on the horizontal axis of the Smith chart, see the circled value labeled 'a'. Locating the +0.3 reactance arc is not as direct as the signs of reactance are missing on the Smith chart. Referring back to Figure 3-19 it is noted that an inductive impedance is in the top half of the Smith chart and so positive reactances are in the top half. Thus the +0.3 reactance arc is in the top half of the Smith chart and the correct arc is identified by 'c'. From the curves identified by 'a' and 'c' the arcs 'b' and 'd' are drawn with the impedance z_L , i.e. point L, at the intersection of the arcs.

It is instructive to determine Γ_L , the reflection coefficient at L. On the Smith chart the reflection coefficient vector Γ_L is drawn from the origin to the point L. Γ_L is evaluated by separately determining its magnitude and angle. To determine the magnitude measure the length of the $|\Gamma_L|$ vector either using a ruler, a compass, or marking the edge of a piece of paper. Then this length can be compared against the reflection coefficient scale shown at the bottom of Figure 3-27 yielding $|\Gamma_L| = 0.644$. The angle of Γ_L is read by extending the Γ_L vector out to the inner most circular scale on the Smith chart. This extension is labeled as e. The angle is read at point 'f' as 115° . Thus $\Gamma_L = 0.644 \angle 115^\circ$.

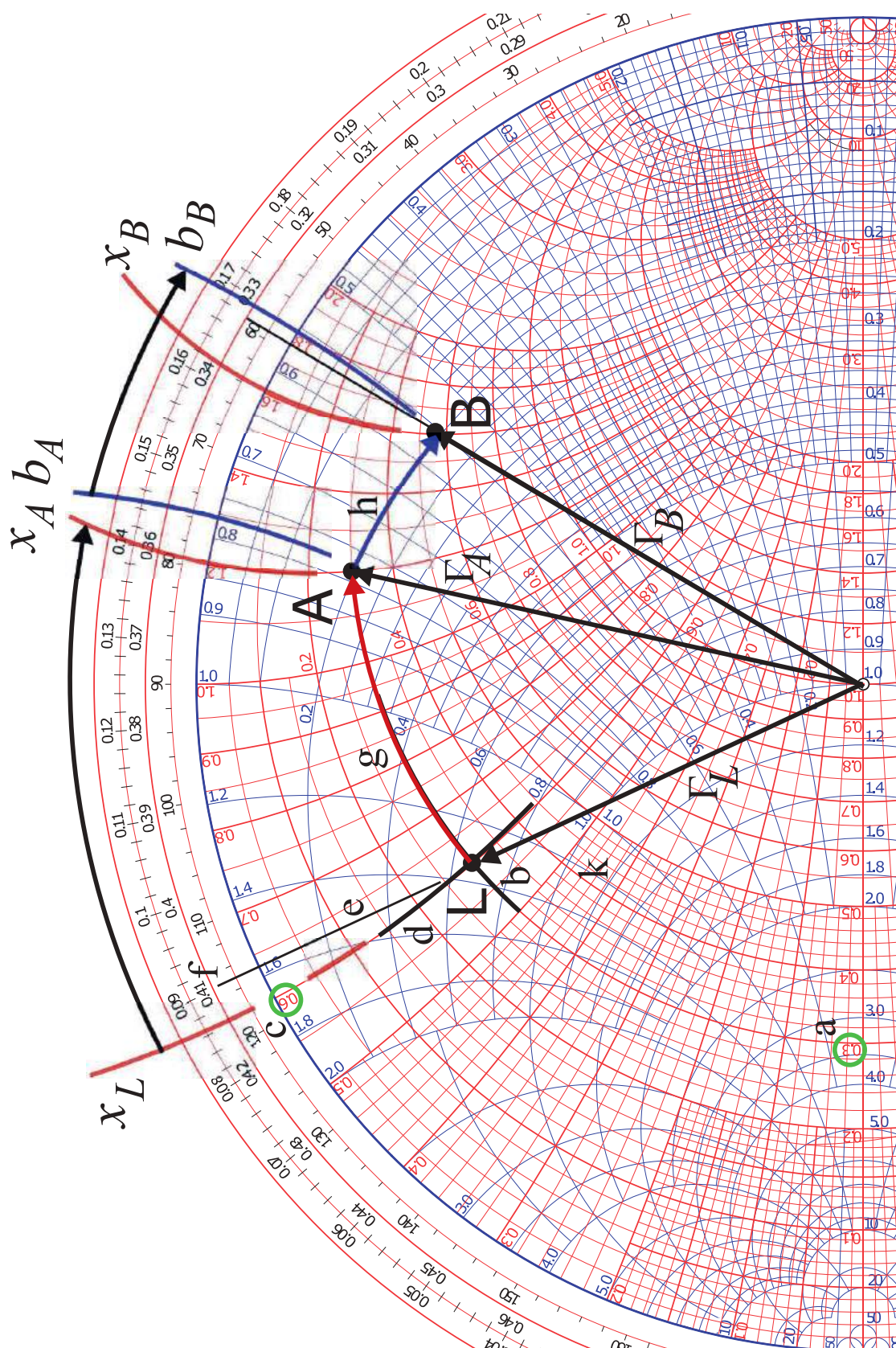


Figure 3-29: The first three steps in the Smith chart manipulations in Figure 3-27.

Step 2 Add the series reactance X_{AL} , path L to A, g

In step 2 an inductor with reactance X_{AL} is in series with Z_L and the reflection coefficient transitions from point L to point A. Now $x_L = \Im\{z_L\} = 0.6$. To this $x_{AL} = 0.6$ is added so that the normalized reactance at A is $x_A = x_L + x_{AL} = 0.6 + 0.6 = 1.2$. The locus of this operation is the arc, 'g', extending from L with gradually increasing series reactance until the full value x_{AL} , at the arrowhead of the locus, is obtained. The procedure is to identify the arc of $x_A = +1.2$ reactance and then follow the circle of constant resistance (since the resistance is not changing) up to this arc. This operation traces out the locus 'g'.

Step 3 Add the shunt susceptance B_{BA} , path A to B, h

In step 3 a capacitor with susceptance X_{BA} is in shunt with Z_A and the reflection coefficient transitions from point A to point B. The locus of this operation follows a circle of constant conductance with only the susceptance changing. The final value must be calculated as $b_B = b_A + b_{BA}$. The susceptance b_B is read from the graph as -0.784 . This value is read by following the arc of constant susceptance out to the unit circle where a value of 0.784 is read. Note that the arc must be interpolated and that the user must realize that the susceptance is negative in the top half of the Smith chart so the susceptance must be negative even though a minus sign is not shown on the Smith chart. Thus the correct reading for x_A is -0.784 . Now $b_{BA} = +0.230$ so the locus, 'h', of the transition follows the circle of constant conductance ending at the (interpolated arc) with susceptance $b_B = b_a + b_{BA} = -0.784 + 0.230 = -0.554$.

Step 4 Add the series reactance X_{CB} , path B to C, i

In step 4 a capacitor with reactance X_{CB} is in series with Z_B and the reflection coefficient transitions from point B to point C. Now x_B is read from the graph as $+1.603$. To this add $x_{CB} = -3.600$ so that the normalized reactance at C is $x_C = x_B + x_{CB} = 1.603 + (-3.600) = -1.997$. The locus from B to C, path 'i', begins at B and follows a circle of constant resistance up to the arc with normalized reactance $x_C = -1.997$. This reactance arc is in the bottom half of the Smith chart as reactances are negative there even though the signs are missing on the labels of the reactance arcs in the bottom half of the chart. The locus of this operation is the arc, 'g', from L with gradually increasing series reactance until the full value z_{CB} , at the arrowhead of the locus, is obtained. The procedure is to identify the arc of $x_C = -1.997$ reactance and then follow the circle of constant resistance (since the resistance is not changing) up to this arc. This traces out the locus 'i'.

Step 5 Insert the transmission line, path C to D, j

Step 5 illustrates a different type of manipulation as now there is a transmission line and the reflection coefficient transitions from Γ_C , i.e. point C to the input reflection coefficient of the line Γ_D . The locus of this transition must be clockwise, i.e. having increasingly negative angle (as discussed in Section 2.3.3 of [11]). The electrical length of the transmission line is $\theta = 83^\circ$ and the reflection coefficient changes by the negative of twice this amount, $\phi_{DC} = -2\theta = -166^\circ$. The locus is drawn in Figure 3-27 with the transmission line gradually increasing in length tracing out a circle which, since $Z_0 = Z_{REF}$, is centered at the origin of the Smith cart. The procedure is to find the scale value of the angle at point C which is read by drawing a line from the origin through C intersecting the reflection coefficient angle scale

(the innermost circular scale) yielding $\phi_C = -50.4^\circ$ and so $\phi_D = \phi_C + \phi_{DC} = -50.4^\circ - 166^\circ + 360^\circ = +143.6^\circ$. The locus from C to D is drawn by first drawing a line from the origin to the $\phi_D = -143.6^\circ$ point on the angle scale. Then point D will be at the intersection of this line and a circle of constant radius drawn through C. The locus is shown as path 'j' in Figure 3-27.

Step 6 Add the shunt susceptance B_{ID} , path D to l, k

The final step is to add the shunt capacitor with susceptance B_{ID} to Z_D . Following the previous procedure b_D is read as -2.71 to which $b_{ID} = 2.71$ is added so that $b_I = 0$ which is just the horizontal line across the middle of the Smith chart. This line corresponds to zero reactance and zero susceptance. The locus, path 'k', extends from D to l following the circle of constant conductance. The final result is that $z_{IN} = 1.00$ and $Z_{IN} = z_{IN} \cdot Z_0 = 50 \Omega$.

Summary

The Smith chart manipulations considered here modified the reflection coefficient of a load by adding shunt and series reactive elements. The final result of the circuit manipulations is that the input impedance is $Z_{IN} = 50 \Omega$. If the source has a Thevenin source impedance of 50Ω then there is maximum power transfer to the circuit. Since all of the elements in the circuit manipulations are lossless this means that there is maximum power transfer from the source to the load Z_L . Of course fewer circuit manipulations could have been used to achieve this result. Note that manipulations resulting from adding series and/or shunt resistances were not considered. It is rare that this would be desired as that simply means that power is absorbed in the resistance and additional noise is added to the circuit.

EXAMPLE 3.7

Reflection Coefficient of a Shorted Microstrip Line on a Smith Chart



Design Environment Project File: RFDesign.Shorted_Microstrip_Line_Smith.emp

The example in Section 3.5.2 of [11] calculated the input reflection coefficient, Γ , of the shorted microstrip line on alumina substrate shown in Figure 3-30. The line had low loss and so Γ was always close to 1. The microstrip line was designed to be 50Ω and the locus of Γ with respect to frequency of the low loss line is plotted on a $50\text{-}\Omega$ Smith chart in Figure 3-31(a). Plotting Γ on a $50\text{-}\Omega$ Smith chart indicates that the reflection coefficient was calculated with respect to 50Ω . At a very low frequency, 0.1 GHz is the lowest frequency here, the locus of the reflection coefficient is very close to $\Gamma = -1$, identifying a short circuit. As the electrical length increases, in this case the frequency increases as the physical length of the line is fixed, the locus of the reflection coefficient moves clockwise, hugging the unity reflection coefficient circle. At the highest frequency, 30 GHz , the reflection coefficient is less than 1 and the locus starts moving in from the unity circle. It is interesting to see what happens with a high-loss line, and this is achieved by changing the loss tangent, $\tan \delta$, of the substrate from 0.001 to 0.1 . The locus of the reflection coefficient of the high-loss line is shown in Figure 3-31(b). Loss increases as the electrical length of the line increases and the locus of the reflection coefficient traces out a clockwise inward spiral.



Figure 3-30: A 50Ω shorted gold microstrip line with width $w = 500 \mu\text{m}$, length $\ell = 1 \text{ cm}$ on a $600 \mu\text{m}$ thick alumina substrate with relative permittivity $\epsilon_r = 9.8$ and loss tangent $\tan \delta = 0.001$.

3.4.5 An Alternative Admittance Chart

Design often requires switching between admittance and impedance. So it is convenient to use the colored combined Smith chart shown in Figure 3-23. Monochrome charts were once the only ones available and an impedance Smith chart was used for admittance-based calculations provided that reflection coefficients are rotated by 180° . This form of the Smith chart is not used now.

3.4.6 Expanded Smith Chart

Another form of the Smith chart is the expanded Smith chart shown in Figure 3-32. This is used to plot reflection coefficients of loads with a negative resistance that have a reflection coefficient magnitude greater than one. An oscillator, for example, presents a negative resistance to a resonator. It is also used to plot transmission parameters that have a magnitude greater than one, such as the forward transmission parameter, S_{21} , of a transistor.

3.4.7 Summary

The Smith chart is the most powerful of tools used in RF and Microwave Design. Design using Smith charts will be considered in other chapters but at this stage the reader should be totally conversant with the techniques described in this section.

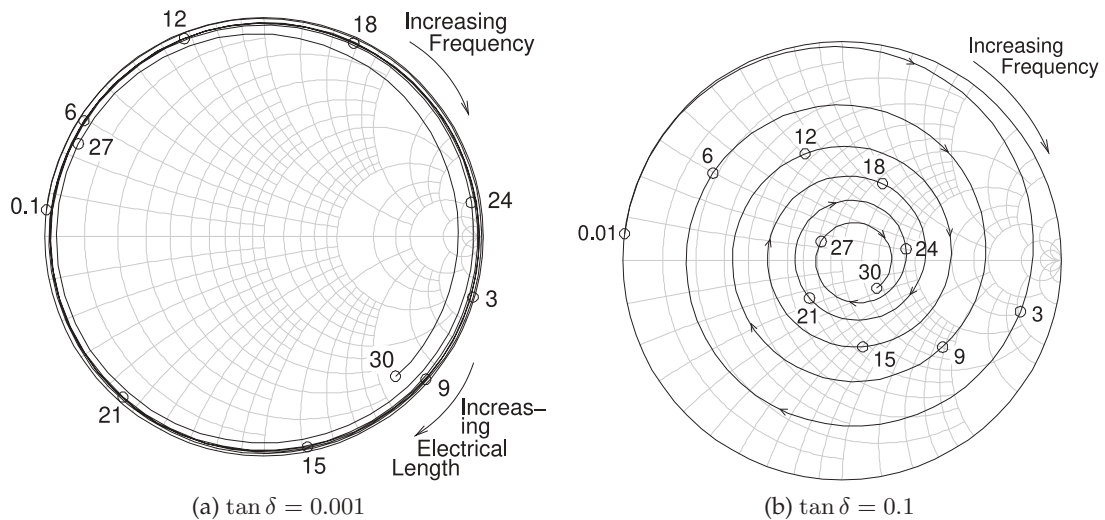


Figure 3-31: Smith chart plot of the reflection coefficient of the shorted 1 cm-long microstrip line in Figure 3-30: (a) a low-loss substrate with $\tan \delta = 0.001$; and (b) a high-loss substrate with $\tan \delta = 0.1$. Frequencies are marked in gigahertz.

3.5 Transmission Lines and Smith Charts

The locus of a transmission line on a Smith chart is a circle. When the characteristic impedance of the line is equal to the system reference impedance this circle is centered at the origin of the Smith chart. The main purpose of this section is to consider the situation where the characteristic impedance and the system reference impedance differ.

3.5.1 Bilinear Transform

Mathematically the input reflection coefficient of a terminated transmission line of characteristic impedance Z_{02} is referenced to a system impedance Z_{01} . The mathematics describing this is based on the bilinear transform. The generalized bilinear transform of two complex numbers z and w is

$$w = \frac{Az + B}{Cz + D}, \quad (3.36)$$

where A, B, C , and D are constants¹ that may themselves be complex. This is of interest in dealing with reflection coefficients where w and z are reflection coefficients and A, B, C , and D describe the two-port network connected to a load with a complex reflection coefficient z , and w is the reflection coefficient looking into the network. The special property of the bilinear transform is that a circle in the complex plane (here the locus of z) is mapped onto another circle (here the locus of w) in the complex plane. (This is shown in Section 1.A.14 of [11].)

¹ These are not the cascadable $ABCD$ parameters, but simply the coefficients commonly used with bilinear transforms.

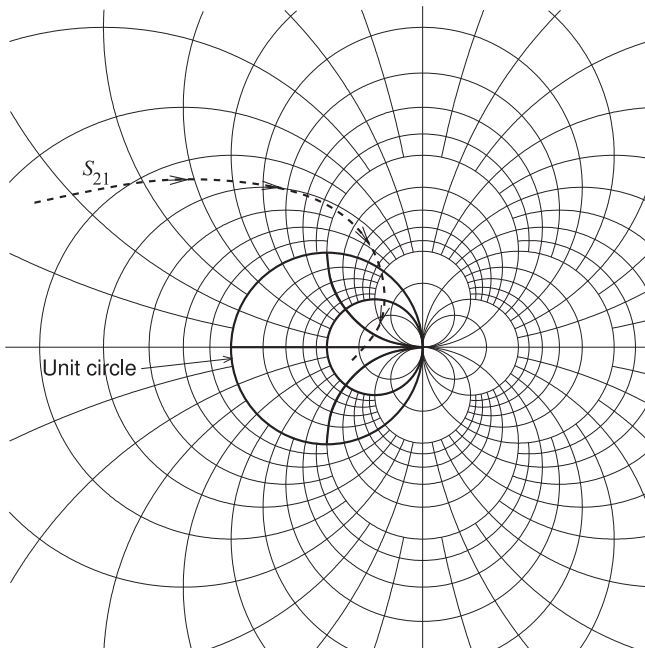


Figure 3-32: Expanded Smith chart used to plot scattering parameters with a magnitude greater than 1. The forward transmission parameter, S_{21} , of a transistor is shown with the arrows in the direction of increasing frequency. The unit circle of a conventional Smith chart is shown

3.5.2 Reference Impedance Change as a Bilinear Transform

In Figure 3-33 a fixed load terminates a transmission line of characteristic impedance Z_{01} and the input reflection coefficient is Γ_{in} . As will be shown, the locus of Γ_{in} , normalized to any system impedance, is a circle on the complex plane as the electrical length of the line increases. The electrical length of the line increases as the frequency increases with the physical length of the line held constant, or as the physical length of the line increases with the frequency held constant.

From Equation ((2.60)) of [11] the reflection coefficient of a load Z_L referenced to Z_{01} is

$$\Gamma_{L,Z01} = \frac{Z_L - Z_{01}}{Z_L + Z_{01}} \quad (3.37)$$

and the input reflection coefficient referenced to Z_{01} is

$$\Gamma_{in,Z01} = \Gamma_{L,Z01} e^{-j2\theta}, \quad (3.38)$$

where $\theta = \beta\ell$ is the electrical length of the line. As θ increases from zero, $\Gamma_{in,Z01}$ plotted on a polar chart traces out a circle rotating in the clockwise direction. The important result that will be developed in this section is that when the input reflection coefficient is referenced to another impedance, the new reflection coefficient will also trace out a circle. The development of $\Gamma_{in,Z02}$ (the input reflection coefficient referred to Z_{02}) begins by calculating the input impedance of the line (in Figure 3-33):

$$Z_{in} = Z_{01} \frac{1 + \Gamma_{in,Z01}}{1 - \Gamma_{in,Z01}} \quad (3.39)$$

so that the reflection coefficient referenced to Z_{02} is

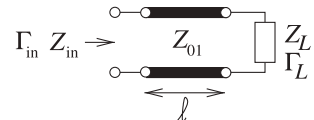
$$\begin{aligned} \Gamma_{in,Z02} &= \frac{Z_{in} - Z_{02}}{Z_{in} + Z_{02}} = \frac{(Z_{in} - Z_{02})(1 - \Gamma_{in,Z01})}{(Z_{in} + Z_{02})(1 - \Gamma_{in,Z01})} \\ &= \frac{(Z_{01} + Z_{02})\Gamma_{in,Z01} + (Z_{01} - Z_{02})}{(Z_{01} - Z_{02})\Gamma_{in,Z01} + (Z_{01} + Z_{02})} \\ &= \frac{\Gamma_{in,Z01} + B}{B\Gamma_{in,Z01} + 1} = \frac{A\Gamma_{in,Z01} + B}{C\Gamma_{in,Z01} + D}. \end{aligned} \quad (3.40)$$

This mapping has the form of a bilinear transform (Equation (3.36)) with

$$A = 1 = D, \quad B = \frac{Z_{01} - Z_{02}}{Z_{01} + Z_{02}} = C. \quad (3.41)$$

Since Equation (3.40) is a general bilinear transform, if the locus of $\Gamma_{in,Z01}$ is a circle, then the locus of $\Gamma_{in,Z02}$ is also a circle.

Figure 3-33: Transmission line of characteristic impedance Z_{01} terminated in a load with a reflection coefficient Γ_L .



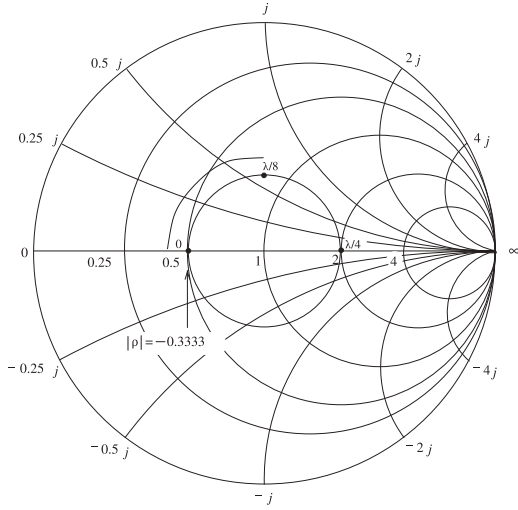


Figure 3-34: A Smith chart normalized to 50 Ω with the input reflection coefficient locus of a 50 Ω transmission line with a load of 25 Ω.

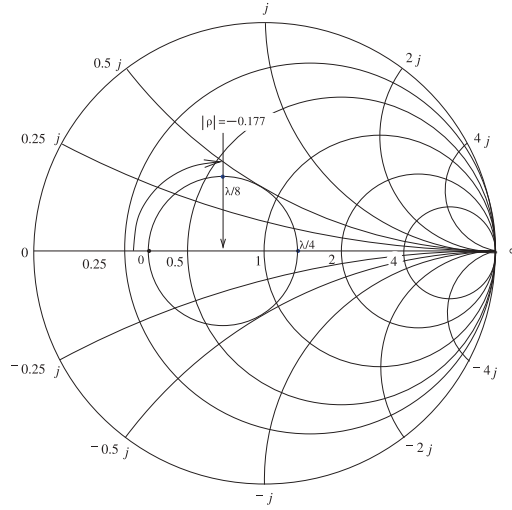
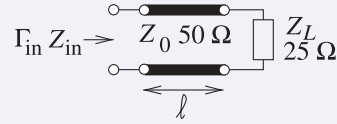


Figure 3-35: A Smith chart normalized to 75 Ω with the input reflection coefficient locus of a 50 Ω transmission line with a load of 25 Ω.

EXAMPLE 3.8

Reflection Coefficient, Reference Impedance Change

In the circuit to the right, a 50-Ω lossless line is terminated in a 25-Ω load. Plot the locus, with respect to the length of the line, of the reflection coefficient looking into the line, referencing it first to a 50-Ω reference impedance and then to a 75-Ω reference impedance.



Solution:

Let the input reflection coefficient referenced to a 50-Ω system be $\Gamma_{in,50}$, and when it is referenced to 75-Ω it is $\Gamma_{in,75}$. In the 50-Ω system the reflection coefficient of the load is

$$\Gamma_{L,50} = \frac{Z_L - 50}{Z_L + 50} = \frac{25 - 50}{25 + 50} = -0.3333 \quad (3.42) \quad \text{and} \quad \Gamma_{in,50} = \Gamma_{L,50} e^{-j2\theta}, \quad (3.43)$$

where $\theta = (\beta\ell)$ is the electrical length of the line. The locus, with respect to electrical length, of $\Gamma_{in,50}$ is plotted in Figure 3-34 as the length ℓ ranges from 0 to $\lambda/8$ to $\lambda/2$, and completes the circle at $\lambda/2$. Now

$$Z_{in} = 50 \frac{1 + \Gamma_{in,50}}{1 - \Gamma_{in,50}}, \quad (3.44)$$

so that the 75-Ω reflection coefficient is

$$\Gamma_{in,75} = \frac{Z_{in} - 75}{Z_{in} + 75}. \quad (3.45)$$

The locus of this reflection coefficient is plotted on a polar plot in Figure 3-35. This locus is the plot of $\Gamma_{in,75}$ as the electrical length of the line, θ , is varied from 0 to π . The center of the circle in Figure 3-35 is taken from the chart and determined to be -0.177 .

A circle is defined by its center and its radius, and Equations ((1.239)) and ((1.240)) of [11], enable the circles for the locus of $\Gamma_{in,Z01}$ and $\Gamma_{in,Z02}$ to be related. $\Gamma_{in,Z01}$ has a center C_{Z01} and a radius R_{Z01} :

$$C_{Z01} = 0 \quad \text{and} \quad R_{Z01} = |\Gamma_{L,Z01}|. \quad (3.46)$$

In Equation ((1.239)) of [11] C_{Z01} replaces the center C_z and $|\Gamma_{L,Z01}|$ takes the place of the radius R_z . Similarly the center of the Γ_{Z02} circle, C_{Z02} , replaces C_w and the radius of the Γ_{Z02} circle, R_{Z02} , replaces R_w . So the locus of the reflection coefficient referenced to Z_{02} is described by a circle with center and radius

$$C_{Z02} = \frac{B - A/C}{1 - |C\Gamma_{L,Z01}|^2} + \frac{A}{C} \quad (3.47) \quad R_{Z02} = \left| \frac{(BC - A)\Gamma_{L,Z01}}{1 - |C\Gamma_{L,Z01}|^2} \right|. \quad (3.48)$$

Since, from Equation (3.41), $A = 1$ and $B = C$ (B is given in Equation (3.41)), this further simplifies to

$$C_{Z02} = \frac{B - 1/B}{1 - |B\Gamma_{L,Z01}|^2} + \frac{1}{B} \quad (3.49) \quad R_{Z02} = \left| \frac{(B^2 - 1)\Gamma_{L,Z01}}{1 - |B\Gamma_{L,Z01}|^2} \right|. \quad (3.50)$$

So the locus (with respect to frequency) of the input reflection coefficient of a terminated transmission line (of characteristic impedance Z_{01}) is a circle no matter what normalization impedance is used and the center of the circle will be on the real axis, the horizontal axis of the Smith chart.

EXAMPLE 3.9

Center of Reflection Coefficient Locus

In Example 3.8 the locus of the input reflection coefficient referenced to 75Ω was plotted for a $50\text{-}\Omega$ line terminated in a load with reflection coefficient (in the $50\text{-}\Omega$ system) of $-1/3$. Calculate the center of the input reflection coefficient when it is referenced to 75Ω .

Solution:

The center of the reflection coefficient normalized to Z_{01} is zero, that is, $C_{50} = 0$. From Equation (3.49), the center of the reflection coefficient normalized to $Z_{02} = 75 \Omega$ is

$$C_{75} = \frac{B - 1/B}{1 - |B\Gamma_{L,50}|^2} + \frac{1}{B}, \quad (3.51)$$

$$\text{where} \quad B = \frac{Z_{01} - Z_{02}}{Z_{01} + Z_{02}} = \frac{50 - 75}{50 + 75} = -0.2. \quad (3.52)$$

$$\text{So} \quad C_{75} = \frac{-0.2 + 5}{1 - (0.2/3)^2} - 5 = -0.17857, \quad (3.53)$$

which compares favorably to a center of -0.177 determined manually from the polar plot in the previous example.

3.5.3 Reflection Coefficient Locus

The direction of the locus of the input reflection coefficient of a terminated transmission line is always clockwise with increasing frequency, even if the Smith chart uses a reference or normalization impedance different from the characteristic impedance of the line. In Figure 3-36, Z_{01} is the characteristic impedance of the line and Z_{02} is the normalization impedance. The center of the circle of the reflection coefficient normalized to Z_{02} is to the left of the origin if $Z_{02} > Z_{01}$, and to the right of the origin if normalized to $Z_{02} < Z_{01}$, but always on the real axis.

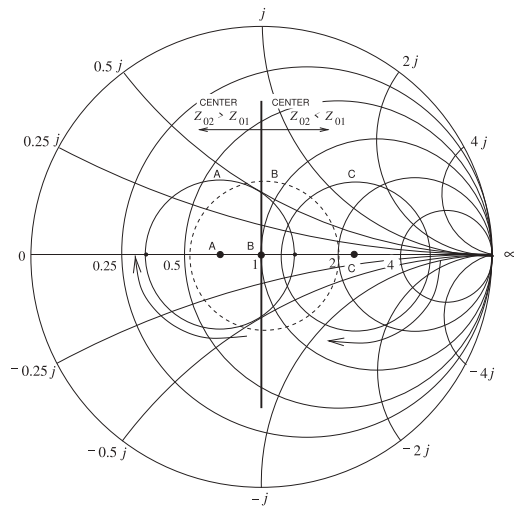


Figure 3-36: The locus of the input reflection coefficient normalized to Z_{02} of a terminated line of characteristic impedance Z_{01} . The locus is with respect to the electrical length of the line and the arrows show the direction of rotation of the reflection coefficient. (Note that for the same terminating impedance the radii will also change, but this is not shown here.)

3.5.4 Summary

Smith charts are indispensable tools for RF and microwave engineers. Even with the ready availability of CAD programs, Smith charts are generally preferred for portraying measured and calculated data because of the easy interpretation of S parameters. With experience, the properties of circuits can be inferred. Also, with experience they are an invaluable design tool enabling the designer to see the beginning and endpoints of a design and infer the type of circuitry required to go from start to finish.

3.6 Summary

Graphical representations of power flow enable RF and microwave engineers to quickly ascertain circuit performance and arrive at qualitative design decisions. Humans are very good at processing graphical information and seeing patterns, anomalies, and the path from one point to another. Two powerful techniques were introduced in this chapter that provide this insight. These are the signal flow graph and the Smith chart. Signal flow graphs enable engineers to solve algebraic problems without using algebraic equations. Signal flow graphs are also a convenient way to develop symbolic expressions. Developing these expressions using algebraic manipulations alone is error prone.

The Smith chart is a richly annotated polar plot for representing reflection and transmission coefficients, and more generally, scattering parameters. The Smith chart representation of scattering parameter data aligns very well with the intuitive understanding of an RF designer. The experienced RF designer is intrinsically familiar with the Smith chart and prefers that circuit performance during design be represented on one. Representing something as simple as an extension of a line length to a two-port is quite complex if described using network parameters other than scattering parameters. However, with scattering parameters this extension results in a change of the angle of a scattering parameter, or on a Smith chart an arc. Scattering parameters relate directly to power flow. So from a Smith chart an

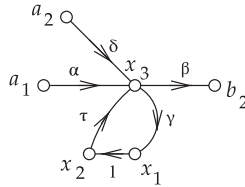
experienced designer can ascertain the effect of circuit design on power flow, which then relates to signal-to-noise ratio and power gain. The Smith chart will be an essential tool in many of the topics considered in later chapters.

3.7 References

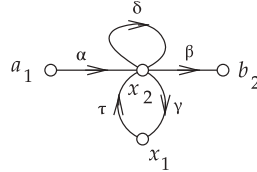
- [1] S. Mason, "Feedback theory-some properties of signal flow graphs," *Proc. of the IRE*, vol. 41, no. 9, pp. 1144–1156, Sep. 1953.
- [2] A. Tustin, *Direct Current Machines for Control Systems*. The Macmillan Company, 1956.
- [3] N. Balabanian, *Fundamentals of Circuit Theory*. Allyn and Bacon, 1961.
- [4] J. Abrahams and G. Coverley, *Signal Flow Analysis*. Pergamon Press, 1965.
- [5] J. Distefano, A. Stubberud, and I. Williams, *Theory and Problems of Feedback Control Systems*. McGraw-Hill, 1990.
- [6] S. Mason, "Feedback theory-further properties of signal flow graphs," *Proc. of the IRE*, vol. 44, no. 7, pp. 920–926, Jul. 1956.
- [7] P. Smith, *Electronic Applications of the Smith Chart: In Waveguide, Circuit, and Component Analysis*. SciTech Publishing, 2000.
- [8] —, "Transmission line calculator," *Electronics*, 1939.
- [9] —, "An improved transmission-line calculator," *Electronics*, 1944.
- [10] —, "R.F. transmission line nomographs," *Electronics*, vol. 22, pp. 112–117, Feb. 1949.
- [11] M. Steer, *Microwave and RF Design, Transmission Lines*, 3rd ed. North Carolina State University, 2019.

3.8 Exercises

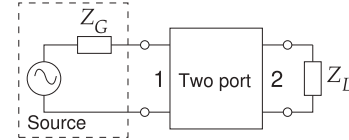
1. Reduce the following signal flow graph to two edges and three nodes. That is, write down the expression for b_2 in terms of a_1 and a_2 , eliminating the variables x_1 , x_2 , and x_3 .



2. Reduce the following signal flow graph to one edge and two nodes. That is, write down the expression for b_2 in terms of a_1 , eliminating the variables x_1 and x_2 .



3. The scattering parameters of a two-port are $S_{11} = 0.25$, $S_{12} = 0$, $S_{21} = 1.2$, and $S_{22} = 0.5$. The system reference impedance is 50Ω and the Thevenin equivalent impedance of the source at Port 1 is $Z_G = 50 \Omega$. The power available from the source connected to Port 1 is 1 mW. The load impedance is $Z_L = 25 \Omega$. Using SFGs, determine the power dissipated by the load at Port 2.



4. Draw the SFG of a two-port with a load at Port 2 having a voltage reflection coefficient of Γ_L , and at Port 1 a source reflection coefficient of Γ_S . Γ_S is the reflection coefficient looking from Port 1 of the two-port toward the generator. Keep the S parameters of the two-port in symbolic form (e.g., S_{11} , S_{12} , S_{21} , and S_{22}). Using SFG analysis, derive an expression for the reflection coefficient looking into the two-port at Port 2. You must show the stages in collapsing the SFG to the minimal form required.
5. A three-port has the scattering parameters:

$$\begin{bmatrix} 0 & \gamma & \delta \\ \alpha & 0 & \epsilon \\ \theta & \beta & 0 \end{bmatrix}.$$

Port 2 is terminated in a load with a reflection coefficient Γ_L . Reduce the three-port to a two-port using signal flow graph theory. Write down the four scattering parameters of the final two-port.

6. The $50\text{-}\Omega$ S parameters of a three-port are

$$\begin{bmatrix} 0.2\angle 180^\circ & 0.8\angle -45^\circ & 0.1\angle 45^\circ \\ 0.8\angle -45^\circ & 0.2\angle 0^\circ & 0.1\angle 90^\circ \\ 0.1\angle 45^\circ & 0.1\angle 90^\circ & 0.1\angle 180^\circ \end{bmatrix}.$$

- (a) Is the three-port reciprocal? Explain your answer.

- (b) Write down the criteria for a network to be lossless.
- (c) Is the three-port lossless? You must show your work.
- (d) Draw the SFG of the three-port.
- (e) A $50\ \Omega$ load is attached to Port 3. Use SFG operations to derive the SFG of the two-port with just Ports 1 and 2. Write down the two-port S parameter matrix.

7. The $50\ \Omega$ S parameters of a three-port are

$$\begin{bmatrix} 0.2\angle 180^\circ & 0.8\angle -45^\circ & 0.1\angle 45^\circ \\ 0.8\angle -45^\circ & 0.2\angle 0^\circ & 0.1\angle 90^\circ \\ 0.1\angle 45^\circ & 0.1\angle 90^\circ & 0.1\angle 180^\circ \end{bmatrix}.$$

- (a) Is the three-port reciprocal? Explain.
 - (b) Write down the criteria for a network to be lossless.
 - (c) Is the three-port lossless? Explain.
 - (d) Draw the SFG of the three-port.
 - (e) A $150\ \Omega$ load is attached to Port 3. Derive the SFG of the two-port with just Ports 1 and 2. Write down the two-port S parameter matrix of the simplified network.
8. A system consists of 2 two-ports in cascade. The S -parameter matrix of the first two-port is \mathbf{S}_A and the S parameter matrix of the second two-port is \mathbf{S}_B . The second two-port is terminated in a load with a reflection coefficient Γ_L . (Just to be clear, \mathbf{S}_A is followed by \mathbf{S}_B , which is then terminated in Γ_L . Port 2 of \mathbf{S}_A is connected to Port 1 of \mathbf{S}_B .) The individual S parameters of the two-ports are as follows:

$$\mathbf{S}_A = \begin{bmatrix} a & c \\ c & b \end{bmatrix} \text{ and } \mathbf{S}_B = \begin{bmatrix} d & f \\ f & e \end{bmatrix}.$$

- (a) Draw the SFG of the system consisting of the two cascaded two-ports and the load.
- (b) Ignoring the load, is the cascaded two-port system reciprocal? If there is not enough information to decide, then say so. Give your reasons.
- (c) Ignoring the load, is the cascaded two-port system lossless? If there is not enough information to decide, then say so. Give your reasons.
- (d) Consider that the load has no reflection (i.e., $\Gamma_L = 0$). Use SFG analysis to find the input reflection coefficient looking into Port 1 of \mathbf{S}_A . Your answer should be Γ_{in} in terms of a, b, \dots, f .

9. A circulator is a three-port device that is not reciprocal and selectively shunts power from one port to another. The S parameters of an ideal cir-

culator are

$$[S] = \begin{bmatrix} 0 & 1 & 0 \\ 0 & 0 & 1 \\ 1 & 0 & 0 \end{bmatrix}.$$

- (a) Draw the three-port and discuss power flow.
- (b) Draw the SFG of the circulator.
- (c) If Port 2 is terminated in a load with reflection coefficient 0.2, reduce the SFG of the circulator to a two-port with Ports 1 and 3 only.
- (d) Write down the 2×2 S parameter matrix of the (reduced) two-port.

10. The S parameters of a certain two-port are $S_{11} = 0.5 + j0.5$, $S_{21} = 0.95 + j0.25$, $S_{12} = 0.15 - j0.05$, $S_{22} = 0.5 - j0.5$. The system reference impedance is $50\ \Omega$.

- (a) Is the two-port reciprocal?
- (b) Which of the following is a true statement about the two-port?
 - (A) It is unitary.
 - (B) Overall power is produced by the two-port.
 - (C) It is lossless.
 - (D) If Port 2 is matched, then the real part of the input impedance (at Port 1) is negative.
 - (E) A and C.
 - (F) A and B.
 - (G) A, B, and C
 - (H) None of the above.
- (c) What is the value of the load required for maximum power transfer at Port 2? Express your answer as a reflection coefficient.
- (d) Draw the SFG for the two-port with a load at Port 2 having a voltage reflection coefficient of Γ_L and at Port 1 a source reflection coefficient of Γ_S .

11. The $50\text{-}\Omega$ S parameters of a three-port are

$$\begin{bmatrix} 0.2 & 0.8 & 0.1 \\ 0.8 & 0.2 & 0.1 \\ 0.1 & 0.1 & 0.1 \end{bmatrix}.$$

- (a) Is the three-port reciprocal? Explain your answer.
- (b) Write down the criteria for a network to be lossless.
- (c) Is the three-port lossless? You must show your work.
- (d) Draw the SFG of the three-port.
- (e) A $50\ \Omega$ load is attached to Port 3. Use SFG operations to derive the SFG of the two-port with just Ports 1 and 2. Write down the two-port S parameter matrix.

12. The $50\text{-}\Omega$ S parameters of a three-port are

$$\begin{bmatrix} 0.5 & 0.4 & 0.5 \\ 0.6 & 0.5 & 0.5 \\ 0.5 & 0.5 & 0.5 \end{bmatrix}.$$

- (a) Is the three-port reciprocal? Explain.
 - (b) Write down the criteria for a network to be lossless.
 - (c) Is the three-port lossless? Explain.
 - (d) Draw the SFG of the three-port.
 - (e) A $150\text{-}\Omega$ load is attached to Port 3. Derive the SFG of the two-port with just Ports 1 and 2. Write down the two-port S parameter matrix.
13. In the distribution of signals on a cable TV system a $75\text{-}\Omega$ coaxial cable is used, with a loss of 0.1 dB/m at 1 GHz . If a subscriber disconnects a television set from the cable so that the load impedance looks like an open circuit, estimate the input impedance of the cable at 1 GHz and 1 km from the subscriber. An answer within 1% is required. Estimate the error of your answer. Indicate the input impedance on a Smith chart, drawing the locus of the input impedance as the line is increased in length from nothing to 1 km . (Consider that the dielectric filling the line has $\epsilon_r = 1$.)
14. A resistive load has a reflection coefficient with a magnitude of 0.7 . If a transmission line is placed in series with the load, on a polar plot sketch the locus of the input reflection coefficient looking into the input of the terminated line as the line increases in electrical length from zero to $\lambda/2$. By reading the Smith chart, determine the normalized input impedance of the line when it has an electrical length of $\pi/2$.
15. A complex load has a reflection coefficient of $0.5 + j0.5$. If a transmission line is placed in series with the load, on a polar plot sketch the locus of the input reflection coefficient looking into the input of the terminated line as the line increases in electrical length from zero to $\pi/2$.
16. A resistive load has a reflection coefficient of -0.5 . If a transmission line is placed in series with the load, on a polar plot sketch the locus of the input reflection coefficient looking into the input of the terminated line as the line increases in electrical length from 0 to $3\lambda/8$.
17. S_{21} of a two-port is 0.5 . If a transmission line is placed in series with Port 1, on a polar plot sketch the locus of S_{21} of the augmented two-port as the electrical length of the line increases from zero to $\lambda/2$.
18. A load has an impedance $Z = 115 - j20\text{-}\Omega$.
- (a) What is the reflection coefficient, Γ_L , of the load in a $50\text{-}\Omega$ reference system?
 - (b) Plot the reflection coefficient on a polar plot of reflection coefficient.
 - (c) If a one-eighth wavelength long lossless $50\text{-}\Omega$ transmission line is connected to the load, what is the reflection coefficient, Γ_{in} , looking into the transmission line? (Again, use the $50\text{-}\Omega$ reference system.) Plot Γ_{in} on the polar reflection coefficient plot of part (b). Clearly identify Γ_{in} and Γ_L on the plot.
 - (d) On the Smith chart, identify the locus of Γ_{in} as the length of the transmission line increases from 0 to $\lambda/8$ long. That is, on the Smith chart, plot Γ_{in} as the length of the transmission line varies.
19. A load has a reflection coefficient with a magnitude of 0.5 . If a transmission line is placed in series with the load, on a polar plot sketch the locus of the input reflection coefficient looking into the input of the terminated line as the line increases in electrical length from zero to $\lambda/2$. What is the normalized input impedance of the line when it has an electrical length of $\lambda/2$?
20. A resistive load has a reflection coefficient with a magnitude of 0.7 . If a transmission line is placed in series with the load, on a polar plot sketch the locus of the input reflection coefficient looking into the input of the terminated line as the line increases in electrical length from zero to $\lambda/4$. By reading the Smith chart, determine the normalized input impedance of the line when it has an electrical length of $\lambda/4$.
- Problems 21 to 27 refer to the normalized Smith chart in Figure 3-38 with reference impedance $Z_{\text{REF}} = 50\text{-}\Omega$ and reflection coefficient Γ , voltage reflection coefficient $^V\Gamma$, current reflection coefficient $^I\Gamma$, and normalized impedance $z = r + jx$ and admittance $y = g + jb$. Γ should be given in magnitude-angle format.
21. (a) What is $^V\Gamma$ at A? (f) What is $|\Gamma|$ at F?
 - (b) What is $^I\Gamma$ at A? (g) What is b at I?
 - (c) What is r at B? (h) What is Γ at P?
 - (d) What is z at C? (i) What is Γ at D?
 - (e) What is y at D? (j) What is Γ at T?
22. (a) What is z at A? (f) What is $|\Gamma|$ at W?
 - (b) What is y at I? (g) What is b at F?
 - (c) What is z at E? (h) What is x at K?
 - (d) What is y at Z? (i) What is Γ at K?
 - (e) What is y at H? (j) What is Γ at R?

23. (a) What is y at A? (h) What is Γ at G?
 (b) What is y at I? (i) What is z at L,
 (c) What is z at G? label this z_L ?
 (d) What is y at O? (j) Use the Smith
 (e) What is y at V? chart to find z_{in} of a $50\ \Omega$
 (f) What is Γ at B? $\lambda/8$ -long line with load
 (g) What is x at C? z_L ?
24. (a) What is $^V\Gamma$ at M? (f) What is $|\Gamma|$ at B?
 (b) What is $^I\Gamma$ at M? (g) What is b at K?
 (c) What is r at W? (h) What is Γ at V?
 (d) What is z at Y? (i) What is Γ at P?
 (e) What is y at V? (j) What is Γ at N?
25. (a) What is z at M? (f) What is $|\Gamma|$ at F?
 (b) What is y at K? (g) What is b at B?
 (c) What is z at S? (h) What is x at I?
 (d) What is Γ at R? (i) What is Γ at I?
 (e) What is g at B? (j) What is Γ at Q?
26. (a) What is g at M? (h) What is Γ at T?
 (b) What is r at K? (i) What is z at O,
 (c) What is y at S? label this z_O ?
 (d) What is z at R? (j) Using the Smith
 (e) What is y at Z? chart find z_{in} of a $3\lambda/8$ -
 (f) What is Γ at W? long $50\ \Omega$ line with load
 (g) What is x at Y? z_O ?
27. (a) What is g at P? (f) What is $|\Gamma|$ at U?
 (b) What is y at J? (g) What is $^V\Gamma$ at X?
 (c) What is Γ at L? (h) What is $^I\Gamma$ at X?
 (d) What is z at N? (i) What is g at B?
 (e) What is y at S? (j) What is x at I?
28. Design a short-circuited stub to realize a normalized susceptance of 2.15. Show the locus of the stub as its length increases from zero to its final length. What is the minimum length of the stub in terms of wavelengths?
29. Design a short-circuited stub to realize a normalized susceptance of -0.56 . Show the locus of the stub as its length increases from zero to its final length. What is the minimum length of the stub in terms of wavelengths?
30. Design a short-circuited stub to realize a normalized susceptance of -2.2 . Show the locus of the stub as its length increases from zero to its final length. What is the minimum length of the stub in terms of wavelengths?
31. A $75\text{-}\Omega$ transmission line is terminated in a load with a reflection coefficient, Γ , normalized to $75\ \Omega$, of $0.5\angle 45^\circ$. If Γ at the input of the line is $0.5\angle -135^\circ$, what is the minimum electrical length of the line in degrees.
32. An open-circuited $75\text{-}\Omega$ transmission line has an input reflection coefficient with an angle of 40° what is the electrical length of the line in degrees? If there is more than one answer provide at least two correct answers.
33. Use a Smith chart to design a microstrip network to match a load $Y_L = 28 - j12\text{ mS}$ to a source $Y_S = 6 + j12\text{ mS}$. Use transmission lines only and use short-circuited stubs. Use a reference impedance of $50\ \Omega$.
 (a) Draw the matching network problem labeling source and load admittances and labeling the admittance looking into the matching network from the source as Y_1 .
 (b) What is the condition for maximum power transfer at the source side of the matching network in terms of admittances?
 (c) What is the condition for maximum power transfer at the source side of the matching network in terms of reflection coefficients?
 (d) What is the reference admittance Y_{REF} ?
 (e) What is the value of the normalized source admittance?
 (f) What is the value of the normalized load admittance?
 (g) On a Smith chart (not a sketch) identify, i.e. draw, the electrical designs of two suitable matching networks. Identify the designs using the labels D1 and D2 on the loci.
 (h) Develop the complete electrical design of a matching network using the Smith chart using $50\ \Omega$ lines only. You only need do one design.
 (i) Draw the microstrip layout of the matching network and identify critical parameters such characteristic impedances and electrical length. Ensure that you identify which is the source side and which is the load side. You do not need to determine the widths of the lines or their physical lengths.
34. Repeat Exercise 33 with $Y_L = 20 + j20\text{ mS}$ to a source $Y_S = 4 + j20\text{ mS}$.
35. Repeat Example 3.4 using the full impedance Smith chart of Figure 3-18.
36. Plot the normalized impedances $z_A = 0.5 + j0.5$, $z_A = 0.5 + j0.5$, and $z_B = 0.185 - j1.05$ on the full impedance Smith chart of Figure 3-18. [Parallels Example 3.4]
37. In Figure 3-37 the results of several different experiments are plotted on a Smith chart. Each experiment measured the input reflection coefficient from a low frequency (denoted by a circle) to a high frequency (denoted by a square) of a one-port. Determine the load that was measured. The loads that were measured are one of those shown below.

Load	Description
i	An inductor
ii	A capacitor
iii	A reactive load at the end of a transmission line
iv	A resistive load at the end of a transmission line
v	A parallel connection of an inductor, a resistor, and a capacitor going through resonance and with a transmission line offset
vi	A series connection of a resistor, an inductor and a capacitor going through resonance and with a transmission line offset
vii	A series resistor and inductor
viii	An unknown load and not one of the above

For each of the measurements below indicate the load or loads using the load identifier above (e.g., i, ii, etc.).

- (a) What load(s) is indicated by curve A?
 (a) What load(s) is indicated by curve A?
 (b) What load(s) is indicated by curve B?
 (c) What load(s) is indicated by curve C?

- (d) What load(s) is indicated by curve D?
 (e) What load(s) is indicated by curve E?
 (f) What load(s) is indicated by curve F?

38. A 50- Ω lossy transmission line is shorted at one end. The line loss is 2 dB per wavelength. Note that since the line is lossy the characteristic impedance will be complex, but close to 50 Ω , since it is only slightly lossy. There is no way to calculate the actual characteristic impedance with the information provided. That is, problems must be solved with small inconsistencies. Microwave engineers do the best they can in design and always rely on measurements to calibrate results.

- (a) What is the reflection coefficient at the load (in this case the short)?
 (b) Consider the input reflection coefficient, Γ_{in} , at a distance ℓ from the load. Determine Γ_{in} for ℓ going from 0.1λ to λ in steps of 0.1λ .
 (c) On a Smith chart plot the locus of Γ_{in} from $\ell = 0$ to λ .
 (d) Calculate the input impedance, Z_{in} , when the line is $3\lambda/8$ long using the telegrapher's equation.
 (e) Repeat part (d) using a Smith chart.

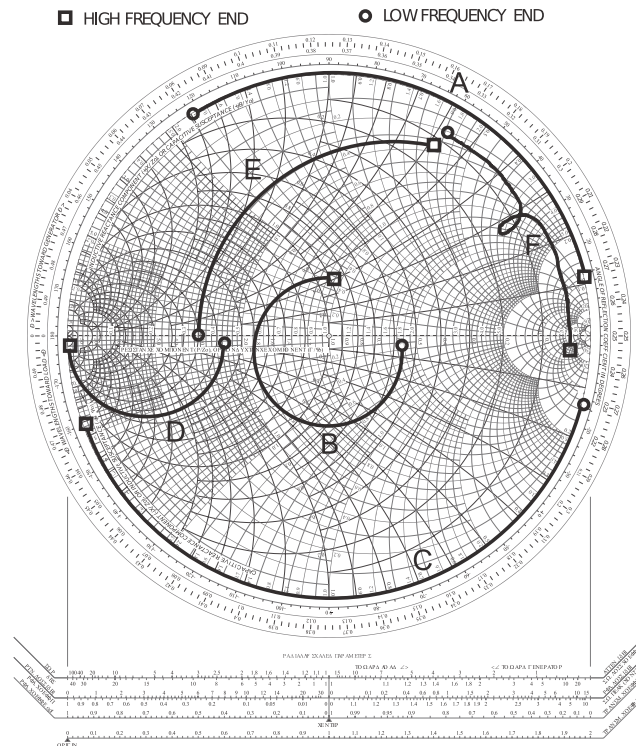
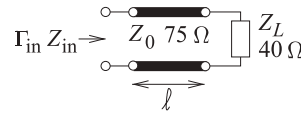
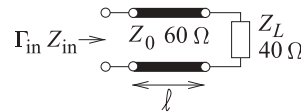


Figure 3-37: The locus of various loads plotted on a Smith chart.

39. Design an open-circuited stub with an input impedance of $+j75\ \Omega$. Use a transmission line with a characteristic impedance of $75\ \Omega$. [Parallels Example 3.5]
40. Design a short-circuited stub with an input impedance of $-j50\ \Omega$. Use a transmission line with a characteristic impedance of $100\ \Omega$. [Parallels Example 3.5]
41. A load has an impedance $Z_L = 25 - j100\ \Omega$.
- What is the reflection coefficient, Γ_L , of the load in a $50\ \Omega$ reference system?
 - If a one-quarter wavelength long $50\ \Omega$ transmission line is connected to the load, what is the reflection coefficient, Γ_{in} , looking into the transmission line?
 - Describe the locus of Γ_{in} , as the length of the transmission line is varied from zero length to one-half wavelength long. Use a Smith chart to illustrate your answer
42. A network consists of a source with a Thevenin equivalent impedance of $50\ \Omega$ driving first a series reactance of $-50\ \Omega$ followed by a one-eighth wavelength long transmission line with a characteristic impedance of $40\ \Omega$ and an element with a reactive impedance of $j25\ \Omega$ in shunt with a load having an impedance $Z_L = 25 - j50\ \Omega$. This problem must be solved graphically and no credit will be given if this is not done.
- Draw the network.
- (b) On a Smith chart, plot the locus of the reflection coefficient first for the load, then with the element in shunt, then looking into the transmission line, and finally the series element. Use letters to identify each point on the Smith chart. Write down the reflection coefficient at each point.
- (c) What is the impedance presented by the network to the source?
43. In the circuit below, a $75\text{-}\Omega$ lossless line is terminated in a $40\text{-}\Omega$ load. On the complex plane plot the locus, with respect to the length of the line, of the reflection coefficient, looking into the line referencing it first to a $50\text{-}\Omega$ impedance. [Parallels Example 3.8]



44. Consider the circuit below, a $60\ \Omega$ lossless line is terminated in a $40\ \Omega$ load. What is the center of the reflection coefficient locus on the complex plane when it is referenced to $55\ \Omega$? [Parallels Example 3.9]



3.8.1 Exercises by Section

[†]challenging

- | | | |
|---|---|--|
| §3.2 1, 2, 3 [†] , 4 [†] , 5 [†] , 6 [†] , 7 [†] , 8 [†] , 9 [†] ,
10 [†] , 11, 12 | 21, 22, 23, 24, 25, 26, 27, 28,
29, 30, 31, 32, 33, 34, 35, 36, | §3.5 43 [†] , 44 [†] |
| §3.4 13, 14, 15, 16, 17, 18, 19, 20, | 37 [†] , 38 [†] , 39 [†] , 40 [†] , 41 [†] , 42 [†] | |

3.8.2 Answers to Selected Exercises

- | | | |
|--|--------------------------------|--------------------------------|
| 1 $\frac{\beta}{1 - \tau\gamma}(\alpha a_1 + \gamma a_2)$ | 8(d) $a + \frac{dc^2}{1 - bd}$ | 38(d) $8.37 - j49.3\ \Omega$ |
| 3 $0.940\ \text{mW}$ | 13 $\Gamma_{IN} = 10^{-10}$ | 41 $0.825\angle -50.9^\circ$ |
| 6 $\begin{bmatrix} -0.2 & 0.8\angle -45^\circ \\ -0.2 & 0.2 \end{bmatrix}$ | 37(c) ii & iii | 42 $\approx 250 - j41\ \Omega$ |
| | | 44 0.0418 |

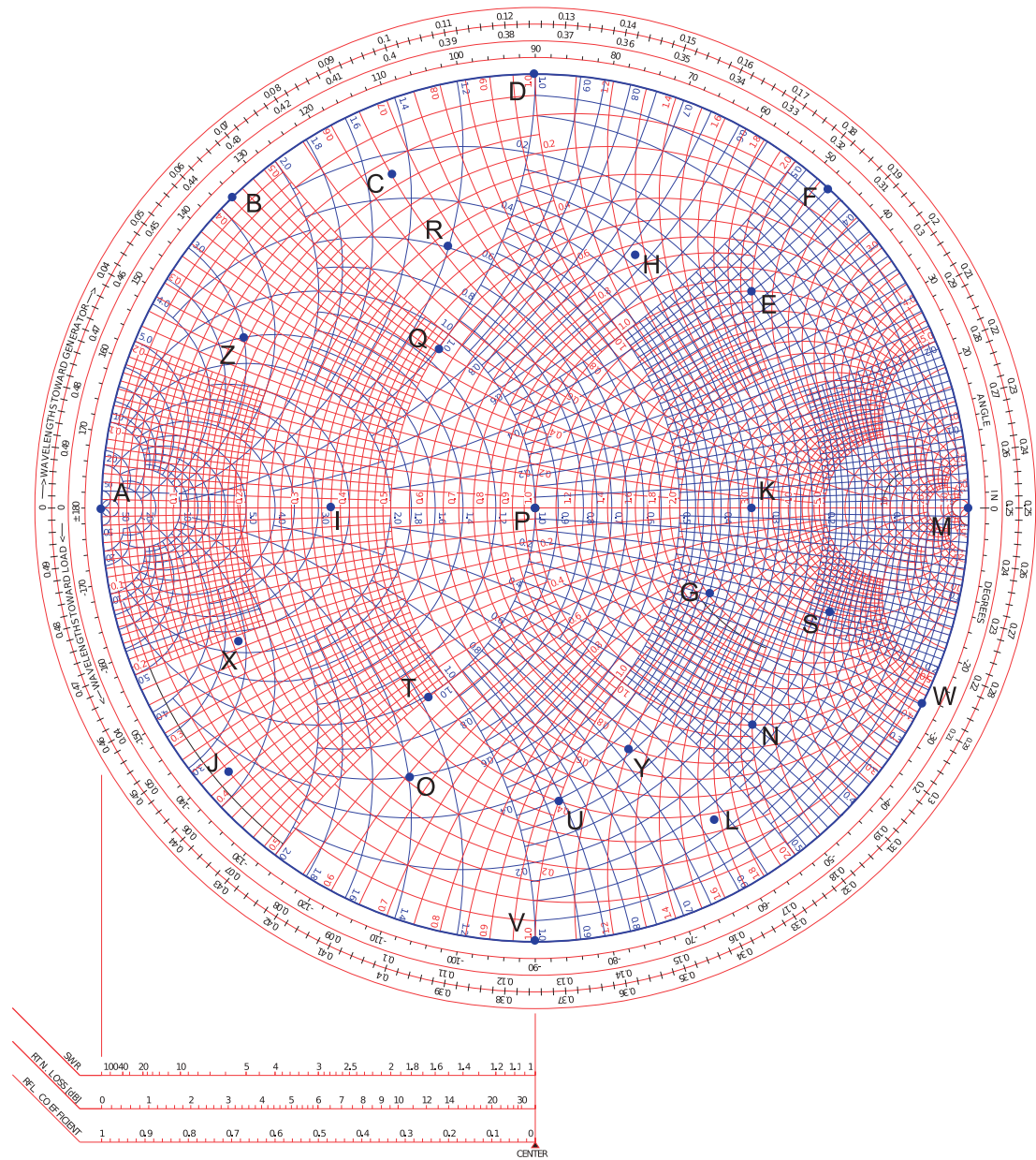


Figure 3-38

Microwave Measurements

4.1	Introduction	89
4.2	Measurement of Scattering Parameters	89
4.3	Calibration	93
4.4	Extraction of Transmission Line Parameters	107
4.5	Determining Z_0 of a Line from the Smith Chart	109
4.6	Summary	110
4.7	References	110
4.8	Exercises	112

4.1 Introduction

At microwave frequencies it is almost never possible to measure voltage and current directly and so it is not possible to measure z and y parameters, and most other network parameters, directly. However S parameters are easy to measure as they are based on power flow and instead of relying on short and open circuit terminations, their definitions require matched loads which minimize reflections and also ensure that circuits are stable.

4.2 Measurement of Scattering Parameters

S parameters are measured using a network analyzer called an **automatic network analyzer (ANA)**, or more commonly a **vector network analyzer (VNA)**.

4.2.1 Vector Network Analyzer

The VNA is based on separating the forward- and backward-traveling voltage waves using a directional coupler. The separated traveling waves are then the total voltages on the coupled lines of the directional coupler. They are down-converted to perhaps 100 kHz and then sampled by an analog-to-digital converter [1]. Schematics of modern VNAs are shown in Figures 4-1 and 4-2 and comprise

1. A frequency synthesizer for stable generation of a sinewave.
2. A display plotting the S parameters in various forms, with a Smith chart being most commonly used.
3. An S parameter test set. This device generally has two measuring ports

so that when required S_{11} , S_{12} , S_{21} , and S_{22} can all be determined under program control. The main components are switches and directional couplers. Directional couplers separate the forward- and backward-traveling wave components. Network analyzers with more than two ports—four-port network analyzers are popular—have more switches and directional couplers. The mixers map the amplitude and phase of the RF signal to the IF, commonly around 100 kHz, which is sampled by the ADC.

4. A computer controller used in correcting errors and converting the results to the desired form.

For RF measurements up to a few tens of gigahertz, most of these functions are incorporated in a single instrument. At higher frequencies and with older equipment multiple units are used. An outline of such a system is shown in Figure 4-3(a) and a photograph in Figure 4-3(c). In the foreground of Figure 4-3(c) is a probe station that has a stage for an IC or RF circuit board and mounts for micromanipulators to which **microprobes** are attached. The vertical tube-shaped object is a microscope-mounted camera.

The probes are mounted on micromanipulators such as those shown in Figure 4-4. These provide precision positioning with x - y - z movement and an axis rotation to accommodate probing on substrates that are not completely flat.

Figure 4-1: Switch-based vector network analyzer system with two receivers. The directional couplers selectively couple forward- or backward-traveling waves. With the directional coupler (see inset), a traveling wave inserted at Port 2 appears only at Port 1. A traveling wave inserted at Port 1 appears at Port 2 and a coupled version at Port 3. A traveling wave inserted at Port 3 appears only at Port 1. Switch positions determine which S parameter is measured.

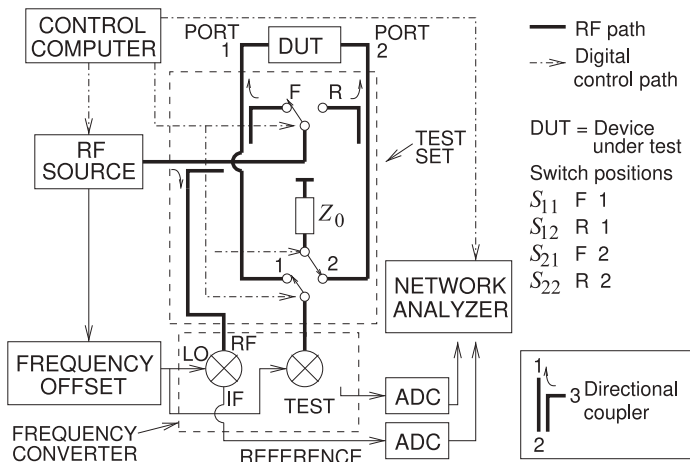
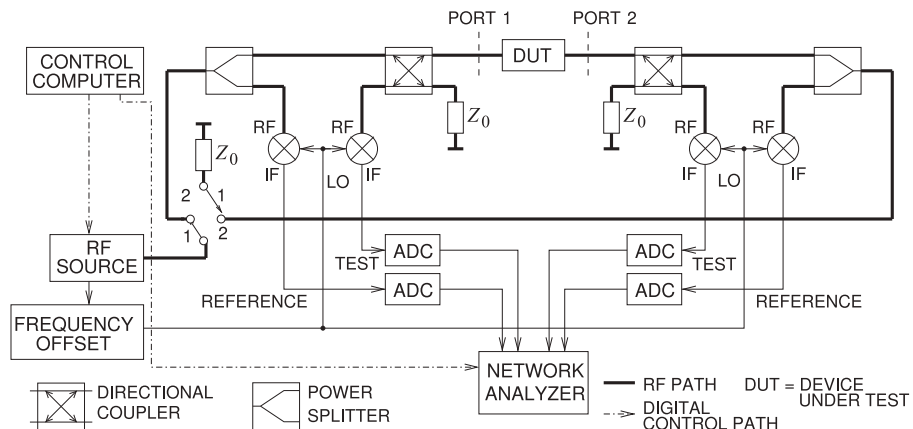


Figure 4-2: Vector network analyzer system with four receivers.



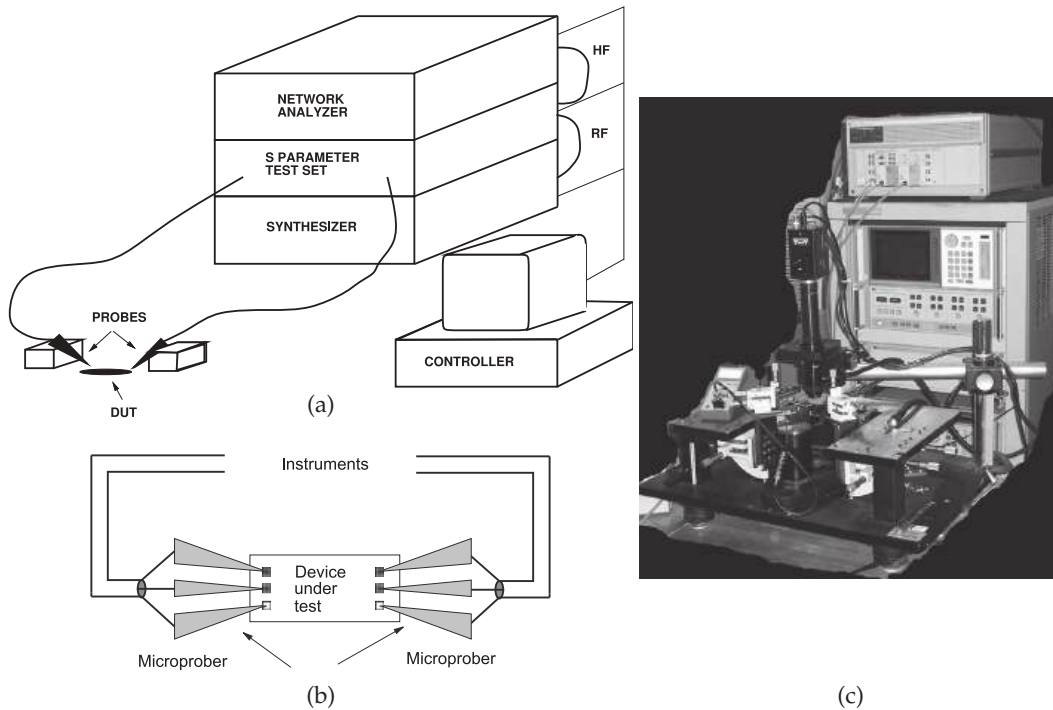


Figure 4-3: *S* parameter measurement system: (a) shown in a configuration to do on-chip testing; (b) details of coplanar probes with a GSG configuration and contacting pads; and (c) a vector network analyzer in the background with probe station including camera.



Figure 4-4: Micropositioners used with coplanar probes. Used with permission of J MicroTechnology, Inc.

Probing elements required for on-wafer measurements are shown in Figure 4-5. Figure 4-5(a) shows a single RF probe that is essentially an extended coaxial line. Figure 4-5(c) shows a microprobe making a connection to a transmission line on an IC and the lower image in Figure 4-5(b) shows greater detail of the contact area.

A typical microprobe is based on a micro coaxial cable with the center conductor (carrying the signal) extended a millimeter or so to form a needle-like contact. Two other needle-like contacts are made by attaching short extensions to the outer conductor of the coaxial line on either side of the signal connection (see the top image in Figure 4-5(b)). Such probes are called

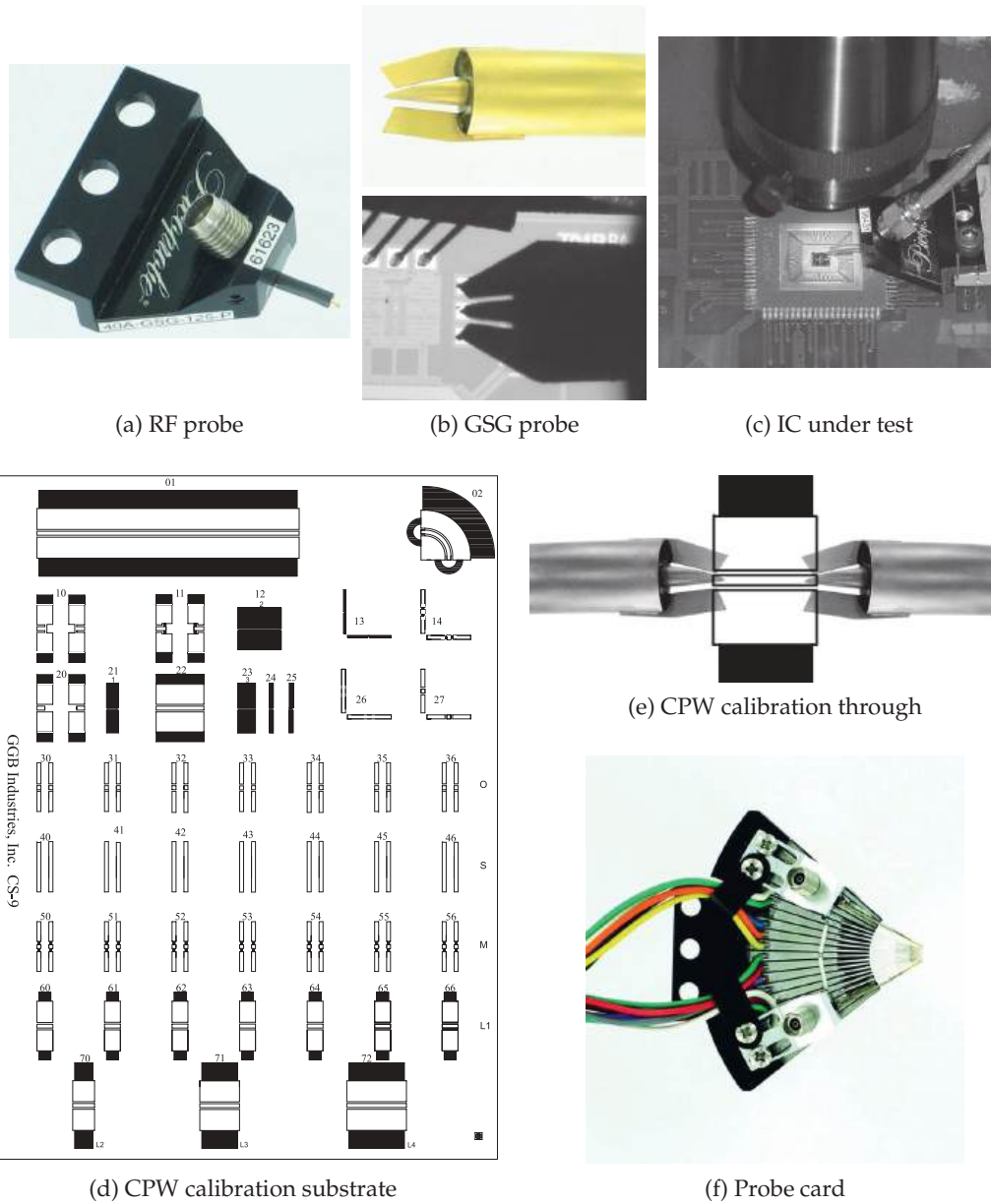


Figure 4-5: RF probes: (a) single RF probe probe; (b) detail of a GSG probe and contacting an IC; (c) an IC under test; (d) layout of a calibration substrate used with GSG probes; (e) probes contacting a through CPW structure on the calibration substrate; and (f) a probe card with 2 RF probes (top and bottom) and 13 needle probes for DC and low-frequency connections. ((a), (b) top, (d), (e), (f) Copyright GGB Industries Inc., used with permission [2].)

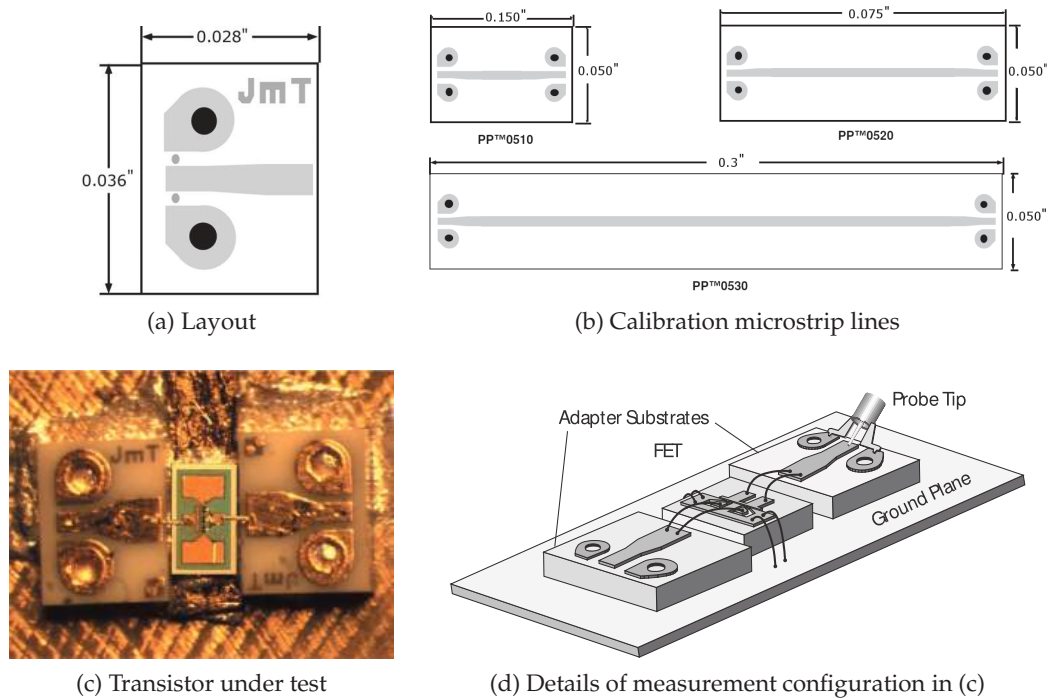


Figure 4-6: Use of a CPW-to-microstrip adaptor enabling coplanar probes to be used in characterizing a non-CPW device. The adaptors provide a low insertion loss CPW-to-microstrip transition. Used with permission of J microTechnology, Inc.

ground-signal-ground (GSG) probes and transition from a coaxial cable to an on-wafer CPW line, providing a smooth transition of the EM fields from those of a coaxial line to those of the CPW line. The on-wafer pads can be as small as 50 μm on a side.

Measurement using CPW probes and manipulators enables repeatable measurements to be made from DC to above 100 GHz. Such measurements require repeatability of probe connections that are better than 1 μm . When the DUT has microstrip connections, it is necessary to use a CPW-to-microstrip adapter, as shown in Figure 4-6. The layout of a suitable adapter is shown in Figure 4-6(a). In Figure 4-6(c and d) two adapters are shown in use in the characterization of a microwave transistor. GSG probes contact the adapters and the grounds are connected to the backside metalization by vias. Calibration uses the microstrip transmission line calibration substrates shown in Figure 4-6(b).

4.3 Calibration

The components of a microwave measurement system introduce substantial errors. Fortunately a network analyzer is a very stable instrument and the errors are faithfully reproduced. This means that a calibration procedure can be used to determine the errors and then the errors can be removed from raw measurements of the device being measured, which, by convention, is called

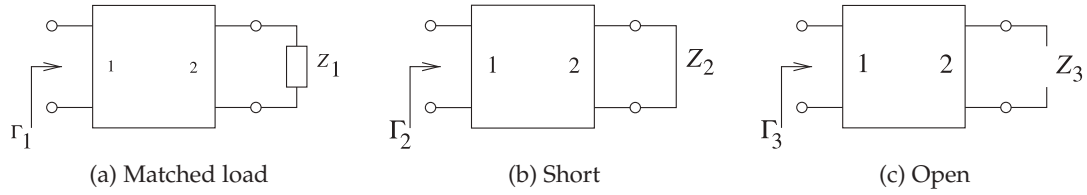


Figure 4-7: Two-port error network with three different calibration loads.

the **device under test (DUT)**. All that is needed to determine the parameters of a two-port are three precisely known loads.

Calibration of the measurement system is critical, as the effect of cabling and connectors can be more significant than that of the device being measured. The process of removing the effect of cabling and connectors is called de-embedding. Ideally, perfect short, open, and matched loads would be available, but these can only be approximated, and numerous schemes have been developed for alternative ways of calibrating an RF measurement system. In some cases, for example, in measuring integrated circuits using what is called on-wafer probing, it is very difficult to realize a good match. A solution is to use calibration standards that consist of combinations of transmission line lengths and repeatable reflections. These calibration procedures are known mostly by combinations of the letters T, R, and L such as **through-reflect-line TRL** [3] (which relies on a transmission line of known characteristic impedance to replace the match); or **through-line (TL)**, [4, 5] (which relies on symmetry to replace the third standard).

4.3.1 One-Port Calibration

In one-port measurements the desired reflection coefficient cannot be obtained directly. Instead, there is effectively an error network between the measurement plane at the load and the ideal internal network analyzer port. The network model [6] of the measurement system is shown in Figure 4-7 together with three ideal calibration standards. Calibration, here, is concerned with determining the S parameters of the error two-port.

Various calibration schemes have been developed, some of which are better in particular measurement environments, such as when measuring on-chip structures. Calibration schemes share certain commonalities. One of these is that the errors can be represented as a two-port (or several two-ports) that exists between an effective reference plane internal to the measurement equipment and the reference plane at the device to be measured. This device is commonly called the device under test (DUT). Known standards are placed at the device reference plane and measurements are made. The concept is illustrated by considering the determination of the S parameters of the two-port shown in Figure 4-7. With Z_1 being a matched load, the input reflection coefficient Γ_1 is S_{11} :

$$S_{11} = \Gamma_1. \quad (4.1)$$

The other commonly used calibration loads are $Z_2 = 0$ (a short circuit) and $Z_3 = \infty$ (an open circuit). In calibration precision shorts and opens are

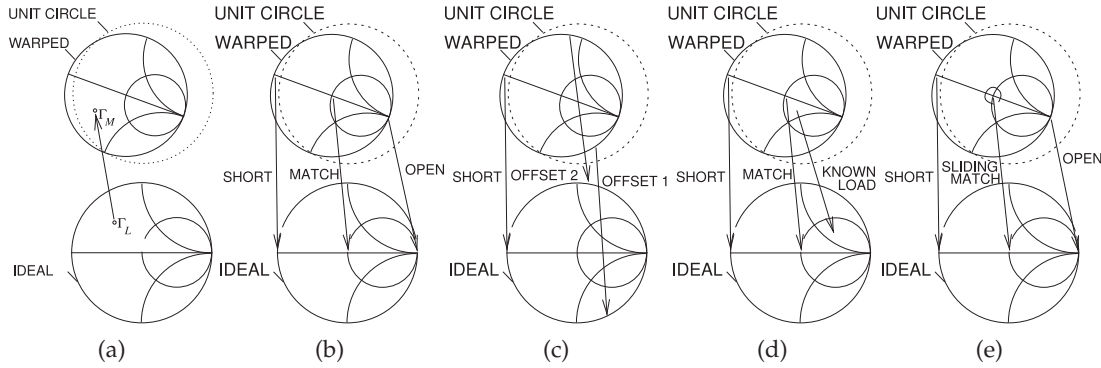


Figure 4-8: Calibrations as mapping operations with each calibration mapping having a warped Smith chart and an ideal Smith chart. The raw measurement of a reflection coefficient of a load is not the actual reflection coefficient, Γ_L , but instead is the raw measurement, Γ_M , which appears on a Smith chart that is warped (see (a)). In calibration, the raw measurements of standards also appear on the warped Smith chart although their actual values are known: (b) calibration as a mapping established using short, match, and open calibration standards; (c) mapping using short and two offset short calibration standards; (d) mapping using a short, a match, and a known load as calibration standards; and (e) mapping using a short, an open, and a sliding matched load as calibration standards.

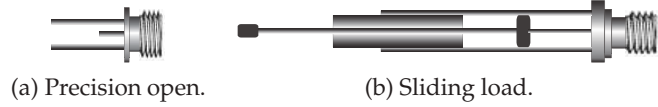
are used and the errors involved are known and incorporated in the more detailed calibration procedure. From these, $S_{12} = S_{21}$ and S_{22} can be derived:

$$S_{22} = \frac{2S_{11} - \Gamma_2 - \Gamma_3}{\Gamma_2 - \Gamma_3} \quad (4.2)$$

$$\text{and} \quad S_{21} = S_{12} = [(\Gamma_3 - S_{11})(1 - S_{22})]^{1/2}. \quad (4.3)$$

The error two-port modifies the actual reflection coefficient of a DUT to a warped (but calibrated) reflection coefficient according to Equation (3.12). In Equation (3.12), the load reflection coefficient, Γ_L , is a complex number that is scaled, rotated, and shifted before being presented at Γ_{in} . Moreover, circles of reflection coefficient are mapped to circles on the warped complex plane; that is, the ideal Smith chart is mapped to a warped Smith chart. Here the actual load reflection coefficient, Γ_L , is warped to present a measured reflection coefficient, Γ_M , to the internal network analyzer. Calibration can be viewed as a mapping operation from the complex plane of raw measurements to the complex plane of ideal measurements, as shown in Figure 4-8(a). That is, calibration develops the required mapping. Figure 4-8(b–e) shows how the corrected mapping is developed using different sets of calibration standards. The mapping operation shown in Figure 4-8(b) uses the short, open, and match loads. This one-port calibration procedure is called open-short-load or SOL calibration and is available as a calibration algorithm in all network analyzers. The three standards are well distributed over the Smith chart and so the mapping can be extracted with good precision. While ideal short, open, and match loads are not available, if the terminations are well characterized then appropriate corrections can be made. The mapping in the one-port case is embodied in the extracted S

Figure 4-9: Precision calibration standards.



parameters of the two-port.

Figure 4-9(a) shows the longitudinal section of a precision coaxial open. The key feature is that the outer coaxial conductor is extended and the fringing capacitance at the end of the center conductor can be calculated analytically. Thus the precision open is not a perfect open, but rather an open that can be modeled as a small capacitor whose frequency variation is known. Figure 4-8(c) uses offset shorts (i.e., short-circuited transmission lines of various lengths). This circumvents the problem of difficult-to-produce open and matched loads. Care is required in the choice of offsets to ensure that the mapping can be determined accurately. The calibration scheme shown in Figure 4-8(d) introduces a known load. The mapping cannot be easily extracted here, but in some situations this is the only option. Figure 4-8(e) introduces a new concept in calibration with the use of a sliding matched load such as that shown in Figure 4-9(b). A perfect matched load cannot be produced and there is always, at best, a small resistance error and perhaps parasitic capacitance. When measured, the reflection will have a small offset from the origin. If the matched load is moved, as with a sliding matched load, a small circle centered on the origin will be traced out and the center of this circle is the ideal matched load.

4.3.2 De-Embedding

The one-port calibration described above can be repeated for two ports, resulting in the two-port error model of Figure 4-10(a), the error model for correcting two-port measurements. Using the chain scattering matrix (or \mathbf{T} matrix¹) introduced in Section 2.6, the \mathbf{T} parameter matrix measured at the internal reference planes of the network analyzer is

$$\mathbf{T}_{\text{MEAS}} = \mathbf{T}_A \mathbf{T}_{\text{DUT}} \mathbf{T}_B, \quad (4.4)$$

where \mathbf{T}_A is the \mathbf{T} matrix of the first error two-port, \mathbf{T}_{DUT} is the \mathbf{T} matrix of the device under test, and \mathbf{T}_B is the \mathbf{T} matrix of the right-hand error two-port. Manipulating Equation (4.4) leads to \mathbf{T}_{DUT} :

$$\mathbf{T}_A^{-1} \mathbf{T}_{\text{MEAS}} \mathbf{T}_B^{-1} = \mathbf{T}_A^{-1} \mathbf{T}_A \mathbf{T}_{\text{DUT}} \mathbf{T}_B \mathbf{T}_B^{-1} \quad (4.5)$$

$$\mathbf{T}_{\text{DUT}} = \mathbf{T}_A^{-1} \mathbf{T}_{\text{MEAS}} \mathbf{T}_B^{-1}, \quad (4.6)$$

from which the S parameters of the DUT can be obtained.

4.3.3 Two-Port Calibration

The VNA architecture introduced in 1968 and still commonly used today is shown in Figure 4-1. A key component of the system is the test set that comprises mechanical microwave switches and directional couplers that selectively couple energy in either the forward- or backward-traveling waves. Many modern VNAs use multiple mixers and electronic switches to

¹ Note that there are several \mathbf{T} matrices, so it necessary to be specific.

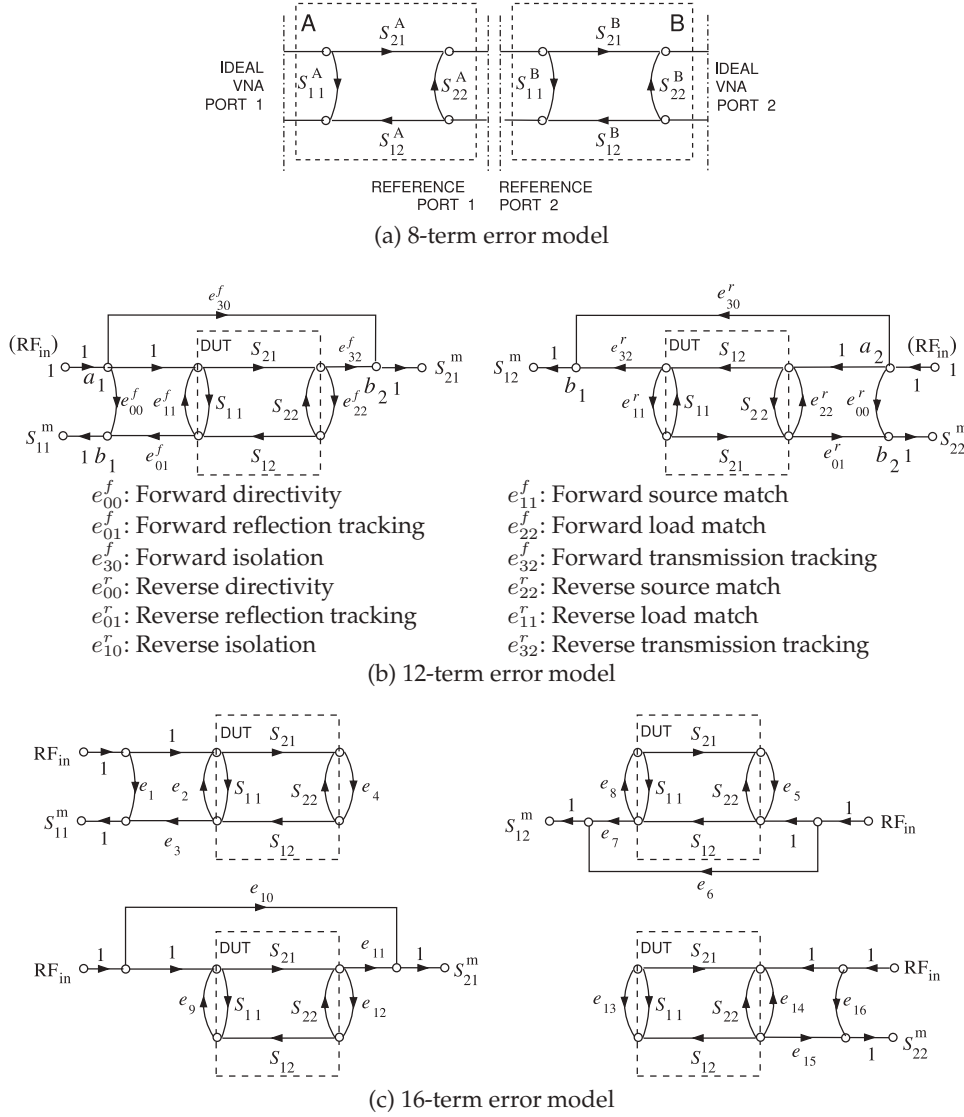


Figure 4-10: Two-port error models: (a) SFG representation of the 8-term two-port error model (1968) [1]; (b) SFG of the 12-term two-port error model (1978) [7]; and (c) SFG of the 16-term two-port error model (circa 1979) [8]. S_{ij}^m are the raw S parameter measurements, S_{ij} are the S parameters of the DUT, and e_{ij} , e_{ij}^r , and e_{ij}^f are error S parameters determined during calibration.

eliminate the need for mechanical switches. Operation is similar. Returning to the architecture of Figure 4-1, this architecture supports a single signal source and a single test port at which the RF signal to be measured is mixed down to a low frequency, typically 100 kHz, where it is captured by an ADC. The mixing component is called the frequency converter, and it mixes the RF signal with a version of the original RF signal offset in frequency to produce a low-frequency version of the RF signal. This has the same phase as the

RF signal and an amplitude that is linearly proportional to the RF signal. When Hackborn introduced this system in 1968 [1], he also introduced the 8-term error model shown in Figure 4-10(a). This is an extension of the one-port error model discussed in Section 4.3.1, with a two-port capturing the measurement errors to each port.

Closer examination of the VNA system of Figure 4-1 indicates that the signal path varies for each of the four scattering parameters for a DUT. Another imperfection that is not immediately obvious is that there is leakage in the system so that Ports 1 and 2 are coupled by a number of mechanisms that do not involve transmission of the signal through the DUT. Leakage is due to finite isolation in the mixers and direct coupling between probes used to make contact at Ports 1 and 2, among other possible causes. The first person to identify this was Shurmer [9] in 1973, leading eventually to the 12-term error model [7, 10] shown in Figure 4-10(b). Calibration yields the error parameters, and the S parameters of the DUT are found as follows:

$$S_{11} = \frac{1}{\delta} \left\{ \left[\frac{S_{11}^m - e_{00}^f}{e_{01}^f} \right] \left[1 + \frac{S_{22}^m - e_{00}^r}{e_{01}^r} e_{22}^r \right] - e_{22}^f \left[\frac{S_{21}^m - e_{30}^f}{e_{32}^f} \right] \left[\frac{S_{12}^m - e_{10}^r}{e_{32}^r} \right] \right\} \quad (4.7)$$

$$S_{21} = \frac{1}{\delta} \left\{ \left[\frac{S_{21}^m - e_{30}^f}{e_{32}^f} \right] \left[1 + \frac{S_{22}^m - e_{00}^r}{e_{01}^r} (e_{22}^r - e_{22}^f) \right] \right\} \quad (4.8)$$

$$S_{12} = \frac{1}{\delta} \left\{ \left[\frac{S_{12}^m - e_{10}^r}{e_{32}^r} \right] \left[1 + \frac{S_{11}^m - e_{00}^f}{e_{01}^f} (e_{11}^f - e_{11}^r) \right] \right\} \quad (4.9)$$

$$S_{22} = \frac{1}{\delta} \left\{ \left[\frac{S_{22}^m - e_{00}^r}{e_{01}^r} \right] \left[1 + \frac{S_{11}^m - e_{00}^f}{e_{01}^f} e_{11}^f \right] - e_{11}^r \left[\frac{S_{21}^m - e_{30}^f}{e_{32}^f} \right] \left[\frac{S_{12}^m - e_{10}^r}{e_{32}^r} \right] \right\} \quad (4.10)$$

$$\delta = \left[1 + \frac{S_{11}^m - e_{00}^f}{e_{01}^f} e_{11}^f \right] \left[1 + \frac{S_{22}^m - e_{00}^r}{e_{01}^r} e_{22}^r \right] - e_{22}^f e_{11}^r \left[\frac{S_{21}^m - e_{30}^f}{e_{32}^f} \right] \left[\frac{S_{12}^m - e_{10}^r}{e_{32}^r} \right]. \quad (4.11)$$

The most complete model is the 16-term error model introduced in 1979 and shown in Figure 4-10(c), which incorporates a different model for each parameter and fully captures the various signal paths resulting from the different switch positions [8]. Nevertheless, the 12-term error model is the one most commonly used in microwave measurements and is sufficient to reliably extract the desired S parameters of the DUT from the raw VNA measurements. This process of extracting the de-embedded parameters is called de-embedding, or less commonly, unterminating.

The 12-term error model models the error introduced by leakage or crosstalk internal to the network analyzer. The 16-term error model captures the leakage or crosstalk of the 12-term error model, but in addition includes switch leakage that results in error signals reflecting from the DUT and leaking to the transmission port as well as common-mode leakage [11]. This method is called two-port 16-term singular value decomposition (SVD) calibration, as the equations are solved in a least squares sense using the singular value decomposition method [11]. In a coaxial environment, the

extra leakage terms are small, provided that the switches have high isolation. However, in wafer probing where direct coupling between the probes can be appreciable, the transmission-related leakage can be important and the 16-term error model captures errors that the 12-term error model does not. These error models and the sequence of measurements to extract them are included in the VNA control software. The user must select which to use.

Coaxial Two-Port Calibration

If the DUT has coaxial connectors then precision open, short, and matched loads are available. While these are not ideal components, the open has fringing capacitance; for example, they are well characterized over frequency. The full set of standards required to develop the 12-term error model includes one-port measurements for each port with open, short, and match connections, a two-port measurement with a through connection, and a two-port measurement with opens at each port. The last measurement determines the internal isolation of the system. Most connectors come in male and female counterparts. As such it is not possible to create a perfect through by joining the connectors and a small delay is introduced. There are, however, sexless connectors, such as the Amphenol precision connector (APC-7) with a 7 mm outer diameter as it has a flush face that can be connected for a near-perfect through. The APC-7 connector is no longer commonly used, with most coaxial systems now using SMA connectors or the higher-tolerance APC 3.5 connectors that come in male and female connectors. The majority of the measurements desired these days are of ICs and other planar structures for which there is no clear connector. The connector, or fixture, problem has resulted in a variety of standards being used.

Planar Circuit Calibration

Calibration standards are required in microwave measurements. For measurements of microstrip and CPW systems, standard calibration alumina substrates are available, see Figure 4-5(d and e). These calibration substrates include various lengths of transmission lines that can be used as standards, as well as an open, a short, and a laser-trimmed matched load.

4.3.4 Transmission Line-Based Calibration Schemes

A drawback of all de-embedding techniques that use repeated fixture measurements during the de-embedding process is the generation of errors caused by the lack of fixture reproducibility during measurements of each of the required standards. These errors can be amplified during the course of de-embedding.

The TRL technique [3] is a calibration procedure used for microwave measurements when classical standards such as open, short, and matched terminations cannot be realized. There are now a family of related techniques, here denoted as TxL methods, with the commonality being the two-port measurement of a through connection and of the same structure with an inserted transmission line. The two-port connections required in the TRL procedure are shown in Figure 4-11. The concept behind the representation is that there is a measurement error that is captured by

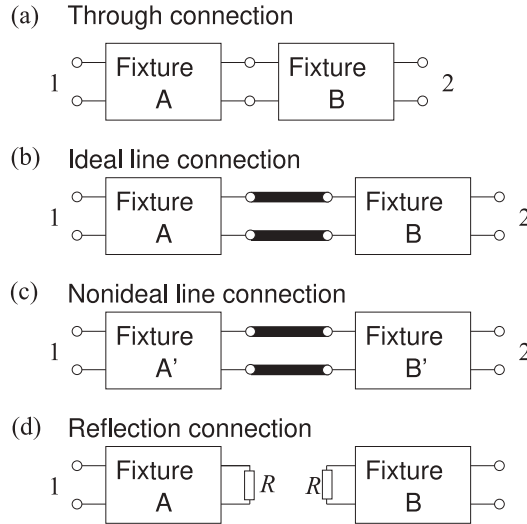


Figure 4-11: Measurement connections in two-port calibration using the TRL procedure: (a) through connection; (b) ideal line connection; (c) realistic configuration with nonidentical fixtures; and (d) with arbitrary reflection.

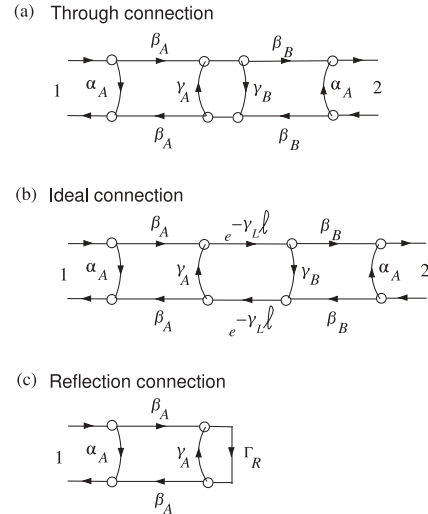


Figure 4-12: SFG representations of the two-port connections shown in Figure 4-11: (a) through connection; (b) ideal line connection; and (c) arbitrary reflection connection.

the fixture two-port. The TRL procedure allows the fixtures on either side, Fixtures A and B here, to have different two-port parameters. The SFG representations of the connections are shown in Figure 4-12. Assuming that the fixtures are faithfully reproduced when going from one connection to another, then the SFGs shown in 4-12(a–c) need to be considered. With each configuration, two-port measurements are made, and as the number of independent S parameter measurements exceed the number of unknowns, it would seem that it may be possible to solve the SFGs to obtain the unknown parameters of the fixtures. This is all that is required to de-embed measurements made with a DUT between the fixtures. Unfortunately this is not possible. However, Engen and Hoer [3] developed a procedure that enabled the complex propagation constant of the line to be extracted from the external S parameter measurements of the through and line connections. This procedure is considered in the next section.

4.3.5 Through-Line Calibration

The through and line measurement structures include fixtures as well as the direct connection (for the through) and the inserted line (for the line) (see Figure 4-11). Two-port measurements of these two structures yield the propagation constant $\gamma_L = \alpha + j\beta$ of the line [3]. Similar but earlier work was presented by Bianco et al. [12]. For the through structure, the error networks between the ideal internal port of a network analyzer and the desired measurement reference plane are designated as Fixture A at Port 1 and Fixture B at Port 2. For the line measurement, fixturing is reestablished (following the through measurement) with the line inserted. In general, the

fixturing cannot be faithfully reproduced and therefore becomes Fixtures A' and B', respectively (see Figure 4-11).

The following is based on the derivation of Engen and Hoer [3]. As well as presenting an important result indicating sources of error in microwave measurement, the development demonstrates a technique for solving measurement problems involving transmission lines.

The development begins using **cascading matrices**, \mathbf{R} , defined as

$$\begin{bmatrix} b_1 \\ a_1 \end{bmatrix} = \mathbf{R} \begin{bmatrix} a_2 \\ b_2 \end{bmatrix}, \quad (4.12)$$

which is related to scattering parameters \mathbf{S} by

$$\mathbf{R} = \begin{bmatrix} R_{11} & R_{12} \\ R_{21} & R_{22} \end{bmatrix} = \begin{bmatrix} \frac{S_{12} S_{21} - S_{11} S_{22}}{S_{21}} & \frac{S_{11}}{S_{21}} \\ -\frac{S_{22}}{S_{21}} & \frac{1}{S_{21}} \end{bmatrix}. \quad (4.13)$$

Thus the parameters describing the A and B fixtures are \mathbf{S}_A , \mathbf{S}_B and \mathbf{R}_A , \mathbf{R}_B , respectively. The cascading matrix of the through is simply a unity matrix and the line of length, ℓ_L , is described by

$$\mathbf{R}_L = \begin{bmatrix} e^{-\gamma_L \ell_L} & 0 \\ 0 & e^{\gamma_L \ell_L} \end{bmatrix}. \quad (4.14)$$

The characteristic impedance of the line is taken as the reference impedance, Z_0 , of the measurement system and results in the off-diagonal zeros in the above definition for the line standard. Because of this simplifying assumption, γ_L can be computed using the equations that follow.

The cascading matrix of the through structure (i.e., the fixture-fixture cascade) is

$$\mathbf{R}_t = \mathbf{R}_A \mathbf{R}_B \quad (\text{the through}). \quad (4.15)$$

For the line structure, a fixturing error Δ is introduced. Δ corresponds to a small additional electrical length of the A fixture (i.e., $\mathbf{R}'_A = \mathbf{R}_A \mathbf{R}_e$), then the cascading matrix of the fixture-line-fixture cascade is

$$\mathbf{R}_d = \mathbf{R}'_A \mathbf{R}_L \mathbf{R}_B = \mathbf{R}_A \mathbf{R}_e \mathbf{R}_L \mathbf{R}_B \quad (\text{the line}) \quad \text{with } \mathbf{R}_e = \begin{bmatrix} e^{-\Delta} & 0 \\ 0 & e^{\Delta} \end{bmatrix}. \quad (4.16)$$

Now introduce the matrix

$$\mathbf{T} = \begin{bmatrix} t_{11} & t_{12} \\ t_{21} & t_{22} \end{bmatrix} = \mathbf{R}_d \mathbf{R}_t^{-1}. \quad (4.17)$$

Thus \mathbf{T} combines the line and through measurements and approximately removes the through measurement from the line measurement. Most importantly, all of the elements of the \mathbf{T} matrix are measured quantities. Continuing (note that if \mathbf{A} and \mathbf{B} are matrices, $(\mathbf{AB})^{-1} = \mathbf{B}^{-1}\mathbf{A}^{-1}$), and using Equations (4.15)–(4.17),

$$\begin{aligned} \mathbf{T} \mathbf{R}_A &= \mathbf{R}_d \mathbf{R}_t^{-1} \mathbf{R}_A = \mathbf{R}'_A \mathbf{R}_L \mathbf{R}_B (\mathbf{R}_A \mathbf{R}_B)^{-1} \mathbf{R}_A \\ &= \mathbf{R}_A \mathbf{R}_e \mathbf{R}_L \mathbf{R}_B^{-1} \mathbf{R}_A^{-1} \mathbf{R}_A \end{aligned} \quad (4.18)$$

$$\text{and so } \mathbf{T} \mathbf{R}_A = \mathbf{R}_A \mathbf{R}_e \mathbf{R}_L, \quad (4.19)$$

which is referred to as the TL (for through-line) equation. Expanding Equation (4.19) leads to a system of equations:

$$t_{11}R_{A11} + t_{12}R_{A21} = R_{A11}e^{-\Delta}e^{-\gamma_L\ell_L} \quad (4.20)$$

$$t_{21}R_{A11} + t_{22}R_{A21} = R_{A21}e^{-\Delta}e^{-\gamma_L\ell_L} \quad (4.21)$$

$$t_{11}R_{A12} + t_{12}R_{A22} = R_{A12}e^{\Delta}e^{\gamma_L\ell_L} \quad (4.22)$$

$$t_{21}R_{A12} + t_{22}R_{A22} = R_{A22}e^{\Delta}e^{\gamma_L\ell_L}, \quad (4.23)$$

which upon solution yields the propagation constant of the line standard [3],

$$\gamma_L = \frac{1}{2\ell_L} \left[\ln \left(\frac{t_{11} + t_{22} \pm \zeta}{t_{11} + t_{22} \mp \zeta} \right) - 2\Delta \right] \quad (4.24)$$

$$\zeta = (t_{11}^2 - 2t_{11}t_{22} + t_{22}^2 + 4t_{21}t_{12})^{1/2}. \quad (4.25)$$

If the fixtures are faithfully reproduced, then networks A and A' are identical, as are networks B and B', and so $\Delta = 0$, and γ_L is

$$\gamma_L = \frac{1}{2\ell_L} \ln \left(\frac{t_{11} + t_{22} \pm \zeta}{t_{11} + t_{22} \mp \zeta} \right). \quad (4.26)$$

The sign to use with ζ is chosen corresponding to the root selection [3].

That is, two-port S parameter measurements of the through connection (shown in Figure 4-11(a)) and two-port S parameter measurements of the line connection (shown in Figure 4-11(b)) enable the propagation constant of the line to be determined. The characteristic impedance of the line standard can be determined as described in Section 4.5.

Extraction of the propagation constant of the transmission line standard is a common property of calibration techniques that use through and line measurements instead of match measurements. Such techniques are called TxL techniques, where x identifies an additional measurement used in calibration. Unfortunately the TxL calibration techniques often result in errors in de-embedding at frequencies where the length of the line standard is a multiple of one-half wavelength (called critical lengths [13, 14]). These are the lengths where the electrical length is a multiple of 180° . Buff et al. [15, 16] showed that small fixture repeatability errors result in errors incorporated in Δ . These errors affect the entire calibration and subsequent de-embedded measurements. These errors are minimized by using measurements where the line standard has an electrical length not within 20° of a critical length. Statistical means and the use of multiple lines have been proposed to minimize the error [17, 18], as well as an optimization scheme to determine the additional electrical length, Δ [15, 16]. The optimization scheme significantly reduces the uncertainty and is based on the assumption that a change of line length is the sole source of error in fixture reproducibility (the fixture here includes, of course, the probe and probe pad). This is seen in Figure 4-13 where the results of optimization are seen most clearly for the attenuation constant in Figure 4-13(a), the curve labeled fixture error de-embedded. The no fixture error curve was selected as the best results from a large number of calibrations (multiple repeats of probe-on-probe pad connections). The fixture error curve is the result of a typical calibration measurement.

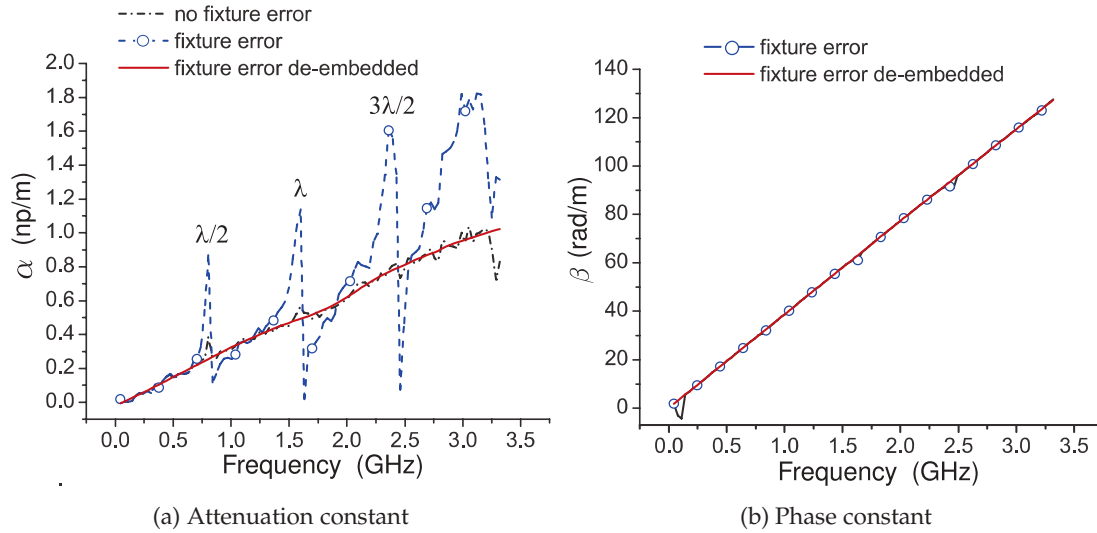


Figure 4-13: Extracted propagation constant from the through and line components of TRL with fixture error introduced during the line measurement.

In the following, several of the TxL calibration techniques are described. These are techniques incorporated in most vector network analyzers and are particularly useful in characterizing on-chip circuits. An example of an on-wafer two-port measurement is shown in Figure 4-14, showing on-chip calibration standards. The VNA software leads the user through the required set of calibration measurements and computes the error models to be used in de-embedding.

Through Short Delay

Matched loads can be difficult to realize, especially when probing ICs and planar circuits using probes. The through short delay (TSD) method uses reflection and transmission measurements [19]. The delay is realized using a line with a $50\ \Omega$ characteristic impedance. TSD experiences the 180° glitches common to TxL schemes. The through could be another delay, but then problems occur when the delay difference (the electrical length difference) of the through and delay is an integer multiple of 180° .

Through Reflect Line

What has become known as the through reflect line (TRL) calibration technique was developed by Bianco et al. [12] and Engen and Hoer [3], who used a through connection, an arbitrary reflection standard, and a delay or line standard. The line standard can be of arbitrary length with its propagation constant unknown, but it is assumed to be nonreflecting. The result of this assumption is that the characteristic impedance of the line becomes the system reference impedance. Also, the reflection standard, can be any repeatable reflection load, with an open or short preferred. Again the transmission line introduces calibration uncertainties when the electrical

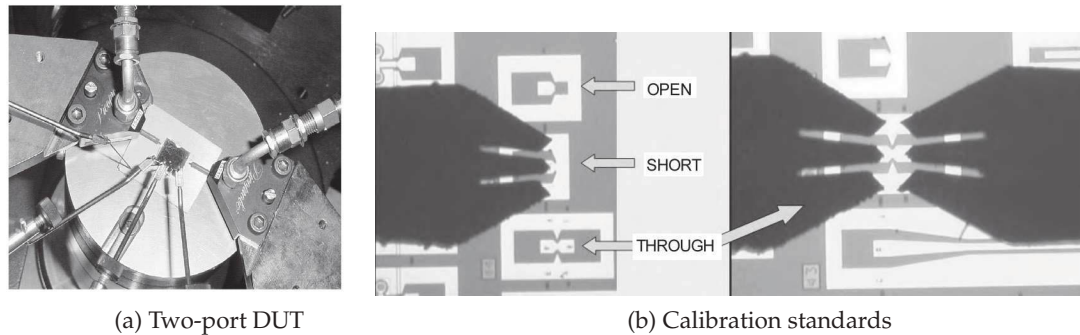


Figure 4-14: Two-port measurements: (a) two-port device under test with DC needle probes at the bottom and GSG probes on the left and right; and (b) open, short, and through calibration standards with GSG probes.

length is a multiple of one-half wavelength [3].

Through Reflect Match

Through reflect match (**TRM**) is a variation of TRL that replaces the through by a matched load and is useful only when a matched load can be realized. It retains the arbitrary reflection standard, which is particularly useful as it can be difficult to produce a short or open with planar circuits. For example, a via used in realizing a microstrip short circuit has finite resistance and inductance and so does not create a good through, but does create a useful repeatable arbitrary reflection. The technique does not have the critical length glitches, but repeatable fixturing is always important.

Other Distributed Calibration Techniques

TRL and TRM are the most commonly accepted standards used in calibrating measurements of planar circuit structures. There are several other related techniques that also use transmission lines and are useful in certain circumstances.

In 1982 Benet [20] developed the open-short-five-offset-line calibration technique. The key concept is that the multiple offset through lines trace out a circle on the Smith chart and the center of the circle provide the matched load. Through least squares fitting Benet derived the propagation constant of the through lines and the remaining error terms to develop the 12-term error model.

Pennock et al. [21] introduced the **double through line (DTL)** calibration system in 1987. This is useful for characterizing transitions between different mediums. There is sufficient information to develop the 6-term error model. SOLT (short-open-load-through) calibration requires precisely characterized standards and is robust to 20 GHz.

SOLR (short-open-load-reciprocal-through) calibration is similar to SOLT using precisely defined reflect standards as a standard.

LRRM, (line-reflect-reflect-match) calibration uses a line instead of a through, one of the reflection standards is a short and the other is an open. This is

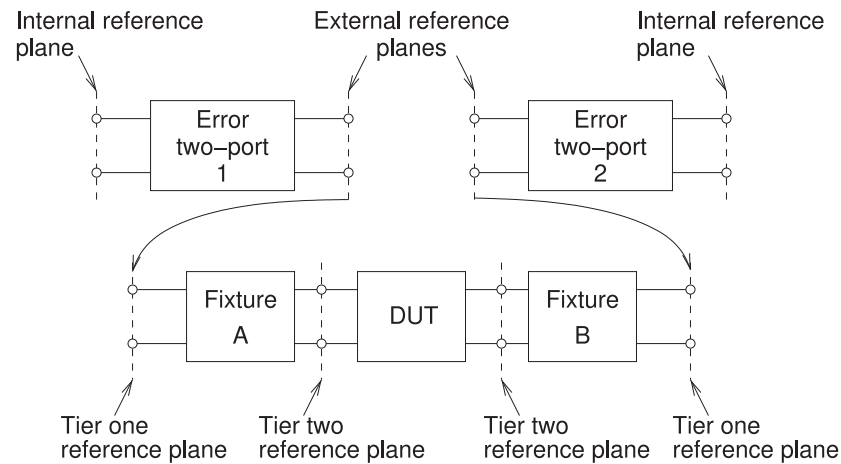


Figure 4-15: Two-tier calibration procedure.

usually the best calibration technique to use with probes, as these standards are straightforward to incorporate in calibration substrates. The calibration standards are the same as those used in SOLT, but LRRM does not require precision short and open standards. The essentials of what must be known are the characteristics of the through and the DC resistance of one of the load standards. The inductance of the load is automatically determined.

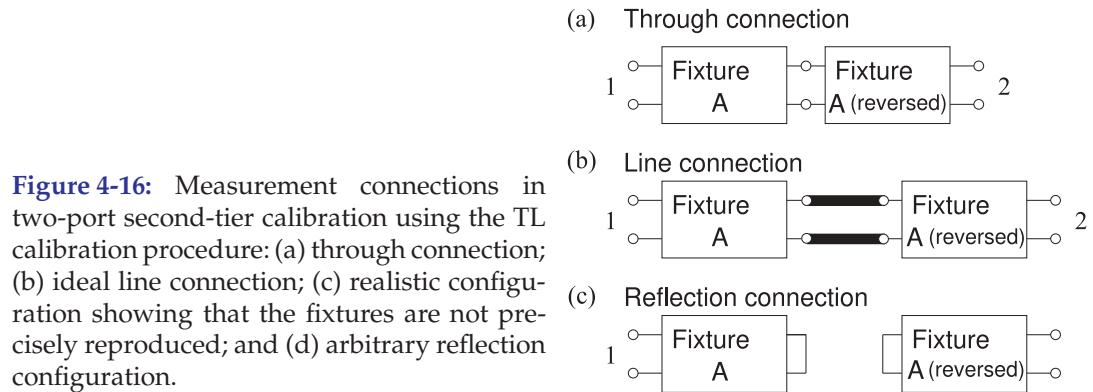
LRM, (load-reflect-match) calibration is similar to LRRM calibration but does not use a precision reflect standard. A modification is LRM+, for which the DC resistances of the loads are required.

4.3.6 Two-Tier Calibration

With measurements in noncoaxial systems, it is difficult to produce precision standards such as shorts, opens, and resistive loads. In these situations, two-tier calibration is sometimes used. In a two-tier calibration procedure, two sets of standards are used to establish first- and second-tier reference planes (see Figure 4-15). It is preferable to use a highly repeatable set of standards in Tier 1 (such as a non-TxL technique), and one that yields more precise characterization in a particular environment (such as a TxL technique for on-wafer measurement).

In the first-tier calibration, a precision set of standards is normally used. This can be achieved using coaxial standards or perhaps a standard calibration substrate used with probes. Referring to Figure 4-15, each of the 2 two-ports from the internal reference planes of the network analyzer to the external reference planes is established. Generally with the second tier, insitu calibration standards are used, and the additional (e.g. on-chip) fixturing is identical for the two ports. Precision calibration should be done using standards fabricated in the medium of the DUT.

Two-tier calibration generally results in the fixtures in the second tier being identical. This enables checks to be made for the integrity of the probe connection. Connections to IC pads can be problematic because of oxide build up, especially with aluminum pads. So ensuring symmetry of second-tier calibrations by comparing the two-port measurements of symmetrical structures such as transmission lines can greatly reduce the impact of the fixture-induced errors discussed in Section 4.3.5. Recall that small fixturing errors, such as bringing the probes down in slightly different positions,



results in measurement errors at the half-wavelength frequencies ($\lambda/2$, λ , $3\lambda/2$, etc.). For example, if the DUT is a device on a silicon wafer, the optimum measurement technique is to realize the calibration standards on the silicon wafer processed in the same way as for the DUT. The two-tier calibration procedure removes fixturing errors associated with fringing effects at the probes and with other nonidealities involved in creating the landing pads for the probes.

In an example two-tier calibration scheme, a first tier is used to establish the 12-term error model. Then a second calibration is used to develop a secondary six-term error model, as in Figure 4-10(a) with $S_{12} = S_{21}$. In such a situation the standards used in developing the 12-term error model would normally include an open, a short, and a matched load. These need not be precise standards. Thus the 12-term error model need not be precise, and this model does not suffer from the half-wavelength errors of the TxL techniques.

Through Line Symmetry

For planar measurements using probes, first-tier calibration using a standard calibration substrate is to the end of the probe tips, and errors with using other substrates (e.g., the probe pads are of different size or the substrate permittivity is different) will be common to both probes (fixtures) in a two-port measurement. With careful design, the fixtures employed in the second tier will be identical and have the same S parameters. In the second-tier calibration, measurements of a through and line will be symmetrical with $S_{11} = S_{22}$ and $S_{12} = S_{21}$. This symmetry is exploited in the **through line (TL)** technique which exploits symmetry and renders the half-wavelength errors of TxL insignificant [4, 5]. The TL calibration connections in second-tier calibration are shown in Figure 4-16. In the first calibration tier, a 12-term error model is developed using open, short, load, and delay. Consequently there are no half-wavelength glitches that occur when transmission line standards are used. In the second calibration tier, probes are used with two lengths of transmission line fabricated on the same substrate as the DUT. One of the lines becomes a through.

The procedure proceeds by calculating the propagation constant of the line using the technique developed for the TRL procedure (Equation (4.26)). There is fixture symmetry in the TL connections (see Figure 4-16) and this is reflected in the SFG representations of the connections as shown in Figure 4-17. As will be shown, this symmetry enables the arbitrary reflection used

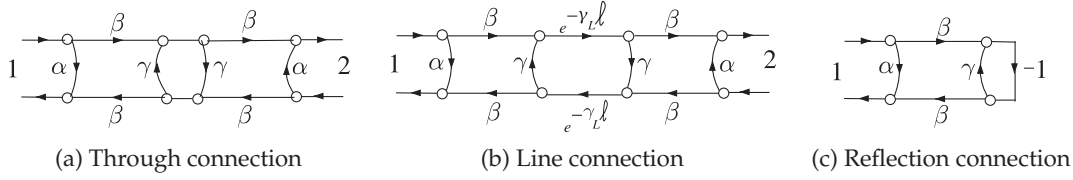


Figure 4-17: SFG representations of the two-port connections shown in Figure 4-16.

in the TRL procedure to be replaced by a virtual precise short or open circuit. Let the S parameters of Fixture A be $\alpha = S_{11}$, $\beta = S_{12} = S_{21}$, and $\gamma = S_{22}$. Using these parameters with the port reversal required to model the Fixture at Port 2, the SFG shown in Figure 4-17(a) relates the measured S parameters to the parameters of the fixtures. The input reflection coefficient of Fixture A with a short circuit placed at Port 2 of A is

$$\rho_{sc} = \alpha - \frac{\beta^2}{1 + \gamma}. \quad (4.27)$$

Let the measured S parameters of the through connection be designated by a leading superscript T . Using the self-loop (or Mason's) rule with the SFG in Figure 4-17(a) relates the measured S parameters to the fixture parameters:

$$^T S_{11} = \alpha + \frac{\beta^2 \gamma}{1 - \gamma^2} \quad \text{and} \quad ^T S_{21} = \frac{\beta^2}{1 - \gamma^2}. \quad (4.28)$$

Subtracting these expressions yields

$$\begin{aligned} ^T S_{11} - ^T S_{21} &= \alpha + \frac{\beta^2 \gamma}{1 - \gamma^2} - \frac{\beta^2}{1 - \gamma^2} = \alpha + \frac{\beta^2 \gamma - \beta^2}{(1 - \gamma)(1 + \gamma)} \\ &= \alpha - \frac{\beta^2 (1 - \gamma)}{(1 - \gamma)(1 + \gamma)} = \alpha - \frac{\beta^2}{1 + \gamma} = \rho_{sc}. \end{aligned} \quad (4.29)$$

That is, the input reflection coefficient of a fixture terminated in a virtual ideal short circuit can be obtained from the through measurement of the back-to-back fixtures in the through configuration:

$$\rho_{sc} = ^T S_{11} - ^T S_{21}. \quad (4.30)$$

Similar results are obtained for a virtual ideal open circuit placed at Port 2 of Fixture A:

$$\rho_{oc} = ^T S_{11} + ^T S_{21}. \quad (4.31)$$

Thus it is possible to effectively insert ideal open and short circuits within a noninsertable medium.

4.4 Extraction of Transmission Line Parameters

This section describes approaches for extracting the per unit length $RLGC$ parameters of a transmission line, and the effective permittivity and permeability of transmission line mediums, from measurements. The measurements could be made experimentally or through simulation.

Ideal Calibration

The procedure described here assumes ideal calibration to the ports of a uniform transmission line that will yield symmetrical transmission line S parameters with $S_{11} = S_{22}$ and $S_{12} = S_{21}$ for the reciprocal structure. The propagation constant of a transmission line is

$$\gamma = \sqrt{(R + j\omega L)(G + j\omega C)} \quad (4.32)$$

and the characteristic impedance is

$$Z_0 = \sqrt{\frac{(R + j\omega L)}{(G + j\omega C)}}. \quad (4.33)$$

Then

$$R = \Re\{\gamma Z_0\}, \quad L = \Im\left\{\frac{\gamma Z_0}{\omega}\right\}, \quad G = \Re\{\gamma/Z_0\}, \quad C = \Im\left\{\frac{\gamma/Z_0}{\omega}\right\}. \quad (4.34)$$

These parameters can be extracted from the measured S parameters of a transmission line provided that sufficiently accurate calibration can be achieved. This extraction was described in [22–24], yielding the line's characteristic impedance

$$Z_0 = Z_{\text{REF}} \sqrt{\frac{(1 + S_{11})^2 - S_{21}^2}{(1 - S_{11})^2 - S_{21}^2}}, \quad (4.35)$$

where Z_{REF} is the reference impedance of the S parameters. The line's propagation constant is obtained from

$$e^{-\gamma \ell} = \left(\frac{1 - S_{11}^2 + S_{21}^2}{2S_{21}} \pm K \right)^{-1}, \quad (4.36)$$

$$\text{where} \quad K = \left[\frac{(S_{11}^2 - S_{21}^2 + 1)^2 - (2S_{11})^2}{(2S_{21})^2} \right]^{\frac{1}{2}}. \quad (4.37)$$

It is also possible to use specialized test structures to obtain the transmission line parameters. In [25] measurements of the input impedances of short- and open-circuited stubs are used to derive the transmission line parameters.

Nonideal Calibration

The measurement of the S parameters of a transmission line described above assumes that the error model of the fixtures can be accurately calibrated. Sometimes it can be difficult to achieve a sufficiently accurate calibration because of the difficulty of inserting a known resistive impedance standard. In the through-line calibration methods described in Section 4.3.5, measurement of a fixtured transmission line and measurement of back-to-back fixtures (a through connection) yields the propagation constant γ of the transmission line, even if an impedance standard is not available. One way of extracting the characteristic impedance, Z_0 , of a line from measurements in this situation was described in Section 4.5. The key idea was varying the electrical length of a transmission line to trace out a circle on the Smith chart. The frequency-dependent characteristic impedance can be obtained by using a number of transmission lines of different length. So with γ and Z_0 known, the $RLGC$ parameters can be obtained using Equation (4.34).

4.4.1 Summary

The complexity and expense of equipment involved in measuring S parameters depends greatly on the frequency range with vector network analyzers able to measure S parameters above a hundred gigahertz costing many 100s of thousands of dollars. Also the time involved in calibration can be significant taking many hours to days at the very highest of microwave frequencies but only a few minutes at single-gigahertz frequencies. Microwave measurement requires the development of considerable expertise.

4.5 Determining Z_0 of a Line from the Smith Chart

It was shown in Section 3.5.2 that the reflection coefficient locus with respect to frequency of a terminated line is a circle on the Smith chart even if the characteristic impedance of the line is not the same as the reference impedance of the Smith chart. The one caveat here is that the reflection coefficient of the termination must be independent of frequency so a resistive termination is sufficient. If the characteristic impedance of the line is Z_{01} and the Smith chart is referenced to Z_{02} , which is usually the same as the system impedance of the measurement system, then Z_{01} can be determined from the center, C_{Z02} , and radius, R_{Z02} , of the reflection coefficient circle. Thus measurements can be used to determine the unknown impedance Z_{01} . Another situation where this is useful is in design where a transmission line circle can be drawn to complete a design problem and from this the characteristic impedance of the line found. In both situations C_{Z02} , R_{Z02} , and Z_{02} are known and Z_{01} must be determined.

A simple closed-form solution for the unknown characteristic impedance Z_{01} cannot be obtained from Equations (3.49) and (3.50). However, by substituting Equation (3.50) in Equation (3.49), and if Z_{01} and Z_{02} are close (so that B is small), then

$$C_{Z02} \approx B - \frac{1}{B} + \frac{1}{B} \approx B. \quad (4.38)$$

The approximation is better for smaller $|\Gamma_{L,Z01}|$. Also

$$R_{Z02} \approx |\Gamma_{L,Z01}|. \quad (4.39)$$

So provided that the characteristic impedance of the line, Z_{01} , is close to the system reference impedance, Z_{02} ,

$$\frac{Z_{01}}{Z_{02}} = \frac{1+B}{1-B} \approx \frac{1+C_{Z02}}{1-C_{Z02}} \quad (4.40)$$

and this is just the normalized impedance reading at the center of the circle. For example, if a line with a characteristic impedance (Z_{01}) of 55 Ω is terminated in a 45 Ω load, then in a ($Z_{02} =$) 50 Ω system, $C_{Z02} = 0.0939$ and $R_{Z02} = 0.0996$. Using Equation (4.40) the derived $Z_{01} = 54.7 \Omega$ and, using Equation (4.39), $\Gamma_{L,Z01} = 0.0996$ compared to the ideal 0.1000.

Table 4-1 presents the actual characteristic impedance of the line as the ratio Z_{01}/Z_{02} for particular center and radius values measured on the polar plot referenced to Z_{02} . The actual value of impedance is compared to the approximate value for $Z_{01}/Z_{02} \approx 1 + C_{Z02}/1 - C_{Z02}$. It is seen that the

approximation in Equation (4.40) provides a good estimate of the unknown characteristic impedance (Z_{01}) improving as the center of the locus is closer to the origin.

4.6 Summary

The vendors of microwave test equipment program their instruments so that they guide the user through the calibration procedure. Usually the calibration procedures take much longer than the actual DUT measurement. The higher the frequency the longer and more fastidious is calibration, with calibration at 200 GHz perhaps taking days. Still calibration is absolutely required and with it surprisingly accurate measurements can be made at microwave and millimeter-wave frequencies.

4.7 References

- [1] R. Hackborn, "An automatic network analyzer system," *Microwave Journal*, pp. 45–52, May 1968.
- [2] <http://www.ggb.com>.
- [3] G. Engen and C. Hoer, "Thru-reflect-line: An improved technique for calibrating the dual six-port automatic network analyzer," *IEEE Trans. on Microwave Theory and Techniques*, vol. 27, no. 12, pp. 987–993, Dec. 1979.
- [4] S. Goldberg, M. Steer, P. Franzon, and J. Kasten, "Experimental electrical characterization of interconnects and discontinuities in high-speed digital systems," *IEEE Trans. on Components, Hybrids, and Manufacturing Technology*, vol. 14, no. 4, pp. 761–765, Dec. 1991.
- [5] M. Steer, S. Goldberg, G. Rinne, P. Franzon, I. Turlik, and J. Kasten, "Introducing the through-line deembedding procedure," in 1992 *IEEE MTT-S Int. Microwave Symp. Dig.*, Jun. 1992, pp. 1455–1458.
- [6] J. Hunton, "Analysis of microwave measurement techniques by means of signal flow graphs," *IRE Trans. on Microwave Theory and Techniques*, vol. 8, no. 2, pp. 206–212, Mar. 1960.
- [7] J. Fitzpatrick, "Error models for systems measurement," *Microwave Journal*, pp. 63–66, May 1978.
- [8] A. A. M. Saleh, "Explicit formulas for error correction in microwave measuring sets with switching-dependent port mismatches," *IEEE Trans. on Instrumentation and Measurement*, vol. 28, no. 1, pp. 67–71, Mar. 1979.
- [9] H. Shurmer, "Calibration procedure for computer-corrected s parameter characterization of devices mounted in microstrip," *Electronics Letters*, vol. 9, no. 14, pp. 323–324, 12 1973.
- [10] *De-embedding and Embedding S-parameter Networks Using a Vector Network Analyzer*, May 2004, Agilent Application Note 1363–1.
- [11] J. Butler, D. Rytting, M. Iskander, R. Pollard, and M. Vanden Bossche, "16-term error model and calibration procedure for on-wafer network analysis measurements," *IEEE Trans. on Microwave Theory and Techniques*, vol. 39, no. 12, pp. 2211–2217, Dec. 1991.
- [12] B. Bianco, M. Parodi, S. Ridella, and F. F. Selvaggi, "Launcher and microstrip characterization," *IEEE Trans. on Instrumentation and Measurement*, vol. 25, no. 4, pp. 320–323, Dec. 1976.
- [13] C. Hoer, "Choosing line lengths for calibrating network analyzers," *IEEE Trans. on Microwave Theory and Techniques*, vol. 31, no. 1, pp. 76–78, Jan. 1983.
- [14] C. A. Hoer, "Some questions and answers concerning air lines as impedance standards," in *29th ARFTG Conf. Digest-Spring*, vol. 11, Jun. 1987, pp. 161–173.
- [15] P. Buff, "Characterization of propagation on wires over lossy earth," Ph.D. dissertation, North Carolina State University, 2006.
- [16] P. Buff, J. Nath, and M. Steer, "Origin of the half-wavelength errors in microwave measurements using through-line calibrations," *IEEE Trans. on Instrumentation and Measurement*, vol. 56, no. 5, pp. 1610–1615, Oct. 2007.
- [17] R. Marks, "A multilayer method of network analyzer calibration," *IEEE Trans. on Microwave Theory and Techniques*, vol. 39, no. 7, pp. 1205–1215, Jul. 1991.
- [18] D. Williams, "De-embedding and unterminating microwave fixtures with nonlinear least squares," *IEEE Trans. on Microwave Theory and Techniques*, vol. 38, no. 6, pp. 787–791, Jun. 1990.
- [19] N. R. Franzen and R. A. Speciale, "A new

Table 4-1: Table of the normalized characteristic impedance Z_{01}/Z_{02} of a terminated transmission line having characteristic impedance Z_{01} plotted on a Smith chart with a reference impedance of Z_{02} in terms of the center, C_{Z02} , of the circular locus (with respect to line length) of the line for various radii, R_{Z02} , of the circular locus. C_{Z02} and R_{Z02} are in terms of reflection coefficient measured on the Smith chart. Also shown is the approximation, $(1 + C_{Z02})/(1 - C_{Z02})$, of Z_{01}/Z_{02} (see Equation (4.40)).

C_{Z02}	$\frac{Z_{01}/Z_{02} \approx (1 + C_{Z02})}{(1 - C_{Z02})}$	$R_{Z02} = 0.2$		$R_{Z02} = 0.3$		$R_{Z02} = 0.4$		$R_{Z02} = 0.5$	
			error	Z_{01}/Z_{02}	error	Z_{01}/Z_{02}	error	Z_{01}/Z_{02}	error
0.00	1.000	1.000	0%	1.000	0%	1.000	0%	1.000	0%
0.02	1.041	1.043	< 1%	1.045	< 1%	1.050	1%	1.050	1%
0.04	1.083	1.088	< 1%	1.093	1%	1.100	2%	1.113	3%
0.06	1.128	1.130	< 1%	1.140	1%	1.155	2%	1.175	4%
0.08	1.174	1.183	< 1%	1.193	2%	1.210	3%	1.250	6%
0.10	1.222	1.230	< 1%	1.245	2%	1.270	4%	1.310	7%
0.12	1.273	1.285	1%	1.305	2%	1.335	5%	1.385	8%
0.14	1.326	1.340	1%	1.365	3%	1.408	6%	1.465	10%
0.16	1.381	1.400	1%	1.428	3%	1.475	6%	1.550	11%
0.18	1.439	1.460	1%	1.495	4%	1.550	7%	1.645	13%
0.20	1.500	1.528	2%	1.565	4%	1.635	8%	1.745	14%
0.22	1.564	1.595	2%	1.645	5%	1.720	9%	1.860	16%
0.24	1.632	1.670	2%	1.725	5%	1.815	10%	1.980	18%
0.26	1.703	1.745	2%	1.810	6%	1.920	11%	2.120	20%
0.28	1.778	1.830	3%	1.905	7%	2.030	12%	2.270	22%
0.30	1.857	1.915	3%	2.005	7%	2.150	14%	2.450	24%
0.32	1.941	2.008	3%	2.110	8%	2.285	15%	2.655	27%
0.34	2.030	2.105	4%	2.225	9%	2.435	16%	2.885	30%
0.36	2.125	2.215	4%	2.350	10%	2.600	18%	3.125	32%
0.38	2.226	2.325	4%	2.490	11%	2.785	20%	3.515	37%
0.40	2.333	2.455	5%	2.640	12%	3.000	22%	3.925	40%
0.42	2.585	2.585	5%	2.805	13%	3.240	24%	–	–
0.44	2.730	2.730	6%	2.985	14%	3.535	27%	–	–
0.46	2.704	2.885	6%	3.180	15%	3.865	30%	–	–

C_{Z02}	$\frac{Z_{01}/Z_{02} \approx (1 + C_{Z02})}{(1 - C_{Z02})}$	$R_{Z02} = 0.6$		$R_{Z02} = 0.7$	
		Z_{01}/Z_{02}	error	Z_{01}/Z_{02}	error
0.00	1.000	1.000	0%	1.000	0%
0.02	1.041	1.065	2%	1.080	4%
0.04	1.083	1.135	5%	1.170	7%
0.06	1.128	1.208	7%	1.265	11%
0.08	1.174	1.285	9%	1.375	15%
0.10	1.222	1.370	11%	1.500	19%
0.12	1.273	1.465	13%	1.640	22%
0.14	1.326	1.565	15%	1.800	26%
0.16	1.381	1.685	18%	1.990	31%
0.18	1.439	1.820	21%	2.230	35%
0.20	1.500	1.965	24%	2.515	40%
0.22	1.564	2.130	27%	2.915	46%
0.24	1.632	2.330	30%	3.440	53%
0.26	1.703	2.555	33%	4.380	61%
0.28	1.778	2.830	37%	–	–
0.30	1.857	3.205	42%	–	–

procedure for system calibration and error removal in automated s-parameter measurements," in *5th European Microwave Conf.*, Sep. 1975, pp. 69–73.

- [20] J. Benet, "The design and calibration of a universal MMIC test fixture," in *Microwave and Millimeter-Wave Monolithic Circuits*, vol. 82, no. 1, Jun. 1982, pp. 36–41.
- [21] S. R. Pennock, C. M. D. Rycroft, P. R. Shepherd, and T. Rozzi, "Transition characterisation for de-embedding purposes," in *17th European Microwave Conf.*, Sep. 1987, pp. 355–360.
- [22] W. Eisenstadt and Y. Eo, "S-parameter-based ic interconnect transmission line characterization," *IEEE Trans. on Components, Hybrids, and Manufacturing Technology*, vol. 15, no. 4, pp. 483–490, Aug. 1992.
- [23] Yungseon Eo, W. Eisenstadt, and Jongin Shim, "S-parameter-measurement-based high-speed signal transient characterization of vlsi interconnects on sio2-si substrate," *IEEE Trans. on Advanced Packaging*, vol. 23, no. 3, pp. 470–479, Aug. 2000.
- [24] Yungseon Eo and W. Eisenstadt, "High-speed vlsi interconnect modeling based on s-parameter measurements," *IEEE Trans. on Components, Hybrids, and Manufacturing Technology*, vol. 16, no. 5, pp. 555–562, Aug. 1993.
- [25] R. Amaudov and R. Borisov, "S-parameters-based extraction of effective dielectric constant in transmission lines on multilayer substrates," in *Telecommunications Forum (TELFOR)*, 2011 19th, Nov. 2011, pp. 900–903.

4.8 Exercises

1. In Section 4.3.1, the S parameters of a reciprocal error network were determined by applying three loads— Z_1 , Z_2 , and Z_3 —and measuring the respective input reflection coefficients. If Z_1 is a matched load, Z_2 is a short circuit, and Z_3 is an open, the S parameters of Equations (4.1), (4.2), and (4.3) are found. Use SFG theory to derive these results.
2. The S parameters of a line with a physical length of 20 cm was measured at 1 GHz in a $Z_{\text{ref}} = 50 \Omega$ system and found to be $S_{11} = S_{22} = 0.1$ and $S_{21} = S_{12} = -0.9$. What are the characteristic impedance, attenuation constant, and phase constant of the line at 1 GHz. It is known that the line is less than a wavelength long.
3. At 10 GHz the propagation constant of a line is $\gamma = 4.6 + j400$ and the characteristic impedance is $Z_0 = 60 - j0.5$. What are the R , L , G and C parameters of the line?
4. At 100 GHz, the propagation constant of a line is $\gamma = 30 + j600$ and the characteristic impedance is $Z_0 = 27 + j0.7$. What are the R , L , G and C parameters of the line?
5. At 1 GHz, the propagation constant of a line is $\gamma = 2.5 + j36$ and the characteristic impedance is $Z_0 = 105j$. What are the R , L , G and C parameters of the line?
6. The S parameters of a line with a physical length of 2 mm was measured at 10 GHz in a $Z_{\text{ref}} = 50 \Omega$ system and found to be $S_{11} = S_{22} = 0.1 - j0.001$ and $S_{21} = S_{12} = -0.7 + j0.3$. It is known that the line is less than a wavelength long. For the line find the following at 10 GHz:
 - (a) Characteristic impedance.
 - (b) Why is it important to know the approximate length of the line in terms of wavelengths?
 - (b) Complex propagation constant.
 - (c) Attenuation constant, .
 - (c) R , L , G , and C parameters.
7. Repeat 6 but now the line is between one and two wavelengths long.
8. The properties of a 5 mm long microstrip line on an unknown substrate are to be determined by terminating the line in a known impedance and measuring Γ_{in} , the reflection coefficient at the input of the line. At 10 GHz the load has a reflection coefficient $\Gamma_L = 0.9 \angle 0^\circ$ and $\Gamma_{\text{in}} = 0.9 \angle 170^\circ$. When the frequency is swept, on a Smith chart Γ_{in} traces out a circle centered at the origin. All measurements are referenced to 50 Ω . It is known that the substrate is not magnetic and so the relative permeability of the substrate is one.
 - (a) At 10 GHz what is the electrical length of the line in degrees? (Assume that the line is less than a half-wavelength long.)
 - (b) What is the electrical length of the line in fractions of a wavelength?
 - (c) Since the line is 5 mm long, what is the guide wavelength, λ_g , of the line?
 - (d) What is the free space wavelength, λ_0 ?
 - (e) What is the relationship between λ_g , λ_0 , and the line's effective relative permittivity ϵ_e ?
 - (f) What is ϵ_e ?
 - (g) What is the characteristic impedance of the line?
 - (h) What is the loss of the line in terms of dB per meter?

- (i) If there was no substrate, i.e. $\epsilon_r = \epsilon_0$, what would the electrical length of the line be in terms of λ_0 ?
- 9 A long slightly lossy line has a frequency-independent input reflection coefficient located at the point $\Gamma_{in} = 0.8$ on a Smith chart. What is the characteristic impedance of the line?
- 10 A long slightly lossy line has a frequency-independent input reflection coefficient located at the point $\Gamma_{in} = -0.7$ on a Smith chart. What is the characteristic impedance of the line?
- 11 Port 2 of a transmission line with characteristic impedance $Z_{01} = 75 \Omega$ is terminated in 75Ω and the input reflection coefficient Γ_{in} at Port 1 is measured and plotted on a 50Ω Smith chart. As the frequency is varied Γ_{in} traces out a circle. What is the center and radius of that circle.
- 12 Port 2 of a transmission line with characteristic impedance $Z_{01} = 75 \Omega$ is left open and the input reflection coefficient Γ_{in} at Port 1 is measured and plotted on a 50Ω Smith chart. As the frequency is varied Γ_{in} traces out a circle. What is the center (use polar coordinates) and radius of that circle.
- 13 The input reflection coefficient Γ_{in} of a transmission line with unknown characteristic impedance Z_{01} and is measured using a VNA in a 50Ω system but the load terminating the line is unknown. On a 50Ω Smith chart the locus of Γ_{in} with respect to frequency is a circle centered at 0.7 on the horizontal axis of the Smith chart with a radius of 0.3. What is Z_{01} ?
- 14 The input reflection coefficient Γ_{in} of a transmission line with unknown characteristic impedance Z_{01} and is measured using a VNA in a 50Ω system but the load terminating the line is unknown. On a 50Ω Smith chart the locus of Γ_{in} with respect to frequency is a circle centered at 1.2 on the horizontal axis of the Smith chart with a radius of 0.25. What is Z_{01} ?

4.8.1 Exercises by Section

[†]challenging

§4.3 1[†]

§4.4 2, 3[†], 4, 5, 6, 7, 8

§4.5 9, 10, 11, 12, 13, 14

4.8.2 Answers to Selected Exercises

$$\begin{array}{ll}
 4 \quad R = 476.0 \Omega/\text{m}, & G = 21.11 \text{ mS/m}, \\
 \quad L = 381.9 \text{ nH/m}, & C = 106.1 \text{ pF/m}
 \end{array}$$

Passive Components

5.1	Introduction	115
5.2	Q Factor	115
5.3	Integrated Lumped Elements	118
5.4	Surface-Mount Components	121
5.5	Terminations and Attenuators	122
5.6	Transmission Line Stubs and Discontinuities	127
5.7	Resonators	131
5.8	Magnetic Transformers	132
5.9	Hybrids	135
5.10	Baluns	139
5.11	Combiners and Dividers	141
5.12	Transmission Line Transformer	143
5.13	Transmission Line-Based Hybrids	150
5.14	Summary	153
5.15	References	154
5.16	Exercises	155

5.1 Introduction

This chapter introduces a wide variety of passive components. It is not possible to be comprehensive, as there is an enormous catalog of microwave elements and scores of variations, and new concepts are introduced every year. At microwave frequencies distributed components can be constructed that have features with particular properties related to coupling, to traveling waves, and to storage of EM energy. Sometimes it is possible to develop lumped-element equivalents of the distributed elements by using the LC ladder model of a transmission line thus realizing lumped-element circuits that would be difficult to imagine otherwise.

5.2 Q Factor

RF inductors and capacitors also have loss and parasitic elements. With inductors there is both series resistance and shunt capacitance mainly from interwinding capacitance, while with capacitors there will be shunt resistance and series inductance. A practical inductor or capacitor is limited

Figure 5-1: Transfer characteristic of a resonant circuit. (The transfer function is V/I for the parallel resonant circuit of Figure 5-2(a) and I/V for the series resonant circuit of Figure 5-2(b).)

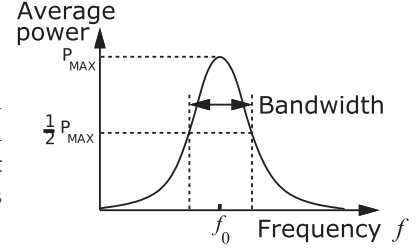
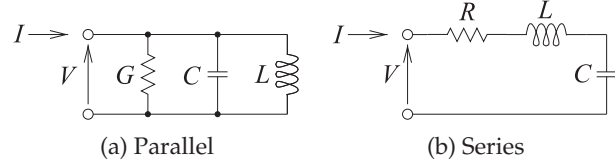


Figure 5-2: Second-order resonant circuits.



to operation below the self-resonant frequency determined by the inductance and capacitance itself resonating with its reactive parasitics. The impact of loss is quantified by the Q factor (the quality factor). Q is loosely related to bandwidth in general and the strict relationship is based on the response of a series or parallel connection of a resistor (R), an inductor (L), and a capacitor (C). The response of an RLC network is described by a second-order differential equation with the conclusion that the 3 dB fractional bandwidth of the response (i.e., when the power response is at its half-power level below its peak response) is $1/Q$. (The fractional bandwidth is $\Delta f/f_0$ where $f_0 = f_r$ is the resonant frequency at the center of the band and Δf is the 3 dB bandwidth.) This is not true for any network other than a second-order circuit, but as a guiding principle, networks with higher Q s will have narrower bandwidths.

5.2.1 Definition

The Q factor of a component at frequency f is defined as the ratio of $2\pi f$ times the maximum energy stored to the energy lost per cycle. In a lumped-element resonant circuit, stored energy is transferred between an inductor, which stores magnetic energy, and a capacitor, which stores electric energy, and back again every period. Distributed resonators function the same way, exchanging energy stored in electric and magnetic forms, but with the energy stored spatially. The quality factor is

$$Q = 2\pi f_r \left(\frac{\text{average energy stored in the resonator at } f_r}{\text{power lost in the resonator}} \right), \quad (5.1)$$

where $f_1 = \omega_r/(2\pi)$ is the resonant frequency.

A simple response is shown in Figure 5-1. For a parallel resonant circuit with elements L , C , and $G = 1/R$ (see Figure 5-2(a)),

$$Q = \omega_r C / G = 1/(\omega_r L G), \quad (5.2)$$

where $f_r = \omega_r/(2\pi)$ is the resonant frequency and is the frequency at which the maximum amount of energy is stored in a resonator. The conductance, G , describes the energy lost in a cycle. For a series resonant circuit (Figure 5-2(b)) with L , C , and R elements,

$$Q = \omega_r L / R = 1/(\omega_r C R). \quad (5.3)$$

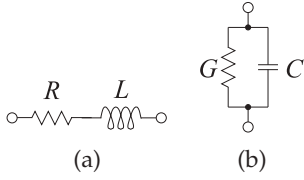


Figure 5-3: Loss elements of practical inductors and capacitors: (a) an inductor has a series resistance R ; and (b) for a capacitor, the dominant loss mechanism is a shunt conductance $G = 1/R$.

These second-order resonant circuits have a bandpass transfer characteristic (see Figure 5-1) with Q being the inverse of the fractional bandwidth of the resonator. The fractional bandwidth, $\Delta f/f_r$, is measured at the half-power points as shown in Figure 5-1. (Δf is also referred to as the two-sided -3 dB bandwidth.) Then

$$Q = f_r/\Delta f. \quad (5.4)$$

Thus the Q is a measure of the sharpness of the bandpass frequency response. The determination of Q using the measurement of bandwidth together with Equation (5.4) is often not very precise, so another definition that uses the much more sensitive phase change at resonance is preferred when measurements are being used. With ϕ being the phase (in radians) of the transfer characteristic, the definition of Q is now

$$Q = \frac{\omega_r}{2} \left| \frac{d\phi}{d\omega} \right|. \quad (5.5)$$

Equation (5.5) is another equivalent definition of Q for parallel RLC or series RLC resonant circuits. It is meaningful to talk about the Q of circuits other than three-element RLC circuits, and then its meaning is always a ratio of the energy stored to the energy dissipated per cycle. The Q of these structures can no longer be determined by bandwidth or by the rate of phase change.

5.2.2 Q of Lumped Elements

Q is also used to characterize the loss of lumped inductors and capacitors. Inductors have a series resistance R , and the main loss mechanism of a capacitor is a shunt conductance G (see Figure 5-3).

The Q of an inductor at frequency $f = \omega/(2\pi)$ with a series resistance R and inductance L is

$$Q_{\text{INDUCTOR}} = \frac{\omega L}{R}. \quad (5.6)$$

Since R is approximately constant with respect to frequency for an inductor, the Q will vary with frequency.

The Q of a capacitor with a shunt conductance G and capacitance C is

$$Q_{\text{CAPACITOR}} = \frac{\omega C}{G}. \quad (5.7)$$

G is due mainly to relaxation loss mechanisms of the dielectric of a capacitor and so varies linearly with frequency. Thus the Q of a capacitor is almost constant with respect to frequency. For microwave components invariably $Q_{\text{CAPACITOR}} \gg Q_{\text{INDUCTOR}}$, and Q_{INDUCTOR} is smaller than the Q of transmission line networks. Thus, if the length of a transmission line is not too long, transmission line networks are preferred. If lumped elements must be used, the use of inductors should be minimized.

5.2.3 Loaded Q Factor

The Q of a component as defined in the previous section is called the unloaded Q , Q_U . However if a component is to be measured or used in any way, it is necessary to couple energy in and out of it. The Q is reduced and thus the resonator bandwidth is increased by the power lost to the external circuit so that the loaded Q , then the loaded Q is

$$Q_L = 2\pi f_0 \left(\frac{\text{average energy stored in the resonator at } f_0}{\text{power lost in the resonator and to the external circuit}} \right) \\ = \frac{1}{1/Q + 1/Q_X}, \quad (5.8)$$

where Q_X is called the external Q . Q_L accounts for the power extracted from the resonant circuit.

So a parallel LCG circuit with elements L_r , C_r , and G_r (at resonance) loaded by a shunt conductance G_l has

$$Q_U = \omega_r C_r / G_r = 1 / (\omega_r L_r G_r) \quad (5.9)$$

$$\text{and} \quad Q_L = \omega_r C_r / (G_r + G_l). \quad (5.10)$$

$$\text{Thus} \quad \frac{1}{Q_L} = \frac{1}{Q_U} + \frac{1}{Q_X} \quad (5.11)$$

$$\text{or} \quad Q_X = \left(\frac{1}{Q_L} - \frac{1}{Q_U} \right)^{-1}. \quad (5.12)$$

Q_X is called the external Q , and it describes the effect of loading. Q_L is the Q that would actually be measured. Q_U normally needs to be determined, but if the loading is kept very small, $Q_L \approx Q_U$.

5.2.4 Summary of the Properties of Q

In summary:

- (a) Q is properly defined and related to the energy stored in a resonator for a second-order network, one with two reactive elements of opposite types.
- (b) Q is not well defined for networks with three or more reactive elements.
- (c) However, Q is a frequently used parameter in the design equations for more complex networks than second-order ones.
- (d) For complex networks the Q is defined as the ratio of a reactance to a resistance when looking into one end of the network at one frequency. This value of Q should not be used to deduce the bandwidth of the network.
- (e) It is only used (as defined or some approximation of it) for guiding the design.

5.3 Integrated Lumped Elements

This section considers lumped-elements used in integrated circuits operating at microwave frequencies. Lumped elements such as capacitors, inductors and resistors can rarely be regarded as pure elements at microwave frequencies. Inductors and capacitors have significant loss and all of the elements store energy in both electric and magnetic forms.

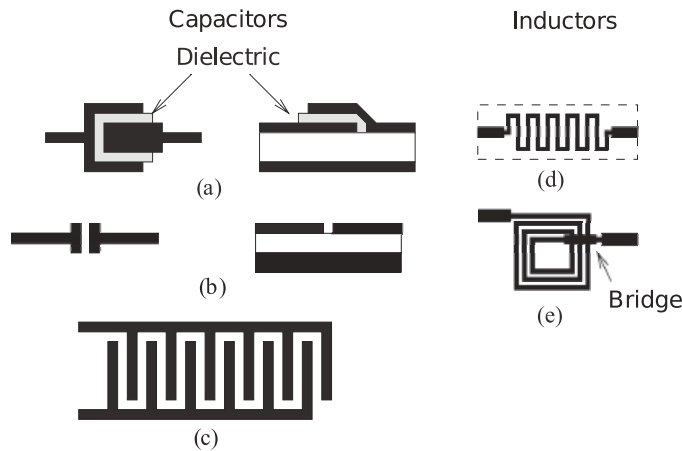


Figure 5-4: Monolithic lumped elements: (a) parallel plate capacitor; (b) gap capacitor; (c) interdigitated capacitor; (d) meander line inductor; and (e) spiral inductor.

5.3.1 On-Chip Capacitors

There are three primary forms of on-chip capacitor:

- (a) Metal-dielectric-metal capacitor—using interconnect metalization.
- (b) Metal-dielectric-semiconductor capacitor—essentially a MOS transistor.
- (c) Semiconductor junction capacitor—either the capacitance of a reverse-biased *pn* junction or Schottky barrier.

In silicon technology it is common to refer to the first capacitor type as a **metal-oxide-metal (MOM)** capacitor or as a **metal-insulator-metal (MIM)** capacitor. A MOM capacitor can be realized as a parallel plate capacitance (see Figure 5-4(a)), and multiple levels of metalization can be used to increase the capacitance density. Relatively low capacitance values of up to $500 \text{ fF}/\mu\text{m}^2$ are typically available.

An alternative MOM capacitance is available using lateral arrangements of conductors on the same layer (see Figure 5-4(b)); that is, adjacent metal structures are separated by a small horizontal gap. Again, there are two distinct metal connections, and a smaller metal separation can be obtained using photolithography than that possible using dielectric separation. However the capacitance density is only increased by a factor of about three. Higher values can be obtained using the **interdigitated capacitor (IDC)** of Figure 5-4(c). Both types of MOM capacitance, parallel plate and lateral, are geometrically defined, are voltage independent, have very low temperature coefficients, and have initial fabrication tolerances of 20%–30%.

The second type of capacitor in MOS technology is referred to as a **metal-oxide-semiconductor (MOS)** capacitor. MOS capacitors use a MOS transistor with a parallel-plate capacitance between the gate of a MOS transistor and a heavily inverted channel. The drain and source are connected in this configuration and the separation between the conductors is thin, being the gate oxide thickness. This leads to high values of capacitance, although with a weak voltage dependence. Junction capacitance is realized as the capacitance of a reverse-biased semiconductor junction. This capacitance can be quite large, but has a strong voltage dependence. This voltage dependence can be utilized to realize tunable circuits (e.g., a voltage-controlled oscillator).

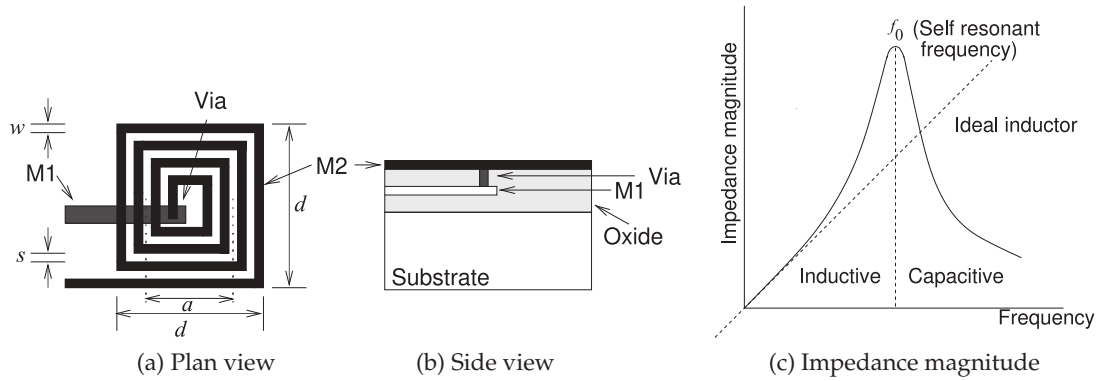


Figure 5-5: An on-chip spiral inductor.

5.3.2 Planar Inductors

Inductors are important components in RF and microwave circuits. In addition to their role in matching networks, they are used to provide bias to active devices while effectively blocking RF signals from the bias circuitry. Inductors of up to 10 nH can be fabricated in compact form, with the spiral inductor of Figure 5-4(e) being typical. Bond wires can also be used to realize small inductances in the 0.5–1 nH range. One of the advantages of having a portion of a large inductance on-chip is reduced sensitivity to die attach (bondwire, etc.) connections used to connect to an external inductance. Small values of inductance can be realized by the meander line inductor of Figure 5-4(d). This is based on a high-impedance length of line (narrow line in microstrip) appearing inductive.

An on-chip **spiral inductor** is shown in Figure 5-5. An approximate expression for the inductance of this structure was developed by Wheeler [1–3]:

$$L \approx \frac{9.4\mu_0 n^2 a^2}{11d - 7a}, \quad (5.13)$$

where a is the mean radius of the spiral and n is the number of turns. This formula was derived for circular coils, but its accuracy for square spirals is within 5% of values obtained using EM simulation [4]. It is therefore a very useful formula in the early stages of design, but EM analysis is required to obtain the necessary accuracy and frequency dependence of the inductor.

Fields produced by a spiral inductor penetrate the substrate, and as the ground plane is located at a short distance away, the eddy currents on the ground plane reduce the inductance that would otherwise be obtained. The eddy current in the ground conductor rotates in a direction opposite to that of the current on the spiral itself. As a result, the flux of the image inductor in the ground is in the opposite direction to that produced by the spiral itself, with the consequent effect that the effective total inductance is reduced. By creating a broken conductor pattern, the ground inductance is largely eliminated as the eddy currents cannot flow [5].

All inductors have appreciable resistive loss of conductors, and for inductors on semiconductor substrates, loss due to induced substrate currents is

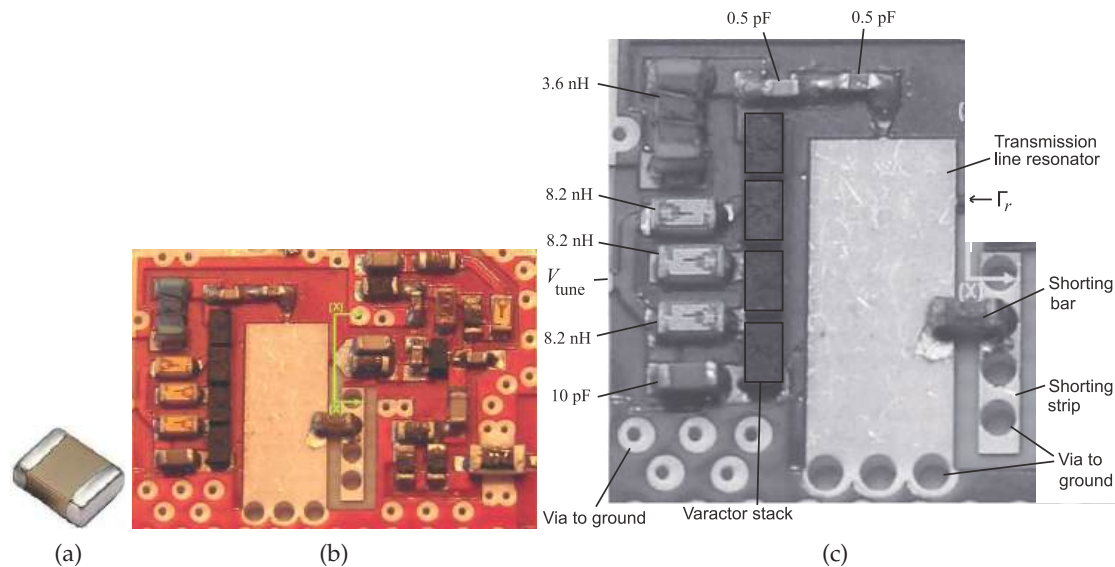


Figure 5-6: Circuit board showing the use of surface-mount components: (a) chip resistor or capacitor with metal terminals at the two ends; (b) populated RF microstrip circuit board of a 5 GHz voltage-controlled oscillator [7] (the larger components have dimensions $1.6 \text{ mm} \times 0.8 \text{ mm}$); and (c) identification of several components including a varactor stack with four varactor diodes and a shunting bar that is a 0Ω resistor.

important and often dominates. Loss in the substrate is particularly large in silicon substrates due to the finite conductivity of the substrate and the resulting current flow. These induced currents follow a path under the conductors of the spiral and, just as with ground plane eddy currents, lowers the inductance achieved. However, the resistance of the lines is unchanged. Thus on silicon it is difficult to achieve very high Q s (the ratio of stored energy to energy dissipated per cycle).

Lumped inductors are based on coils of conductor, and there is parasitic capacitance between the windings [6]. As a result there will be a frequency where the capacitance and inductance resonate at what is called the self-resonant frequency. The impedance of a realistic inductor is shown in Figure 5-5(c). If the practical inductor was purely inductive, then its impedance would increase linearly with frequency. However, because of resonance, the effective inductance increases just before resonance causing the impedance of the practical inductor to increase more rapidly than linearly. This is seen in Figure 5-5(c), and this effect is often used in narrowband microwave circuits.

5.4 Surface-Mount Components

The majority of the RF and microwave design effort goes into developing modules and interconnecting modules on circuit boards. With these the most common type of component to use is surface-mount. Figure 5-6(a) shows a two-terminal element, such as a resistor or capacitor, in the form of a surface-mount component. Figure 5-6(b and c) show the use of surface-mount components on a microwave circuit board.

Table 5-1: Sizes and designation of two-terminal surface mount components. Note the designation of a surface-mount component refers (approximately) to its dimensions in hundredths of an inch.

Designation	Size (inch \times inch)	Metric designation	Size (mm \times mm)
01005	0.016×0.0079	0402	0.4×0.2
0201	0.024×0.012	0603	0.6×0.3
0402	0.039×0.020	1005	1.0×0.5
0603	0.063×0.031	1608	1.6×0.8
0805	0.079×0.049	2012	2.0×1.25
1008	0.098×0.079	2520	2.5×2.0
1206	0.13×0.063	3216	3.2×1.6
1210	0.13×0.098	3225	3.2×2.5
1806	0.18×0.063	4516	4.5×1.6
1812	0.18×0.13	4532	4.5×3.2
2010	0.20×0.098	5025	5.0×2.5
2512	0.25×0.13	6432	6.4×3.2
2920	0.29×0.20	—	7.4×5.1

Table 5-2: Parameters of the inductors in Figure 5-7(a). L_{nom} is the nominal inductance, SRF is the self-resonance frequency, R_{DC} is the inductor's series resistance, and I_{max} is the maximum RMS current supported.

L_{nom} (nH)	900 MHz		1.7 GHz		SRF (GHz)	R_{DC} (Ω)	I_{max} (mA)
	L (nH)	Q	L (nH)	Q			
1.0	0.98	39	0.99	58	16.0	0.045	1600
2.0	1.98	46	1.98	70	12.0	0.034	1900
5.1	5.12	68	5.18	93	5.50	0.050	1400
10	10.0	67	10.4	85	3.95	0.092	1100
20	20.2	67	21.6	80	2.90	0.175	760
56	59.4	54	75.4	48	1.75	0.700	420

A two-terminal surface-mount resistor or capacitor is commonly called a chip resistor or chip capacitor. These can be very small, and the smaller the component often the higher the operating frequency due to reduced parasitic capacitance or inductance. Common sizes of two-terminal chip components are listed in Table 5-1. With a chip resistor or chip capacitor, the parasitic inductance determines the maximum operating frequency with the self-resonant frequency, in the case of a chip capacitor, being when the capacitance resonates with the parasitic inductance. The usable maximum frequency is below the self-resonant frequency.

Figure 5-7(a) shows an inductor in a surface-mount package and details are shown in Figure 5-7(b). This inductor is wound on a dielectric former, which, unfortunately, increases the inductor's parasitic capacitance. The resonance of this capacitance with the inductance establishes the self-resonant frequency (SRF) of the inductor. The inductor is useable as an inductor at a frequency backed-off from the SRF. The parasitic capacitance is reduced if the inductor has an air core, as for the inductors shown in Figure 5-7(c), with details shown in Figure 5-7(d). The air enables the inductor performance to be improved if the size remains the same or the inductor is smaller for comparable performance. The performance of the two types of inductors is listed in Tables 5-2 and 5-3.

5.5 Terminations and Attenuators

5.5.1 Terminations

Terminations are used to completely absorb a forward-traveling wave and the defining characteristic is that the reflection coefficient of a termination is ideally zero. If a transmission line has a resistive characteristic impedance

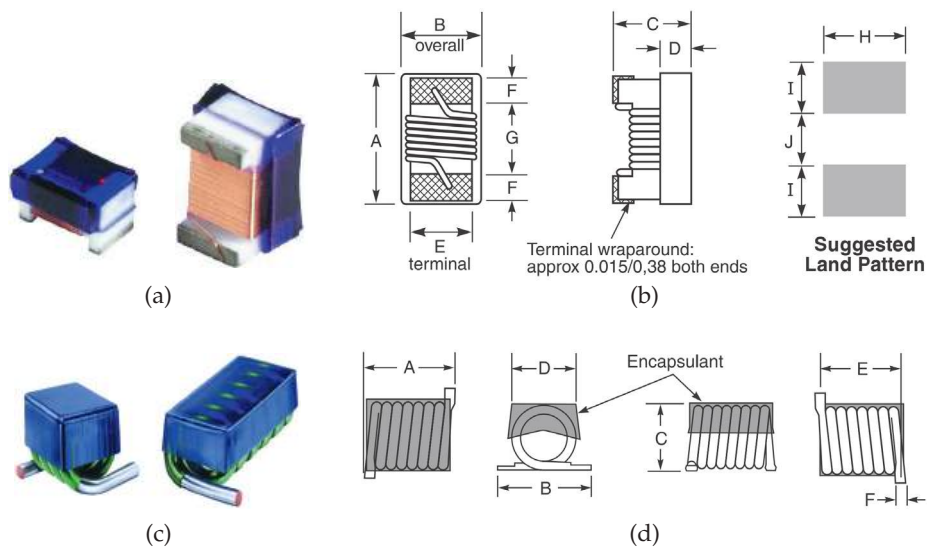


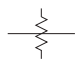
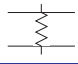
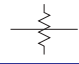
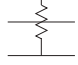
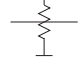
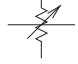

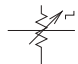
Figure 5-7: Chip inductors: (a) inductor in an 0603 surface-mount package; (b) schematic showing sizes and pads to be provided on a circuit board (A=64 mils (1.63 mm), B=33 mils (0.84 mm), C=24 mils (0.61 mm), D=13 mils (0.33 mm), E=30 mils (0.76 mm), F=25 mils (0.64 mm), G=25 mils (0.64 mm), and H=40 mils (1.02 mm)); (c) 0201 surface-mount air-core inductor; and (d) detail (A=23 mils (0.58 mm), B=18 mils (0.46 mm), C=17.7 mils (0.45 mm), D=4 mils (0.1 mm), E=15 mils (0.38 mm), F=9 mils (0.23 mm), G=7 mils (0.18 mm), and H=18 mils (0.46 mm)). Copyright Coilcraft, Inc., used with permission [8].

L_{nom} (nH)	900 MHz		1.7 GHz		SRF	R_{DC}	I_{max}
	L (nH)	Q	L (nH)	Q	(GHz)	(Ω)	(mA)
0.5	0.5	29	0.49	43	23.5	0.020	1250
1.2	1.16	42	1.16	60	17.9	0.042	870
2.3	2.28	45	2.28	64	16.5	0.070	670
5.2	5.21	36	5.21	55	10.0	0.170	430
9.6	9.62	38	9.64	53	6.2	0.400	280
14.0	14.13	37	14.37	51	5.1	0.440	270

Table 5-3: Parameters of the inductors in Figure 5-7(c). L_{nom} is the nominal inductance, SRF is the self-resonance frequency, R_{DC} is the inductor’s series resistance, and I_{max} is the maximum RMS current supported.

$R_0 = Z_0$, then terminating the line in a resistance R_0 will fully absorb the forward-traveling wave and there will be no reflection. The line is then said to be matched. At RF and microwave frequencies some refinements to this simple circuit connection are required. On a transmission line the energy is contained in the EM fields. For the coaxial line, a simple resistive connection between the inner and outer conductors would not terminate the fields and there would be some reflection. Instead, coaxial line terminations generally comprise a disk of resistive material (see Figure 5-8(a)). The total resistance of the disk from the inner to the outer conductor is the characteristic resistance of the line, however, the resistive material is distributed and so creates a good termination of the fields guided by the coaxial conductors. Terminations are a problem with microstrip, as the characteristic impedance varies with frequency, is in general complex, and the vias that would be required if a lumped resistor was used has appreciable inductance at

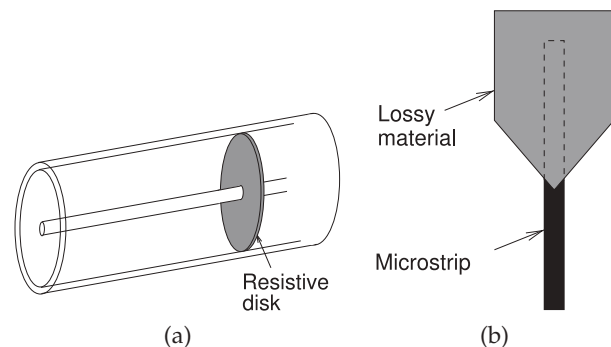
Table 5-4: IEEE standard symbols for attenuators [9].

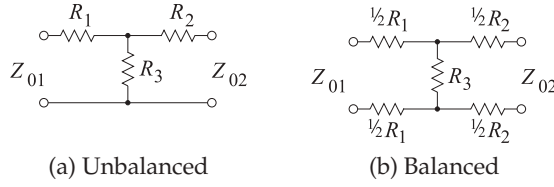
Component	Symbol	Alternate
Attenuator, fixed		
Attenuator, balanced		
Attenuator, unbalanced		
Attenuator, variable		
Attenuator, continuously variable		
Attenuator, stepped variable		

frequencies above a few gigahertz. A high-quality termination is realized using a section of lossy line as shown in Figure 5-8(b). Here lossy material is deposited on top of an open-circuited microstrip line. This increases the loss of the line appreciably without significantly affecting the characteristic impedance of the line. If the length of the lossy line is sufficiently long, say one wavelength, the forward-traveling wave will be totally absorbed and there will be no reflection. Tapering the lossy material, as shown in Figure 5-8(b), reduces the discontinuity between the lossless microstrip line and the lossy line by ensuring that some of the power in the forward-traveling wave is dissipated before the maximum impact of the lossy material occurs. Thus a matched termination is achieved without the use of a via.

5.5.2 Attenuators

An attenuator is a two-port network used to reduce the amplitude of a signal and it does this by absorbing power and without distorting the signal. The input and output of the attenuator are both matched, so there are no reflections. An attenuator may be fixed, continuously variable, or discretely variable. The IEEE standard symbols for attenuators are shown in Table 5-4. When the attenuation is fixed, an attenuator is commonly called a **pad**. Resistive pads can be used to minimize the effect of shorts and opens on

Figure 5-8: Terminations: (a) coaxial line resistive termination; (b) microstrip matched load.



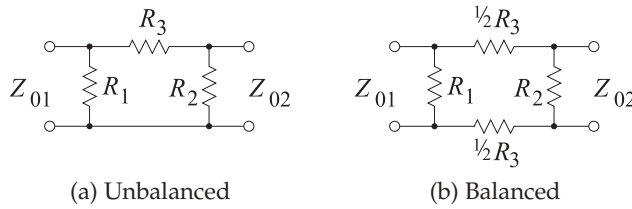
$$R_1 = \frac{Z_{01}(K+1) - 2\sqrt{KZ_{01}Z_{02}}}{K-1} \quad R_2 = \frac{Z_{02}(K+1) - 2\sqrt{KZ_{01}Z_{02}}}{K-1}$$

$$R_3 = \frac{2\sqrt{KZ_{01}Z_{02}}}{K-1} \quad (5.14)$$

If $Z_{01} = Z_{02} = Z_0$, then

$$R_1 = R_2 = Z_0 \left(\frac{\sqrt{K}-1}{\sqrt{K}+1} \right) \quad \text{and} \quad R_3 = \frac{2Z_0\sqrt{K}}{K-1} \quad (5.15)$$

Figure 5-9: T (Tee) attenuator. K is the (power) attenuation factor, e.g. a 3 dB attenuator has $K = 10^{3/10} = 1.995$.



$$R_1 = \frac{Z_{01}(K-1)\sqrt{Z_{02}}}{(K+1)\sqrt{Z_{02}} - 2\sqrt{KZ_{01}}} \quad R_2 = \frac{Z_{02}(K-1)\sqrt{Z_{01}}}{(K+1)\sqrt{Z_{01}} - 2\sqrt{KZ_{02}}} \quad (5.16)$$

$$R_3 = \frac{(K-1)}{2} \sqrt{\frac{Z_{01}Z_{02}}{K}} \quad (5.17)$$

If $Z_{01} = Z_{02} = Z_0$, then

$$R_1 = R_2 = Z_0 \left(\frac{\sqrt{K}+1}{\sqrt{K}-1} \right) \quad \text{and} \quad R_3 = \frac{Z_0(K-1)}{2\sqrt{K}}. \quad (5.18)$$

If $R_1 = R_2$, then $Z_{01} = Z_{02} = Z_0$

$$Z_0 = \sqrt{\frac{R_1^2 R_3}{2R_1 + R_3}}, \quad \text{and} \quad K = \left(\frac{R_1 + Z_0}{R_1 - Z_0} \right)^2. \quad (5.19)$$

Figure 5-10: Pi (Pi) attenuator. K is the (power) attenuation factor, e.g. a 20 dB attenuator has $K = 10^{20/10} = 100$.

the integrity of an RF circuit. An example of attenuator use in this situation is in a cable TV system, where it is critical that the integrity of the system is not compromised by a consumer disconnecting appliances from a cable outlet.

Balanced and unbalanced resistive pads are shown in Figures 5-9 and 5-10 together with their design equations. The attenuators in Figure 5-9 are T or Tee attenuators, where Z_{01} is the system impedance to the left of the pad and Z_{02} is the system impedance to the right of the pad. The defining characteristic is that the reflection coefficient looking into the pad from the left is zero when referred to Z_{01} . Similarly, the reflection coefficient looking

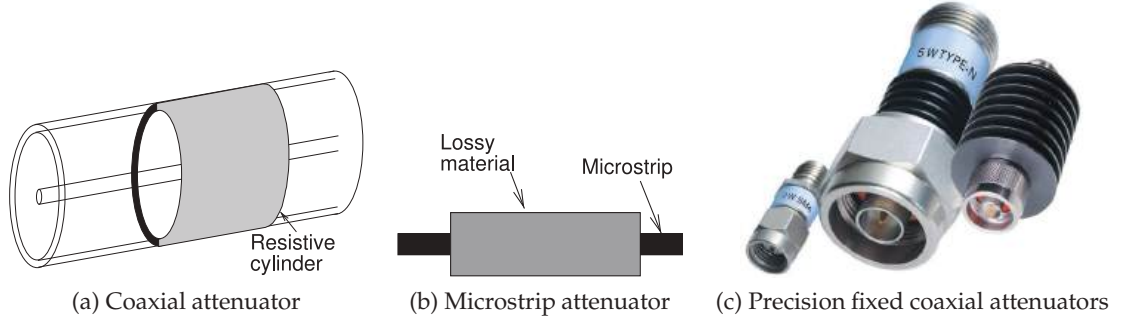


Figure 5-11: Distributed attenuators. The attenuators in (c) have power handling ratings of 2W, 5W and 20 W (left to right). Copyright 2012 Scientific Components Corporation d/b/a Mini-Circuits, used with permission [11].

from the right of the pad is zero with respect to Z_{02} . The attenuation factor is

$$K = \frac{\text{Power in}}{\text{Power out}}. \quad (5.20)$$

In decibels, the attenuation is

$$K|_{\text{dB}} = 10 \log_{10} K = (\text{Power in})|_{\text{dBm}} - (\text{Power out})|_{\text{dBm}}. \quad (5.21)$$

If the left and right system impedances are different, then there is a minimum attenuation factor that can be achieved [10]:

$$K_{\text{MIN}} = \begin{cases} \left[\frac{2Z_{01} - Z_{02} + 2\sqrt{Z_{01}(Z_{01} - Z_{02})}}{Z_{02}} \right] / Z_{02} & , Z_{01} \geq Z_{02} \\ \left[\frac{2Z_{02} - Z_{01} + 2\sqrt{Z_{02}(Z_{02} - Z_{01})}}{Z_{01}} \right] / Z_{01} & , Z_{01} \leq Z_{02} \end{cases} \quad (5.22)$$

This limitation comes from the simultaneous requirement that the pad be matched. If there is a single system impedance, $Z_0 = Z_{01} = Z_{02}$, then $K_{\text{MIN}} = 1$, and so any value of attenuation can be obtained.

Lumped attenuators are useful up to 10 GHz above which the size of resistive elements becomes large compared to a wavelength. Also, for planar circuits, vias are required, and these are undesirable from a manufacturing standpoint, and electrically they have a small inductance. Fortunately attenuators can be realized using a lossy section of transmission line, as shown in Figure 5-11. Here, lossy material results in a section of line with a high-attenuation constant. Generally the lossy material has little effect on the characteristic impedance of the line, so there is little reflection at the input and output of the attenuator. Distributed attenuators can be used at frequencies higher than lumped-element attenuators can, and they can be realized with any transmission line structure.

Another example of the use of attenuators in combining the output of two sources is shown in Figure 5-12. This is a common situation in measurements where the outputs of two instrumentation sources are to be combined. The attenuators reduce the level of the signal presented to the output of one source by the other. If the level of the second signal is high, most sources would produce nonlinear distortion, including nonlinear mixing products.

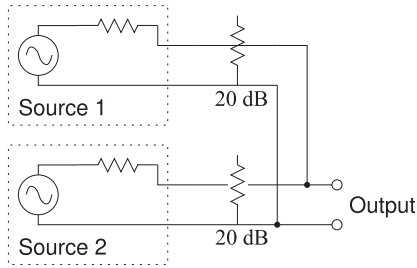


Figure 5-12: The use of attenuators to isolate the outputs of two sources that are combined.

EXAMPLE 5.1 Pad Design

Design an unbalanced 20 dB pad in a 75 Ω system.

Solution:

There are two possible designs using resistive pads. These are the unbalanced Tee and Pi pads shown in Figures 5-9 and 5-10. The Tee design will be chosen. The K factor is

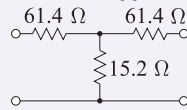
$$K = 10^{(K|_{\text{dB}}/10)} = 10^{(20/10)} = 100. \quad (5.23)$$

Since $Z_{01} = Z_{02} = 75 \Omega$, Equation (5.15) yields

$$R_1 = R_2 = 75 \left(\frac{\sqrt{100} - 1}{\sqrt{100} + 1} \right) = 75 \left(\frac{9}{11} \right) = 61.4 \Omega \quad (5.24)$$

$$R_3 = \frac{2 \cdot 75 \sqrt{100}}{100 - 1} = 150 \left(\frac{10}{99} \right) = 15.2 \Omega. \quad (5.25)$$

The final design is



5.6 Transmission Line Stubs and Discontinuities

Interruptions of the magnetic or electric field create regions where additional magnetic energy or electric energy is stored. If the additional energy stored is predominantly magnetic, the discontinuity will introduce an inductance. If the additional energy stored is predominantly electric, the discontinuity will introduce a capacitance. Such discontinuities occur with all transmission lines. In some cases transmission line discontinuities introduce undesired parasitics, but they also provide an opportunity to effectively introduce lumped-element components. In this section microstrip discontinuities will be considered, but the principles apply to all transmission line structures.

The simplest microwave circuit element is a uniform section of transmission line that can be used to introduce a time delay or frequency-dependent phase shift. More commonly it is used to interconnect other components. Line segments including bends and junctions are shown in Figure 5-13.

5.6.1 Open

Many transmission line discontinuities arise from fringing fields. One element is the microstrip open, shown in Figure 5-14. The fringing fields at the end of the transmission line in Figure 5-14(a) store energy in the electric field, and this can be modeled by the fringing capacitance, C_F , shown in Figure 5-14(b). This effect can also be modeled by an extended transmission

line, as shown in Figure 5-14(c). For a typical microstrip line with $\epsilon_r = 9.6$, $h = 600 \mu\text{m}$, and $w/h = 1$, C_F is approximately 36 fF. However, C_F varies with frequency, and the extended length is a much better approximation to the effect of fringing [12]. For the same dimensions, the length of the extension is approximately $0.35h$ and almost independent of frequency [13]. As with many fringing effects, a capacitance or inductance can be used to model the effect of fringing, but generally a distributed model is better.

5.6.2 Discontinuities

Several microstrip discontinuities and their equivalent circuits are shown in Figure 5-15. Discontinuities (Figure 5-15(b–g)) are modeled by capacitive elements if the E field is affected and by inductive elements if the H field (or current) is disturbed. The stub shown in Figure 5-15(b), for example, is best modeled using lumped elements describing the junction as well as the transmission line of the stub itself. Current bunches at the right angle bends from the through line to the stub. The current bunching leads to excess energy being stored in the magnetic field, and hence an inductive effect. There is also excess charge storage in the parallel plate region bounded by the left- and right-hand through lines and the stub. This is modeled by a capacitance.

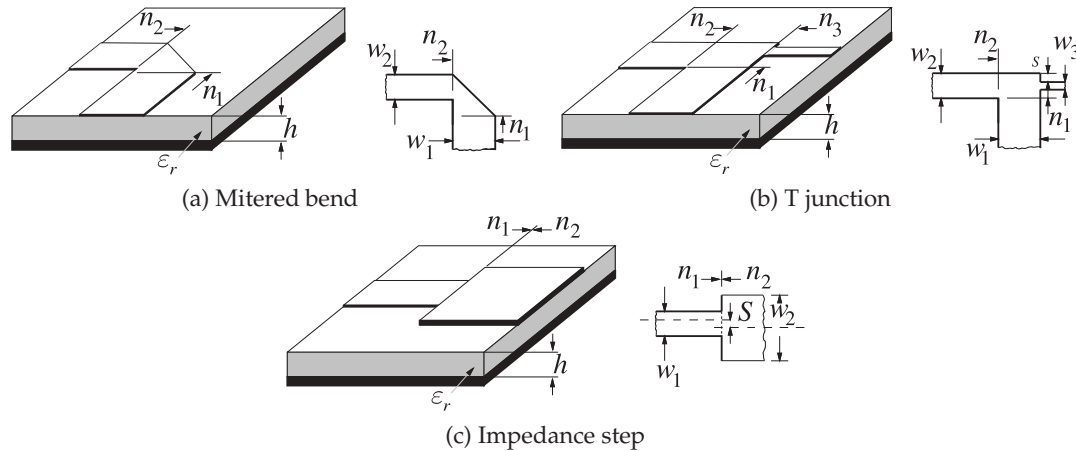
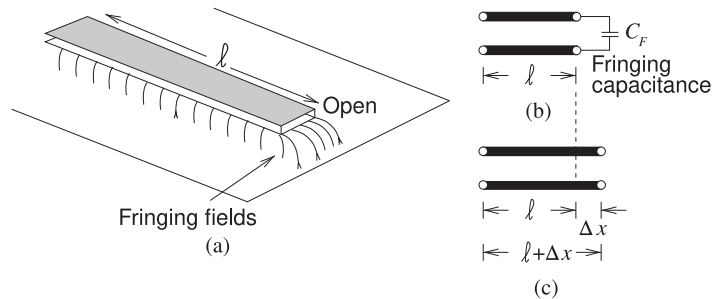


Figure 5-13: Microstrip discontinuities.

Figure 5-14: An open on a microstrip transmission line: (a) microstrip line showing fringing fields at the open; (b) fringing capacitance model of the open; and (c) an extended line model of the open with Δx being the extra transmission line length that captures the open.



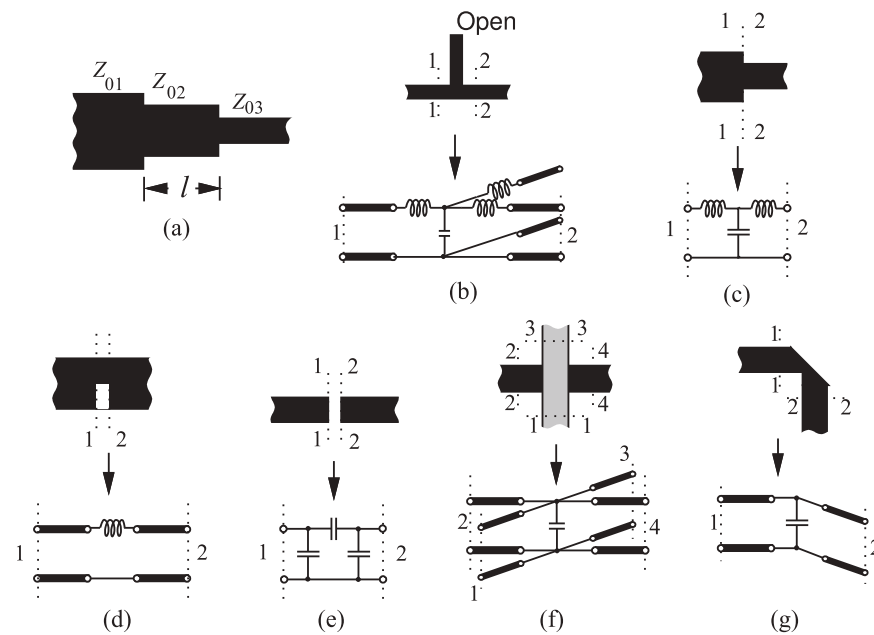


Figure 5-15: Microstrip discontinuities: (a) quarter-wave impedance transformer; (b) open microstrip stub; (c) step; (d) notch; (e) gap; (f) crossover; and (g) bend.

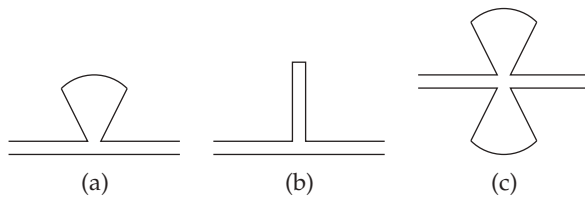


Figure 5-16: Microstrip stubs: (a) radial shunt-connected stub; (b) conventional shunt stub; and (c) butterfly radial stub.

5.6.3 Impedance Transformer

Impedance transformers interface two lines of different characteristic impedance. The smoothest transition and the one with the broadest bandwidth is a tapered line. This element can be long and then a quarter-wave impedance transformer (see Figure 5-15(a)) is sometimes used, although its bandwidth is relatively small and centered on the frequency at which $l = \lambda_g/4$. Ideally $Z_{0,2} = \sqrt{Z_{0,1}Z_{0,3}}$. This topic is considered further in Section 7.5 where the design of tapered lines and multi-stage quarter-wave transformers are considered in detail.

5.6.4 Planar Radial Stub

The use of a radial stub (Figure 5-16(a)), as opposed to the conventional microstrip stub (Figure 5-16(b)), can improve the bandwidth of many microstrip circuits. A major advantage of a radial stub is that the input impedance presented to the through line generally has broader bandwidth than that obtained with the conventional stub. When two shunt-connected radial stubs are introduced in parallel (i.e., one on each side of the microstrip feeder line) the resulting configuration is termed a “butterfly” stub (see Figure 5-16(c)). Critical design parameters include the radius, r , and the angle of the stub.


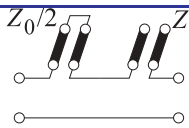
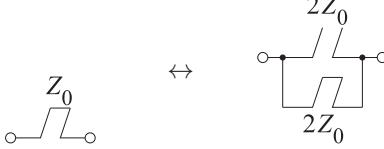
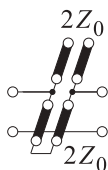
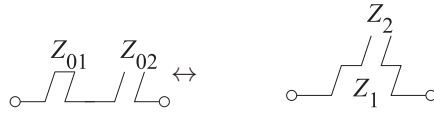
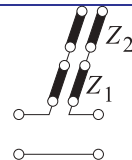
	Stub transformations	Transmission line circuit
(a)	 Electrical length = θ Electrical length = $\theta/2$	
(b)	 Electrical length = θ Electrical length = $\theta/2$	
(c)	 $Z_{01} = Z_1^2 / (Z_1 + Z_2)$ $Z_{02} = Z_1 Z_2 / (Z_1 + Z_2)$	

Figure 5-17: Stub network transformations: (a) open- and (b) short-circuited stubs after application of the half-angle transform [14]; and (c) equivalence between series connection of open- and short-circuited stubs and stepped impedance transmission line.

5.6.5 Stub Transformations

The stub transformations in Figure 5-17 enable the lengths of stubs to be reduced. The first two stub transformations (Figure 5-17(a and b)) are called half-angle transformations and enable a stub to be replaced by two shorter stubs. The third stub transformation (Figure 5-17(c)) enables two stubs to be replaced by two cascaded transmission lines.

Figure 5-17(a) is a half-angle transform of a series open-circuited stub. Mathematically the transform is described as follows. Consider the input impedance of an open-circuited stub [14] with electrical length $\theta = \beta\ell$ at frequency f and which is a quarter-wavelength long at f_0 (i.e., $\theta = \pi/2$ at f_0) (from Section 2.4.4 of [15] and using Equation ((1.105)) of [15]):

$$Z_{oc} = -jZ_0 \cot(\theta) = j(Z_0/2) \tan(\theta/2) - j(Z_0/2) / \tan(\theta/2). \quad (5.26)$$

In general, $\theta = (\pi/2)(f/f_0)$. The right-hand side of Equation (5.26) describes the series connection of short- and open-circuited stubs having characteristic impedances of $Z_0/2$ and half the original electrical length. This implies that the resulting transmission line resonators are one-quarter wavelength long at $2f_0$ (i.e., they are one-eighth wavelength long at f_0). The half-angle transformation applies at all frequencies and not just frequencies near f_0 .

Through a similar analytical treatment, the short-circuited stub has the equivalence shown in Figure 5-17(b). The series short-circuited stub on the left in Figure 5-17(b) has the series admittance

$$Y_T = \frac{1}{jZ_0 \tan(\theta)} = \frac{1}{jZ_0} \cot(\theta) \quad (5.27)$$

and the stubs in the transformation have an input impedance

$$Z_{oc} = -j\frac{1}{2}Z_0 \cot(\theta/2) \quad \text{and} \quad Z_{sc} = j\frac{1}{2}Z_0 \tan(\theta/2). \quad (5.28)$$

These stubs are in parallel so that the total input admittance is

$$\begin{aligned} Y_T &= \frac{1}{Z_{oc}} + \frac{1}{Z_{sc}} = \frac{2}{-jZ_0 \cot(\theta/2)} + \frac{1}{jZ_0 \tan(\theta/2)} \\ &= \frac{2}{jZ_0} \left[-\tan(\theta/2) + \frac{1}{c} \cot(\theta/2) \right] = \frac{1}{jZ_0} \cot(\theta). \end{aligned} \quad (5.29)$$

Examining Equations (5.27) and (5.29) it is seen that they are identical, thus Figure 5-17(b) represents another half-angle transformation.

For the series open- and short-circuited stubs in Figure 5-17(c), the input impedances of the open- and short-circuited stubs are

$$Z_{oc} = -jZ_{02} \cot(\theta) \quad \text{and} \quad Z_{sc} = jZ_{01} \tan(\theta), \quad (5.30)$$

respectively, so that the total series impedance is

$$Z_T = Z_{oc} + Z_{sc} = -jZ_{02} \cot(\theta) + jZ_{01} \tan(\theta). \quad (5.31)$$

For the transformation on the right, the impedance looking into the open circuit (outer) stub is

$$Z_x = -jZ_2 \cot(\theta) \quad (5.32)$$

and the total impedance is

$$Z_T = Z_1 \left[\frac{-jZ_2 \cot(\theta) + jZ_1 \tan(\theta)}{Z_1 + Z_2 \cot(\theta) \tan(\theta)} \right] = \frac{-jZ_1 Z_2 \cot(\theta)}{Z_1 + Z_2} + \frac{jZ_1^2 \tan(\theta)}{Z_1 + Z_2}. \quad (5.33)$$

Equating Equations (5.31) and (5.33) and collecting terms,

$$Z_{02} = Z_1 Z_2 / (Z_1 + Z_2) \quad \text{and} \quad Z_{01} = Z_1^2 / (Z_1 + Z_2), \quad (5.34)$$

and the transmission line segments (of characteristic impedance Z_{01} , Z_{02} , Z_1 and Z_2) all have the same electrical length.

In summary, the stub transformations hold no matter what the lengths of the stubs. The half-angle stub transformations enable transmission line circuits to be miniaturized.

5.7 Resonators

Near resonance, the response of a microwave resonator is very similar to the resonance response of a parallel or series LC resonant circuit, shown in Figure 5-18(e and f). These equivalent circuits can be used over a narrow frequency range of perhaps 5% fractional bandwidth.

Several types of resonators are shown in Figure 5-18. Figure 5-18(a) is a rectangular cavity resonator coupled to an external coaxial line by a small coupling loop. Figure 5-18(b) is a microstrip patch reflection resonator. This resonator has large coupling to the external circuit. The coupling can be reduced and photolithographically controlled by introducing a gap, as shown in Figure 5-18(c), to create what is called a microstrip gap-coupled transmission line reflection resonator. The Q of a resonator can be dramatically increased by using a low-loss, high-dielectric constant material, as shown in Figure 5-18(d), for a dielectric transmission resonator in microstrip.

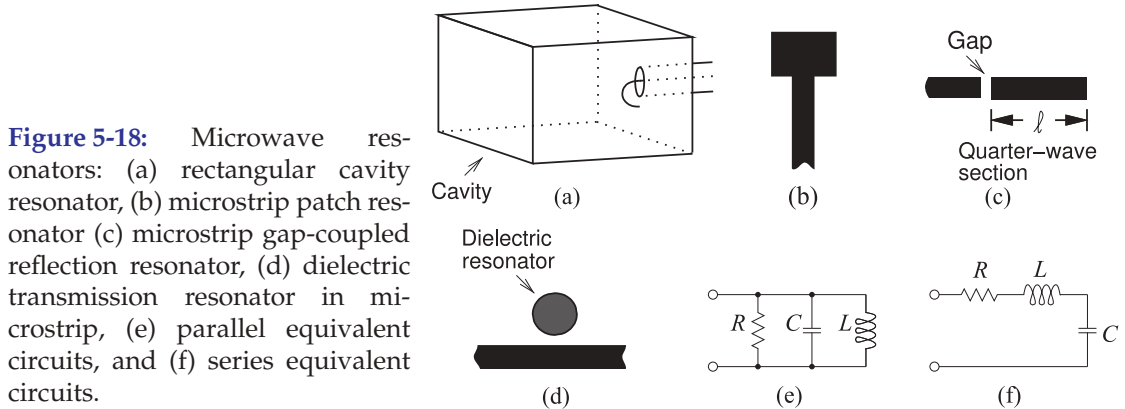


Figure 5-18: Microwave resonators: (a) rectangular cavity resonator, (b) microstrip patch resonator (c) microstrip gap-coupled reflection resonator, (d) dielectric transmission resonator in microstrip, (e) parallel equivalent circuits, and (f) series equivalent circuits.

5.7.1 Dielectric Resonators

Any dielectric structure can store EM energy, with the resonant frequency dependent on both the permittivity and the physical dimensions. At the resonance frequency, all resonators store the maximum amount of energy. Two resonators that store particularly large amounts of energy are the cavity resonator shown in Figure 5-18(a) and the dielectric resonator shown in Figure 5-18(d).

Microwave ceramics can have very low loss and high permittivity (which results in small wavelengths and hence small size) and are commonly used in microwave resonators. Low-loss ceramic materials with permittivities in the range of 21 to 150 are generally available and unloaded Q factors are in the 5,000 to 10,000 range. Physical dimensions generally depend upon the resonant frequencies desired.

The general theoretical expression for the resonant frequencies, applying to a cylindrical dielectric resonator of radius a and height d , is

$$f_{mnl} = \frac{c}{2\sqrt{\epsilon_r}} \sqrt{\left(\frac{\chi_{mn}}{\pi a}\right)^2 + \left(\frac{l}{d}\right)^2}, \quad (5.35)$$

where the integer l denotes the number of half wavelengths in the vertical direction and χ_{mn} is the m th extremum of the Bessel function J_n for a TM mode (or alternatively the m th zero for a TE mode).

Figure 5-18(d) shows a common use of a dielectric resonator, often called a **puck**, coupling to the fields of a microstrip line. The puck has a resonance defined by the radius of the high permittivity puck. There can be several modes of resonance, with some modes introducing a parallel resonant circuit (Figure 5-18(e)) in shunt across the line and others introducing a series resonant circuit in shunt across the line (Figure 5-18(f)).

5.8 Magnetic Transformer

In this section the use of magnetic transformers in microwave circuits will be discussed. Magnetic transformers can be used directly up to a few hundred megahertz or so, but the same transforming properties can be achieved using coupled transmission lines.

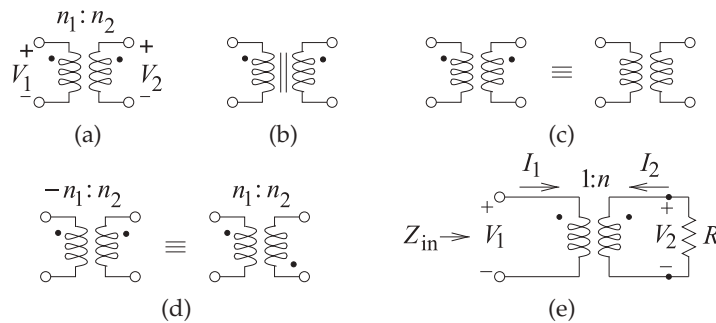


Figure 5-19: Magnetic transformers: (a) a transformer as two magnetically coupled windings with n_1 windings on the primary (on the left) and n_2 windings on the secondary (on the right) (the dots indicate magnetic polarity so that the voltages V_1 and V_2 have the same sign); (b) a magnetic transformer with a magnetic core; (c) identical representations of a magnetic transformer with the magnetic polarity implied for the transformer on the right; (d) two equivalent representations of a transformer having opposite magnetic polarities (an **inverting transformer**); and (e) a magnetic transformer circuit.

5.8.1 Properties of a Magnetic Transformer

A magnetic transformer (see Figure 5-19) magnetically couples the current in one wire to current in another. The effect is amplified using coils of wires and using a core of magnetic material (material with high permeability) to create greater magnetic flux density. When coils are used, the symbol shown in Figure 5-19(a) is used, with one of the windings called the primary winding and the other called the secondary winding. If there is a **magnetic core** around which the coils are wound, then the symbol shown in Figure 5-19(b) is used, with the vertical lines indicating the core. However, even if there is a core, the simpler transformer symbol in Figure 5-19(a) is more commonly used. Magnetic cores are useful up to several hundred megahertz and rely on the alignment of magnetic dipoles in the core material. Above a few hundred megahertz the magnetic dipoles cannot react quickly enough and so the core looks like an open circuit to magnetic flux. Thus the core is not useful for magnetically coupling signals above a few hundred megahertz. As mentioned, the dots above the coils in Figure 5-19(a) indicate the polarity of the magnetic flux with respect to the currents in the coils so that, as shown, V_1 and V_2 will have the same sign. Even if the magnetic polarity is not specifically shown, it is implied (see Figure 5-19(c)). There are two ways of showing inversion of the magnetic polarity, as shown in Figure 5-19(d), where a negative number of windings indicates opposite magnetic polarity. The interest in using magnetic transformers in high-frequency circuit design is that configurations of magnetic transformers can be realized using coupled transmission lines to extend operation to hundreds of gigahertz. The transformer is easy to conceptualize, so it is convenient to first develop a circuit using the transformer and then translate it to transmission line form. That is, in “back-of-the-envelope” microwave design, transformers can be used to indicate coupling, with the details of the coupling left until later when the electrical design is translated into a physical design. Restrictions must be followed as not all transformer configurations can be translated this

way. Transformer characteristics are developed below.

The following notation is used with a magnetic transformer:

L_1, L_2 : the self-inductances of the two coils

M : the mutual inductance

k : the coupling factor,

$$k = \frac{M}{\sqrt{L_1 L_2}}. \quad (5.36)$$

Referring to Figure 5-19(e), the voltage transformer ratio is

$$V_2 = nV_1, \quad (5.37)$$

where n is the ratio of the number of secondary to primary windings. An ideal transformer has “perfect coupling,” indicated by $k = 1$, and the self-inductances are proportional to the square of the number of windings, so

$$\frac{V_2}{V_1} = \sqrt{\frac{L_2}{L_1}}. \quad (5.38)$$

The general equation relating the currents of the circuit in Figure 5-19(e) is

$$RI_2 + j\omega L_2 I_2 + j\omega M I_1 = 0, \quad (5.39)$$

and so

$$\frac{I_1}{I_2} = -\frac{R + j\omega L_2}{j\omega M}. \quad (5.40)$$

If $R \ll \omega L_2$, then the current transformer ratio is

$$\frac{I_1}{I_2} \approx -\frac{L_2}{M} = -\sqrt{\frac{L_2}{L_1}}. \quad (5.41)$$

Notice that combining Equations (5.38) and (5.41) leads to calculation of the transforming effect on impedance. On the Coil 1 side, the input impedance is (referring to Figure 5-19(e))

$$Z_{\text{in}} = \frac{V_1}{I_1} = -\frac{V_2}{I_2} \left(\frac{L_1}{L_2} \right) = R \frac{L_1}{L_2}. \quad (5.42)$$

In practice, however, there is always some magnetic field leakage—not all of the magnetic field created by the current in Coil 1 goes through (or links) Coil 2—and so $k < 1$. Then from Equations (5.38)–(5.42),

$$V_1 = j\omega L_1 I_1 + j\omega M I_2 \quad (5.43)$$

$$0 = RI_2 + j\omega L_2 I_2 + j\omega M I_1. \quad (5.44)$$

Again, assuming that $R \ll \omega L_2$, a modified expression for the input impedance is obtained that accounts for nonideal coupling:

$$Z_{\text{in}} = R \frac{L_1}{L_2} + j\omega L_1 (1 - k^2). \quad (5.45)$$

Imperfect coupling, $k < 1$, causes the input impedance to be reactive and this limits the bandwidth of the transformer. Stray capacitance is another factor that impacts the bandwidth of the transformer.

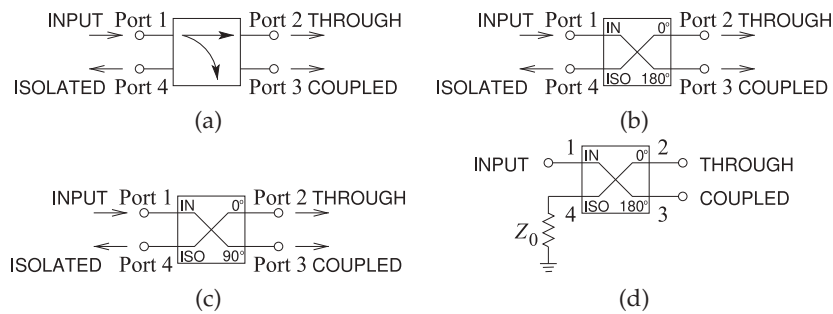


Figure 5-20: Commonly used symbols for hybrids: (a) through and coupled ports; (b) 180° hybrid; (c) 90° hybrid; and (d) hybrid with the isolated port terminated in a matched load.

5.9 Hybrids

Hybrids are transformers that combine or divide microwave signals among a number of inputs and outputs. They can be implemented using distributed or lumped elements and are not restricted to RF and microwave applications. For example, a magnetic transformer is a hybrid and can be used to combine the outputs of two or more transistor stages, or to obtain appropriate impedance levels. A 3 dB directional coupler based on parallel coupled lines is also a type of hybrid. Specific implementations will be considered later in this chapter, but for now the focus is on their idealized characteristics. The symbols commonly used for hybrids are shown in Figure 5-20.

A hybrid is a special type of four-port junction with the property that if a signal is applied at any port, it emerges from two of the other ports at half power, while there is no signal at the fourth or isolated port. The two outputs have specific phase relationships and all ports are matched. Only two fundamental types of hybrids are used: 180° and 90° hybrids. A hybrid is a type of directional coupler, although the term directional coupler, or just coupler, is most commonly used to refer to devices where only a small fraction of the power of an input signal is sampled. Also, a balun is a special type of hybrid.

5.9.1 Quadrature Hybrid

The ideal 90° **hybrid**, or **quadrature hybrid**, shown in Figure 5-20(c), has the scattering parameters

$$S_{90^\circ} = \frac{1}{\sqrt{2}} \begin{bmatrix} 0 & -j & 1 & 0 \\ -j & 0 & 0 & 1 \\ 1 & 0 & 0 & -j \\ 0 & 1 & -j & 0 \end{bmatrix}. \quad (5.46)$$

The 90° phase difference between the through and coupled ports is indicated by $-j$. The actual phase shift, that is, $+90^\circ$ or -90° (indicated by j), between the input and output ports depends on the specific hybrid implementation. Another quadrature hybrid could have the parameters

$$S_{90^\circ} = \frac{1}{\sqrt{2}} \begin{bmatrix} 0 & j & 1 & 0 \\ j & 0 & 0 & 1 \\ 1 & 0 & 0 & j \\ 0 & 1 & j & 0 \end{bmatrix}. \quad (5.47)$$

Recall the requirement of quadrature modulators that the local oscillator be supplied as two components equal in magnitude but 90° out of phase. A quadrature hybrid is just the circuit that can do this.

To convince yourself that Equation (5.47) describes a network that splits the power, consider the power flow implied by Equation (5.47). The fraction of power transmitted from Port i to Port j is described by $|S_{ji}|^2$. Consider the power that enters Port 1. No power is reflected for an ideal hybrid, as the input at Port 1 is matched and $S_{11} = 0$. Port 4 should be isolated so no power will come out of Port 4, and so $S_{41} = 0$. The power should be split between Ports 2 and 3, and these should be equal to half the power entering Port 1. From Equation (5.47),

$$|S_{21}|^2 = \left(\frac{1}{\sqrt{2}} |j| \right)^2 = \frac{1}{2} \quad \text{and} \quad |S_{31}|^2 = \left(\frac{1}{\sqrt{2}} |1| \right)^2 = \frac{1}{2}. \quad (5.48)$$

Thus the power entering Port 1 is split, with half going to Port 2 and half to Port 3.

5.9.2 180° Hybrid

The scattering parameters of the 180° **hybrid**, shown in Figure 5-20(b), are

$$S_{180^\circ} = \frac{1}{\sqrt{2}} \begin{bmatrix} 0 & 1 & -1 & 0 \\ 1 & 0 & 0 & 1 \\ -1 & 0 & 0 & 1 \\ 0 & 1 & 1 & 0 \end{bmatrix}, \quad (5.49)$$

and this defines the operation of the hybrid. In terms of the root power waves a and b , the outputs at the ports are

$$\begin{aligned} b_1 &= (a_2 - a_3)/\sqrt{2} & b_2 &= (a_1 + a_4)/\sqrt{2} \\ b_3 &= (-a_1 + a_4)/\sqrt{2} & b_4 &= (a_2 + a_3)/\sqrt{2} \end{aligned} \quad (5.50)$$

Imperfections in fabricating the hybrid will result in nonzero scattering parameters at the ports where ideally $S_{ji} = 0$, so that it is best to terminate

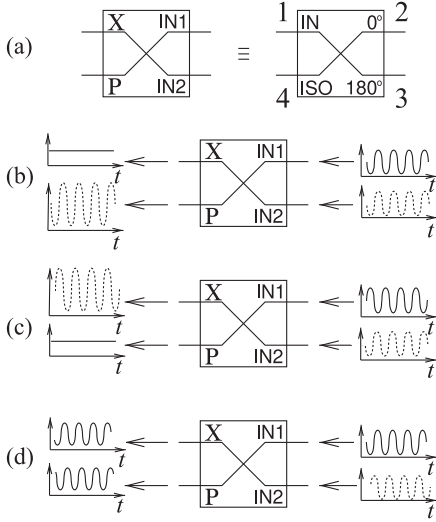


Figure 5-21: A 180° hybrid as a combiner (with output at the sum port, Σ) and as a comparator (with output at the difference port, Δ): (a) equivalence between a 180° hybrid and a sum-and-difference hybrid; (b) the two inputs are in phase; (c) the two inputs are 180° out of phase; and (d) the two inputs are 90° out of phase.

the isolated port of the hybrid, as shown in Figure 5-20(d), to ensure that there is no reflected signal (i.e., no a_4) entering the hybrid at the isolated port. Equation (5.50) shows that ports are interchangeable. That is, if a signal is applied to Port 3, then it is split between Ports 1 and 4, and Port 2 becomes the isolated port.

A hybrid can be used in applications other than splitting the input signal into a through and a coupled component. An example of another use is in a system that combines or compares two signals, as in Figure 5-21. Here a 180° hybrid with the scattering parameters of Equation (5.49) is shown. With a signal $x(t)$ applied to Port 2 in Figure 5-20(b), and another signal $y(t)$ applied to Port 3, the output at Port 4 is the sum signal, $x(t) + y(t)$, and the output at Port 1 is the difference signal, $x(t) - y(t)$. More common names for the output ports (when the 180° hybrid is used as a combiner) are to call Port 4 the sigma or sum port, often designated using the symbol Σ . Port 1 is called the difference or delta port, Δ . Notice that if a signal is applied to the Δ port it will generate out-of-phase outputs.

5.9.3 Magnetic Transformer Hybrid

In the hybrid circuits of Figures 5-22 and 5-23, the number of windings of each coil (there are three in each structure) is the same. The impedance levels given are those required for maximum power transfer and indicate the impedance transformations of the structures. Considering Figure 5-23 and equating powers,

$$\frac{1}{2} \frac{(2V)^2}{Z_2} = \frac{1}{2} \frac{V^2}{Z_0}, \quad \frac{4}{Z_2} = \frac{1}{Z_0}, \quad \text{and so} \quad Z_2 = 4Z_0. \quad (5.51)$$

That is, if $Z_2 = 4Z_0$, the impedance seen looking into Port 4 (of the transformer in Figure 5-23) is Z_0 , and so the transformer has provided matching to the large load. For example, if $Z_2 = 200 \, \Omega$ (perhaps the input of a transistor), the transformer matches this to $50 \, \Omega$.

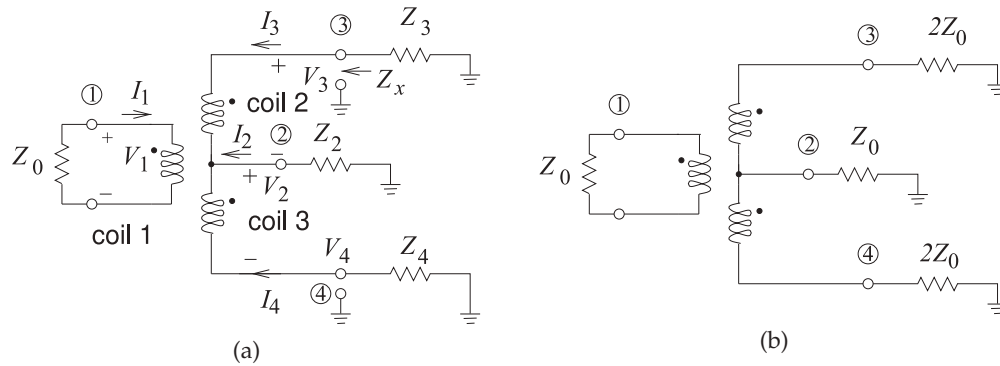


Figure 5-22: Magnetic transformer hybrid with each coil having the same number of windings: (a) showing general loading impedance; and (b) optimum loading to function as a 180° hybrid with Port 2 (terminal 2 to ground) isolated and the balanced input at Port 1. For example, an antenna could be attached to Port 1. A common flux passes through the three coils.

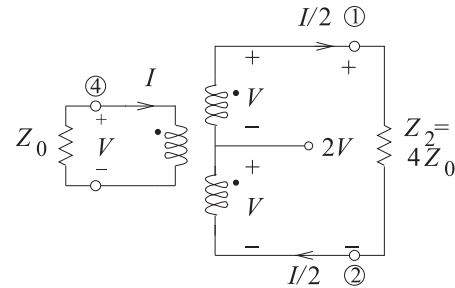


Figure 5-23: The magnetic transformer of Figure 5-22 as an impedance transforming balun.

EXAMPLE 5.2 Magnetic Transformer Hybrid

Consider the magnetic transformer hybrid of Figure 5-22(a) with Z_0 real. Determine what type of hybrid this is and calculate the impedance transformations. Assume ideal coupling ($k = 1$).

Solution:

Since the coupling is ideal and each coil has the same number of windings,

$$(V_3 - V_2) = V_1 \quad \text{and} \quad (V_2 - V_4) = V_1. \quad (5.52)$$

The current levels in the transformer depend on the attached circuitry. For this circuit to function as a hybrid with Port 2 isolated, the current I_2 must be zero so that I_3 and I_4 are equal in magnitude but 180° out of phase. The loading at Ports 3 and 4 must be the same. Now $V_2 = 0$, since $I_2 = 0$, and so Equation (5.52) become

$$V_3 = V_1 \quad \text{and} \quad V_4 = -V_1, \quad (5.53)$$

so this circuit is a 180° hybrid.

To determine loading conditions at Ports 2, 3, and 4 the following transformer equation is used:

$$V_3 = j\omega L_2 I_3 + j\omega M I_1 - j\omega M I_4, \quad (5.54)$$

where L_2 is the inductance of Coil 2 and M is the mutual inductance. Now $I_1 = -V_1/Z_0$, $L_2 = L_3 = M$ since coupling is ideal, and $V_3 = V_1$. So Equation (5.54) becomes

$$V_3 = j\omega M(2I_3 - V_3/Z_0). \quad \text{That is,} \quad V_3(1 + j\omega M/Z_0) = j2\omega M I_3. \quad (5.55)$$

$$\text{If } j\omega M \gg |Z_0|, \text{ this reduces to} \quad Z_x = V_3/I_3 = 2Z_0. \quad (5.56)$$

For maximum power transfer $Z_3 = Z_x^*$, but since Z_0 is real, $Z_3 = Z_x = 2Z_0$. From symmetry, $Z_4 = Z_3$. Also, $I_3 = -I_4 = I_1/2$.

(The above result can also be obtained by considering only maximum power transfer considerations. The argument is as follows. An impedance Z_0 is attached to Coil 1. Maximum power transfer to the transformer through the coil requires that the input impedance be Z_0 (since it is real). In the ideal hybrid operation the power is split evenly between the powers delivered to the loads at Ports 3 and 4, since $V_1 = (V_3 - V_2) = (V_2 - V_4)$ and the power delivered to Coil 1 is $V_1^2/(2Z_0)$. The power delivered to Z_3 (and Z_4) is $(V_3 - V_2)^2/(2Z_3) = V_1^2/(2Z_3) = V_1^2/(4Z_0)$. That is, $Z_3 = 2Z_0 = Z_4$. It is a small extrapolation to say that $Z_3 = 2Z_0^* = Z_4$.)

The problem is not yet finished, as Z_2 must be determined. For hybrid operation, a signal applied to Port 2 should not have a response at Port 1. So the current at Port 2, I_2 , should be split between Coils 2 and 3 so that $I_3 = -I_2/2 = I_4$. Thus

$$V_4 = -I_4(2Z_0) = (I_2/2)(2Z_0) = I_2 Z_0 = V_3. \quad (5.57)$$

$$\text{Now} \quad V_3 - V_2 = V_1 = 0 = V_2 - V_4, \quad \text{and so} \quad V_2 = V_4 = I_2 Z_0. \quad (5.58)$$

$$\text{That is,} \quad Z_2 = V_2/I_2 = Z_0. \quad (5.59)$$

The final 180° hybrid circuit is shown in Figure 5-22(b) with the loading conditions for matched operation as a hybrid.

In the example above it is seen that the number of windings in the coils are the same so that the current in Coils 2 and 3 (of the transformer in Figure 5-22) is half that in Coil 1. The general rule is that with an ideal transformer, the sum of the amp-turns around the magnetic circuit must be zero. The precise way the sum is calculated depends on the direction of the windings indicated by the “dot” convention. A generalization of the rule for the transformer shown in Figure 5-22 is

$$n_1 I_1 - n_2 I_2 - n_3 I_3 = 0, \quad (5.60)$$

where n_j is the number of windings of Coil j with current I_j . The example serves to illustrate the type of thinking behind the development of many RF circuits. Considering maximum power transfer provided an alternative, simpler start to the solution of the problem than one that used the full transformer equations.

5.10 Baluns

A balun [16, 17] is a structure that joins balanced and unbalanced circuits. The word itself (balun) is a contraction of balanced-to-unbalanced

Figure 5-24: A balun: (a) as a two-port with four terminals; (b) IEEE standard schematic symbol for a balun [9]; and (c) an (unbalanced) coaxial cable driving a dipole antenna through a balun.

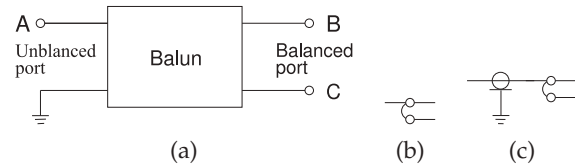


Figure 5-25: Balun: (a) schematic representation as a transformer showing unbalanced and balanced ports; and (b) connected to a single-ended unbalanced amplifier yielding a balanced output.

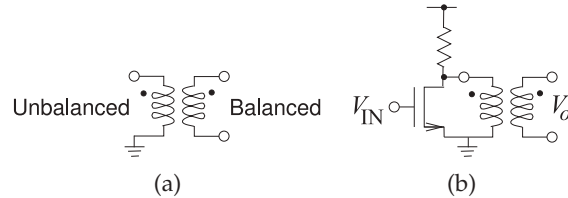
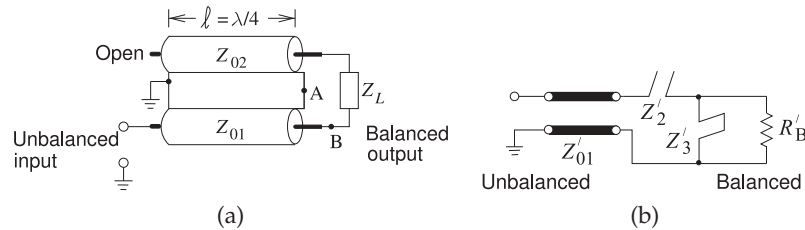


Figure 5-26: Marchand balun: (a) coaxial form of the Marchand balun; and (b) its equivalent circuit.



transformer. Representations of a balun are shown in Figure 5-24. A situation when a balun is required is with an antenna. Many antennas do not operate correctly if part of the antenna is at the same potential electrically as the ground. Instead, the antenna should be electrically isolated from the ground (i.e., balanced). The antenna would usually be fed by a coaxial cable with its outer conductor connected to ground, and so a balun is required between the cable and the antenna.

A balun is a key component of many RF and microwave communications systems [18, 19]. Baluns are used in balanced circuits, such as antennas, double-balanced mixers, push-pull amplifiers, and frequency doublers [20]. Another application of a balun is in a system using RFICs, where a balun transforms the differential outputs of an RFIC to unbalanced microwave circuitry. The schematic of a magnetic transformer used as a balun is shown in Figure 5-25(a) with one terminal of the unbalanced port grounded. Figure 5-24(b) is the standard schematic symbol for a balun and its use with a dipole antenna is shown in Figure 5-24(c). The second port is floating and is not referenced to ground. An example of the use of a balun is shown in Figure 5-25(b), where the amplifier is called a single-ended amplifier and its output is unbalanced, being referred to ground. A balun transitions from the unbalanced transistor output to a balanced output.

5.10.1 Marchand Balun

The most common form of microwave balun is the Marchand balun [16, 20–23]. An implementation of the Marchand balun using coaxial transmission lines is shown in Figure 5-26(a) [24]. It can also be realized in planar form [16]. The Z_{02} line acts as both a series stub and a shunt stub. Thus the model of the Marchand balun is as shown in Figure 5-26(b).

The drawback of the conventional Marchand balun is that the center frequency of the balun is actually the resonant frequency of the transmission

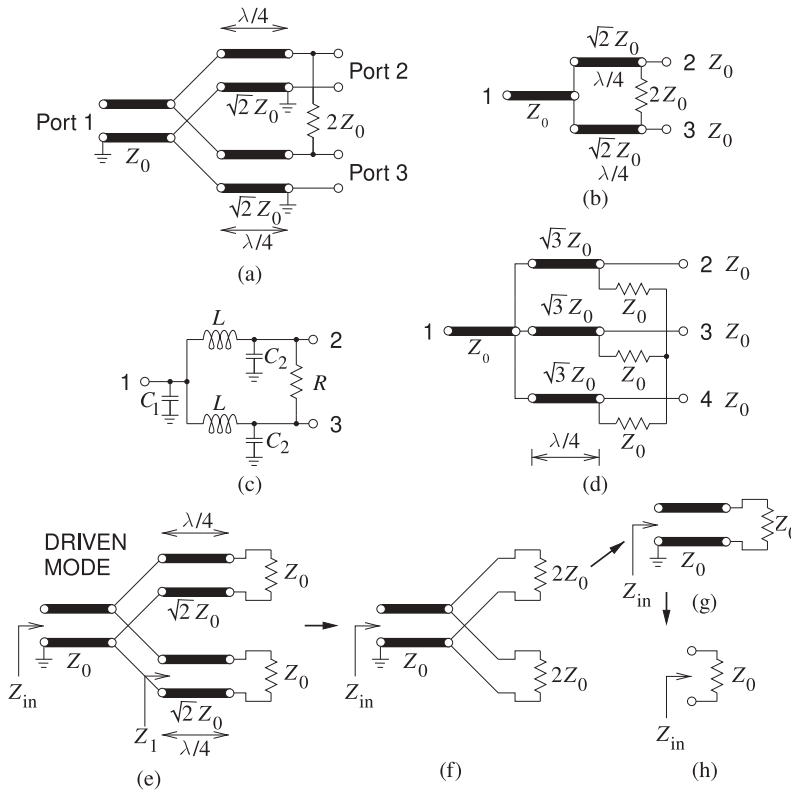


Figure 5-27: Wilkinson divider: (a) two-way divider with Port 1 being the combined signal and Ports 2 and 3 being the divided signals; (b) less cluttered representation; (c) lumped-element implementation; (d) three-way divider with Port 1 being the combined signal and Ports 2, 3, and 4 being the divided signals; and (e)–(h) steps in the derivation of the input impedance.

line resonators forming the balun. Thus the overall size of a conventional Marchand balun can be large, with the size determined by the transmission line sections, which are one-quarter wavelength long at the balun center frequency. Network synthesis can lead to miniaturized baluns by shifting the one-quarter wavelength frequency up while maintaining the balun center frequency [23].

5.11 Combiners and Dividers

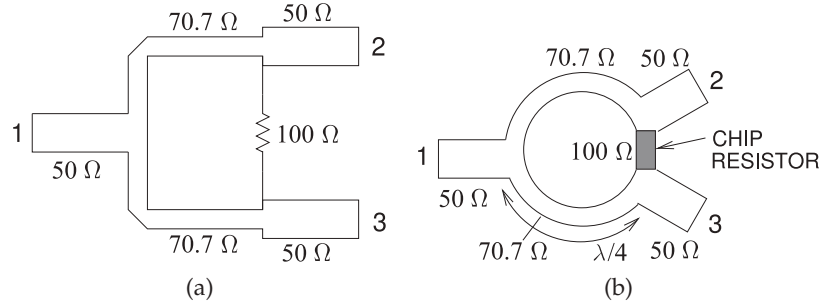
Combiners are used to combine power from two or more sources. A typical use is to combine power from two high power amplifiers to obtain a higher power than would otherwise be available. Dividers divide power so that the power from an amplifier can be routed to different parts of a circuit.

5.11.1 Wilkinson Combiner and Divider

The Wilkinson divider can be used as a combiner or divider that divides input power among the output ports [25]. Figure 5-27(a) is a two-way divider that splits the power at Port 1 equally between the two output ports at Ports 2 and 3. A particular insight that Wilkinson brought was the introduction of the resistor between the output ports and this acts to suppress any imbalance between the output signals due to nonidealities. If the division is exact, no current will flow in the resistor. The circuit works less well as a general purpose combiner. Ideally power entering Ports 2 and 3 would combine losslessly and appear at Port 1. A typical application is to combine the power at the output of two matched transistors where the amplitude and the phase

Figure 5-28:

Wilkinson combiner and divider: (a) microstrip realization; and (b) higher performance microstrip implementation.



of the signals can be expected to be closely matched. However, if the signals are not identical, power will be absorbed in the resistor. The bandwidth of the Wilkinson combiner/divider is limited by the one-quarter wavelength long lines. However, the bandwidth is relatively large, approaching $\pm 50\%$ [25]. Arbitrary power ratios can also be obtained [26–28].

The operation of the Wilkinson divider can be seen by deriving the input impedance of the two-way Wilkinson divider driven at Port 1 (see Figure 5-27(e)). Since the Wilkinson divider is driven, the signals at Ports 2 and 3 will be identical, so it is as though the resistor in the Wilkinson divider is not there. The input impedance of one of the one-quarter wavelength long sections in Figure 5-27(e) is

$$Z_1 = \frac{(\sqrt{2}Z_0)^2}{Z_0} = 2Z_0, \quad (5.61)$$

and so the Wilkinson model reduces to that in Figure 5-27(f). The two $2Z_0$ resistors are in parallel, resulting in the further model reductions in Figures 5-27(g) and 5-27(h). Thus Port 1 is matched. A similar analysis shows that Ports 2 and 3 are matched (have an input impedance of Z_0). The S parameters of the two-way Wilkinson power divider with an equal split of the output power are therefore

$$\mathbf{S} = \begin{bmatrix} 0 & -j/\sqrt{2} & -j/\sqrt{2} \\ -j/\sqrt{2} & 0 & 0 \\ -j/\sqrt{2} & 0 & 0 \end{bmatrix}. \quad (5.62)$$

Figure 5-27(b) is a compact representation of the two-way Wilkinson divider, and a three-way Wilkinson divider is shown in Figure 5-27(d). This pattern can be repeated to produce N -way power dividing. The lumped-element version of the Wilkinson divider shown in Figure 5-27(c) is based on the LC model of a one-quarter wavelength long transmission line segment. With a $50\ \Omega$ system impedance and center frequency of 400 MHz, the elements of the lumped element are (from Figure 2-37(c)) $L = 28.13\ \text{nH}$, $C_1 = 11.25\ \text{pF}$, $C_2 = 5.627\ \text{pF}$, and $R = 100\ \Omega$.

Figure 5-28(a) is the layout of a direct microstrip realization of a Wilkinson divider. The obvious problem is how to incorporate the resistor. As long as the resistor is placed symmetrically this is not as severe a problem as it would initially seem, as power is not dissipated in the resistor unless there is an imbalance. A higher-performance microstrip layout is shown in Figure 5-28(b), where the transmission lines are curved to bring the output ports near each other so that a chip resistor can be used.

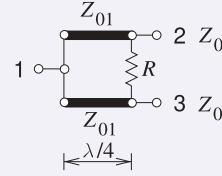
EXAMPLE 5.3 Lumped-Element Wilkinson Divider

Design a lumped-element 2-way Wilkinson divider in a $60\ \Omega$ system. The center frequency of the design should be 10 GHz.

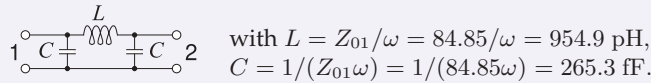
Solution:

The design begins with the transmission line form of the Wilkinson divider which will be converted to a lumped-element form latter. The design parameters are $Z_0 = 60\ \Omega$, $f = 10\ \text{GHz}$, $\omega = 2\pi 10^{10} = 2.283 \cdot 10^{10}\ \text{rads/s}$ and so

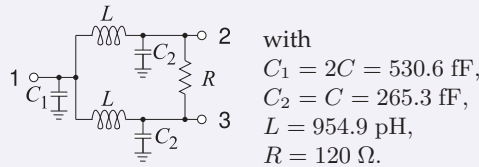
$$Z_{01} = \sqrt{2}Z_0 = 84.85\ \Omega, \quad R = 2Z_0 = 120\ \Omega.$$



The next stage is to convert the transmission lines to lumped elements. A broadband design of a quarter-wavelength transmission line was presented in Figure 2-37(b) of [15]. That is, each of the quarter-wave lines has the model



So the final lumped element design is

**5.11.2 Chireix Combiner**

One of the problems with the Wilkinson structure when it is used as a combiner is that it is only efficient at combining when the two signals to be combined are in phase. A better combiner is the Chireix combiner [29] shown in Figure 5-29. This combiner is often used when combining the outputs of two amplifiers achieving efficient combining even when the signals to be combined are not identical [30–33].

5.12 Transmission Line Transformer

One of the challenges in RF engineering is achieving broadband operation of transformers from megahertz up to several gigahertz. In this section, several structures are presented that operate as magnetic transformers at frequencies below several hundred megahertz but as coupled transmission line structures at high frequencies. A transformer that achieves this and,

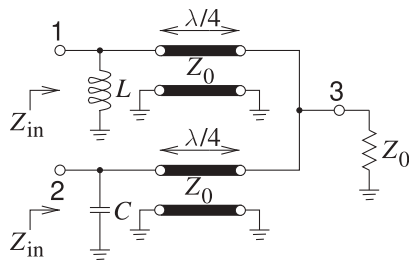


Figure 5-29: Chireix combiner.

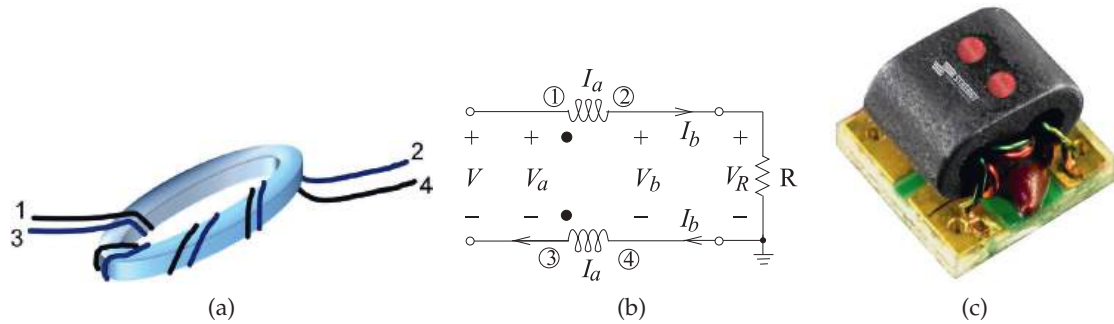


Figure 5-30: A broadband RF balun as coupled lines wound around a ferrite core: (a) physical realization (the wires 1–2 and 3–4 form a single transmission line); (b) equivalent circuit using a wire-wound transformer (the number of primary and secondary windings are equal); and (c) packaged as a module (Model TM1-9 with a frequency range of 100–5000 MHz. Copyright Synergy Microwave Corporation, used with permission [34]).

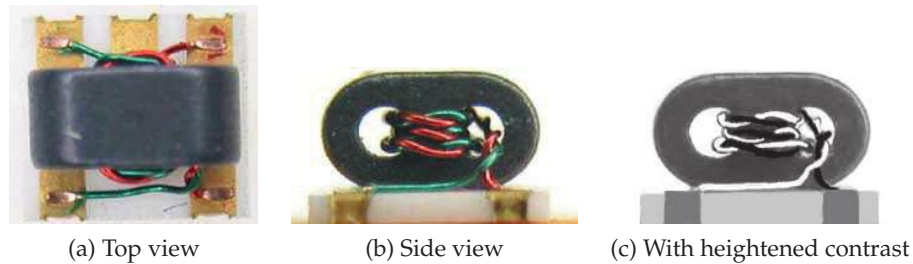


Figure 5-31: Open-core surface-mount transformer. Copyright 2012 Scientific Components Corporation d/b/a Mini-Circuits, used with permission [11].

in this configuration, realizes a balun is shown in Figure 5-30(a). Below a few hundred megahertz this functions as a magnetic transformer. Above this frequency the ferrite core cannot respond to the signal and the magnetic circuit through the core appears as an open circuit. Then, since the transformer is not operating as a magnetic transformer anymore, magnetic leakage is inconsequential. At high frequencies the wire transmission lines are closely coupled and appear as a perfect coupler if the lines (or wires here) are long enough. The equivalent circuit of this structure is shown in Figure 5-30(b). At high frequencies, stray capacitances between the windings becomes important but become part of the transmission line capacitance. Many types of transformers operating from several megahertz to several gigahertz can be realized using the same principle and are available as surface-mount components (see Figure 5-30(c)).

High-frequency coupling is enhanced by twisting the conductors as shown in Figure 5-31. The combination of magnetic coupling at low frequencies with transmission line coupling at high frequencies yields a transformer that operates over very wide bandwidths.

5.12.1 Transmission Line Transformer as a Balun

The schematic of a broadband 1:1 RF balun is shown in Figure 5-30(b) and a realization of it is shown in Figure 5-30(a and c). The 1:1 designation indicates that there is no impedance transformation. The circuit equations describing this balun are (from the $ABCD$ parameters of a transmission line; see Table 2-1)

$$V_a = V_b \cos(\beta\ell) + jI_b Z_0 \sin(\beta\ell) \quad \text{and} \quad I_a = I_b \cos(\beta\ell) + j \frac{V_b}{Z_0} \sin(\beta\ell) \quad (5.63)$$

and the load resistance creates a third equation,

$$V_b = I_b R. \quad (5.64)$$

The aim in the following is the development of a design equation that describes the essential properties of the structure. Substituting Equation (5.64) in Equation (5.63) leads to

$$V_a = V_b \left[\cos(\beta\ell) + j \frac{Z_0}{R} \sin(\beta\ell) \right] \quad \text{and} \quad I_a = \frac{V_b}{R} \left[\cos(\beta\ell) + j \frac{R}{Z_0} \sin(\beta\ell) \right]. \quad (5.65)$$

Choosing $Z_0 = R$ yields (since $e^{j\beta\ell} = \cos(\beta\ell) + j \sin(\beta\ell)$)

$$V_a = V_b e^{j\beta\ell} \quad \text{and} \quad I_a = (V_b/R) e^{j\beta\ell}, \quad (5.66)$$

and so

$$Z_{\text{in}} = V_a / I_a = R. \quad (5.67)$$

This analysis is idealized, as parasitics are eliminated (mainly parasitic capacitances), but the above equation indicates that the essential function of the structure is that of a balun with no impedance transformation.

The transformer arrangement shown in Figure 5-30(b) is of particular interest as it can be realized using coupled transmission lines.

5.12.2 4:1 Impedance Transformer at High Frequencies

By changing the connection of the transformer terminals it is possible to achieve impedance transformation. A 4:1 impedance transformer is shown in Figure 5-32(a). A specific arrangement of the primary and secondary windings puts this into what is called the transmission line form, shown in Figure 5-33. At high frequencies port conditions are enforced so that the currents at Ports 1 and 3 (and at Ports 2 and 4) are matched, as shown in Figure 5-33. Showing that $Z_{\text{in}} = R$ begins with

$$\begin{aligned} V_a &= V_b \cos(\beta\ell) + jI_b Z_0 \sin(\beta\ell), & I_a &= I_b \cos(\beta\ell) + j \frac{V_b}{Z_0} \sin(\beta\ell), \\ V_{\text{in}} &= V_a + R(I_a + I_b), & \text{and} & \quad V_b = (I_a + I_b)R. \end{aligned} \quad (5.68)$$

So the aim is to find $Z_{\text{in}} = V_{\text{in}}/I_a$, as this defines the required electrical function. Now

$$V_{\text{in}} = V_a + V_b = V_b [1 + \cos(\beta\ell)] + jI_b Z_0 \sin(\beta\ell), \quad (5.69)$$

Figure 5-32: A 4:1 impedance transformer: (a) Schematic (the coils have the same number of windings); and (b) realization as transformer with twisted coupled wires twisted around a magnetic core.

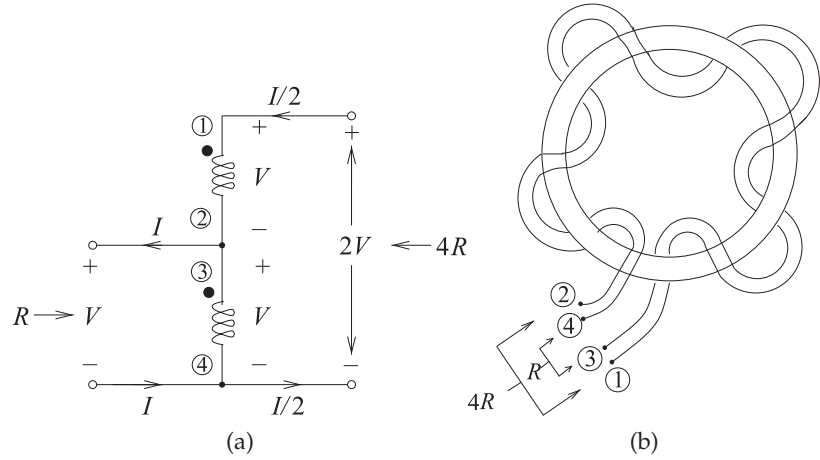
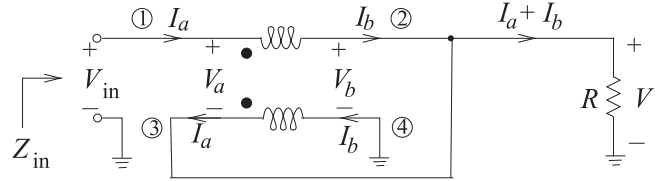


Figure 5-33: A transmission line form of the 4:1 impedance transformer of Figure 5-32, after [35]. (The number of primary and secondary windings are the same.)



and using the equations above

$$\begin{aligned} I_a &= I_b \cos(\beta\ell) + j(I_a + I_b) \frac{R}{Z_0} \sin(\beta\ell) \\ I_b &= I_a \frac{Z_0 - jR \sin(\beta\ell)}{Z_0 \cos(\beta\ell) + jR \sin(\beta\ell)}. \end{aligned} \quad (5.70)$$

Thus

$$Z_{in} = \frac{V_{in}}{I_a} = Z_0 \frac{2R[1 + \cos(\beta\ell)] + jZ_0 \sin(\beta\ell)}{Z_0 \cos(\beta\ell) + jR \sin(\beta\ell)}. \quad (5.71)$$

At very low frequencies the electrical length of the transmission line, $\beta\ell$, is negligibly small and $Z_{in} = 4R$. To see what happens when the length of the transmission line has a significant effect, consider the special case when $Z_0 = 2R$, then

$$Z_{in} = 2R(1 + e^{-j\beta\ell}). \quad (5.72)$$

For a short line, that is, $\ell < 0.1\lambda$ or $\beta\ell < 0.2\pi$, Equation (5.72) can be approximated as

$$Z_{in} \approx 2R[1 + 1 - j\beta\ell] = 4R - jR(2\beta\ell). \quad (5.73)$$

The imaginary component, $-jR2\beta\ell$, is a capacitance and it must be resonated out (e.g., by a series inductor) to obtain the required resistance transformation.

The general approach described above can be used to design transformers with higher impedance ratios. Two more, a 9:1 transformer and a 16:1 transformer, are shown in Figure 5-34.

A practical broadband transmission line realization of the 4:1 transformer is shown in Figure 5-32(b), where the transmission line is a pair of twisted wires.

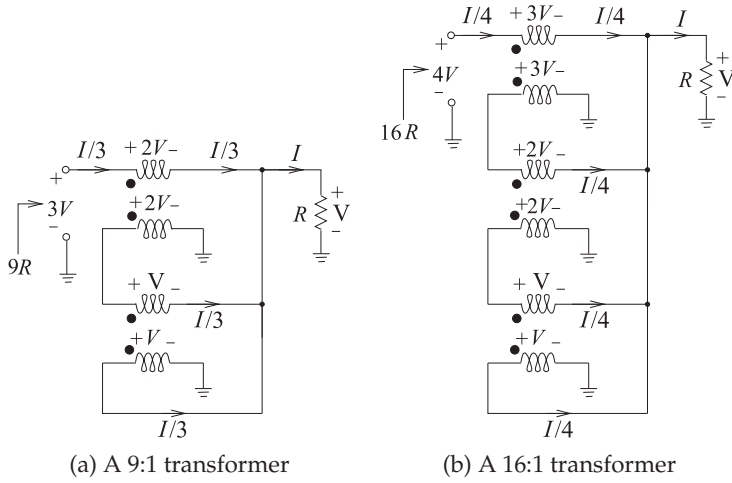


Figure 5-34: High-order impedance transformers.

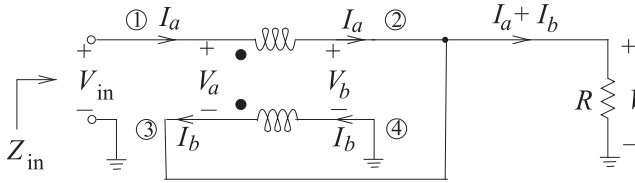


Figure 5-35: Low-frequency schematic of the 4:1 impedance transformer shown in Figure 5-32(a).

5.12.3 4:1 Impedance Transformer at Low Frequencies

In the previous section it was shown that the impedance transformer in Figure 5-32(a) acts as a 4:1 impedance transformer at high frequencies where the structure can be considered to be a transmission line. In this section it will be shown that the transformer is also a 4:1 impedance transformer at low frequencies where the structure can be considered to be a wire-wound transformer.

At low frequencies, the port conditions¹ at the ends of the transmission line are not enforced and so a better low frequency representation of the transformer currents is shown in Figure 5-35. If at low frequencies the transformer of Figure 5-33 has a self-inductance of L_s and a mutual inductance of M , then the circuit equations for the transformer are

$$V_{in} - V_b = j\omega L_s I_a - j\omega M I_b \quad (5.74)$$

$$V_b = -j\omega L_s I_b + j\omega M I_a \quad (5.75)$$

$$V_b = (I_a + I_b)R. \quad (5.76)$$

Equating Equations (5.75) and (5.76) and rearranging,

$$I_b = -\left(\frac{R - j\omega M}{R + j\omega L_s}\right) I_a. \quad (5.77)$$

Combining Equations (5.74) and (5.76) and rearranging,

$$V_{in} = (R + j\omega L_s) I_a + (R - j\omega M) I_b. \quad (5.78)$$

¹ Currents at the pair of terminals of a port are equal in magnitude and opposite in direction.

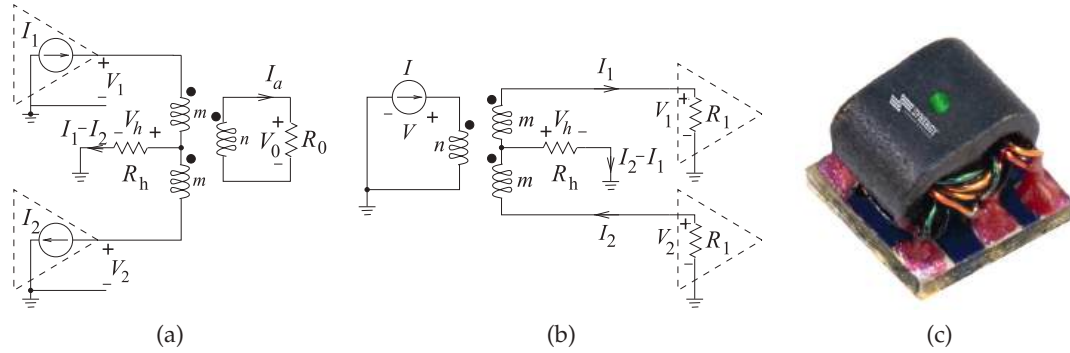


Figure 5-36: A 180° hybrid transformer: (a) used as a combiner; (b) used as a splitter; and (c) center-tapped transformer as a surface-mount component (Model TM1-2 with a frequency range of 20–1200 MHz. Copyright Synergy Microwave Corporation, used with permission [34]).

Replacing I_b in Equation (5.78) using Equation (5.77) yields

$$V_{in} = \left[(R + j\omega L_s) - \frac{(R - j\omega M)^2}{R + j\omega L_s} \right] I_a. \quad (5.79)$$

Thus the input impedance is

$$Z_{in} = \frac{V_{in}}{I_a} = \frac{R^2 + j2R\omega L_s - (\omega L_s)^2 - R^2 + j2R\omega M + (\omega M)^2}{R + j\omega L_s}. \quad (5.80)$$

If ideal coupling is assumed (i.e., $M = L_s$) then Equation (5.80) reduces to

$$Z_{in} = \frac{j4R\omega L_s}{R + j\omega L_s}. \quad (5.81)$$

If $j\omega L_s \gg R$, then

$$Z_{in} \approx 4R. \quad (5.82)$$

Thus the transformer is a 4:1 impedance transformer both at low frequencies when the structure acts as a magnetic transformer and, as seen in Section 5.12.2, at higher frequencies when the structure acts like a transmission line. Design of the impedance transformer is then directed at managing the frequency transition region and ensuring that the required impedance transformation occurs there as well. In practice, very broadband operation is not difficult to achieve.

5.12.4 Hybrid Transformer Used as a Combiner

In Figure 5-36(a) a 180° hybrid transformer is used to combine the outputs of two power amplifiers that are driven 180° out of phase with respect to each other. This is commonly done when the power available from just one solid-state transistor amplifier is not sufficient to meet power requirements. Since the sum of the amp-turns of an ideal transformer must be zero,

$$nI_o = m(I_1 + I_2) \quad (5.83)$$

and $I_1 = I_2$ since the two amplifiers are driven identically but 180° out of phase. Then $V_h = 0$, $V_1 = V_2 = (m/n)V_o$, and both power amplifiers deliver equal power to the load. Also, each amplifier sees a load impedance

$$R_{in} = \frac{V_1}{I_1} = \left(\frac{m}{n}\right)^2 2R_o. \quad (5.84)$$

EXAMPLE 5.4**Transformer Design**

The Thevenin equivalent output impedance of each amplifier in Figure 5-36(a) is $1\ \Omega$ and the system impedance, R_o , is $50\ \Omega$. Choose the transformer windings for maximum power transfer.

Solution:

For maximum power transfer, $R_{in} = 1\ \Omega$, and so from Equation (5.84),

$$1 = \left(\frac{m}{n}\right)^2 \cdot 2 \cdot 50 \quad \text{and} \quad \frac{m}{n} = 0.1. \quad (5.85)$$

Thus with a 10:1 winding ratio the required impedance transformation can be achieved.

5.12.5 Hybrid Transformer Used as a Power Splitter

The hybrid transformer can also be used to split power from a source to drive two loads. The circuit of Figure 5-36(b) splits power from a current source driver into two loads. With the number of primary and secondary windings equal (i.e., $m = n$), the circuit equations are

$$I = I_1 + I_2, \quad V_1 = V + V_h, \quad \text{and} \quad V_2 = V_h - V. \quad (5.86)$$

$$\text{Thus} \quad V_1 - V_h = V_h - V_2. \quad (5.87)$$

Using $V_1 = R_1 I_1$, $V_2 = -I_2 R_2$, and $V_h = (I_2 - I_1)R_h$, the desired electrical characteristics of the splitter are obtained:

$$\frac{I_2}{I_1} = \frac{R_1 + 2R_h}{R_2 + 2R_h}. \quad (5.88)$$

Several observations can be made about the performance of the power splitter. If $R_1 = R_2$, then $I_1 = I_2$ for any value of R_h . Conversely, if $R_1 \neq R_2$, $I_1 \neq I_2$ for a finite R_h . To obtain equal drive currents in both power amplifiers in spite of variations in R_1 and R_2 , the center tap of the transformer needs to be omitted so that $R_h = \infty$.

5.12.6 Broadband Hybrid Combiner

A broadband hybrid combiner is shown in Figure 5-37. In what follows, it is shown that this combiner has the property of accommodating mismatches of the amplifiers. The development begins by assuming that the transformers have an equal number of turns on each winding. These two transformers are used to make a broadband (transmission line transformer) hybrid coupler. The circuit equations are

$$I_1 = I_a + I_b \quad \text{and} \quad I_2 = I_a - I_b, \quad (5.89)$$

$$I_a = \frac{1}{2}(I_1 + I_2) \quad \text{and} \quad I_b = \frac{1}{2}(I_1 - I_2), \quad (5.90)$$

$$V_1 = \frac{V_o}{2} + V_h \quad \text{and} \quad V_2 = \frac{V_o}{2} - V_h. \quad (5.91)$$

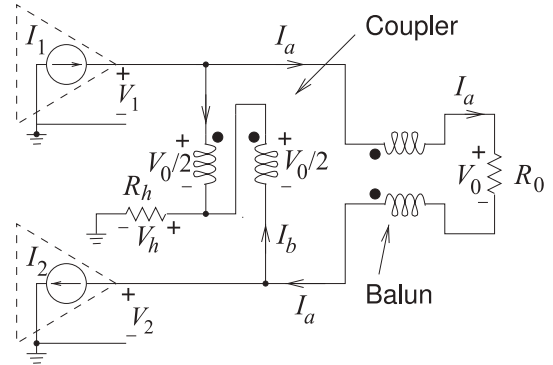


Figure 5-37: Broadband hybrid power combiner.

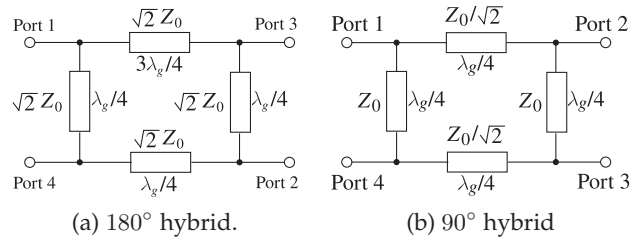


Figure 5-38: Topologies of ring-type hybrids.

Thus

$$\frac{V_1}{I_1} = R_h \left(1 - \frac{I_2}{I_1} \right) + \frac{R_0}{2} \left(1 - \frac{I_2}{I_1} \right) \quad (5.92)$$

$$\frac{V_2}{I_2} = \frac{R_0}{2} \left(1 + \frac{I_1}{I_2} \right) - R_h \left(\frac{I_1}{I_2} - 1 \right). \quad (5.93)$$

A special situation is when $R_h = R_0/2$, and then $V_2/I_2 = R_0$ and $V_1/I_1 = R_0$. Thus each of the amplifiers sees a constant load resistance, R_0 , even if the amplifiers are mismatched, resulting, for example, when the amplifiers have slightly different gains.

5.13 Transmission Line-Based Hybrids

Hybrids can be realized in a variety of transmission line structures. A few of these, but representative ones, are discussed here. Hybrids can also be realized using lumped-elements by modeling the transmission line segments.

5.13.1 Branch-Line Hybrids Based on Transmission Lines

A branch-line hybrid is based on transmission line segments that introduce phase delay. Two such hybrids are shown in Figure 5-38 where the different signal paths result in constructive and destructive interference of signals. This is a very different way of realizing the hybrid function than that obtained using magnetic transformers. The operation of the 180° hybrid (Figure 5-38(a)) can be verified approximately by counting the total number of one-quarter wavelength (90°) phase shifts in each path. It is not so easy to verify the operation of the 90° hybrid. The various characteristic impedances of the transmission line segments adjust the levels of the signals. The operation of the 90° hybrid is examined in the example in this section. (A complete analysis could be done using signal flow graphs.)

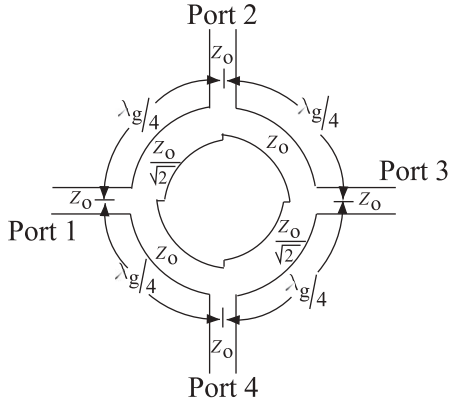


Figure 5-39: Planar implementation of the 3 dB ring-type branch-line hybrid with the topology of Figure 5-38(b).

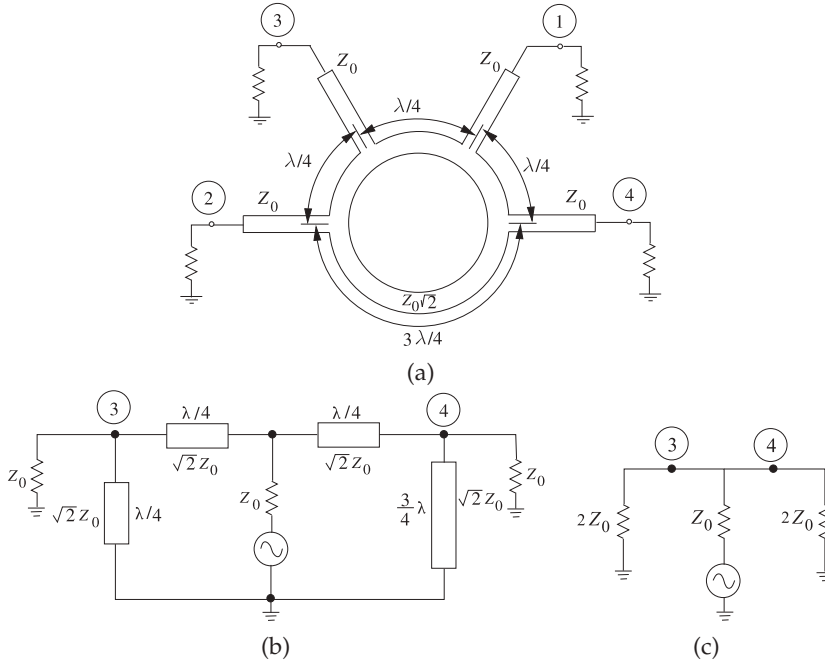


Figure 5-40: Rat-race hybrid with input at Port 1, outputs at Ports 3 and 4, and virtual ground at Port 2: (a) implementation as a planar circuit; (b) transmission line model; and (c) equivalent circuit model.

These branch-line hybrids may be formed into a ring shape, as shown in Figure 5-39. It is also worth considering the so-called rat-race or hybrid-ring circuit shown in Figure 5-40(a). Output signals from Ports 2 and 4 differ in phase by 180° (in contrast to the branch-line coupler, where the phase difference is 90°). An interesting and important design feature arises when considering the quarter-wave transformer action of this coupler. Only Ports 2 and 4 exhibit this action, because Port 3 is half-wave separated from the input feeding Port 1. Thus the net effective load on the inner ring lines feeding Ports 2 and 4 amounts to $2Z_0$ (two Z_0 loads appearing, equivalently, in series). Now the characteristic impedance Z_0 of any quarter-wave transforming line between two impedances, Z_{01} and Z_{02} , is equal to $\sqrt{Z_{01}Z_{02}}$. In this case the two impedances are Z_0 and $2Z_0$, respectively, so (from Section 2.4.6 of [15]) the input impedance of the intervening quarter-wave line is

$$Z'_0 = \sqrt{Z_0 \cdot 2Z_0} = \sqrt{2}Z_0. \quad (5.94)$$

Thus the characteristic impedance of the line forming the ring itself is $\sqrt{2}$ times that of the feeder line impedances. So when the impedance of all ports is $50\ \Omega$, the ring characteristic impedance is $70.7\ \Omega$.

EXAMPLE 5.5**Rat-Race Hybrid**

In this example the rat-race circuit shown in Figure 5-40(a) is considered. One of the functions of this circuit is that with an input at Port 1, the power of this signal is split between Ports 3 and 4. At the same time, no signal appears at Port 2. This example is an exercise in exploiting the impedance transformation properties of the transmission line.

From Figure 5-40(a) it is seen that each port is separated from the other port by a specific electrical length. Intuitively one can realize that there will be various possible outputs for excitation from different ports. Each case will be studied.

When Port 1 of the hybrid is excited or driven, the outputs at Ports 3 and 4 are in phase, as both are distanced from Port 1 by an electrical length of $\lambda_g/4$, while Port 2 remains isolated, as the electrical length of the two paths from Port 1 to Port 2 differ by an even multiple of $\lambda_g/2$. Thus Port 2 will be an electrical short circuit to the signal at Port 1.

In a similar way, a signal excited at Port 2 will result in outputs at Ports 3 and 4, though with a phase difference of 180° between the two output ports and Port 1 remains isolated.

Finally, a signal excited at Ports 3 and 4 will result in the sum of the two signals at Port 1 and the difference of two signals at Port 2. This combination of output is again due to varying electrical length between every port and every other port in the rat-race hybrid. The equivalent transmission line model and equivalent circuit of the rat-race hybrid are shown in Figures 5-40(b and c), respectively.

5.13.2 Lumped-Element Hybrids

Hybrids are developed based on transmission line principles, but it is possible to create hybrids using lumped-element equivalents of transmission line segments. In some cases the full circle of design can begin with the magnetic transformer conceptualization, followed by a transmission line realization, and then a lumped-element approximation. At least this is valid over a bandwidth centered at a particular frequency, $f = \omega_0/(2\pi)$. The lumped-element equivalent of the 180° hybrid in Figure 5-38(a) is shown in Figure 5-41(a) with

$$\omega_0 L = \frac{1}{\omega_0 C} = \sqrt{2} Z_0. \quad (5.95)$$

This result comes from the broadband equivalent circuit of a $\lambda/4$ line shown in Figure 2-37. The lumped-element quadrature hybrid of Figure 5-41(b), based on Figure 5-38(b), has

$$\omega_0 Z_0 C_a = 1, \quad C_a + C_b = \frac{1}{\omega_0^2 L}, \quad \text{and} \quad \omega_0 L = \frac{Z_0}{\sqrt{2}}, \quad (5.96)$$

where Z_0 is the port impedance.

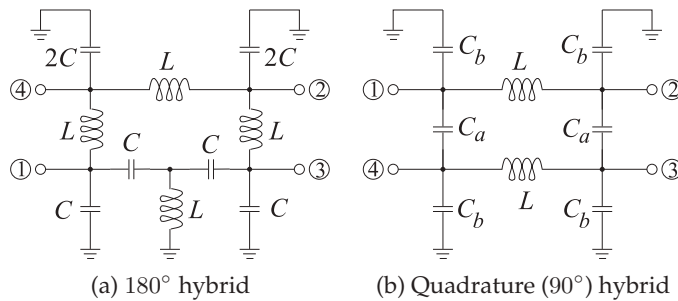


Figure 5-41:
Lumped-
element
hybrids.

5.14 Summary

This chapter introduced the richness of microwave components available to the RF designer. Microwave lumped-element R , L , and C components are carefully constructed so that they function as intended up to 20 GHz or so. They are usually in surface-mount form so that they can be integrated in design without the parasitic effects of leads. To a limited extent, transmission line discontinuities can be used as small-valued lumped elements. Even if the transmission line discontinuities are not specifically introduced for this purpose, their lumped-element equivalent circuits must be included in circuit analysis. Transmission line stubs are widely used to introduce capacitance and inductance in circuits. In most transmission line technologies only shunt stubs are available, and thus there is a strong preference for shunt elements in circuit designs. Many functionalities can be developed using the interactions of forward- and backward-traveling waves on transmission lines. Classic examples seen in this chapter are the combiners and hybrids. Sometimes the functionality can only be visualized using transmission line structures. Then coming full circle, lumped-element equivalents can be realized.

There are many more passive components in the repertoire of the RF designer. However, this chapter reviewed the most important and introduced the concepts that can be used to analyze other structures and to invent new ones. Each year new variants of microwave elements are developed and documented in patents and publications. Microwave engineers monitor these developments, especially in their field of expertise.

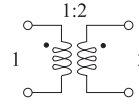
5.15 References

- [1] H. Wheeler, "Simple inductance formulas for radio coils," *Proc. of the Institute of Radio Engineers*, vol. 16, no. 10, pp. 1398–1400, Oct. 1928.
- [2] —, "Inductance formulas for circular and square coils," *Proc. IEEE*, vol. 70, no. 12, pp. 1449–1450, Dec. 1982.
- [3] —, "Inductance chart for solenoid coil," *Proc. IRE*, vol. 38, no. 12, pp. 1398–1400, Dec. 1950.
- [4] T. Lee, *The Design of CMOS Radio-Frequency Integrated Circuits*. Cambridge University Press, 2004.
- [5] C. Yue and S. Wong, "On-chip spiral inductors with patterned ground shields for silicon-based RF ICs," *IEEE J. of Solid-State Circuits*, vol. 33, no. 5, pp. 743–752, May 1998.
- [6] W. Liu, J. Suryanarayanan, J. Nath, S. Mohammadi, L. Katehi, and M. Steer, "Toroidal inductors for radio-frequency integrated circuits," *IEEE Trans. on Microwave Theory and Techniques*, vol. 52, no. 2, pp. 646–654, Feb. 2004.
- [7] A. Victor and M. Steer, "Reflection coefficient shaping of a 5-GHz voltage-tuned oscillator for improved tuning," *IEEE Trans. on Microwave Theory and Techniques*, vol. 55, no. 12, pp. 2488–2494, Dec. 2007.
- [8] <http://www.coilcraft.com>.
- [9] IEEE Standard 315-1975, Graphic Symbols for Electrical and Electronics Diagrams (Including Reference Designation Letters), Adopted Sept. 1975, Reaffirmed Dec. 1993. Approved by American National Standards Institute, Jan. 1989. Approved adopted for mandatory use, Department of Defense, United States of America, Oct. 1975. Approved by Canadian Standards Institute, Oct. 1975.
- [10] P. Vizmuller, *RF Design Guide: Systems, Circuits, and Equations*. Artech House, 1995.
- [11] <http://www.minicircuits.com>.
- [12] P. Katehi and N. Alexopoulos, "Frequency-dependent characteristics of microstrip discontinuities in millimeter-wave integrated circuits," *IEEE Trans. on Microwave Theory and Techniques*, vol. 33, no. 10, pp. 1029–1035, Oct. 1985.
- [13] T. Edwards and M. Steer, *Foundations for Microstrip Circuit Design*. John Wiley & Sons, 2016.
- [14] J. Malherbe, "Realization of elliptic function bandstop filters by means of a resonated prototype," *IEEE Trans. on Microwave Theory and Techniques*, vol. 25, no. 8, p. 717, Aug. 1977.
- [15] M. Steer, *Microwave and RF Design, Transmission Lines*, 3rd ed. North Carolina State University, 2019.
- [16] R. Mongia, I. Bahl, and P. Bhartia, *RF and Microwave Coupled-line Circuits*. Artech House, 1999.
- [17] W. Fathelbab and M. Steer, "Broadband network design," in *Multifunctional Adaptive Microwave Circuits and Systems*, M. Steer and W. Palmer, Eds., 2008, ch. 8.
- [18] D. Kuylenstierna and P. Linner, "Design of broad-band lumped-element baluns with inherent impedance transformation," *IEEE Trans. on Microwave Theory and Techniques*, vol. 52, no. 12, pp. 2739–2745, Dec. 2004.
- [19] B. Minnis and M. Healy, "New broadband balun structures for monolithic microwave integrated circuits," in *1991 IEEE MTT-S Int. Microwave Symp. Dig.*, Jul. 1991, pp. 425–428.
- [20] I. Robertson and S. Lucyszyn, *RFIC and MMIC Design and Technology*. IEEE, 2001, IEEE Circuits, Devices and Systems Series.
- [21] C. Goldsmith, A. Kikel, and N. Wilkens, "Synthesis of marchand baluns using multilayer microstrip structures," *Int. J. of Microwave & Millimeter-Wave Computer-Aided Eng.*, pp. 179–188, 1992.
- [22] N. Marchand, "Transmission line conversion transformers," *Electronics*, pp. 142–145, 1944.
- [23] W. Fathelbab and M. Steer, "New classes of miniaturized planar marchand baluns," *IEEE Trans. on Microwave Theory and Techniques*, vol. 53, no. 4, pp. 1211–1220, Apr. 2005.
- [24] J. J. Cloete, "Graphs of circuit elements for the marchand balun," *Microwave Journal*, vol. 24, no. 5, pp. 125–128, May 1981.
- [25] E. Wilkinson, "An n-way hybrid power divider," *IRE Trans. on Microwave Theory and Techniques*, vol. 8, no. 1, pp. 116–118, Jan. 1960.
- [26] Y.-L. Wu, H. Zhou, Y.-X. Zhang, and Y.-A. Liu, "An unequal wilkinson power divider for a frequency and its first harmonic," *IEEE Microwave and Wireless Components Letters*, vol. 18, no. 11, pp. 737–739, Nov. 2008.
- [27] S. Oh, J.-J. Koo, M.-S. Hwang, C. Park, Y.-C. Jeong, J.-S. Lim, K.-S. Choi, and D. Ahn, "An unequal wilkinson power divider with variable dividing ratio," in *2007 IEEE MTT-S Int. Microwave Symp. Dig.*, Jun. 2007, pp. 411–414.
- [28] J.-S. Lim, S.-W. Lee, C.-S. Kim, J.-S. Park, D. Ahn, and S. Nam, "A 4.1 unequal wilkinson power divider," *IEEE Microwave and Wireless Components Letters*, vol. 11, no. 3, pp. 124–126, Mar. 2001.
- [29] H. Chireix, "High power outphasing modulation," *Proc. of the Institute of Radio Engineers*, vol. 23, no. 11, pp. 1370–1392, Nov. 1935.

- [30] I. Hakala, D. Choi, L. Gharavi, N. Kajakine, J. Koskela, and R. Kaunisto, "A 2.14-GHz chireix outphasing transmitter," *IEEE Trans. on Microwave Theory and Techniques*, vol. 53, no. 6, pp. 2129–2138, Jun. 2005.
- [31] F. Raab, "Efficiency of outphasing RF power-amplifier systems," *IEEE Trans. on Communications*, vol. 33, no. 10, pp. 1094–1099, Oct. 1985.
- [32] S. Moloudi, K. Takinami, M. Youssef, M. Mikhemar, and A. Abidi, "An outphasing power amplifier for a software-defined radio transmitter," in *IEEE Int. Solid-State Circuits Conf., 2008 (ISSCC 2008) Dig. of Technical Papers*, Feb. 2008, pp. 568–636.
- [33] W. Gerhard and R. Knoechel, "Novel transmission line combiner for highly efficient outphasing RF power amplifiers," in *37th European Microwave Conf.*, Oct. 2007, pp. 1433–1436.
- [34] <http://www.synergymwave.com>.
- [35] C. Ruthroff, "Some broad-band transformers," *Proc. of the IRE*, vol. 47, no. 8, pp. 1337–1342, Aug. 1959.

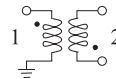
5.16 Exercises

- The Thevenin equivalent output impedance of each of the amplifiers in Figure 5-36(a) is $5\ \Omega$, and the system impedance, R_0 , is $75\ \Omega$. Choose the transformer windings for maximum power transfer. [Parallels Example 5.4]
- A spiral inductor is modeled as an ideal inductor of $10\ \text{nH}$ in series with a $5\ \Omega$ resistor. What is the Q of the spiral inductor at $1\ \text{GHz}$?
- Consider the design of a $50\ \text{dB}$ resistive T attenuator in a $75\ \Omega$ system. [Parallels Example 5.1]
 - Draw the topology of the attenuator.
 - Write down the design equations.
 - Complete the design of the attenuator.
- Consider the design of a $50\ \text{dB}$ resistive Pi attenuator in a $75\ \Omega$ system. [Parallels Example 5.1]
 - Draw the topology of the attenuator.
 - Write down the design equations.
 - Complete the design of the attenuator.
- A $20\ \text{dB}$ attenuator in a $17\ \Omega$ system is ideally matched at both the input and output. Thus there are no reflections and the power delivered to the load is reduced by $20\ \text{dB}$ from the applied power. If a $5\ \text{W}$ signal is applied to the attenuator, how much power is dissipated in the attenuator?
- A resistive Pi attenuator has shunt resistors of $R_1 = R_2 = 294\ \Omega$ and a series resistor $R_3 = 17.4\ \Omega$. What is the attenuation (in decibels) and the characteristic impedance of the attenuator?
- A resistive Pi attenuator in a system with characteristic impedance Z_0 has equal shunt resistors of $R_1 = R_2$ and a series resistor R_3 . Show that $Z_0 = \sqrt{(R_1^2 R_3)/(2R_1 + R_3)}$ and the attenuation factor $K = \sqrt{(R_1 + Z_0)/(R_1 - Z_0)}$. [Start with Equation (5.15).]
- Design a resistive Pi attenuator with an attenuation of $10\ \text{dB}$ in a $100\ \Omega$ system.
- Design a $3\ \text{dB}$ resistive Pi attenuator in a $50\ \Omega$ system.
- A resistive Pi attenuator has shunt resistors $R_1 = R_2 = 86.4\ \Omega$ and a series resistor $R_3 = 350\ \Omega$. What is the attenuation (in decibels) and the system impedance of the attenuator?
- Derive the $50\ \Omega$ scattering parameters of the ideal transformer shown below where the number of windings on the secondary side (Port 2) is twice the number of windings on the primary side (Port 1).



- What is S_{11} ? [Hint: Terminate Port 2 in $50\ \Omega$ and determine the input reflection coefficient.]
- What is S_{21} ?
- What is S_{22} ?
- What is S_{12} ?

- Derive the two-port $50\ \Omega$ scattering parameters of the magnetic transformer below. The primary (Port 1) has 10 turns, the secondary (Port 2) has 25 turns.



- What is S_{11} ?
- What is S_{21} ?
- What is S_{22} ?
- What is S_{12} ?

- An ideal quadrature hybrid has the scattering parameters

$$S_{90^\circ} = \frac{1}{\sqrt{2}} \begin{bmatrix} 0 & -j & 1 & 0 \\ -j & 0 & 0 & 1 \\ 1 & 0 & 0 & -j \\ 0 & 1 & -j & 0 \end{bmatrix}.$$

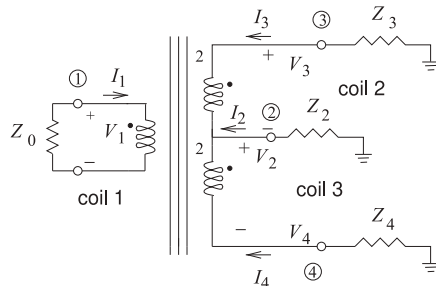
Draw the signal flow graph of the hybrid, labeling each of the edges and assigning a_1, b_1 , etc., to the nodes. (Do not start with the SFG of a generic 4-port network.)

14. An ideal 180° hybrid has the scattering parameters

$$S_{180^\circ} = \frac{1}{\sqrt{2}} \begin{bmatrix} 0 & 1 & -1 & 0 \\ 1 & 0 & 0 & 1 \\ -1 & 0 & 0 & 1 \\ 0 & 1 & 1 & 0 \end{bmatrix}.$$

Draw the signal flow graph of the hybrid, labeling each of the edges and assigning a_1, b_1 , etc., to the nodes. (Note, do not start with the SFG of a generic 4-port network.)

15. A signal is applied to Ports 2 and 3 of a 180° hybrid, as shown in Figure 5-20(b). If the signal consists of a differential component of 0 dBm and a common mode component of 10 dBm:
- Determine the power delivered at Port 1.
 - Determine the power delivered at Port 4. Assume that the hybrid is lossless.
16. Silicon RFICs use differential signal paths to minimize the introduction of substrate noise. As well, differential amplifiers are an optimum topology in current-biased circuits. Off-chip signals are often on microstrip lines and so the source and load, being off-chip, are not differential. The off-chip circuits are then called single-ended. Using 180° hybrids, diagrams, and explanations, outline a system architecture accommodating this mixed differential and single-ended environment.
17. Consider the hybrid shown in the figure below. If the number of windings of Coils 2 and 3 are twice the number of windings of Coil 1, show that for matched hybrid operation $2Z_2 = Z_3 = 8Z_0$.



18. The balun of Figure 5-23 transforms an unbalanced system with a system impedance of Z_0 to a balanced system with an impedance of $4Z_0$. The actual impedance transformation is determined by the number of windings of the coils.

Design a balun of the type shown in Figure 5-23 that transforms an unbalanced 50Ω system to a balanced 377Ω system. [Hint: Find the ratio of the windings of the coils.]

19. A balun can be realized using a wire-wound transformer, and by changing the number of windings on the transformer it is possible to achieve impedance transformation as well as balanced-to-unbalanced functionality. A 500 MHz balun based on a magnetic transformer is required to achieve impedance transformation from an unbalanced impedance of 50Ω to a balanced impedance of 200Ω . If there are 20 windings on the balanced port of the balun transformer, how many windings are there on the unbalanced port of the balun?
20. Design a lumped-element two-way power splitter in a 75Ω system at 1 GHz. Base your design on a Wilkinson power divider.
21. Design a three-way power splitter in a 75Ω system. Base your design on a Wilkinson power divider using transmission lines and indicate lengths in terms of wavelengths.
22. Design a lumped-element three-way power splitter in a 75Ω system at 1 GHz. Base your design on a Wilkinson power divider.
23. A resistive power splitter is a three-port device that takes power input at Port 1 and delivers power at Ports 2 and 3 that are equal; that is, $S_{21} = S_{31}$. However, the sum of the power at Ports 2 and 3 will not be equal to the input power due to loss. Design a 75Ω resistive three-port power splitter with matched inputs, $S_{11} = 0 = S_{22} = S_{33}$. That is, draw the resistive circuit and calculate its element values.
24. Design a balun based on a magnetic transformer if the balanced load is 300Ω and the unbalanced impedance is 50Ω .
- Draw the schematic of the balun with the load and indicate the ratio of windings.
 - If the number of windings on the unbalanced side of the transformer is 20, how many windings are on the unbalanced side?
25. Develop the electrical design of a rat-race hybrid at 30 GHz in a 50Ω system.
26. Develop the electrical design of a rat-race hybrid at 30 GHz in a 100Ω system.
27. Design a lumped-element 180° hybrid at 1900 MHz using 1 nH inductors.
28. Design a 90° lumped-element hybrid at 1900 MHz using 1 nH inductors.
29. Design a 90° lumped-element hybrid at 500 MHz for a 75Ω system.

30. Design a lumped-element 180° hybrid at 1900 MHz matched to $50\ \Omega$ source and load impedances.

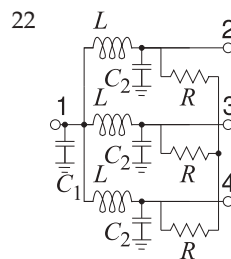
5.16.1 Exercises by Section

[†]challenging, [‡]very challenging

- | | | |
|--|--|--|
| §5.1 1 | §5.8 11 [†] , 12 [†] | §5.11 20 [†] , 21 [†] , 22 [†] |
| §5.2 2, 3, 4, 5 | §5.9 13 [†] , 14 [†] , 15 [†] , 16 [†] , 17 [‡] | §5.12 23 [†] |
| §5.5 6 [†] , 7 [†] , 8, 9, 10 [†] | §5.10 18 [†] , 19 [†] | §5.13 24 [‡] , 25 [†] , 26 [†] , 27, 28, 29, 30 |

5.16.2 Answers to Selected Exercises

- 2 12.57
 3 $R_1=R_2=74.5\ \Omega$
 4 $75.48\ \Omega$
 5 4.95 W
 11(c) 0.6
 12 -0.6897
 15 10 dBm



- $L=20.7\ \text{nH}$, $C_1=3.68\ \text{pF}$
 $C_2=1.23\ \text{pF}$, $R=75\ \Omega$
 24 ratio of windings is 2.45
 30 Fig. 5-41(a)
 $L=5.92\ \text{nH}$, $C=1.19\ \text{pF}$

Impedance Matching

6.1	Introduction	159
6.2	Matching Networks	159
6.3	Impedance Transforming Networks	162
6.4	The L Matching Network	164
6.5	Dealing with Complex Loads	168
6.6	Multielement Matching	171
6.7	Impedance Matching Using Smith Charts	179
6.8	Distributed Matching	183
6.9	Matching Using the Smith Chart	187
6.10	Summary	197
6.11	References	198
6.12	Exercises	198

6.1 Introduction

The maximum transfer of signal power is one of the prime objectives in RF and microwave circuit design. Power traverses a network from a source to a load generally through a sequence of two-port networks. Maximum power transfer requires that the Thevenin equivalent impedance of a source be matched to the impedance seen from the source. That is, the source should be presented with the complex conjugate of the source impedance. This is achieved by designing what is called a matching network inserted between the source and load. As long as the load has some nonzero real part (and so can dissipate power), a matching network can always be found. Design of the matching network is called impedance matching.

Section 6.2 describes two common matching objectives. Then design approaches for impedance matching are presented first with an algorithmic approach in Sections 6.3–6.6 and then a graphical approach based on using a Smith chart in Sections 6.7–6.9.

6.2 Matching Networks

Matching networks are constructed using lossless elements such as lumped capacitors, lumped inductors and transmission lines and so have, ideally, no loss and introduce no additional noise. This section discusses matching objectives and the types of matching networks.

Figure 6-1: A source with Thevenin equivalent impedance Z_S and load with impedance Z_L interfaced by a matching network presenting an impedance Z_{in} to the source.

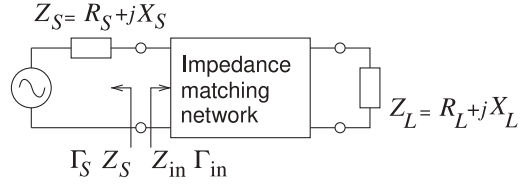


Table 6-1: Matching conditions with reference to Figure 6-1. Γ_{in} , Γ_S , must be with respect to a real Z_{REF} .

Reflection-less match	Maximum power transfer
$Z_{in} = Z_S$	$Z_{in} = Z_S^*$ $\Gamma_{in} = \Gamma_S^*$

6.2.1 Matching for Zero Reflection or for Maximum Power Transfer

With RF circuits the aim of matching is to achieve maximum power transfer. With reference to Figure 6-1 the condition for maximum power transfer is $Z_{in} = Z_S^*$ (see Section 2.6.2 of [1]). An alternative matching objective, used most commonly with digital circuits, is a reflection-less match. The reflection-less match and the maximum power transfer match are only equivalent if Z_S and Z_L are real. Nearly always in RF design the matching objective is maximum power transfer, and this is assumed unless the reflection-less match is specifically indicated.

The maximum power transfer matching condition can also be specified in terms of reflection coefficients with respect to an real reference impedance Z_{REF} . (In the definition of reflection coefficient Z_{REF} can be complex, but many of the manipulations in this book only apply when Z_{REF} is real and this should be assumed unless it is specifically stated that it can be complex.) The condition for maximum power transfer is $Z_{in} = Z_S^*$ which is equivalent to $\Gamma_{in} = \Gamma_S^*$. The proof is as follows:

$$\Gamma_{in} = \left(\frac{Z_{in} - Z_{REF}}{Z_{in} + Z_{REF}} \right), \quad (6.1)$$

and for maximum power transfer $Z_{in} = Z_S^*$, so

$$\begin{aligned} \Gamma_{in}^* &= \frac{Z_{in} - Z_{REF}}{Z_{in} + Z_{REF}} = \left(\frac{Z_S^* - Z_{REF}}{Z_S^* + Z_{REF}} \right)^* = \frac{(Z_S^* - Z_0)^*}{(Z_S^* + Z_0)^*} \\ &= \frac{(Z_S^*)^* - Z_{REF}^*}{(Z_S^*)^* + Z_{REF}^*} = \frac{Z_S - Z_{REF}^*}{Z_S + Z_{REF}^*} = \Gamma_S. \end{aligned} \quad (6.2)$$

If Z_{REF} is real, $Z_{REF}^* = Z_{REF}$ and then the condition for maximum power transfer is

$$\Gamma_{in}^* = \frac{Z_S - Z_{REF}}{Z_S + Z_{REF}} = \Gamma_S. \quad (6.3)$$

Thus, provided that Z_{REF} is real, the condition for maximum power transfer in terms of reflection coefficients is $\Gamma_{in}^* = \Gamma_S$ or $\Gamma_{in} = \Gamma_S^*$. The matching conditions are summarized in Table 6-1.

6.2.2 Types of Matching Networks

Up to a few gigahertz, lumped inductors and capacitors can be used in matching networks. Above a few gigahertz, distributed parasitics (losses

and additional capacitive or inductive effects) can render lumped-element networks impractical. Inductors in particular have high loss and high parasitic capacitances at microwave frequencies. Lumped capacitors are useful circuit elements at much higher frequencies than are lumped inductors. Segments of transmission lines are used in matching networks and are used instead of lumped elements when loss must be kept to a minimum, power levels are high, or the parasitics of lumped elements render them unusable. This is because the loss of an appropriate transmission line component is always much less than the loss of a lumped inductor.

Many factors affect the selection of the components of a matching network. The most important of these are size, complexity, bandwidth, and adjustability. The impact on a circuit of a distributed element is directly related to its length compared to one-quarter of a wavelength ($\lambda/4$). At 1 GHz a circuit board, for example, with a relative permittivity of 4 has $\lambda/4 = 3.75$ cm. This is far too large to fit in consumer wireless products operating at 1 GHz.

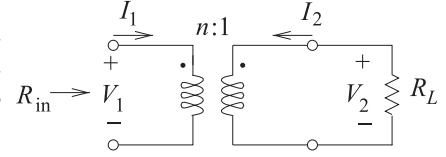
Performance of lumped-element capacitors and inductors refers to both the self-resonant frequency of an element and its loss. Inductors are a particular case in point. An actual inductor must be modeled using capacitive elements, capturing inter-winding capacitance as well as the primary inductive element. At some frequency the inductive and capacitive elements will resonate and this is called the self-resonant frequency of the element. The self-resonant frequency is the maximum operating frequency of the element. With regards to complexity, the simplest matching network design is most often preferred. A simpler matching network is usually more reliable, less lossy, and cheaper than a complex design. The pursuit of small size and/or higher bandwidth, however, may necessitate that the simplest circuit not be selected. Any type of matching network can ideally give, ignoring resistive losses, a perfect match at a single frequency. Away from this center frequency the match will not be ideal. From experience, achieving a reasonable match over a 5% fractional bandwidth based on a single-frequency match can usually be achieved with simple matching networks..

An impedance matching network may consist of

- (a) Lumped elements only. These are the smallest networks, but have the most stringent limit on the maximum frequency of operation. The relatively high resistive loss of an inductor is the main limiting factor limiting performance. The self resonant frequency of an inductor limits operation to low microwave frequencies.
- (b) Distributed elements (microstrip or other transmission line circuits) only. These have excellent performance, but their size restricts their use in systems to above a few gigahertz.
- (c) A hybrid design combining lumped and distributed elements, primarily small sections of lines with capacitors. These lines are shorter than in a design with distributed elements only, but the hybrid design has higher performance than a lumped-element-only design.
- (d) Adhoc solutions (suggested by input impedance behavior and features of various components).

This chapter concentrates on matching network design. One emphasis here is on the development of design equations and synthesis of desired results. The second emphasis is on graphical techniques for matching network design based on using A Smith chart. This is particularly powerful as it enables

Figure 6-2: A transformer as a matching network. Port 1 is on the left or primary side and Port 2 is on the right or secondary side.



typologies to traded-off. An alternative design approach used by some designers is to choose a circuit topology and then use a circuit optimizer to arrive at circuit values that yield the desired characteristics. This is sometimes a satisfactory design technique, but is not a good solution for new designs as it does not provide insight and does not help in choosing new topologies.

6.2.3 Summary

There are many design choices in the type of matching network to be developed but the common guidelines are to minimize losses and to keep the matching network compact. These objectives are not always compatible. Matching network design in this chapter is based on perfect matching at one frequency and design decisions are made to maximize, or otherwise manipulate, the bandwidth of the match. True broadband matching network design is more like filter design.

6.3 Impedance Transforming Networks

Transformers and reactive elements considered in this section can be used to losslessly transform impedance levels. This is a basic aspect of network design.

6.3.1 The Ideal Transformer

The ideal transformer shown in Figure 6-2 can be used to match a load to a source if the source and load impedances are resistances. This will be shown by starting with the constitutive relations of the transformer:

$$V_1 = nV_2 \quad \text{and} \quad I_1 = -I_2/n. \quad (6.4)$$

Here n is the transformer ratio. For a wire-wound transformer, n is the ratio of the number of windings on the primary side, Port 1, to the number of windings on the secondary side, Port 2. Thus the input resistance, R_{in} , is related to the load resistance, R_L , by

$$R_{in} = \frac{V_1}{I_1} = -n^2 \frac{V_2}{I_2} = n^2 R_L. \quad (6.5)$$

The matching problem with purely resistive load and source impedances is solved by choosing the appropriate winding ratio, n . However, resistive-only problems are rare at RF, and so other matching circuits must be used.

6.3.2 A Series Reactive Element

Matching using lumped elements is based on the impedance and admittance transforming properties of series and shunt reactive elements. Even a single reactive element can achieve limited impedance matching. Consider the series reactive element shown in Figure 6-3(a). Here the reactive element, X_S ,

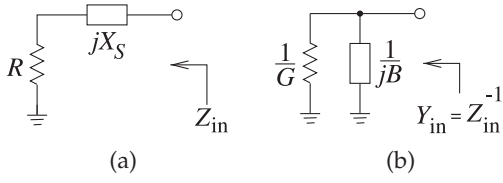


Figure 6-3: Matching using a series reactance: (a) the series reactive element; and (b) its equivalent shunt circuit.

is in series with a resistance R . The shunt equivalent of this network is shown in Figure 6-3(b) with a shunt susceptance of B . In this transformation the resistance R has been converted to a resistance $R_P = 1/G$. The mathematics describing this transformation is as follows. The input admittance of the series connection (Figure 6-3(a)) is

$$Y_{in}(\omega) = \frac{1}{Z_{in}(\omega)} = \frac{1}{R + jX_S} = \frac{R}{R^2 + X_S^2} - j\frac{X_S}{R^2 + X_S^2}. \quad (6.6)$$

Thus the elements of the equivalent shunt network, Figure 6-3(b), are

$$G = \frac{R}{R^2 + X_S^2} \quad \text{and} \quad B = -\frac{X_S}{R^2 + X_S^2}. \quad (6.7)$$

The “resistance” of the network, R , has been transformed to a new value,

$$R_P = G^{-1} = \frac{R^2 + X_S^2}{R} > R. \quad (6.8)$$

This is an important start to matching, as X_S can be chosen to convert R (a load, for example) to any desired resistance value (such as the resistance of a source). However there is still a residual reactance that must be removed to complete the matching network design. Before moving on to the solution of this problem consider the following example.

EXAMPLE 6.1 Capacitive Impedance Transformation

Consider the impedance transforming properties of the capacitive series element in Figure 6-4(a). Show that the capacitor can be adjusted to obtain any positive shunt resistance.

Solution:

The concept here is that the series resistor and capacitor network has an equivalent shunt circuit that includes a capacitor and a resistor. By adjusting C_S any value can be obtained for R_P . From Equation (6.8),

$$R_P = \frac{R_0^2 + (1/\omega^2 C_S^2)}{R_0} = \frac{1 + \omega^2 C_S^2 R_0^2}{\omega^2 C_S^2 R_0} \quad (6.9)$$

$$\text{and the susceptance is } B = \frac{(1/\omega C_S)}{R_0^2 + 1/\omega^2 C_S^2} = \omega \frac{C_S}{1 + \omega^2 C_S^2 R_0^2}. \quad (6.10)$$

$$\text{Thus } C_P = \frac{B}{\omega} = \frac{C_S}{1 + \omega^2 C_S^2 R_0^2}. \quad (6.11)$$

To match R_0 to a resistive load $R_P (> R_0)$ at a radian frequency ω_d , then, from Equation (6.9), the series capacitance required, i.e. the design equation for C_S , comes from

$$\omega_d C_S = 1/\sqrt{R_0 R_P - R_0^2}, \quad (6.12)$$

To complete the matching design, use a shunt inductor L , as shown in Figure 6-4(c), where $\omega_d C_P = 1/(\omega_d L)$. The equivalent impedance in Figure 6-4(c) is a resistor of value R_P , with a value that can be adjusted by choosing C_S which then requires L to be adjusted.

Figure 6-4: Impedance transformation by a series reactive element: (a) a resistor with a series capacitor; (b) its equivalent shunt circuit; and (c) an LC network.

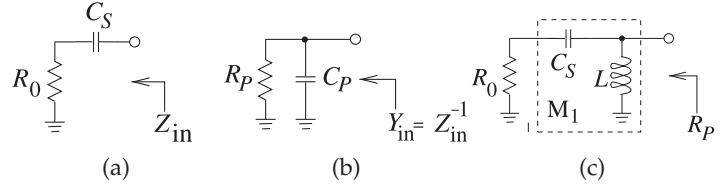
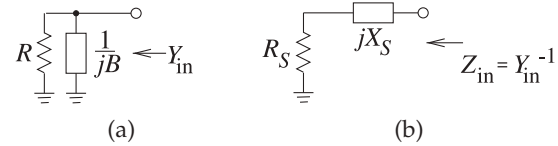


Figure 6-5: A resistor with (a) a shunt parallel reactive element where B is a susceptance, and (b) its equivalent series circuit.



6.3.3 A Parallel Reactive Element

The dual of the series matching procedure is the use of a parallel reactive element, as shown in Figure 6-5(a). The input admittance of the shunt circuit

$$Y_{in} = \frac{1}{R} + jB. \quad (6.13)$$

This can be converted to a series circuit by calculating $Z_{in} = 1/Y_{in}$:

$$Z_{in} = \frac{R}{1 + jBR} = \frac{R}{1 + B^2R^2} - j\frac{BR^2}{1 + B^2R^2}. \quad (6.14)$$

$$\text{So } R_S = \frac{R}{1 + B^2R^2} \text{ and } X_S = \frac{-BR^2}{1 + B^2R^2}. \quad (6.15)$$

Notice that $R_S < R$.

EXAMPLE 6.2

Parallel Tuning

As an example of the use of a parallel reactive element to tune a resistance value, consider the circuit in Figure 6-6(a) where a capacitor tunes the effective resistance value so that the series equivalent circuit (Figure 6-6(b)) has elements

$$R_S = \frac{R_0}{1 + \omega^2 C_P^2 R_0^2} \text{ and } X_S = -\frac{\omega C_P R_0^2}{1 + \omega^2 C_P^2 R_0^2} = -\frac{1}{\omega C_S}. \quad (6.16)$$

$$\text{So } C_S = \frac{1 + \omega^2 C_P^2 R_0^2}{\omega^2 C_P R_0^2}. \quad (6.17)$$

Now consider matching R_0 to a resistive load R_S , which is less than R_0 at a given frequency ω_d . This requires that

$$\omega_d C_P = \sqrt{1/(R_S R_0) - 1/R_0^2}.$$

To complete the design, use a series inductor to remove the reactive effect of the capacitor, as shown in Figure 6-6(C). The value of the inductor required is found from

$$\omega_d L = \frac{1}{\omega_d C_S}, \text{ that is, } L = \frac{1}{\omega_d^2 C_S}. \quad (6.18)$$

6.4 The L Matching Network

The examples in the previous two sections suggest the basic concept behind lossless matching of two different resistance levels using an L network:

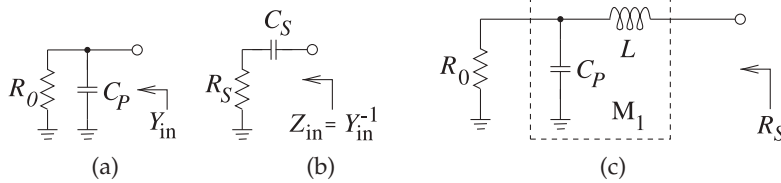


Figure 6-6: Parallel-to-series transformation: (a) resistor with shunt capacitor; (b) its equivalent series circuit; and (c) the transforming circuit with added series inductor.

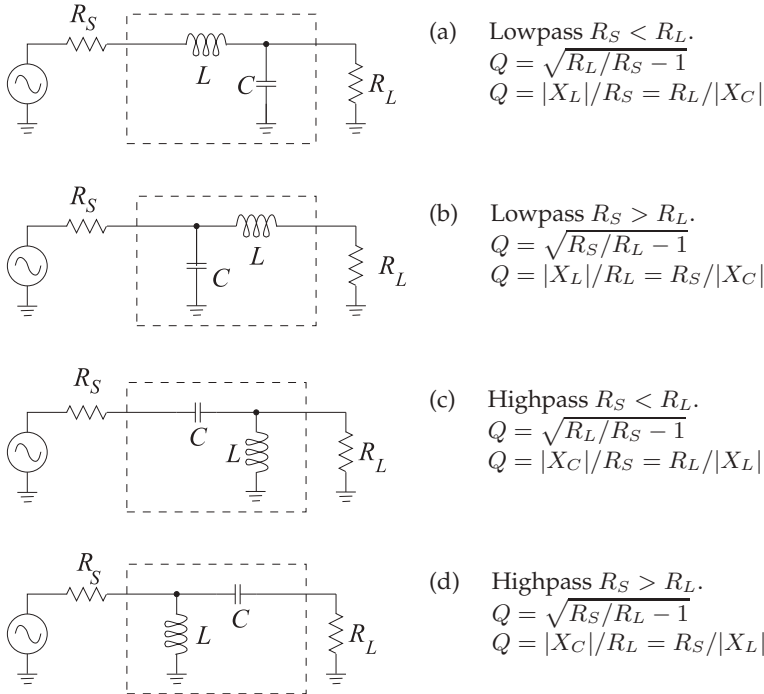


Figure 6-7: L matching networks consisting of one shunt reactive element and one series reactive element. (R_S is matched to R_L .) X_C is the reactance of the capacitor C , and X_L is the reactance of the inductor L . Note that with a two-element matching network the Q and thus bandwidth of the match is fixed.

Step 1: Use a series (shunt) reactive element to transform a smaller (larger) resistance up (down) to a larger (smaller) value with a real part equal to the desired resistance value.

Step 2: Use a shunt (series) reactive element to resonate with (or cancel) the imaginary part of the impedance that results from Step 1.

So a resistance can be transformed to any resistive value by using an LC transforming circuit.

Formalizing the matching approach described above, note that there are four possible two-element L matching networks (see Figure 6-7). The two possible cases, $R_S < R_L$ and $R_L < R_S$, will be considered in the following subsections.

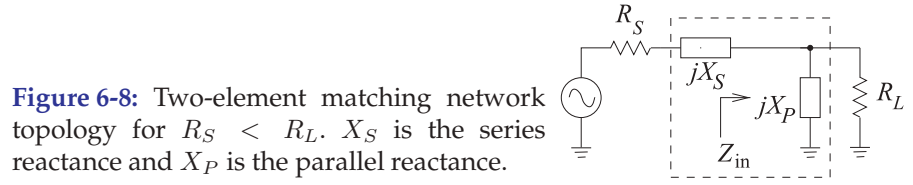


Figure 6-8: Two-element matching network topology for $R_S < R_L$. X_S is the series reactance and X_P is the parallel reactance.

6.4.1 Design Equations for $R_S < R_L$

Consider the matching network topology of Figure 6-8. Here

$$Z_{in} = \frac{R_L(jX_P)}{R_L + jX_P} = \frac{R_L X_P^2}{R_L^2 + X_P^2} + j \frac{X_P R_L^2}{R_L^2 + X_P^2} \quad (6.19)$$

and the matching objective is $Z_{in} = R_S - jX_S$ so that

$$R_S = \frac{R_L X_P^2}{R_L^2 + X_P^2} \quad \text{and} \quad X_S = \frac{-X_P R_L^2}{X_P^2 + R_L^2}. \quad (6.20)$$

$$\text{From these} \quad \frac{R_S}{R_L} = \frac{1}{(R_L/X_P)^2 + 1} \quad \text{and} \quad -\frac{X_S}{R_S} = \frac{R_L}{X_P}. \quad (6.21)$$

Introducing the quantities

$$Q_S = \text{the } Q \text{ of the series leg} = |X_S/R_S| \quad (6.22)$$

$$Q_P = \text{the } Q \text{ of the shunt leg} = |R_L/X_P| \quad (6.23)$$

leads to the final design equations for $R_S < R_L$:

$$|Q_S| = |Q_P| = \sqrt{\frac{R_L}{R_S} - 1}. \quad (6.24)$$

The L matching network principle is that X_P and X_S will be either capacitive or inductive and they will have the opposite sign (i.e., the L matching network comprises one inductor and one capacitor). Also, once R_S and R_L are given, the Q of the network and thus bandwidth is defined; with the L network, the designer does not have a choice of circuit Q .

EXAMPLE 6.3

Matching Network Design

Design a circuit to match a $100 \, \Omega$ source to a $1700 \, \Omega$ load at $900 \, \text{MHz}$. Assume that a DC voltage must also be transferred from the source to the load.

Solution:

Here $R_S < R_L$, and so the topology of Figure 6-9(a) can be used and there are two versions, one with a series inductor and one with a series capacitor. The series inductor version (see Figure 6-9(b)) is chosen as this enables DC bias to be applied. From Equations (6.22)–(6.24) the design equations are

$$|Q_S| = |Q_P| = \sqrt{\frac{1700}{100} - 1} = \sqrt{16} = 4, \quad \frac{X_S}{R_S} = 4, \quad \text{and} \quad X_S = 4 \cdot 100 = 400. \quad (6.25)$$

This indicates that $\omega L = 400 \, \Omega$, and so the series element is

$$L = \frac{400}{2\pi \cdot 9 \cdot 10^8} = 70.7 \, \text{nH}. \quad (6.26)$$

For the shunt element next to the load, $|R_L/X_C| = 4$, and so

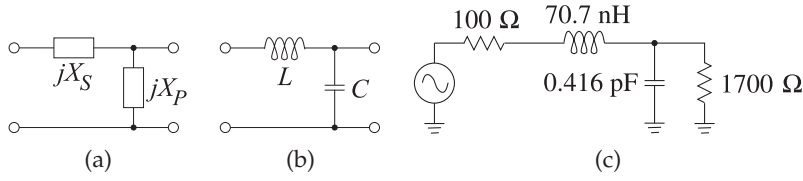


Figure 6-9: Matching network development for Example 6.3.

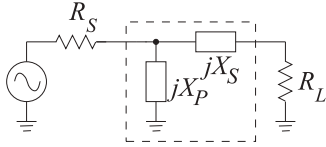


Figure 6-10: Two-element matching network topology for $R_S > R_L$.

$$|X_C| = \frac{R_L}{4} = \frac{1700}{4} = 425. \quad (6.27)$$

$$\text{Thus } 1/\omega C = 425 \text{ and } C = \frac{1}{2\pi \cdot 9 \cdot 10^8 \cdot 425} = 0.416 \text{ pF}. \quad (6.28)$$

The final matching network design is shown in Figure 6-9(c).

6.4.2 L Network Design for $R_S > R_L$

For $R_S > R_L$, the topology shown in Figure 6-10 is used. The design equations for the L network for $R_S > R_L$ are similarly derived and are

$$|Q_S| = |Q_P| = \sqrt{\frac{R_S}{R_L}} - 1 \quad (6.29)$$

$$-Q_S = Q_P, \quad Q_S = \frac{X_S}{R_L}, \quad \text{and} \quad Q_P = \frac{R_S}{X_P}. \quad (6.30)$$

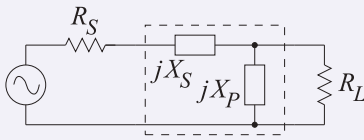
EXAMPLE 6.4

Two-Element Matching Network

Design a passive two-element matching network that will achieve maximum power transfer from a source with an impedance of 50Ω to a load with an impedance of 75Ω . Choose a matching network that will not allow DC to pass.

Solution:

$R_L > R_S$, so, from Figure 6-7, the appropriate matching network topology is



This topology can be either high pass or low pass depending on the choice of X_S and X_P . Design proceeds by finding the magnitudes of X_S and X_P . In two-element matching the circuit Q is fixed. With $R_L = 75 \Omega$ and $R_S = 50 \Omega$.

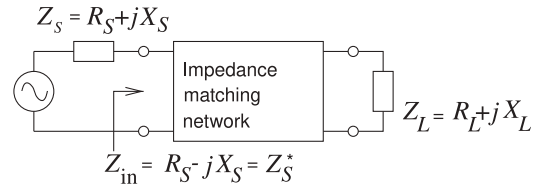
The Q of the matching network is the same for the series and parallel elements:

$$|Q_S| = \frac{|X_S|}{R_S} = \sqrt{\frac{R_L}{R_S}} - 1 = 0.7071 \quad \text{and} \quad |Q_P| = \frac{R_L}{|X_P|} = |Q_S| = 0.7071,$$

therefore $|X_S| = R_S \cdot |Q_S| = 50 \cdot 0.7071 = 35.35 \Omega$. Also

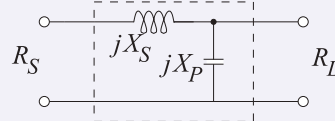
$$|X_P| = R_L / |Q_P| = 75 / 0.7071 = 106.1 \Omega.$$

Figure 6-11: A matching network matching a complex load to a source with a complex Thevenin impedance.



Specific element types can now be assigned to X_S and X_P , and note that they must be of opposite type.

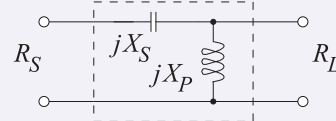
The lowpass matching network is



$$X_S = +35.35 \, \Omega, \quad X_P = -106.1 \, \Omega.$$

This highpass design satisfies the design criterion that DC is not passed, as DC is blocked by the series capacitor.

The highpass matching network is



$$X_S = -35.35 \, \Omega, \quad X_P = +106.1 \, \Omega.$$

6.5 Dealing with Complex Sources and Loads

This section presents strategies for dealing with complex loads. In the algorithmic matching approach design proceeds first by ignoring the complex load and source and then accounting for them either through topology choice or canceling their effect through resonance.

6.5.1 Matching

Input and output impedances of transistors, mixers, antennas, etc., contain both resistive and reactive components. Thus a realistic impedance matching problem looks like that shown in Figure 6-11. The matching approaches that were presented in the previous sections can be directly applied if X_S and X_L are treated as stray reactances that need to be either canceled or, ideally, used as part of the matching network. There are two basic approaches to handling complex impedances:

- Absorption:** Absorb source and load reactances into the impedance matching network itself. This is done through careful placement of each matching element such that capacitors are placed in parallel with source and load capacitances, and inductors in series with source and load inductances. The stray values are then subtracted from the L and C values for the matching network calculated on the basis of the resistive parts of Z_S and Z_L only. The new (smaller) values, L' and C' , constitute the elements of the matching network. Sometimes it is necessary to perform a series-to-parallel, or parallel-to-series, conversion of the source or load impedances so that the reactive elements are in the correct series or shunt arrangement for absorption.
- Resonance:** Resonate source and load reactances with an equal and opposite reactance at the frequency of interest.

The very presence of a reactance in a load indicates energy storage, and therefore bandwidth limiting of some kind. In the above approaches to handling a reactive load, the resonance approach could easily result in a

narrowband matching solution. The major problem in matching is often to obtain sufficient bandwidth. What is sufficient will vary depending on the application. To maximize bandwidth the general goal is to minimize the total energy storage. Roughly the total energy stored will be proportional to the sum of the magnitudes of the reactances in the circuit. Of course, the actual energy storage depends on the voltage and current levels, which will themselves vary in the circuit. A good approach leading to large bandwidths is to incorporate the load reactance into the matching network. Thus the choice of appropriate matching network topology is critical. However, if the source and load reactance value is larger than the calculated matching network element value, then absorption on its own cannot be used. In this situation resonance must be combined with absorption. Overall, the majority of impedance matching designs are based on some combination of resonance and absorption.

EXAMPLE 6.5 Matching Network Design Using Resonance

For the configuration shown in Figure 6-12, design an impedance matching network that will block the flow of DC current from the source to the load. The frequency of operation is 1 GHz. Design the matching network, neglecting the presence of the 10 pF capacitance at the load. Since $R_S = 50 \Omega < R_L = 500 \Omega$, and from Figure 6-7, consider the topologies of Figures 6-13(a) and 6-13(b). The design criterion of blocking flow of DC from the source to the load narrows the choice to the topology of Figure 6-13(b).

Solution:

$$\text{Step 1: } |Q_S| = \left| \frac{X_S}{R_S} \right| = |Q_P| = \left| \frac{R_L}{X_P} \right| = \sqrt{\frac{R_L}{R_S} - 1} = 3 \quad \text{and} \quad Q_P = \frac{R_L}{X_P}. \quad (6.31)$$

So $X_P = \omega L = R_L/Q_P = 500/3$. Reducing this gives

$$\omega L = \frac{500}{3}, \quad \text{and so} \quad L = \frac{500}{3 \times 2\pi \times 10^9} = 26.5 \text{ nH}. \quad (6.32)$$

Similarly $-X_S/R_S = 3$ and so

$$\frac{1/(\omega C)}{R_S} = 3 \quad \text{or} \quad C = \frac{1}{3\omega R_S} = \frac{1}{3 \times 2\pi \times 10^9 \times 50} = 1.06 \text{ pF}. \quad (6.33)$$

Step 2:

Resonate the 10 pF capacitor using an inductor in parallel:

$$(\omega L')^{-1} = \omega \times 10 \times 10^{-12} \quad (6.34)$$

$$L' = \frac{1}{\omega^2 10^{-11}} = \frac{1}{(2\pi)^2 10^{18} \times 10^{-11}} = 2.533 \text{ nH}. \quad (6.35)$$

Thus Figure 6-13(c) is the required matching network. Two inductors are in parallel and the circuit can be simplified to that shown in Figure 6-14, where

$$L_X = (26.5 \text{ nH} \parallel 2.533 \text{ nH}) = \frac{2.533 \times 26.5}{2.533 + 26.5} \text{ nH} = 2.312 \text{ nH}. \quad (6.36)$$

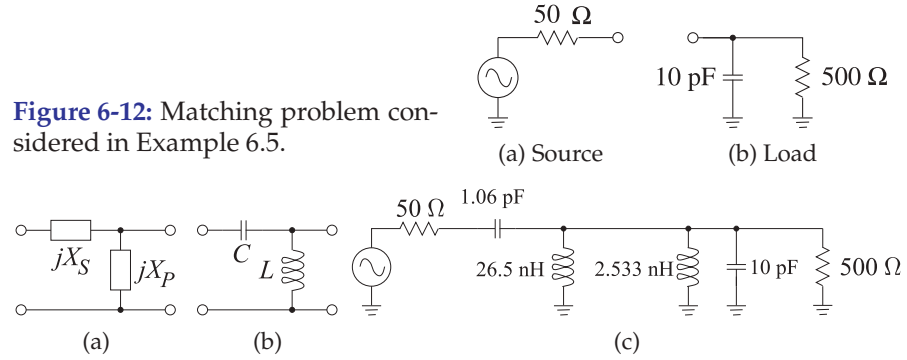


Figure 6-12: Matching problem considered in Example 6.5.

Figure 6-13: Matching network topology used in Example 6.5: (a) and (b) topology; and (c) intermediate matching network.

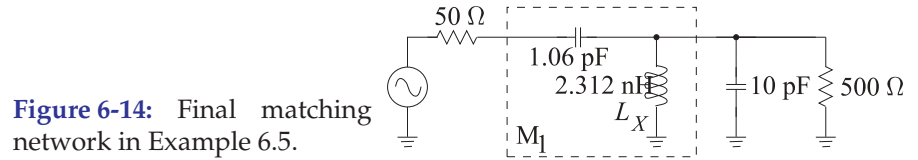


Figure 6-14: Final matching network in Example 6.5.

EXAMPLE 6.6

Matching Network Design Using Resonance and Absorption

For the source and load configurations shown in Figure 6-15, design a lowpass impedance matching network at $f = 1$ GHz.

Solution:

Since $R_S < R_L$, use the topology shown in Figure 6-16(a). For a lowpass response, the topology is that of Figure 6-16(b). Notice that absorption is the natural way of handling the 3 nH at the source and the 5 pF at the load. The design process is as follows:

Step 1:

Design the matching network, neglecting the reactive elements at the source and load:

$$|Q_S| = |Q_P| = \sqrt{\frac{R_L}{R_S}} - 1 = \sqrt{10 - 1} = 3 \quad (6.37)$$

$$\frac{X_S}{R_S} = 3, \quad X_S = 3 \times 100, \quad \omega L = 300 \quad \text{and} \quad L = \frac{300}{2\pi \times 10^9} = 47.75 \text{ nH} \quad (6.38)$$

$$\frac{R_P}{X_P} = -3 \quad \text{and} \quad \frac{1000}{-(1/\omega C)} = -3 \quad \text{and} \quad C = \frac{3}{1000 \times 2\pi \times 10^9} = 0.477 \text{ pF}. \quad (6.39)$$

This design is shown in Figure 6-17(a). This is the matching network that matches the 100 Ω source resistance to the 1000 Ω load with the source and load reactances ignored.

Step 2:

Figure 6-17(b) is the interim matching solution. The source inductance is absorbed into the matching network, reducing the required series inductance of the matching network. The capacitance of the load cannot be fully absorbed. The design for the resistance-only case requires a shunt capacitance of 0.477 pF, but 5 pF is available from the load. Thus there is an excess capacitance of 4.523 pF that must be resonated out by the inductance L'' :

$$\frac{1}{\omega L''} = \omega 4.523 \times 10^{-12}. \quad \text{So} \quad L'' = \frac{1}{(2\pi)^2 \times 10^{18} \times 4.523 \times 10^{-12}} = 5.600 \text{ nH}. \quad (6.40)$$

The final matching network design (Figure 6-17(c)) fully absorbs the source inductance into the matching network, but only partly absorbs the load capacitance.

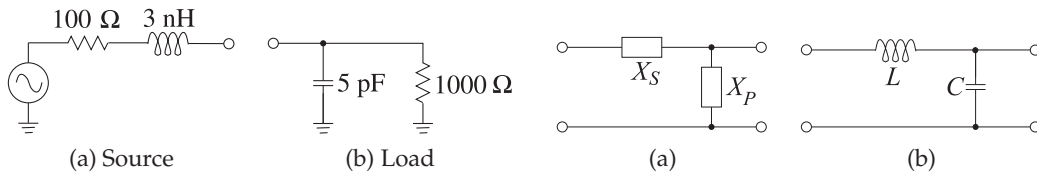


Figure 6-15: Matching problem in Example 6.6. **Figure 6-16:** Topologies referred to in Example 6.6.

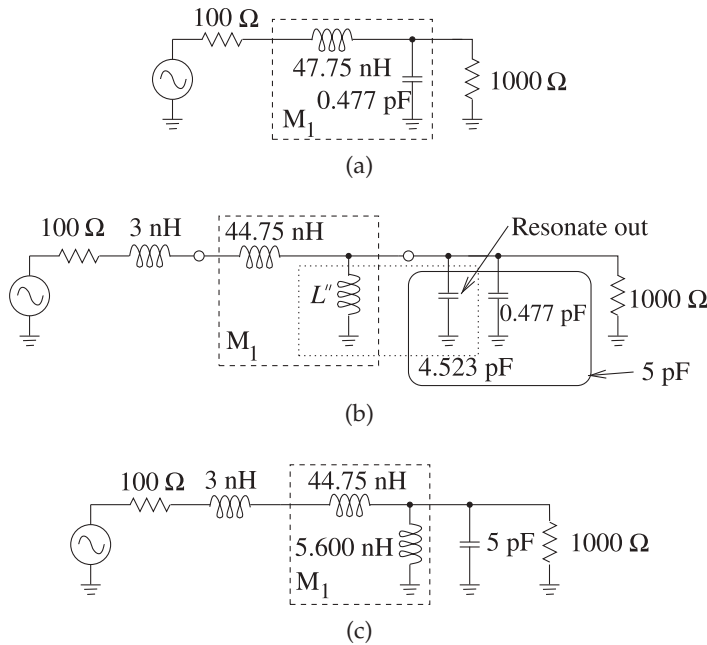


Figure 6-17: Evolution of the matching network in Example 6.6: (a) matching network design considering only the source and load resistors; (b) matching network with the reactive parts of the source and load impedances included; and (c) final design.

6.6 Multielement Matching

The bandwidth of a matching network can be controlled by using multiple matching stages either making the matching bandwidth wider or narrower. This concept is elaborated on in this and several design approaches presented.

6.6.1 Design Concept for Manipulating Bandwidth

The concept for manipulating matching network bandwidth is to do the matching in stages as shown in Figure 6-18. Figure 6-18(a) shows the one-stage matching problem using the common identification of the matching network as 'M'. The one-stage matching problem is repeated in Figure 6-18(b) without explicitly showing the source generator. A two-stage matching problem is shown in Figure 6-18(c) with the introduction of a virtual resistor R_V between the first, M_1 , and second, M_2 , stage matching networks. R_V is shown as a virtual connection as it is not actually inserted in the circuit. Instead this is a short-hand way of indicating the matching problem to be done in two stages as shown in Figure 6-18(d and e) with the first stage matching the source resistor R_S to R_V and the second stage matching R_V

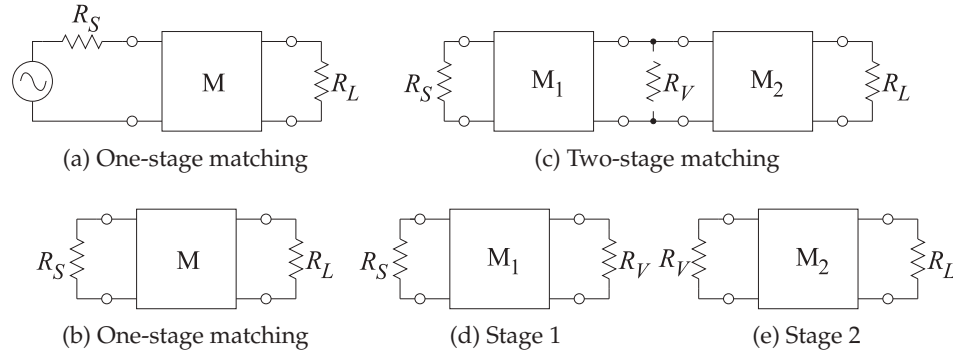


Figure 6-18: Matching in stages: (a) matching network M matching R_S to R_L ; (b) without an explicit source; (c) two-stage matching with a virtual resistor R_V ; (d) matching R_S to R_V ; and (e) matching R_V to R_L .

to the load resistor R_L . After M_1 has been designed the resistance looking into the right-hand port of M_1 , see Figure 6-18(d), will be R_V so R_V is the Thevenin equivalent source resistance to M_2 . Similarly the input impedance looking into the left-hand port of M_2 is R_V so R_V is the effective load resistor of M_1 . Of course these are the impedances at the center frequency and away from the center frequency of the match the input impedances will be complex.

The concept behind multi-stage matching network design is shown in Figure 6-19 where the standard one-stage match is shown in Figure 6-19(a). While this is shown for $R_L > R_S$ the concept holds for $R_L < R_S$. The arrows follow the convention that design begins with the load and ends at the source. With the one stage match the circuit Q is fixed designated here as the total circuit Q , Q_T being the same as the Q of the one-stage R_L to R_S matching network, Q_{SL} . The two-stage match that reduces bandwidth (compared to the one-stage match) is shown in Figure 6-19(b). The total Q , Q_T , of the second stage is higher than for the one-stage design because the ratio of R_L to R_V is greater than the ratio of R_V to R_S . Bandwidth can also be reduced relative to the one-stage match by assigning R_V to be greater than both R_L and R_S , see Figure 6-19(c).

Choosing R_V to be between R_S and R_L will result in a circuit with lower Q_T and the bandwidth of the match will increase, see Figure 6-19(d). The maximum bandwidth for a two-stage match is to choose R_V as the geometric mean of R_S and R_L . This concept can be extended to multiple stages as shown for a three-stage match in Figure 6-19(e).

This section presents various matching network designs for manipulating bandwidth and all are based on the concept of choosing a virtual resistor.

6.6.2 Three-Element Matching Networks

With the L network (i.e., two-element matching), the circuit Q is fixed once the source and load resistances, R_S and R_L , are fixed:

$$Q = \sqrt{\frac{R_L}{R_S}} - 1, \quad (R_L > R_S). \quad (6.41)$$

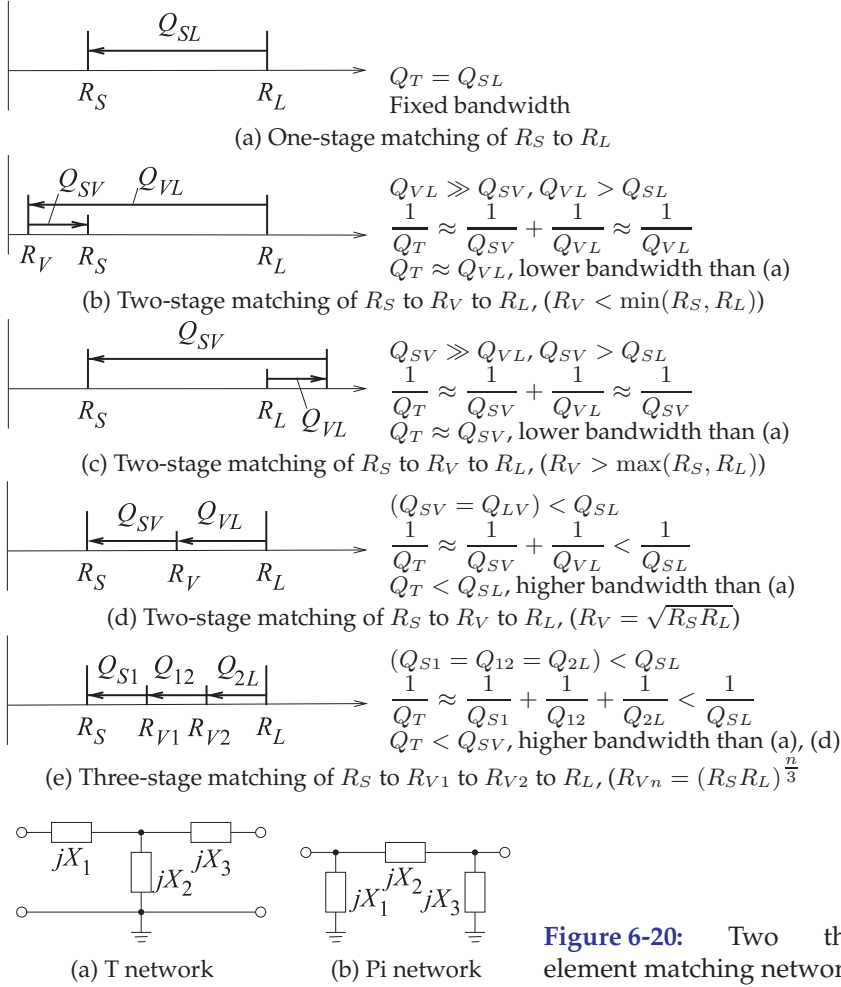


Figure 6-19: Effect of multi-stage matching on total circuit Q , Q_T , and matching bandwidth (which is approximately inversely proportional to Q_T .)

Figure 6-20: Two three-element matching networks.

Thus the designer does not have a choice of circuit Q . Breaking the matching problem into parts enables the circuit Q to be controlled. Introducing a third element in the matching network provides the extra degree of freedom in the design for adjusting Q , and hence bandwidth.

Two three-element matching networks, the T network and the Pi network, are shown in Figure 6-20. Which network is used depends on

- the realization constraints associated with the specific design, and
- the nature of the reactive parts of the source and load impedances and whether they can be used as part of the matching network.

The three-element matching network comprises 2 two-element (or L) matching networks and is used to increase the overall Q and thus narrow bandwidth. Given R_S and R_L , the circuit Q established by an L matching network is the minimum circuit Q available in the three-element matching arrangement. With three-element matching, the Q can only increase, so three-element matching is used for narrowband (high- Q) applications. However, lower Q can be obtained with more than three elements. The next subsections consider matching with more than three elements.

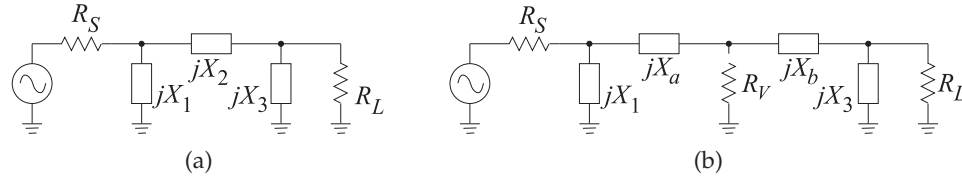


Figure 6-21: Pi matching networks: (a) view of a Pi network; and (b) as two back-to-back L networks with a virtual resistance, R_V , between the networks.

6.6.3 The Pi Network

The Pi network may be thought of as two back-to-back L networks that are used to match the load and the source to a virtual resistance, R_V , placed at the junction between the two networks, as shown in Figure 6-21(b). The design of each section of the Pi network is as for the L network matching. R_S is matched to R_V and R_V is matched to R_L .

R_V must be selected smaller than R_S and R_L since it is connected to the series arm of each L section. Furthermore, R_V can be any value that is smaller than the smaller of R_S, R_L . However, it is customarily used as the design parameter for specifying the desired Q .

As a useful design approximation, the loaded Q of the Pi network can be taken as the Q of the L section with the highest Q :

$$Q = \sqrt{\frac{\max(R_S, R_L)}{R_V}} - 1. \quad (6.42)$$

Given R_S, R_L , and Q , the above equation yields the value of R_V .

EXAMPLE 6.7

Three-Element Matching Network Design

Design a Pi network to match a 50Ω source to a 500Ω load. The desired Q is 10. A suitable matching network topology is shown in Figure 6-22 together with the virtual resistance, R_V , to be used in design.

Solution: $R_S = 50 \Omega$ and $R_L = 500 \Omega$ so $\max(R_S, R_L) = 500 \Omega$ and so the virtual resistor is

$$R_V = \frac{\max(R_S, R_L)}{Q^2 + 1} = \frac{500}{101} = 4.95 \Omega. \quad (6.43)$$

Design proceeds by separately designing the L networks to the left and right of R_V . For the L network on the left,

$$Q_{\text{left}} = \sqrt{\frac{50}{4.95}} - 1 = 3.017. \quad \text{so} \quad Q_{\text{left}} = \frac{|X_a|}{R_V} = \frac{R_S}{|X_1|} = 3.017, \quad (6.44)$$

Note that X_1 and X_a must be of opposite types (one is capacitive and the other is inductive). The left L network has elements

$$|X_a| = 14.933 \Omega \quad \text{and} \quad |X_1| = 16.6 \Omega. \quad (6.45)$$

For the L network on the right of R_V ,

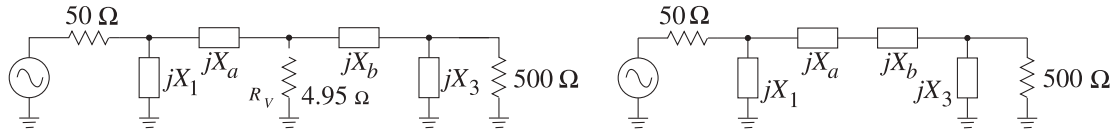


Figure 6-22: Matching network problem of Example 6.7.

Figure 6-23: Final matching network in Example 6.7.

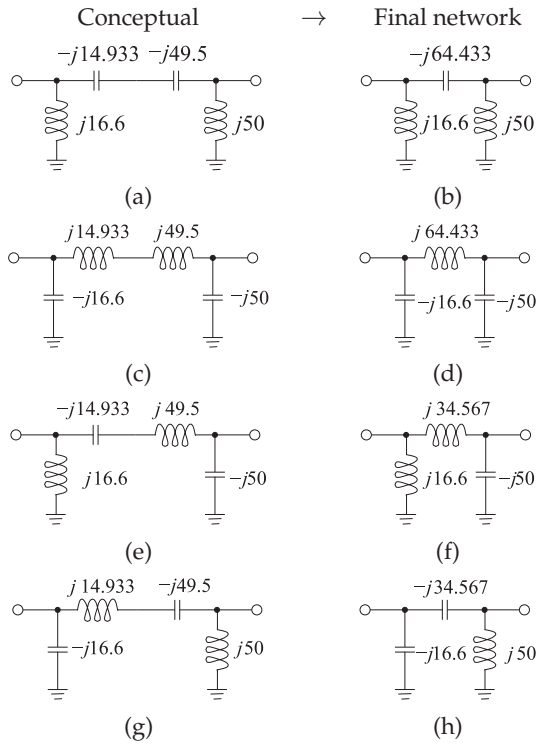


Figure 6-24: Four possible Pi matching networks: (a), (c), (e), and (g) conceptual circuits; and (b), (d), (f), and (h), respectively, their final reduced Pi networks.

$$Q_{\text{right}} = Q = 10, \quad \text{thus} \quad \frac{|X_b|}{R_V} = \frac{R_L}{X_3} = 10. \quad (6.46)$$

X_b , X_3 are of opposite types, and

$$|X_b| = 49.5 \, \Omega \quad \text{and} \quad |X_3| = 50 \, \Omega. \quad (6.47)$$

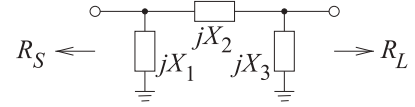
The resulting Pi network is shown in Figure 6-23 with the values

$$|X_1| = 16.6 \, \Omega, \quad |X_3| = 50 \, \Omega, \quad |X_a| = 14.933 \, \Omega, \quad \text{and} \quad |X_b| = 49.5 \, \Omega. \quad (6.48)$$

Note that the pair X_a , X_1 are of opposite types and similarly X_b , X_3 are of opposite types. So there are four possible realizations, as shown in Figure 6-24.

In the previous example there were four possible realizations of the three-element matching network, and this is true in general. The specific choice of one of the four possible realizations will depend on specific application-related factors such as

Figure 6-25: A three-element matching network.



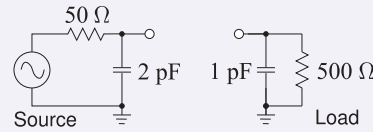
- (a) elimination of stray reactances,
- (b) the need to pass or block DC current, and
- (c) the need for harmonic filtering.

It is fortunate that it may be possible to achieve multiple functions with the same network.

EXAMPLE 6.8

Three-Element Matching with Reactive Source and Load

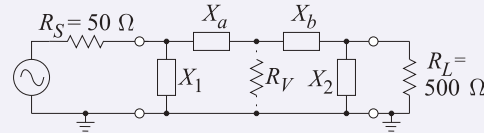
Design a Pi network to match the source to the load shown. The design frequency is 900 MHz and the desired Q is 10.



Solution:

The design objective is to arrive at an overall network which has a Q of 10. To achieve this it is necessary to absorb the source and load reactances into the matching network. If they were resonated instead, the overall Q of the network can be expected to higher than the Q of the L matching network on its own.

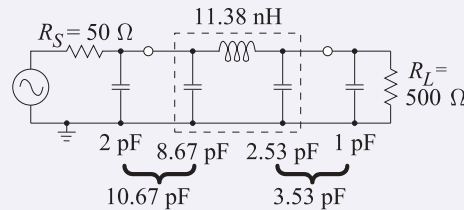
Design begins by considering the matching of $R_S = 50 \Omega$ to $R_L = 500 \Omega$. Since the Q is specified, three (or more) matching elements must be used. The design starting point is shown on the right:



The virtual resistor $R_V = \max(R_S, R_L)/(1 + Q^2) = (500 \Omega)/(1 + 100) = 4.95 \Omega$. The left subnetwork with X_1 and X_a has $Q_{\text{LEFT}} = \sqrt{R_S/R_V - 1} = \sqrt{50/4.95 - 1} = 3.017$. The right subnetwork with X_2 and X_b has $Q_{\text{RIGHT}} = \sqrt{R_L/R_V - 1} = \sqrt{500/4.95 - 1} = 10.001$.

Note that Q_{RIGHT} is almost exactly the desired Q of the network and Q_{LEFT} will have little effect on the Q of the overall circuit. Now $Q_{\text{LEFT}} = |X_a|/R_V = R_S/|X_1|$, so $|X_a| = 14.9 \Omega$ and $|X_1| = 16.57 \Omega$. $Q_{\text{RIGHT}} = |X_b|/R_V = R_S/|X_2|$, so $|X_b| = 49.5 \Omega$ and $|X_2| = 50.0 \Omega$.

X_1 must be chosen to be a capacitor $C_1 = 10.67 \text{ pF}$ so that the 2 pF source capacitance can be absorbed. Similarly X_2 is a capacitor $C_2 = 3.53 \text{ pF}$. X_a and X_b are both inductors that combine in series for a total inductance $L_3 = 11.38 \text{ nH}$. This leads to the final design shown on the right where the matching network is in the dashed box.



6.6.4 Matching Network Q Revisited

To demonstrate that the circuit Q established by an L matching network is the minimum circuit Q for a network having at most three elements, consider the design equations for $R_S > R_L$. Referring to Figure 6-25,

$$X_1 = \frac{R_S}{Q}, \quad X_3 = R_L \left(\frac{R_S/R_L}{Q^2 + 1 - R_S/R_L} \right)^{\frac{1}{2}}, \quad X_2 = \frac{QR_S + R_S R_L / X_3}{Q^2 + 1}. \quad (6.49)$$

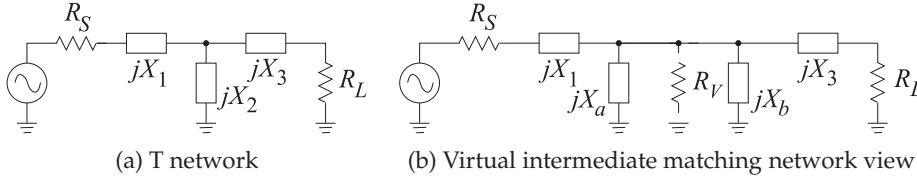


Figure 6-26:
T network
design
approach.

Notice that the denominator of X_3 can be written as

$$Q^2 + 1 - \frac{R_S}{R_L} = \left(Q + \sqrt{\frac{R_S}{R_L} - 1} \right) \left(Q - \sqrt{\frac{R_S}{R_L} - 1} \right). \quad (6.50)$$

Then for a real solution we must have

$$Q \geq \sqrt{\frac{R_S}{R_L} - 1}, \quad (6.51)$$

and so $Q \geq Q_{L \text{ network}}$. For $Q = Q_{L \text{ network}}$, $X_3 \rightarrow \infty$ and the Pi network reduces to an L network that has two elements. Thus it is not possible to have a lower Q with a three-element matching network than the Q of a two-element matching network. Thus a three-element matching network must have lower bandwidth than that of a two-element matching network.

6.6.5 The T Network

The T network may be thought of as two back-to-back L networks that are used to match the load and the source to a virtual resistance, R_V , placed at the junction between the two L networks (see Figure 6-26). R_V must be selected to be larger than both R_S and R_L since it is connected to the shunt leg of each L section. R_V is chosen according to the equation

$$Q = \sqrt{\frac{R_V}{\min(R_S, R_L)} - 1}, \quad (6.52)$$

where Q is the desired loaded Q of the network. Each L network is calculated in exactly the same manner as was done for the Pi network matching. That is, R_S is matched to R_V and R_V is matched to R_L . Once again there will be four possible designs for the T network, given R_S , R_L , and Q .

6.6.6 Broadband (Low Q) Matching

L network matching does not allow the circuit Q , and hence bandwidth, to be selected. However, Pi network and T network matching allows the circuit Q to be selected independent of the source and load impedances, provided that the chosen Q is larger than that which can be obtained with an L network. Thus the Pi and T networks result in narrower bandwidth designs.

One design solution for broadband matching is to use two (or more) series-connected L sections (see Figure 6-27). Design is still based on the concept of a virtual resistor, R_V , placed at the junction of the two L networks (as in Figure 6-28), but now R_V is chosen to be between R_S and R_L :

$$R_{\min} \leq R_V \leq R_{\max}, \quad (6.53)$$

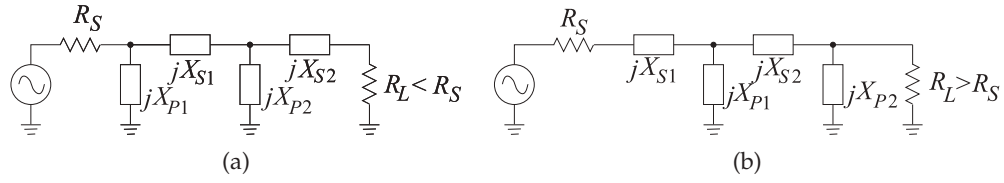


Figure 6-27: Broadband matching networks.

Figure 6-28: Matching network with two L networks.

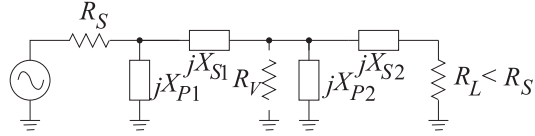
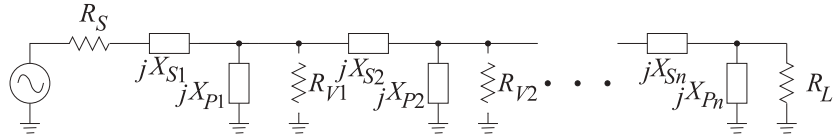


Figure 6-29: Cascaded L networks for broadband matching.



where $R_{\min} = \min(R_L, R_S)$ and $R_{\max} = \max(R_L, R_S)$. Then one of the two networks will have

$$Q_1 = \sqrt{\frac{R_V}{R_{\min}}} - 1 \quad \text{and the other} \quad Q_2 = \sqrt{\frac{R_{\max}}{R_V}} - 1. \quad (6.54)$$

The maximum bandwidth (minimum Q) available is obtained when

$$Q_1 = Q_2 = \sqrt{\frac{R_V}{R_{\min}}} - 1 = \sqrt{\frac{R_{\max}}{R_V}} - 1. \quad (6.55)$$

That is, the maximum matching bandwidth is obtained when R_V is the geometric mean of R_S and R_L :

$$R_V = \sqrt{R_L R_S}. \quad (6.56)$$

Even wider bandwidths can be obtained by cascading more than two L networks, as shown in Figure 6-29. In this circuit

$$R_S < R_{V1} < R_{V2} \dots < R_{Vn-1} < R_L. \quad (6.57)$$

For optimum bandwidth the ratios should be equal,

$$\frac{R_{V1}}{R_S} = \frac{R_{V2}}{R_{V1}} = \frac{R_{V3}}{R_{V2}} = \dots = \frac{R_L}{R_{Vn-1}}, \quad (6.58)$$

and the Q is given by

$$Q = \sqrt{\frac{R_{V1}}{R_S}} - 1 = \sqrt{\frac{R_{V2}}{R_{V1}}} - 1 = \dots = \sqrt{\frac{R_L}{R_{Vn-1}}} - 1. \quad (6.59)$$

If there are N L networks used in the match, the maximum bandwidth will be obtained if the i th virtual resistor is

$$R_{Vi} = (R_S R_L)^{i/N}, \quad i = 1, \dots, (N - 1). \quad (6.60)$$

EXAMPLE 6.9 Two-Section Matching Network Design

Consider matching a $10\ \Omega$ source to a $1000\ \Omega$ load using two L matching networks and designing for a Q of 3. How many matching sections are required?

Solution:

Here the approximate Q s achieved with a single L matching network and with an optimum two-section design are compared. For a single L network design

$$Q = \sqrt{\frac{R_L}{R_S} - 1} = 9.95. \quad (6.61)$$

Now consider an optimum two-section design:

$$R_V = \sqrt{R_S R_L}; \quad Q_2 = \sqrt{\frac{R_L}{R_V} - 1} = \sqrt{\sqrt{\frac{R_L}{R_S}} - 1} = 3. \quad (6.62)$$

Thus the Q is 3 compared to the Q of an L section of 9.95. If the fractional bandwidth is inversely proportional to Q , then the bandwidth of the two-section design is $9.95/3 = 3.32$ times more than that of the L section.

Now consider how many sections are required to obtain a Q of 2:

$$(1 + Q^2) = \frac{R_{V_1}}{R_S} = \frac{R_{V_2}}{R_{V_1}} = \dots = \frac{R_L}{R_{V_{n-1}}} \Rightarrow \quad (6.63)$$

$$(1 + Q^2)^n = \frac{R_L}{R_S} \Rightarrow n \ln(1 + Q^2) = \ln \frac{R_L}{R_S} \Rightarrow n = \frac{\ln(R_L/R_S)}{\ln(1 + Q^2)}. \quad (6.64)$$

For $Q = 2$ and $R_L/R_S = 100$, $n = 2.86$, which rounds to $n = 3$, and three sections are required.

6.7 Impedance Matching Using Smith Charts

The lumped-element matching networks presented up to now can also be developed using Smith charts which provide a fairly intuitive approach to network design. With experience it will be found that this is the preferred approach to developing designs, as trade-offs can be captured graphically. Smith chart-based design will be presented using examples.

6.7.1 Two-Element Matching

The examples here build on the preceding lumped-element matching network designs now using the Smith chart introduced in Chapter 3. Capacitive and inductive regions on the Smith chart are shown in Figure 6-30. In the design examples presented here, circles of constant resistance or constant conductance are followed and these correspond to varying reactance or susceptance, respectively.

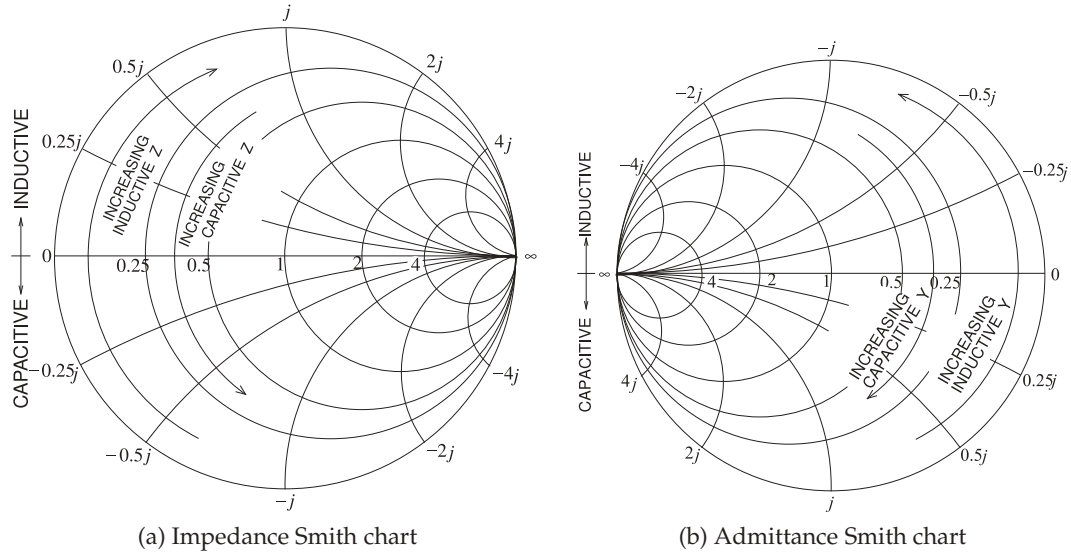


Figure 6-30: Inductive and capacitive regions on Smith charts. Increasing capacitive impedance (Z) indicates smaller capacitance; increasing inductive admittance (Y) indicates smaller inductance.

EXAMPLE 6.10

Two-Element Matching Network Design Using a Smith Chart

Develop a two-element matching network to match a source with an impedance of $R_S = 25 \Omega$ to a load $R_L = 200 \Omega$ (see Figure 6-31).

Solution:

The design objective is to present conjugate matched impedances to the source and load. However, since here the source and load impedances are real, the design objective is $Z_1 = R_S$ and $Z_2 = R_L$. The load and source resistances are plotted on the Smith chart in Figure 6-33(a) after choosing a normalization impedance of $Z_0 = 50 \Omega$ (and so $r_S = R_S/Z_0 = 0.5$ and $r_L = R_L/Z_0 = 4$). The normalized source impedance, r_S , is Point A, and the normalized load impedance, r_L , is Point C. The matching network must be lossless, which means that the design must follow lines of constant resistance (on the impedance part of the Smith chart) or constant conductance (on the admittance part of the Smith chart). So Points A and C must be on the above circles and the circles must intersect if a design is possible. The design can be viewed as moving back from the source toward the load or moving back from the load toward the source. (The views result in identical designs.) Here the view taken is moving back from the source toward the load.

One possible design is shown in Figure 6-33(a). From Point A, the line of constant resistance is followed to Point B (there is increasing series reactance along this path). From Point B, the locus follows a line of constant conductance to the final point, Point C. There is also an alternative design that follows the path shown in Figure 6-33(b). There are only two designs that have a path from A to B following just two arcs. At this point two designs have been outlined. The next step is assigning element values.

The design shown in Figure 6-33(a) begins with r_S followed by a series reactance, x_S , taking the locus from A to B. Then a shunt capacitive susceptance, b_P , takes the locus from B to C and r_L . At Point A the reactance $x_A = 0$, at Point B the reactance $x_B = 1.323$. This value is read off the Smith chart, requiring that an arc as shown be interpolated between the arcs provided. It should be noted that not all versions of Smith charts include negative signs, as the chart becomes too complicated. Thus the user needs to be aware and add signs where appropriate. The normalized series reactance is

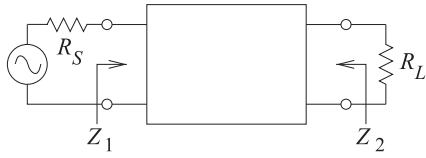


Figure 6-31: Design objectives for Example 6.10.
 $R_S = 25 \Omega$, $R_L = 200 \Omega$.

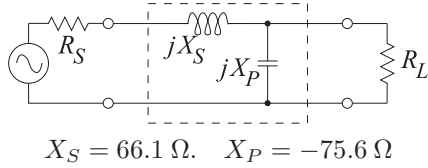


Figure 6-32: Final design for Example 6.10 using the path shown in Figure 6-33(a).

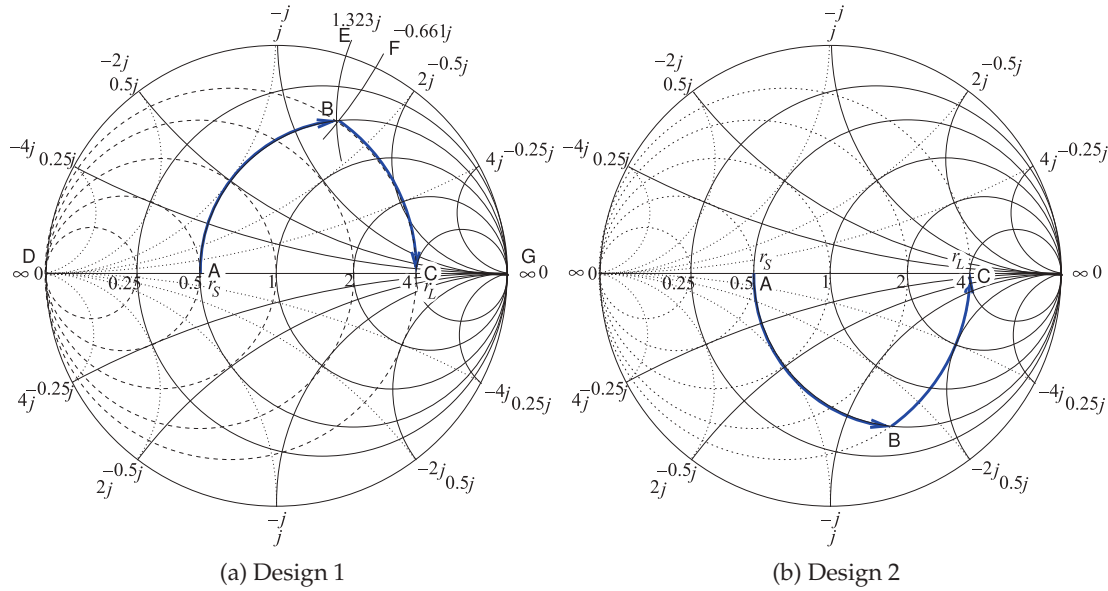


Figure 6-33: Alternative designs for Example 6.10. The normalization impedance is 50Ω .

$$x_S = x_B - x_A = 1.323 - 0 = 1.323, \quad (6.65)$$

that is,

$$X_S = x_S Z_0 = 1.323 \times 50 = 66.1 \Omega. \quad (6.66)$$

A shunt capacitive element takes the locus from Point B to Point C and

$$b_P = b_C - b_B = 0 - (-0.661) = 0.661, \quad (6.67)$$

$$\text{so } B_P = b_P / Z_0 = 0.661 / 50 = 13.22 \text{ mS} \quad \text{or} \quad X_P = -1 / B_P = -75.6 \Omega. \quad (6.68)$$

The final design is shown in Figure 6-32.

One of the advantages of using the Smith chart is that the design progresses in stages, with the structure of the design developed before actual numerical values are calculated. Of course, it is difficult to extract accurate values from a chart, so designs are regularly roughed out on a Smith chart and refined using CAD tools. Example 6.10 matched a resistive source to a resistive load. The next example considers the matching of complex load and source

impedances. In the earlier algorithmic approach to matching network design absorption and resonance were introduced as strategies for dealing with complex terminations. Design was not always straightforward. It will be seen that this complication disappears with a Smith chart-based design, as it is conceptually not much different from the resistive problem of Example 6.10.

EXAMPLE 6.11**Matching Network Design With Complex Impedances**

Develop a two-element matching network to match a source with an impedance of $Z_S = 12.5 + 12.5j \Omega$ to a load $Z_L = 50 - 50j \Omega$, as shown in Figure 6-34.

Solution:

The design objective is to present conjugate matched impedances to the source and load; that is, $Z_1 = Z_S^*$ and $Z_2 = Z_L^*$. The choice here is to design for Z_1 ; that is, elements will be inserted in front of Z_L to produce the impedance Z_1 . The normalized source and load impedances are plotted in Figure 6-35(a) using a normalization impedance of $Z_0 = 50 \Omega$, so $z_S = Z_S/Z_0 = 0.25 + 0.25j$ (Point S) and $z_L = Z_L/Z_0 = 1 - j$ (Point C).

The impedance to be synthesized is $z_1 = Z_1/Z_0 = z_S^* = 0.25 - 0.25j$ (Point A). The matching network must be lossless, which means that the lumped-element design must follow lines of constant resistance (on the impedance part of the Smith chart) or constant conductance (on the admittance part of the Smith chart). Points A and C must be on the above circles and the circles must intersect if a design is possible.

The design can be viewed as moving back from the load impedance toward the conjugate of the source impedance. The direction of the impedance locus is important. One possible design is shown in Figure 6-35(a). From Point C the line of constant conductance is followed to Point B (there is increasing positive [i.e., capacitive] shunt susceptance along this path). From Point B the locus follows a line of constant resistance to the final point, Point A.

The design shown in Figure 6-35(a) begins with a shunt susceptance, b_P , taking the locus from Point C to Point B and then a series inductive reactance, x_S , taking the locus to Point A. At Point C the susceptance $b_C = 0.5$, at Point B the susceptance $b_B = 1.323$. This value is read off the Smith chart, requiring that an arc of constant susceptance, as shown, be interpolated between the constant susceptance arcs provided. The normalized shunt susceptance is

$$b_P = b_B - b_C = 1.323 - 0.5 = 0.823, \quad (6.69)$$

$$\text{that is, } B_P = b_P/Z_0 = 0.823/(50 \Omega) = 16.5 \text{ mS or } X_P = -1/B_P = -60.8 \Omega. \quad (6.70)$$

A series reactive element takes the locus from Point B to Point A, so

$$x_S = x_A - x_B = -0.25 - (-0.661) = 0.411, \quad (6.71)$$

$$\text{so } X_S = x_S Z_0 = 0.411 \times 50 \Omega = 20.6 \Omega. \quad (6.72)$$

The final design is shown in Figure 6-36.

There are only two designs that have a path from Point C to Point A following just two arcs. In Design 1, shown in Figure 6-35(a), Path CBA is much shorter than Path CHA for Design 2 shown in Figure 6-35(b). The path length is an approximate indication of the total reactance required, and the higher the reactance, the greater the energy storage and hence the narrower the bandwidth of the design. (The actual relative bandwidth depends on the voltage and current levels in the network; the path length criteria, however, is an important rule of thumb.) Thus Design 1 can be expected to have a much higher bandwidth than Design 2. Since designing broader bandwidth is usually an objective, a design requiring a shorter path on a Smith chart is usually preferable.

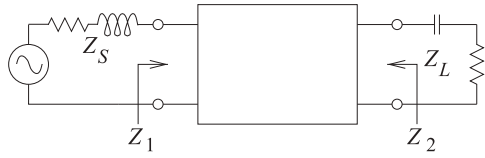


Figure 6-34: Design objectives for Example 6.11.

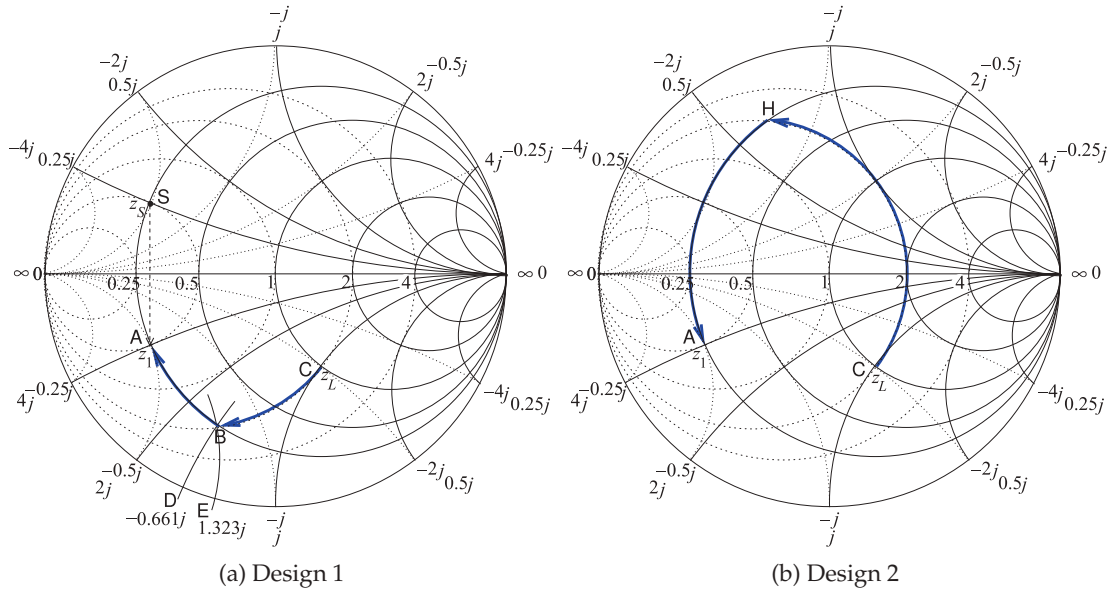


Figure 6-35: Smith chart-based designs used in Example 6.11. (50 Ω normalization used.)

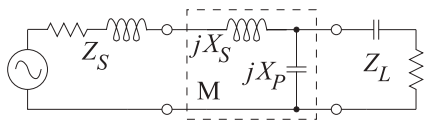


Figure 6-36: Final circuit for Design 1 of Example 6.11.
 $X_S = 20.6 \Omega$, $X_P = -60.8 \Omega$.

6.8 Distributed Matching

Matching using lumped elements leads to series and shunt lumped elements. The shunt elements can be implemented using shunt transmission lines, as a short length (less than one-quarter wavelength long) of short-circuited transmission line looks like an inductor and a short section of open-circuited transmission line looks like a capacitor. However, in most transmission line technologies it is not possible to realize the series elements as lengths of transmission lines. While it has been shown that a short length of transmission line is inductive, replacing series inductors by a length of transmission line of high characteristic impedance is not the best approach to realizing networks. The solution is to use lengths of transmission line together with shunt elements. If space is not at a premium, this is an optimum solution, as transmission lines have much lower loss than a lumped inductor. The series transmission lines rotate the reflection coefficient on the Smith chart.

As with all matching design, using transmission lines begins with a topology in mind. Several topologies are shown in Figure 6-37. Figure 6-37(a) is the

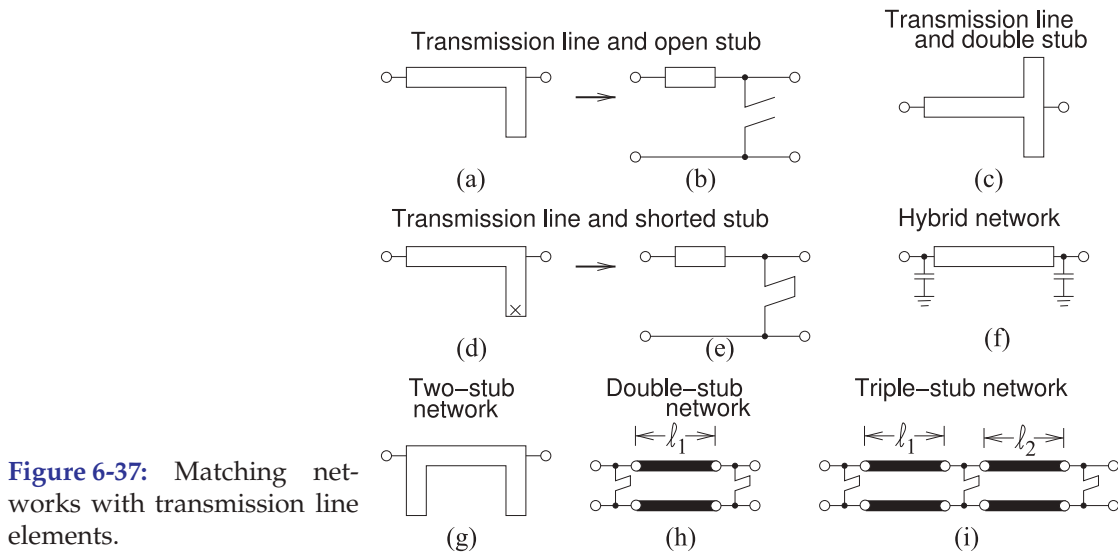


Figure 6-37: Matching networks with transmission line elements.

top view of a microstrip matching network with a series transmission line and stub realized as an open-circuited transmission line. Figure 6-37(b) is a shorthand schematic for this circuit. Matching network design then becomes a problem of choosing the lengths and characteristic impedances of the lines. The stub here is used to realize a capacitive shunt element. This network corresponds to two-element matching with a shunt capacitor. The value of the shunt capacitance can be increased using a dual stub, as shown in Figure 6-37(c), where the capacitive input impedances of each stub are in parallel. The dual circuit to that in Figure 6-37(a) is shown in Figure 6-37(d) together with its schematic representation in Figure 6-37(e). This circuit has a short-circuited stub that realizes a shunt inductance.

Mixing lumped capacitors with a transmission line element, as shown in Figure 6-37(f), realizes a much more space-efficient network design. There are many variations to stub-based matching network design, including the two-stub design in Figure 6-37(g).

A common situation encountered in the laboratory is the matching of circuits that are in development. Laboratory items available for matching include the **stub tuner**, shown in Figure 6-38(a), and the **double-stub tuner**, shown in Figure 6-38(b). With the double-stub tuner the length of the series transmission line is fixed, but stubs can have variable length using lengths of transmission lines with sliding short circuits. Not all impedances can be matched using a double stub tuner, however. A triple-stub tuner can match all impedances presented to it [2]. The **double-slug tuner** shown in Figure 6-38(c) has dielectric slugs each of which introduces a short section of lower impedance line. The slugs are moved up and down the line and avoid the rapid changes in impedances that occur with the stub tuners and as a result the double-slug tuner provides a broader bandwidth match than does the double stub tuner. The **slide-screw slug tuner** shown in Figure 6-38(d) can achieve a broadband match. Here a metal slug can be lowered into the slabline changing the impedance of a section of transmission line and mostly affects the magnitude of the reflection coefficient while moving the metal slug along the line mostly affects the phase. This is the type of tuner incorporated in computer-controlled automated tuners.

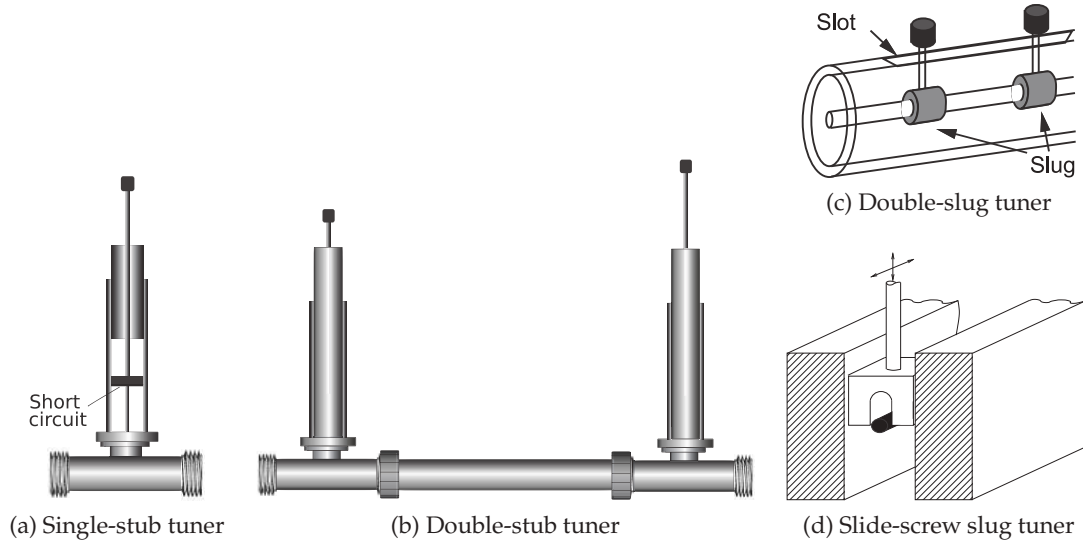
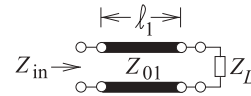
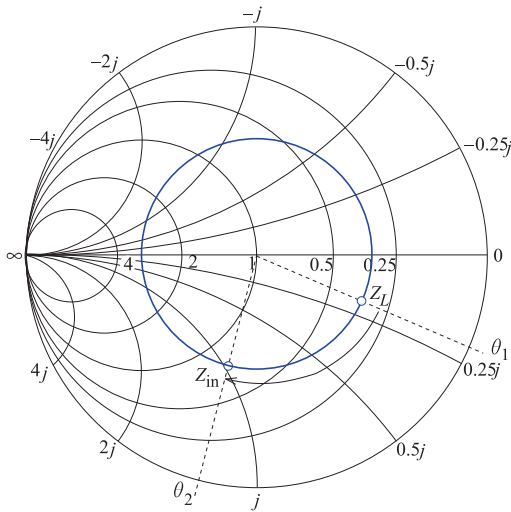


Figure 6-38: Laboratory tuners.


 Figure 6-39: Rotation of the input impedance of a transmission line on a Smith chart normalized to Z_{01} as the line length increases.

6.8.1 Stub Matching

In this section matching using one series transmission line and one stub will be considered. This corresponds to the microstrip circuit topologies shown in Figures 6-37(a and d). First, consider the terminated transmission line shown in Figure 6-39. When the length, ℓ_1 , of the line is zero, the input impedance of the line, Z_{in} , equals Z_L . How it changes is best described by considering the input reflection coefficient, Γ_{in} , of the line. If the reflection coefficient is normalized to Z_{01} , then the magnitude of Γ_{in} and its phase varies as twice the electrical length of the line. This situation is shown on the Smith chart in Figure 6-39, where Z_L is chosen arbitrarily. The input reflection coefficient of

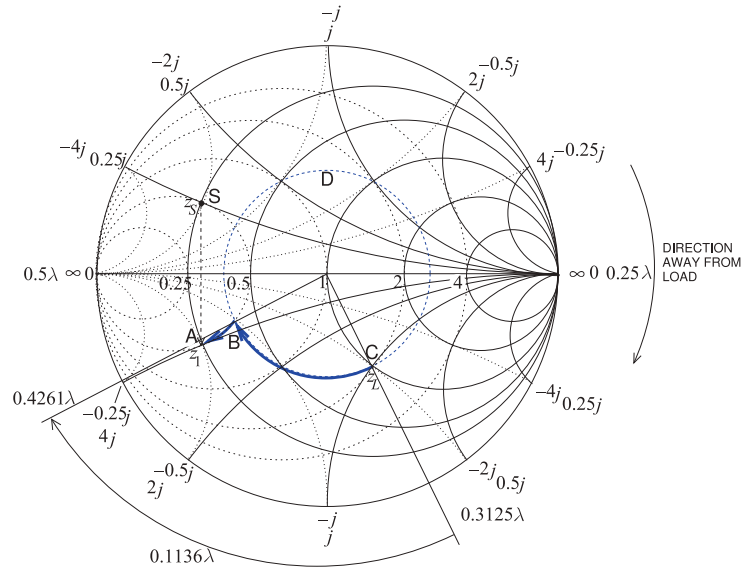
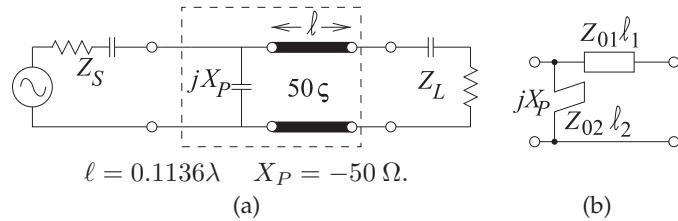


Figure 6-40: Design for Example 6.12.

Figure 6-41: Single-stub matching network design of Example 6.12: (a) electrical design; and (b) electrical design with a shunt stub.



the line rotates in a clockwise direction as the length of the line increases. One way of remembering this is to consider an open-circuited line. When the line length is zero, $Y_{in} = 0$ and $\Gamma_{in} = +1$. A short length of this line is capacitive so that its reflection coefficient will be in the bottom half of the Smith chart. A length of line can be used to rotate the impedance to an appropriate point to follow a line of constant conductance to the desired input impedance.

EXAMPLE 6.12

Matching Network Design With a Transmission Line and a Single Stub

Design a two-element matching network to match a source with an impedance $Z_S = 12.5 + 12.5j \Omega$ to a load $Z_L = 50 - 50j \Omega$, as shown in Figure 6-34. This example repeats the design in Example 6.11, but now using a transmission line.

Solution:

As in Example 6.11, choose $Z_0 = 50 \Omega$ and the design path is from $z_L = Z_L/Z_0 = 1 - j$ to z_s^* , where $z_s = 0.25 + 0.25j$. One possible design solution is indicated in Figure 6-40. The line length, ℓ (taking the locus from Point C to Point B), is

$$\ell = 0.4261\lambda - 0.3125\lambda = 0.1136\lambda,$$

and the normalized shunt susceptance, b_P (taking the locus from Point B to Point C), is

$$b_P = b_A - b_B = 2 - 1 = 1.$$

Thus $X_P = (-1/b_P) \times 50 \Omega = -50 \Omega$. The final design is shown in Figure 6-41(a). The stub design of Figure 6-41(b) follows the procedure described in Example 6.5.

6.8.2 Hybrid Lumped-Distributed Matching

A lossless matching network can have transmission lines as well as inductors and capacitors. If the system reference or normalization impedance is the characteristic impedance of a transmission line, then the locus of the input impedance (or reflection coefficient) of the line with respect to the length of the line is an arc on a circle centered at the origin of the Smith chart. The direction of the arc is clockwise as the electrical length of the line moves away from the load. So a hybrid matching network is possible that combines a length of transmission line with a lumped element (preferably a capacitor rather than an inductor as the inductor would have a relatively lower Q).

6.9 Matching Options Using the Smith Chart

The purpose of this section is to use the Smith chart to present several design options for matching a source to a load, see Figure 6-42. The designs here provide another view of design using the Smith chart.

6.9.1 Locating the Design Points

The first design choice to be made is the reference impedance to use. Here $Z_{\text{REF}} = 50 \Omega$ will be chosen largely because this is in the center of the design space for microstrip lines. Generally the characteristic impedance, Z_0 , of a microstrip line needs to be between 20Ω and 100Ω . A microstrip line with $Z_0 < 20 \Omega$ will be wide and there is a possibility of multimoding due to transverse resonance. Also 20Ω line is about six times wider than a 50Ω line and so takes up a lot of room and there is a good chance that it could be close to other microstrip lines or perhaps the wall of an enclosure. This is based on the rule of thumb (developed in Example 3.4 of [1]) that $Z_0 \propto \sqrt{h/w}$ where h is the substrate thickness and w is the strip width. The thickness is usually fixed, i.e. it is not always a readily changed design choice. If $Z_0 > 100 \Omega$ the characteristic impedance is getting close to the wave impedance of free space and of the dielectric of the substrate. As such it is likely that field lines are not tightly constrained by the metal of the strip and the fields can more likely radiate. Then radiation loss can be high or coupling to a neighboring microstrip can be high.

The normalized source and load impedances are $z_S = Z_S/Z_{\text{REF}} = [(29.36 - j12.05) \Omega]/(50 \Omega) = 0.587 - j0.241$ and $z_L = Z_L/Z_{\text{REF}} = [(132.7 - j148.8) \Omega]/(50 \Omega) = 2.655 - j2.976 = r_L + jx_L$, respectively. Maximum power transfer requires that the input impedance of the matching network terminated in Z_L be $Z_1 = Z_S^*$, i.e. $z_1 = z_S^* = 0.587 + j0.241 = r_1 + jx_1$. These impedances are plotted on the normalized Smith chart in Figure 6-43.

The normalized load impedance is Point L. To locate this point the arcs corresponding to the real and imaginary parts of z_L are considered separately. The resistive part of z_L is $r_L = 2.655$ and the resistance labels are

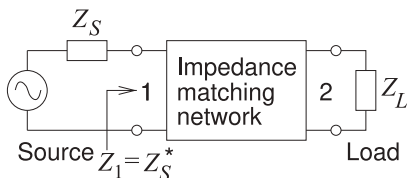


Figure 6-42: Matching problem with the matching network between the source and load designed for maximum power transfer. $Z_S = R_S + jX_S = 29.36 - j12.05$, $Z_1 = R_1 + jX_1 = Z_S^* = R_S - jX_S = 29.36 + j12.05$, and $Z_L = R_L + jX_L = 132.7 - j148.8$.

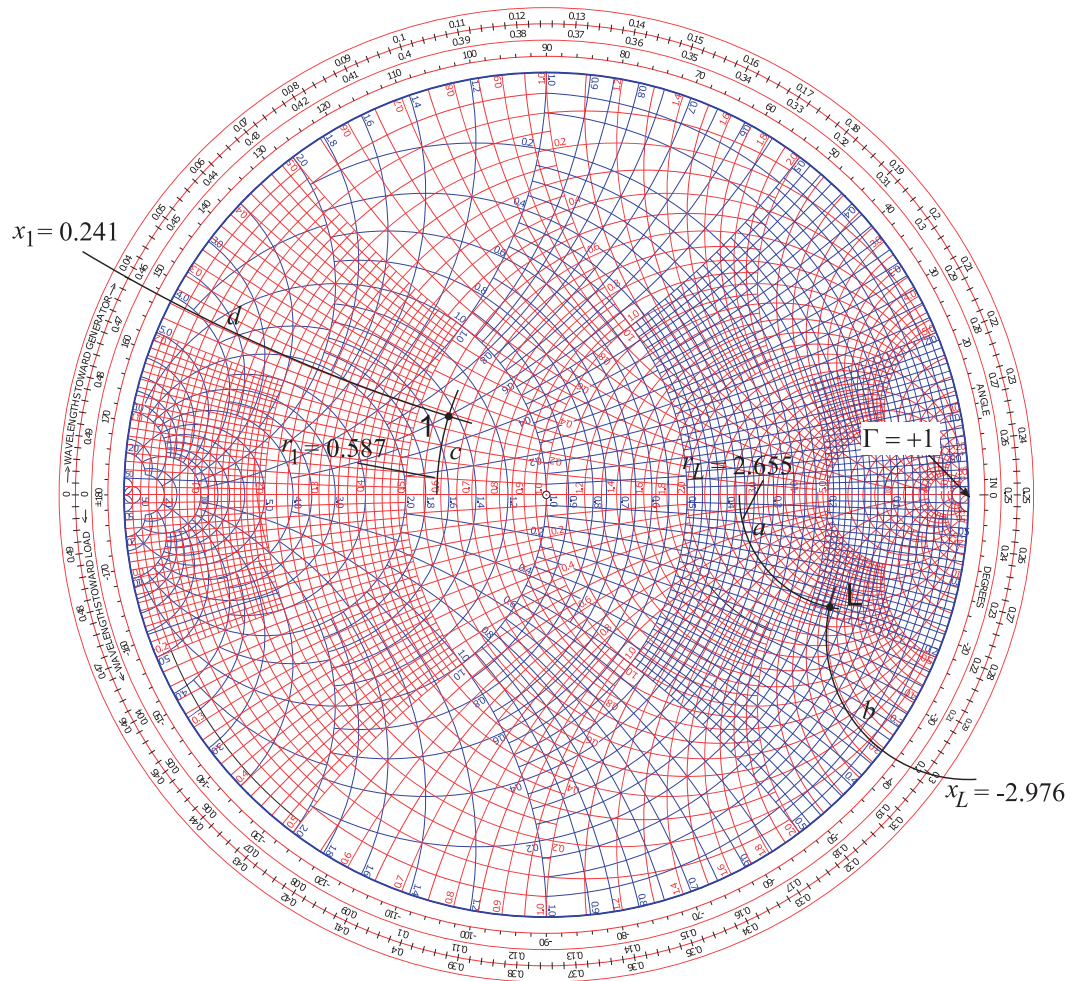


Figure 6-43: Locating Z_L at Point L and $Z_1 = Z_S^*$ at Point 1.

located on the horizontal axis (or equator) of the Smith chart. There are two sets of labels, one for normalized resistance, r (which is above the horizontal axis), and one for normalized conductance, g (which is below the horizontal axis). The way to remember which is which is to realize that the infinite impedance point is at the $\Gamma = +1$ (open circuit) location on the right of the graph. At the origin (center) of the Smith chart $r = 1 = g$ and to the right of the center the values of r should be greater than one. The closest r labels to $r_L = 2.655$ are $r = 2.0$ and $r = 3.0$. There are five divisions so the unlabeled curves correspond to 2.2, 2.4, \dots . The arc corresponding to $r = 2.655$ must be interpolated and this interpolation is shown as the Path 'a'.

The imaginary part of z_L is $x_L = -2.976$. The labels for the arcs of constant reactance are given adjacent to the unit circle. There are two sets of labels, one for reactance and one for susceptance. To recall which is which, the point of infinite impedance can be used and the required reactance labels should increase towards the $\Gamma = +1$ point. Recall that the Smith chart does not

include signs of reactances (there is not enough room) so note must be made that positive reactances are in the top half of the Smith chart and negative reactances are in the bottom half. Since x_L is negative it will be in the bottom half of the Smith chart. The closest labels are $x = 2.0$ (this is actually -2.0) and $x = 3.0$ (this is actually -3.0) so the arc for $x = -2.976$ is interpolated as the Path 'b'. Point L, i.e. z_L , is located at the intersection of Paths 'a' and 'b'. The normalized impedance z_1 is located similarly at Point 1 by finding the point of intersection of the $r_1 = 0.587$ arc, Path 'c', and the $x_1 = +0.241$ arc, Path 'd'.

6.9.2 Design Options

By convention design follows a process of beginning with z_L and adding series and shunt elements in front of it evolving the impedance (or reflection coefficient) until the input impedance is $z_1 = z_S^*$. Three electrical designs are shown in Figure 6-44 and the corresponding lumped-element and microstrip topologies are shown in Figure 6-45. The subscript on the circuit elements correspond to the paths on the Smith chart in Figure 6-44. The designs will be elaborated in the following subsections.

6.9.3 Design 1, Hybrid Design

Design 1 on its own is shown in Figure 6-46. The concept here is to use a transmission line and a shunt to go from the load Point L to the Point 1. The reason why a shunt element is chosen and not a series element is that the shunt element can be implemented as stub line and a series element, i.e. a series stub, cannot be implemented in microstrip. A lumped element limits a design to the low microwave range as losses become prohibitively large especially for inductors. Also if a microstrip line is going to be used anyway then a decision already has been made that there is enough room to implement a transmission-line based design and so the shunt lumped element can reasonably be replaced by a stub.

Design follows trial and error. The first attempt, and the one that works here, is to draw a circle through L centered on the origin at Point O. This circle describes a transmission line whose characteristic impedance is the same as the reference impedance of the Smith chart, here $50\ \Omega$. The next step is to draw a circle of constant conductance through Point 1. The combination path from L to 1 needs to lie on these circles and the intermediate point will be where these circles intersect. One other constraint is that with a transmission line the locus (as the line length increases) of the input reflection coefficient of the line must rotate in the clockwise direction. It is seen that there are two points of intersection and the first of these, at A, is chosen in design. So the electrical design is defined by the directed Paths 'g' and 'h'. Path 'g' defines the properties of the transmission line and Path 'h' defines the properties of the shunt element. As 'h' is directed towards the infinite inductive susceptance point, Path 'h' defines an inductor. The topology of this design is shown in Figure 6-45(a).

The characteristic impedance of the transmission line (defined by Path 'g') is $Z_{0g} = 50\ \Omega$. The electrical length of the line is defined by the angle subtended by the arc 'g'. The electrical length of the line is determined from the outermost circular scale which is labeled 'WAVELENGTHS TOWARDS

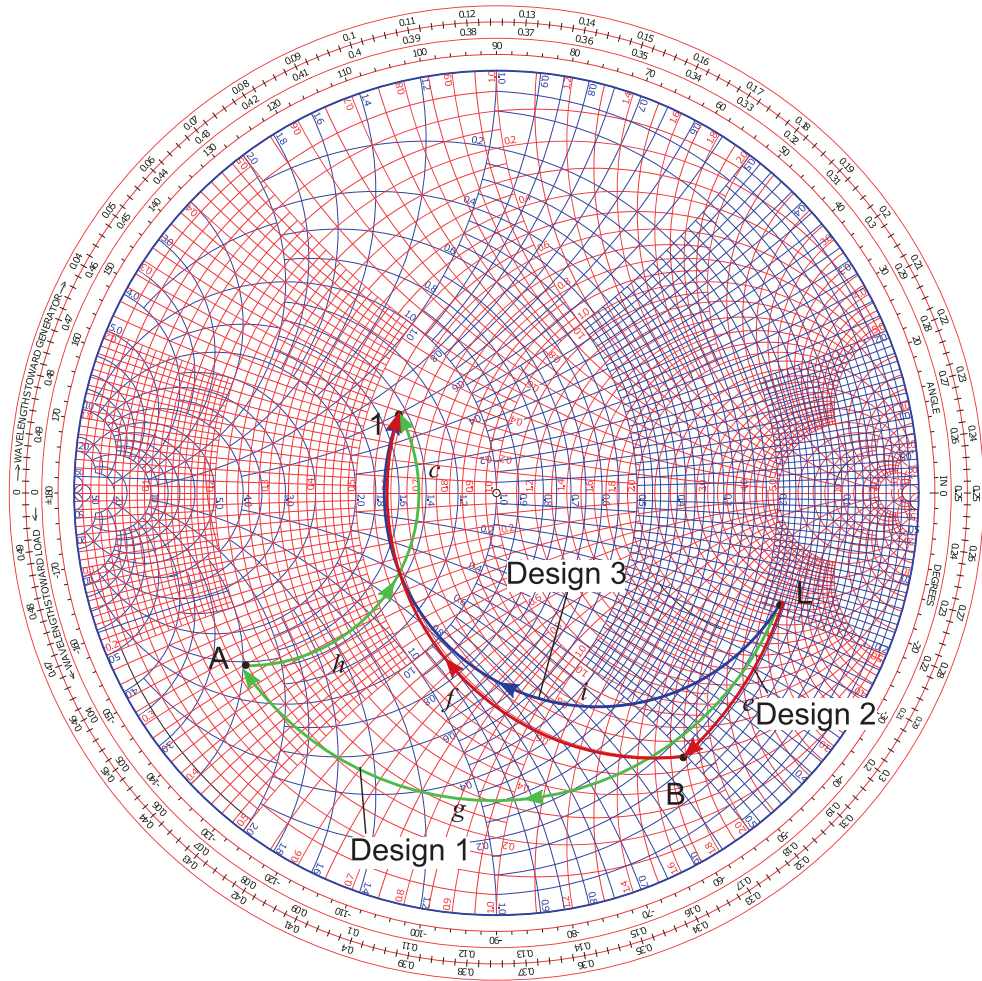


Figure 6-44: Three matching network electrical designs matching a load impedance Z_L at Point L to a source Z_S showing $Z_1 = Z_S^*$ at Point 1.

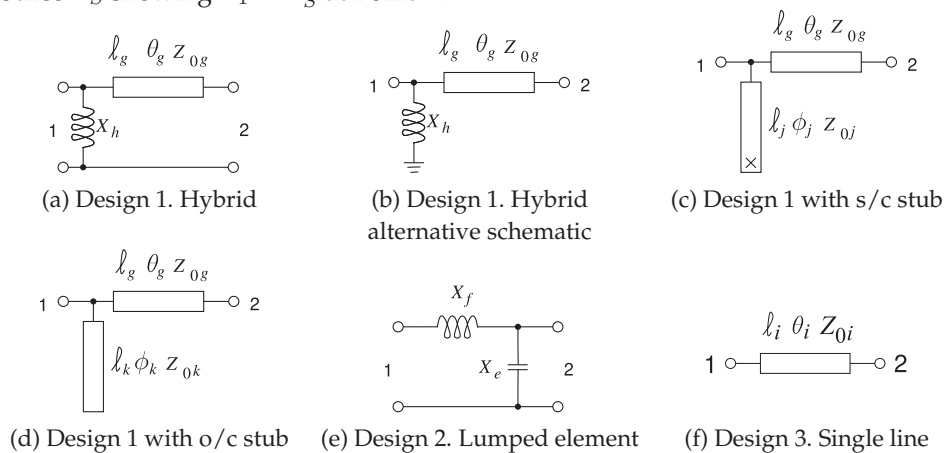


Figure 6-45: Matching network topologies using lumped elements and microstrip lines. In the stub layouts x is a via to the ground plane implementing a short circuit (s/c) and an open circuit (o/c) simply does not show a connection to the microstrip ground plane.

Design 1

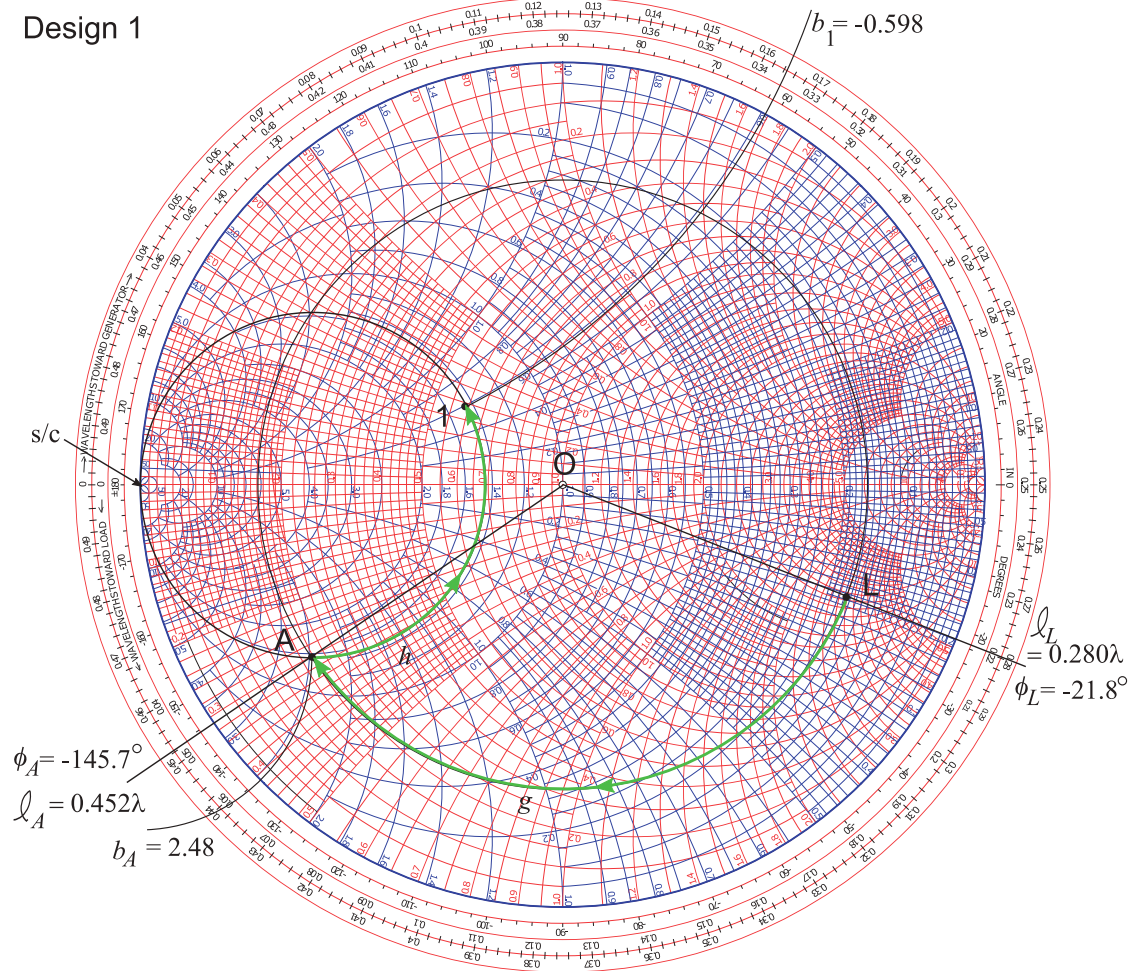


Figure 6-46: Design 1. Hybrid design combining a transmission line with a lumped element in shunt. The design is identified by paths 'g' and 'h'.

GENERATOR.' A line drawn from O through L intersecting the scale has a scale reading of $\ell_L = 0.280\lambda$. Then the scale reading at A is similarly found as $\ell_A = 0.452\lambda$ and so the line length is $\ell_g = \ell_A - \ell_L = 0.452\lambda - 0.280\lambda = 0.172\lambda$. Another way of determining the electrical length of the line is from the change in reflection coefficient angle. For L the reflection coefficient angle is $\phi_L = -21.8^\circ$ read from the innermost circular scale. This angle is just the angle from the polar plot. Then the angle at A is read as $\phi_A = -145.7^\circ$. The difference is $|\phi_A - \phi_L| = |-145.7 - (-21.8)| = 124.9^\circ$. The electrical length of the line is half the change in reflection coefficient angle and so the electrical length of the line is $\theta_g = \frac{1}{2}124.9^\circ = 62.5^\circ$. Now λ corresponds to an electrical length of 360° so θ_g corresponds to $62.5/360\lambda = 0.174\lambda$ corresponding to the previously determined length of 0.172λ which is very good agreement given that these were derived from graphical readings.

Path 'h' defines a shunt inductor and a circle of constant conductance is

followed with only the susceptance changing. The susceptance indicated by Path 'g' is $b_g = b_1 - b_A$. To obtain b_A extend the circle of constant susceptance through A out to the unit circle. The extended circle cross the unit circle between the susceptance labels 2.0 and 3.0. A check is that susceptance is positive in the bottom half of the Smith chart so the signs of the labels do not need to be adjusted. There are two scales adjacent to the unit circle, one for normalized susceptance and one for normalized reactance. Since the intersection is close to the infinite susceptance point at the s/c (short-circuit) so the values that are becoming very large towards s/c are used. Interpolation results in the reading $b_A = 2.48$. A similar process applied to Point 1 results in $b_1 = -0.598$ where the negative sign has been applied to the scale reading since the point of intersection between the arc of constant susceptance passing through Point 1 and the unit circle is in the top half of the Smith chart. Thus $b_h = b_1 - b_A = -0.598 - 2.48 = -3.08$ and so the normalized reactance of the shunt element is $x_h = -1/b_h = 0.325$. The un-normalized reactance of the shunt element is $X_h = x_h Z_{\text{REF}} = 16.2 \Omega$.

The final Design 1 hybrid layout is shown in Figure 6-45(a) with $X_h = 16.2 \Omega$, $Z_{0g} = 50 \Omega$, and $\ell_g = 0.172\lambda$. That is all that is needed to define the electrical design, providing the electrical length in degrees, $\theta_g = 62.5^\circ$ is redundant but provided anyway. The transmission line in Figure 6-45(a) is shown as the top view of the strip of a microstrip line as is commonly done. A more common way of representing this schematic is shown in Figure 6-45(b) where the ground connections at Ports 1 and 2 have been removed and the ground connection of the inductor shown separately.

6.9.4 Design 1 with an Open-Circuited Stub

In the previous section Design 1 was left as a hybrid design with a transmission line and a lumped-element inductor. In this section the lumped-element inductor is implemented as an open-circuited stub, see Figure 6-45(d). Recall that the 50Ω -normalized susceptance of the inductor is $b_h = -3.08$. If the stub is also implemented as a 50Ω line then b_h can be used unchanged. Point C in Figure 6-47 corresponds to the normalized admittance $0 - j3.08$. The unit circle is the zero conductance circle (and is also the zero resistance circle) and the susceptance is read from the scale adjacent to the unit circle again using as reference that susceptances in the top half of the Smith chart need to incorporate a negative sign and the susceptance scale is identified by the susceptance values becoming larger approaching the s/c point. Point C also corresponds to $x_h = -1/b_h = 3.25$ and indeed this is the value read from the normalized reactance scale.

A transmission line needs to be designed to have a normalized input susceptance of $b_h = -3.08$. Choosing an open circuit, o/c, termination the point corresponding to o/c is as identified in the figure. At the o/c point the length scale reads $\ell_{o/c} = 0.250\lambda$. The locus rotates in the clockwise direction up to Point C where the direct electrical reading is $\ell_C = 0.050\lambda$. Using this directly to determine the line length $\ell_k = \ell_C - \ell_{o/c} = 0.050\lambda - 0.250\lambda = -0.20\lambda$ which indicates that the stub has a negative length. Clearly an erroneous result. This apparent discrepancy comes about because the length scale resets at the short circuit point where the length scale abruptly goes from 0.5λ to 0λ . Thus the corrected ℓ_C reading needs to have an additional 0.5λ . Thus the corrected value of $\ell_C = (0.5 + 0.050)\lambda = 0.550\lambda$

Design 1 Stub design

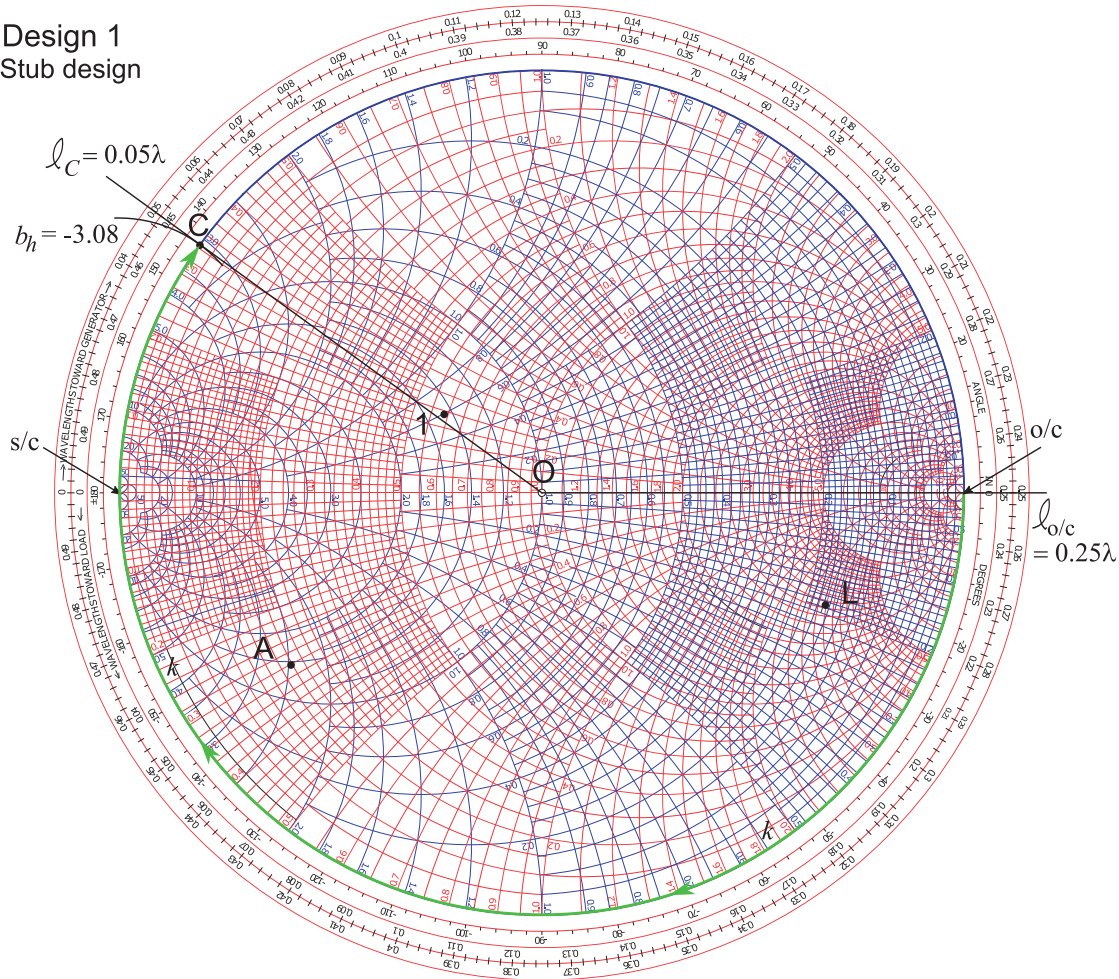


Figure 6-47: Design 1. Design of an open-circuit stub having normalized input susceptance b_h .

and $\ell_k = \ell_C - \ell_{o/c} = 0.550\lambda - 0.250\lambda = 0.300\lambda$.

Thus the final design is as shown in Figure 6-45(d) with $Z_{0k} = 50 \Omega$, and $\ell_g = 0.300\lambda$, $Z_{0g} = 50 \Omega$, and $\ell_g = 0.172\lambda$.

The stub could also have been implemented as a short-circuit stub as shown in Figure 6-45(c). Now the beginning of the line would be at the s/c point and the line length would be 0.050λ

6.9.5 Design 2, Lumped-Element Design

Design 2 is a lumped-element design and the Smith-chart-based electrical design is shown in Figure 6-48 resulting in the schematic shown in Figure 6-45(e). Design proceeds by identifying where circles of constant conductance and constant resistance passing through the Points L and 1 intersect. One solution is shown in Figure 6-48. A circle of constant conductance passes through L and part of a circle of constant resistance passes through 1. If the circle had continued there would have been a second intersection with

Design 2

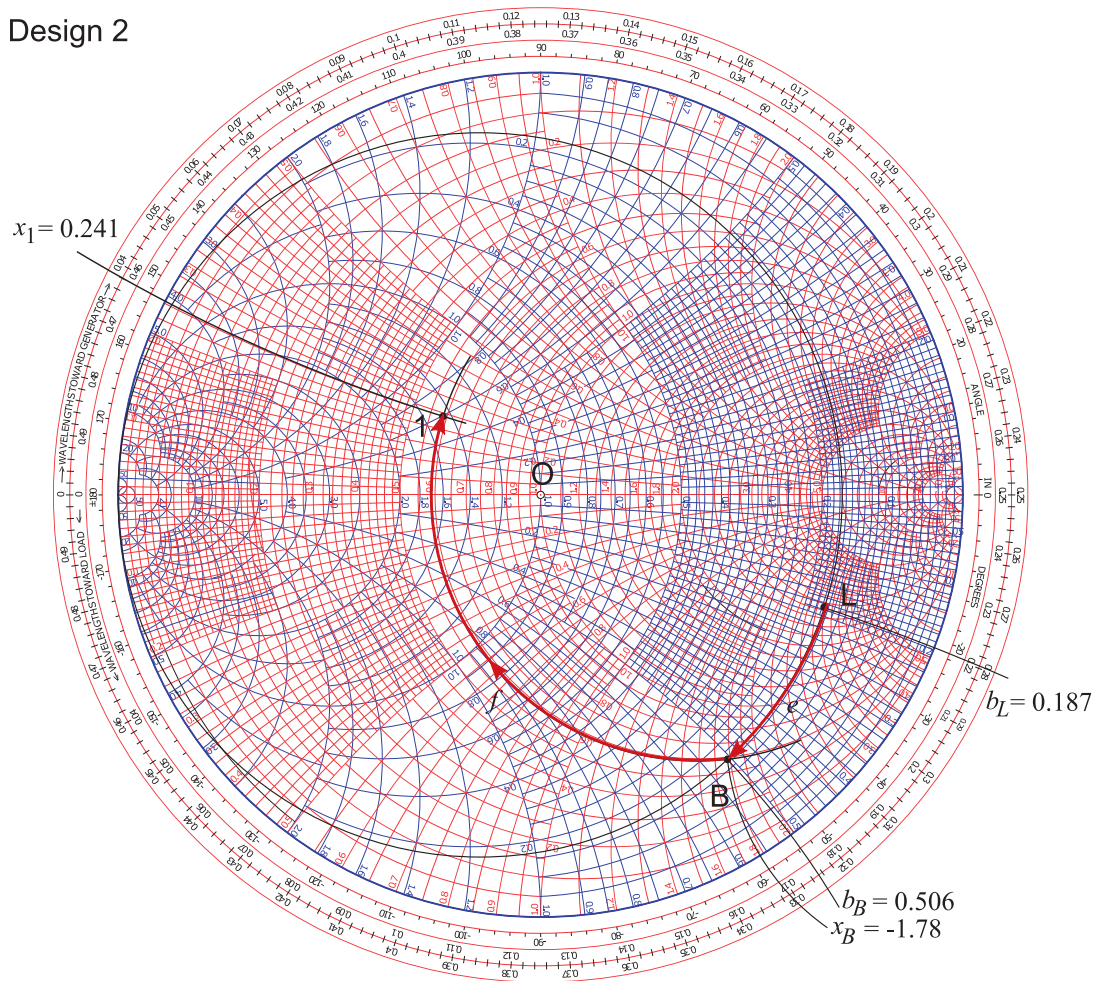


Figure 6-48: Design 2.

the circle through L. Both of these intersections mean that there is a shunt element adjacent to the load and series element adjacent to the source. Recall that in a lumped-element design that under no circumstances can the locus of a lumped element pass through the short circuit point (if it is a susceptance) or open-circuit point (if it is a reactance), the susceptance and reactance infinity points respectively.

Returning to the actual design shown in Figure 6-48. The first intersection of the two circles is Point B so that the design is specified by the Paths 'e' and 'f'. Design has largely been completed by identifying these paths and the next stage is determining the circuit elements that correspond to these paths. Path 'e' follows a circle of constant conductance and so indicates a shunt susceptance and the direction of the locus indicates a capacitance. The value of this normalized susceptance is $b_e = b_B - b_L = 0.506 - 0.187 = 0.319$. (Remember to check the signs of the readings since the Smith chart omits signs of the reactances and susceptances.) Path 'f' identifies a series inductor

with a reactance $x_f = x_1 - x_B = 0.241 - (-1.78) = 2.02$. The final design is shown in Figure 6-45(e) with $X_e = Z_0/b_e = 50/0.319 \Omega = 158 \Omega$ and $X_f = Z_0x_f = 50 \cdot 2.02 \Omega = 101 \Omega$.

6.9.6 Design 3, Single Line Matching

Design 3 uses a single transmission line to match the source and load as shown in the schematic of Figure 6-45(f). This design is akin to using a quarter-wave transmission line transformer but with a Smith chart being used the approach can now be used with complex source and load impedances. Recall from Sections 3.5.2 and 4.5 that the locus of a terminated transmission line is a circle on the Smith chart even if the characteristic impedance of the transmission line, Z_{0i} in Design 3, and the reference impedance, Z_{REF} , are not the same. Furthermore the center of the circle will be on the horizontal axis. The Smith-chart-based electrical design of Design 3 is shown in Figure 6-49 where $Z_{\text{REF}} = 50 \Omega$. There is only one way to draw a circle that passes through two points with the center of the circle constrained to be on the horizontal axis. That circle is shown in Figure 6-49 with Path 'i' on the circle going from Points L to 1 tracing out the locus of the reflection coefficient. This locus must be in the clockwise direction. The center of the circle is at Point D and the center of the circle is (the reflection coefficient normalized to Z_{REF}) is $C_D = 0.240$. (The radius is also given but this is not necessary.) The angle subtended by Path 'i' is twice the electrical length of the line. This angle cannot be directly measured from the scales (although it is possible by placing a chart over the top and aligning the center of the polar plot with D) and here was read using a protractor. The angle is $\phi_D = 150^\circ$ so that the electrical length of the line is $\theta_i = \frac{1}{2}150^\circ = 75^\circ$, i.e. $\ell_i = 74/360\lambda = 0.208\lambda$. The only parameter not known is the characteristic impedance, Z_{0i} , of the line. This must be arrived at iteratively. From Equation (4.40) (after replacing Z_{01} , Z_{02} and C_{Z02} by Z_{0i} , Z_{REF} and C_D , respectively)

$$Z_{0i} \approx Z_{\text{REF}}(1 + C_D)/(1 - C_D) \quad (6.73)$$

with the approximation improving the closer Z_{0i} is to Z_{REF} . Substituting $Z_{\text{REF}} = 50 \Omega$ and $C_D = 0.240$, the first iteration of Z_{0i} is

$$^1Z_{0i} = 50 \left(\frac{1 + 0.240}{1 - 0.240} \right) \Omega = 82 \Omega. \quad (6.74)$$

Re-plotting using a new reference impedance of $Z_{\text{REF}} = 82 \Omega$ yields a new center of 0.07 from which an updated iterate is $^2Z_{0i} = 94 \Omega$ and then a new center of 0.02 and $^3Z_{0i} = 98 \Omega$. Continuing to iterate results in an asymptotic value $Z_{0i} = 100 \Omega$. Z_{0i} can also be estimated from the tabulated values in Table 4-1. Reading the line with radius of 0.5 and center of 0.24 yields $Z_{0i} = 50 \cdot 1.980 = 99 \Omega$.

The final design is as shown in Figure 6-45(f) with $\ell_i = 0.208\lambda$, $\theta_i = 75^\circ$, and $Z_{0i} = 100 \Omega$.

As was seen with the quarter-wave transformer design using multiple stages significantly increases bandwidth by matching to intermediate resistances determined as geometric means of the source and load resistance. The corresponding strategy here is to draw a line between the Points 1 and L and, if there are to be two stages, choose the intermediate matching impedance

Design 3

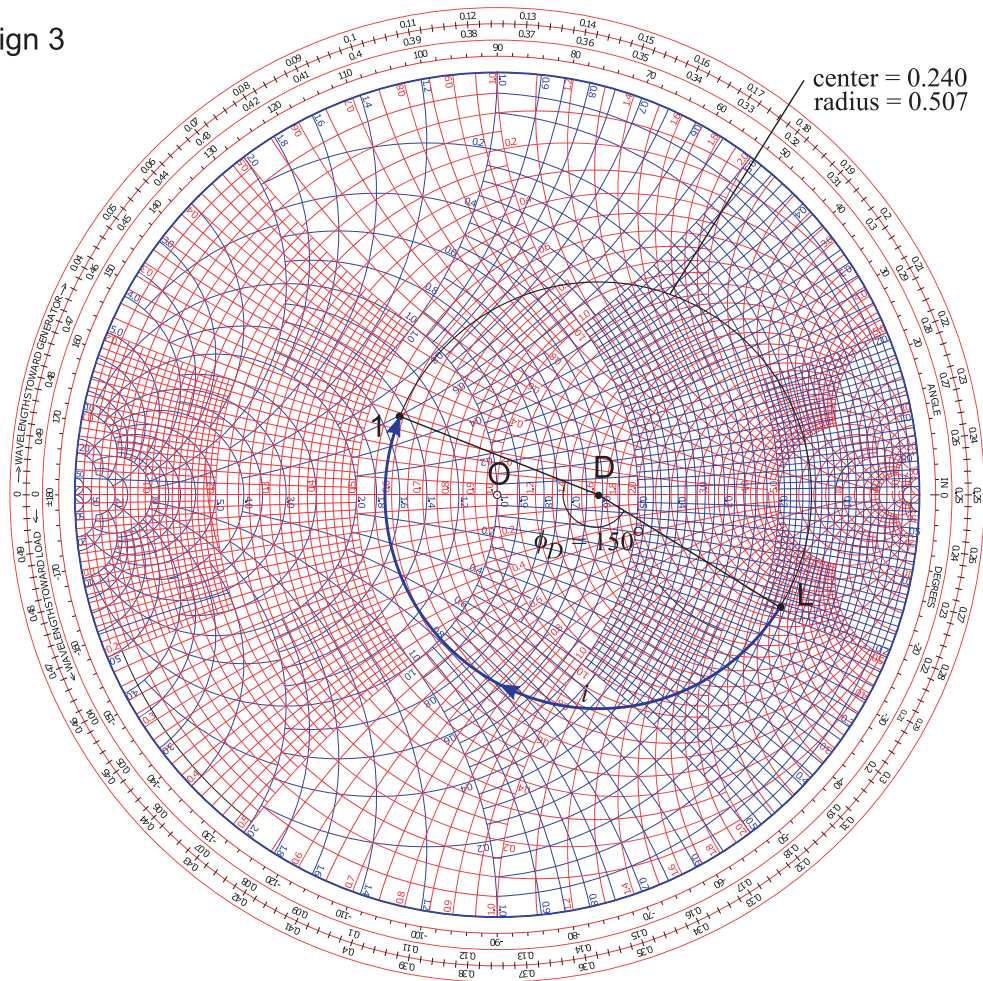


Figure 6-49: Design 3.

at the mid-point of the line. If the source and loads are complex then the reactive storage elements in the source and load will set a limit on maximum achievable bandwidth.

6.9.7 Summary

This section presented three quite different designs for a matching network. One of the particular benefits of using the Smith chart is identifying topologies and initial design values. Design can then transfer to a microwave circuit simulator. The Smith chart enables back-of-the-envelope design studies. While with experience it is possible to complete many of these steps with a computer-based Smith chart tool, even experienced designers doodle with a printed Smith chart when exploring design options.

6.10 Summary

This chapter presented techniques for impedance matching that achieve maximum power transfer from a source to a load. The simplest matching network uses a series and a shunt element, a two-element matching network, to realize a single-frequency match. This type of impedance matching network uses lumped elements and can be used up to a few gigahertz. Performance is limited by the self-resonant frequency of lumped elements and by their loss, particularly that of inductors. The shunt element can be replaced by a shunt stub, but in most transmission line technologies, including microstrip, the series element cannot be implemented as a stub. Matching networks can also be realized using transmission line segments only, principally shunt stubs and cascaded transmission lines. A tunable double-stub matching network, which uses two stubs separated by a transmission line, is standard equipment in microwave laboratories and facilitates matching of a circuit under development.

The bandwidth of a matching network is set by the maximum allowable reflection coefficient of the terminated network. Two-element matching nearly always results in a narrow match and for typical communications applications often achieves acceptable matching over bandwidths of only 1%–3%. The most significant determinant of the quality of the match that can be achieved is the ratio of the source and load resistances, as well as the reactive energy storage of the source and load. Clearly if the load and source are resistances of the same value, the bandwidth of the matching network is infinite, as it is no more than a wired connection.

An important concept in matching network design is a technique for controlling bandwidth. The concept is based on matching to an intermediate resistance R_v . Increased bandwidth is obtained if R_v is the geometric mean of the source and load resistances. This new network consists of two two-element matching networks. If R_v is greater or less than both the source and load resistances, then the bandwidth of the matching network is reduced. Matching network synthesis can also be addressed using filter design techniques, enabling simultaneous control over the quality and bandwidth of the match. It is always a good idea to have no more bandwidth in the system than is needed, as this minimizes the propagation of noise.

A powerful graphical matching tool is the Smith chart on which the load and source can be plotted. The design objective is then to determine the path, subject to constraints, from the load back to an input, which is the complex conjugate of the source, a task that a human is particularly adept at performing. Alternatively the perspective could be flipped and the role of the source and load interchanged.

Design becomes increasingly more difficult as the required bandwidth increases. Many times it is sufficient to have small-to-moderate bandwidths that can be tuned rather than providing one large instantaneous bandwidth. Also many of the evolving wireless systems require multiple functionality, which in turn requires adjustability of a matching network. In some applications the matching network may require adjustment to match a variable load impedance. A good example is dealing with a cell phone antenna where the user may put his or her hand over the antenna and alter the load seen by the RF frontend. Some types of matching network designs are more adjustable than others. Such designs require variable components, so matching design can be a source of competitive advantage.

6.11 References

- [1] M. Steer, *Microwave and RF Design, Transmission Lines*, 3rd ed. North Carolina State University, 2019.
- [2] R. Collins, *Foundations for Microwave Engineering*. McGraw Hill, 1966.

6.12 Exercises

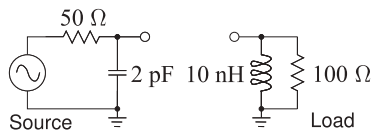
- Consider the design of a magnetic transformer that will match the $3\ \Omega$ output resistance of a power amplifier (this is the source) to a $50\ \Omega$ load. The secondary of the transformer is on the load side.
 - What is the ratio of the number of primary turns to the number of secondary turns for ideal matching?
 - If the transformer ratio could be implemented exactly (the ideal situation), what is the reflection coefficient normalized to $3\ \Omega$ looking into the primary of the transformer with the $50\ \Omega$ load?
 - What is the ideal return loss of the loaded transformer (looking into the primary)? Express your answer in dB.
 - If there are 100 secondary windings, how many primary windings are there in your design? Note that the number of windings must be an integer. (This practical situation will be considered in the rest of the problem.)
 - What is the input resistance of the transformer looking into the primary?
 - What is the reflection coefficient normalized to $3\ \Omega$ looking into the primary of the transformer with the $50\ \Omega$ load?
 - What is the actual return loss (in dB) of the loaded transformer (looking into the primary)?
 - If the maximum available power from the amplifier is 20 dBm, how much power (in dBm) is reflected at the input of the transformer?
 - Thus, how much power (in dBm) is delivered to the load ignoring loss in the transformer?
- Consider the design of a magnetic transformer that will match a $50\ \Omega$ output resistance to the $100\ \Omega$ load presented by an amplifier. The secondary of the transformer is on the load (amplifier) side.
 - What is the ratio of the number of primary turns to the number of secondary turns for ideal matching?
 - If the transformer ratio could be implemented exactly (the ideal situation), what is the reflection coefficient normalized to $50\ \Omega$ looking into the primary of the transformer with the load?
 - What is the ideal return loss of the loaded transformer (looking into the primary)? Express your answer in dB.
 - If there are 20 secondary windings, how many primary windings are there in your design? Note that the number of windings must be an integer? (This situation will be considered in the rest of the problem.)
 - What is the input resistance of the transformer looking into the primary?
 - What is the reflection coefficient normalized to $50\ \Omega$ looking into the primary of the loaded transformer?
 - What is the actual return loss (in dB) of the loaded transformer (looking into the primary)?
 - If the maximum available power from the source is $-10\ \text{dBm}$, how much power (in dBm) is reflected from the input of the transformer?
 - Thus, how much power (in dBm) is delivered to the amplifier ignoring loss in the transformer?
- Consider the design of an L-matching network centered at 1 GHz that will match the $2\ \Omega$ output resistance of a power amplifier (this is the source) to a $50\ \Omega$ load. [Parallels Example 6.3 but note the DC blocking requirement below.]
 - What is the Q of the matching network?
 - The matching network must block DC current. Draw the topology of the matching network.
 - What is the reactance of the series element in the matching network?
 - What is the reactance of the shunt element in the matching network?
 - What is the value of the series element in the matching network?
 - What is the value of the shunt element in the matching network?
 - Draw and label the final design of your matching network including the source and load resistances.
 - Approximately, what is the 3 dB bandwidth

of the matching network?

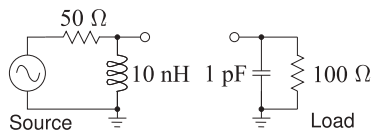
4. Consider the design of an L-matching network centered at 100 GHz that will match a source with a Thevenin resistance of $50\ \Omega$ to the input of an amplifier presenting a load resistance of $100\ \Omega$ to the matching network. [Parallels Example 6.4 but note the DC blocking requirement below.]

- What is the Q of the matching network?
- The matching network must block DC current. Draw the topology of the matching network.
- What is the reactance of the series element in the matching network?
- What is the reactance of the shunt element in the matching network?
- What is the value of the series element in the matching network?
- What is the value of the shunt element in the matching network?
- Draw and label the final design of your matching network including the source and load resistance.
- Approximately, what is the 3 dB bandwidth of the matching network?

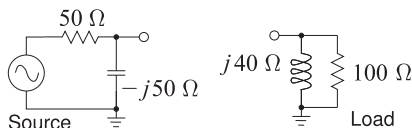
5. Design a Pi network to match the source configuration to the load configuration below. The design frequency is 900 MHz and the desired Q is 10. [Parallels Example 6.8]



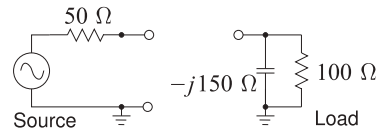
6. Design a Pi network to match the source configuration to the load configuration below. The design frequency is 900 MHz and the desired Q is 10. [Parallels Example 6.8]



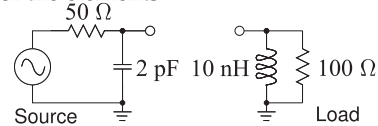
7. Develop the electrical design of an L-matching network to match the source to the load below.



8. Develop the electrical design of an L-matching network to match the source to the load below.



9. Design a lowpass lumped-element matching network to match the source and load shown below. The design frequency is 1 GHz. You must use a Smith Chart and clearly show your working and derivations. You must develop the final values of the elements.



10. Consider the design of an L-matching network centered at 100 GHz that will match a source with a Thevenin resistance of $50\ \Omega$ to the input of an amplifier presenting a load resistance of $200\ \Omega$ to the matching network. [Parallels Example 6.4 but note the DC blocking requirement below.]

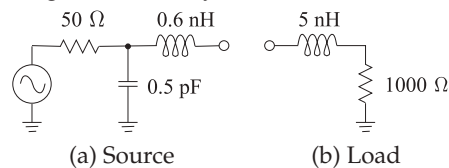
- What is the Q of the matching network?
- The matching network must block DC current. Draw the topology of the matching network.
- What is the reactance of the series element in the matching network?
- What is the reactance of the shunt element in the matching network?
- What is the value of the series element in the matching network?
- What is the value of the shunt element in the matching network?
- Draw and label the final design of your matching network including the source and load resistance.
- Approximately, what is the 3 dB bandwidth of the matching network?

11. Consider the design of the output matching network of a 15 GHz small-signal amplifier. The amplifier consists of an active two-port and input and output matching networks. Port 1 is the input of the active device and Port 2 is its output, and its $50\ \Omega$ S parameters are $S_{11} = 0.5\angle 45^\circ$, $S_{12} = 0.1\angle 0^\circ$, $S_{21} = 2\angle 90^\circ$, and $S_{22} = 0.75\angle -45^\circ$.

- If the input of the active device is terminated in $50\ \Omega$, what is the impedance looking into the output of the amplifier?
- Design a two-element lumped-element matching network for maximum power transfer from the output of the transistor

into a $50\ \Omega$ load. Develop at least two designs and compare them. (Note that the output of the active device physically appears as a resistance in parallel with a capacitance and this can be used in contrasting your designs.)

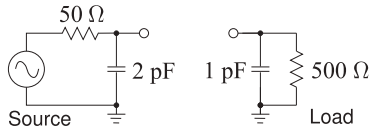
12. Develop a two-element matching network for the source/load configuration shown in the figure below. The matching network must pass DC. The center frequency of the matching network is $f = 1\text{ GHz}$. There are a number of design considerations that should be considered before embarking on network synthesis.



Consider the following:

- (i) The source needs to be collapsed to an equivalent circuit with one resistance and one reactance.
 - (ii) The reactive elements in the source and the load will be accommodated using absorption or resonance. Absorption is preferred, but not always possible.
 - (iii) The DC requirements necessitate a low-pass matching network. So there must be a series inductance and a shunt capacitor in the matching network. Since the load resistance is greater than the source resistance, the most likely design has a shunt capacitor on the load side. However, this may change when the transforming properties of the source and load reactances are considered.
 - (iv) The source reactance should be handled by a series inductor or a shunt capacitor. The input impedance of the source must be considered to determine which.
 - (v) The load reactance will be resonated out by a shunt capacitor. Looks like absorption will be a possibility at the load.
- (a) What is the input impedance of the source? Treat the voltage generator as a short circuit.
 - (b) What is the reactance of the series element that will resonate the effective input reactance of the source?
 - (c) What is the input admittance of the load?
 - (d) What is the shunt reactance required to resonate the load?
 - (e) What is the resistive matching problem? That is, since the reactances of the load and source have been resonated out of consid-
- eration, what are the effective source and load resistances. Derive the required matching network. Keep the element values of the matching network as reactances.
 - (f) Draw the complete matching network showing source and load elements required for resonance as well as the matching network for the resistive problem. Keep the element values as reactances.
 - (g) Draw the final matching network combining all resonant and matching elements. Keep the element values as reactances. This is the electrical design of the matching network.
 - (h) Calculate the inductance and capacitance values of the matching network.
13. Design a two-element matching network to interface a source with a $25\ \Omega$ Thevenin equivalent impedance to a load consisting of a capacitor in parallel with a resistor so that the load admittance is $Y_L = 0.02 + j0.02\text{ S}$. Use the absorption method to handle the reactive load.
14. Design a matching network to interface a source with a $25\ \Omega$ Thevenin equivalent impedance to a load consisting of a capacitor in parallel with a resistor so that the load admittance is $Y_L = 0.01 + j0.01\text{ S}$.
- (a) If the complexity of the matching network is not limited, what is the minimum Q that could possibly be achieved in the complete network consisting of the matching network and the source and load impedances?
 - (b) Outline the procedure for designing the matching network for maximum bandwidth if only four elements can be used in the network. You do not need to design the network.
15. Design a lumped-element matching network to match a source, with a Thevenin equivalent impedance of $50\ \Omega$, to a load that consists of a $100\ \Omega$ resistor in parallel with a 5 pF capacitor. Design the matching network for maximum bandwidth at 1 GHz using no more than four lumped elements.
- (a) How many elements are there in the matching network?
 - (b) Outline how you will design the matching network.
 - (c) Design the matching network. You must draw the final design, including the source and load elements, and label each of the lumped elements using reactance values. (That is, do not calculate values of the inductance and capacitances in your design.) (Do not use a Smith chart.)

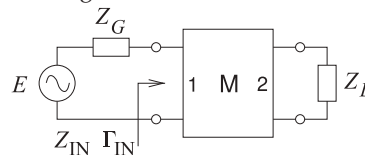
16. The output of a transistor amplifier is modeled as a current source in parallel with both a $50\ \Omega$ resistor and a $1\ \text{pF}$ capacitor. This is to be matched to a load consisting of a $25\ \Omega$ resistor in series with a $0.02\ \text{nH}$ inductor. The task is to design a matching network that will enable DC bias to be applied from the load to the transistor output, thus the matching network must be a lowpass type. The center frequency of the system is $10\ \text{GHz}$ and a bandwidth of $50\ \text{MHz}$ is required.
- What is the fractional bandwidth of the system?
 - What is the Q of the system?
 - Indicate the form of the matching network if no more than four reactive elements are to be used; that is, sketch the matching network.
 - Complete the design of the amplifier providing numerical element values.
17. Design a Pi network to match the source configuration to the load configuration below. The design frequency is $900\ \text{MHz}$ and the desired Q is 10.



18. Design a passive matching network that will achieve maximum bandwidth matching from a source with an impedance of $2\ \Omega$ (typical of the output impedance of a power amplifier) to a load with an impedance of $50\ \Omega$. The matching network can have a maximum of three reactive elements. You need only calculate reactances and not the capacitor and inductor values.
19. Design a passive matching network that will achieve maximum bandwidth matching from a source with an impedance of $20\ \Omega$ to a load with an impedance of $125\ \Omega$. The matching network can have a maximum of four reactive elements. You need only calculate reactances and not the capacitor and inductor values.
- Will you use two, three, or four elements in your matching network?
 - With a diagram, and perhaps equations, indicate the design procedure.
 - Design the matching network. It is sufficient to use reactance values.
20. Design a passive matching network that will achieve maximum bandwidth matching from a source with an impedance of $60\ \Omega$ to a load with an impedance of $5\ \Omega$. The matching network can

have a maximum of four reactive elements. You need only calculate reactances and not the capacitor and inductor values.

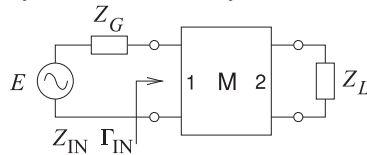
- Will you use two, three, or four elements in your matching network?
 - With a diagram and perhaps equations, indicate the design procedure.
 - Design the matching network. It is sufficient to use reactance values.
21. Design a T network to match a $50\ \Omega$ source to a $1000\ \Omega$ load. The desired loaded Q is 15.
22. Repeat Example 6.2 with an inductor in series with the load. Show that the inductance can be adjusted to obtain any positive shunt resistance value.
23. Design a three-lumped-element matching network that interfaces a source with an impedance of $5\ \Omega$ to a load with an impedance consisting of a resistor with an impedance of $10\ \Omega$. The network must have a Q of 6.
24. A source with a Thevenin equivalent impedance of $75\ \Omega$ must drive a load with an impedance of $5\ \Omega$. A matching network with maximum possible bandwidth between the source and the load must be designed to achieve maximum power transfer. Design the matching network for maximum possible bandwidth using no more than four reactive elements.
- Sketch the schematic of the matching network.
 - Describe the design procedure.
 - Complete the design of the matching network. Determine the values of the elements if the center frequency is $1\ \text{GHz}$.
25. A two-port matching network is shown below with a generator and a load. The generator impedance is $40\ \Omega$ and the load impedance is $Z_L = 50 - j20\ \Omega$. Use a Smith chart to design the matching network.



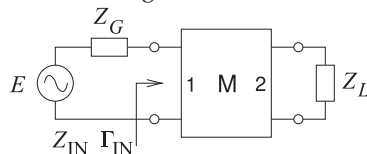
- What is the condition for maximum power transfer from the generator? Express your answer using impedances.
- What is the condition for maximum power transfer from the generator? Express your answer using reflection coefficients.
- What system reference impedance are you going to use to solve the problem?

- (d) Plot Z_L on the Smith chart and label the point. (Remember to use impedance normalization if required.)
- (e) Plot Z_G on the Smith chart and label the point.
- (f) Design a matching network using only transmission lines. Show your work on the Smith chart. You must express the lengths of the lines in terms of electrical length (either degrees or wavelengths). Characteristic impedances of the lines are required. (You will therefore have a design that consists of one stub and one other length of transmission line.)

26. A two-port matching network is shown below with a generator and a load. The generator impedance is 60Ω and the load impedance is $Z_L = 30 + j30 \Omega$. Use a Smith chart to design a lossless matching network. It is important that your solution can be followed, so you must indicate your solution clearly on the chart.



- (a) What is the condition for maximum power transfer from the generator? Express your answer using impedances.
 - (b) What is the condition for maximum power transfer from the generator? Express your answer using reflection coefficients.
 - (c) What system reference impedance are you going to use to solve the problem?
 - (d) Plot Z_L on the Smith chart and label the point. (Remember to use impedance normalization if required.)
 - (e) Plot Z_G on the Smith chart and label the point.
 - (f) Design a lossless lumped-element matching network showing your design process on the Smith chart. Label critical points on the Smith chart. Draw the matching network and show the reactance values.
27. A two-port matching network is shown below with a generator and a load. The generator impedance is 30Ω and the load impedance is $Z_L = 90 - j30 \Omega$. Use a Smith chart to design a lossless matching network.



- (a) What is the condition for maximum power transfer from the generator? Express your answer using impedances.
- (b) What is the condition for maximum power transfer from the generator? Express your answer using reflection coefficients.
- (c) What system reference impedance are you going to use to solve the problem?
- (d) Plot Z_L on the Smith chart and label the point. (Remember to use impedance normalization if required.)
- (e) Plot Z_G on the Smith chart and label the point.
- (f) Design a lossless matching network showing your design process on the Smith chart. Label critical points on the Smith chart. Draw the matching network and show the reactance values.

28. Use Smith chart techniques to design a double-stub matching network to match a load with a normalized admittance $y_L = 0.7 - j5$ to a source with a normalized admittance of 1. The stubs are short-circuited and are separated by a transmission line of length $\lambda/8$. The load is at the position of the first stub. All transmission lines have the system characteristic impedance. Your design should yield the lengths of the two stubs.

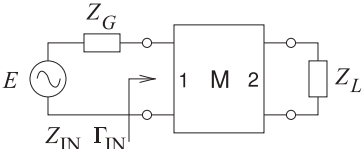
- (a) Plot the load on a Smith chart. Clearly indicate the load.
- (b) Determine the admittances of each of the stubs. Clearly show and describe your design technique so that it can be understood. Label your efforts on a Smith chart and describe the design steps. Note that a description is required and not simply markings on a Smith chart.
- (c) Determine the electrical lengths of the stubs (express your answer in terms of wavelengths or degrees).

29. Use a lossless transmission line and a series reactive element to match a source with a Thevenin equivalent impedance of $25 + j50 \Omega$ to a load of 100Ω . (That is, use one transmission line and one series reactance only.)

- (a) Draw the matching network with the source and load.
- (b) What is the value of the series reactance in the matching network (you can leave this in ohms)?
- (c) What is the length and characteristic impedance of the transmission line?

30. Consider a load $Z_L = 100 - j150 \Omega$. Use the Smith chart to design a two-stub matching network that will match the load to a 50Ω genera-

tor. Use $50\ \Omega$ transmission lines throughout and assume that the load is immediately next to the first stub. The two stubs are separated by a line with an electrical length of 45° . Both stubs are short-circuited.

- (a) Draw the matching stub system.
 - (b) What is the normalized load impedance?
 - (c) Briefly indicate the procedure used to design the two-stub matching network. You will need to use stylized Smith charts.
 - (d) Plot the load on a Smith chart.
 - (e) What is the admittance of the first stub (Stub 1)?
 - (f) What is the electrical length of Stub 1? (Note that the stub is short circuited.)
 - (g) What is the admittance of the second stub near the generator (Stub 2)?
 - (h) What is the electrical length of Stub 2? (Note that the stub is short circuited.)
31. Consider a load $Z_L = 80 + j40\ \Omega$. Use the Smith chart to design a matching network consisting of only two transmission lines that will match the load to a generator of $40\ \Omega$.
- (a) Draw the matching network with transmission lines. If you use a stub, it should be a short-circuited stub.
 - (b) Indicate your choice of characteristic impedance for your transmission lines. What is the normalized load impedance? What is the normalized source impedance?
 - (c) Briefly outline the design procedure you will use. You will need to use Smith chart sketches.
 - (d) Plot the load and source on a Smith chart.
 - (e) Complete the design of the matching network, providing the lengths of the transmission lines.
32. A two-port matching network is shown below with a generator and a load. The generator impedance is $40\ \Omega$ and the load impedance is $Z_L = 20 - j50\ \Omega$. Use a Smith chart to design the matching network.
- 
- (a) What is the condition for maximum power transfer from the generator? Express your answer using impedances.
 - (b) What is the condition for maximum power transfer from the generator? Express your answer using reflection coefficients.
 - (c) What system reference impedance are you going to use to solve the problem?
 - (d) Plot Z_L on a Smith chart and label the point. (Remember to use impedance normalization if required.)
 - (e) Plot Z_G on a Smith chart and label the point.
 - (f) Design a matching network using only transmission lines and show your work on a Smith chart. You must express the lengths of the lines in terms of electrical length (either degrees or wavelengths long). Characteristic impedances of the lines are required. (You will therefore have a design that consists of one stub and one other length of transmission line.)
33. Use a Smith chart to design a microstrip network to match a load $Z_L = 10 - j30\ \Omega$ to a source $Z_S = 60 + j40\ \Omega$. Use a substrate with permittivity $\epsilon_r = 10.0$ and thickness $500\ \mu\text{m}$.
- (a) What is the condition for maximum power transfer?
 - (b) Develop the electrical design of the matching network using the Smith chart using $50\ \Omega$ lines only.
 - (c) Develop the full physical design of the matching network. Draw the microstrip layout and label critical dimensions. That is, you need to find the dimensions of the microstrip circuit.
34. Use a Smith chart to develop the electrical design of a microstrip network to match a load $Z_L = 25\ \Omega$ to a source $Z_S = 250\ \Omega$. Use only $50\ \Omega$ transmission lines. Use one series transmission line and one open-circuited stub. You must use an actual Smith chart and not a sketch of one. Answer parts b, c, and j-q, on a sheet separate from the Smith chart. Make your work easy to follow.
- (a) Draw the matching network problem labeling the matching network as M.
 - (b) What is the condition for maximum power transfer in terms of the source impedance?
 - (c) What is the condition for maximum power transfer in terms of the source reflection coefficient?
 - (d) Use a $50\ \Omega$ reference impedance and plot the normalized source and load impedances on a Smith chart.
 - (e) Draw the locus (as the line length increases) of the reflection coefficient looking into a $50\ \Omega$ line terminated in the source impedance.
 - (f) Draw the locus of the reflection coefficient looking into a $50\ \Omega$ line terminated in the load impedance.

- (g) Draw the locus of a shunt susceptance in parallel with the source (with the shunt susceptance varying in value).
- (h) Draw the locus of a shunt susceptance in parallel with the load.
- (i) Hence identify two matching network designs on the Smith chart identifying them as Design 1 and Design 2. Make the trajectory of the designs clearly visible including directions and label the critical lengths and susceptances on the Smith chart.
- (j) Draw the topology of your Design 1 indicating the source and load ends and labeling critical dimensions?
- (k) What is the length of the series transmission line in your Design 1?
- (l) What is the normalized input admittance of the stub in your Design 1?
- (m) What is the length of the open-circuited stub in your Design 1?
- (n) Draw the topology of your Design 2 indicating the source and load ends and labeling critical dimensions?
- (o) What is the length of the series transmission line in your Design 2?
- (p) What is the normalized input admittance of the stub in your Design 2?
- (q) What is the length of the open-circuited stub in your Design 2?
35. Repeat exercise 34 but now with $Z_L = 200 \Omega$ and $Z_S = 20 \Omega$.
36. Use a Smith chart to design a microstrip network to match a load $Z_L = 100 - j100 \Omega$ to a source $Z_S = 34 - j40 \Omega$. Use transmission lines only and do not use short-circuited stubs. Use a reference impedance of 40Ω .
- (a) Draw the matching network problem labeling impedances and the impedance looking into the matching network from the source as Z_1 .
- (b) What is the condition for maximum power transfer in terms of impedances?
- (c) What is the condition for maximum power transfer in terms of reflection coefficients?
- (d) Identify, i.e. draw, at least two suitable microstrip matching networks.
- (e) Develop the electrical design of the matching network using the Smith chart using 40Ω lines only. You only need do one design.
- (f) Draw the microstrip layout of the matching network identify critical parameters such characteristic impedances and electrical length. Ensure that you identify which is the source side and which is the load side. You do not need to determine the widths of the lines or their physical lengths.
37. Repeat exercise S10.31 but now with $Z_L = 10 - j40 \Omega$ and $Z_S = 28 - j28 \Omega$.
38. Use a Smith chart to design a two-element lumped-element lossless matching network to interface a source with an admittance $Y_S = 6 - j12 \text{ mS}$ to a load with admittance $Y_L = 70 - j50 \text{ mS}$.
39. Use a Smith chart to design a two-element lumped-element lossless matching network to interface a load $Z_L = 50 + j50 \Omega$ to a source $Z_S = 10 \Omega$.

6.12.1 Exercises by Section

[†]challenging

§6.3 1, 2

§6.4 3, 4

§6.5 5, 6, 7, 8, 9, 10, 11[†], 12[†], 13[†],

14[†], 15[†], 16[†], 17[†]

§6.6 18[†], 19[†], 20[†], 21[†], 22[†], 23[†],

24[†]

§6.7 25[†], 26[†], 27[†], 28[†], 29[†], 30[†],

31[†], 32[†]

§6.9 33[†], 34, 35, 36, 37, 38, 39

6.12.2 Answers to Selected Exercises

11 $43.6 - j106 \Omega$

12(g) series: $j219 \Omega$, shunt: $-j225 \Omega$

16(b) 200

19(c) $Q = 1.22467$

22 $C = 1/(\omega_d^2 L_P)$

25(d) $1.25 - j0.5$

29(b) $-j50 \Omega$

32(f) 40Ω , 0.085λ long line before load, 40Ω , 0.076λ long shorted stub

Broadband Matching

7.1	Introduction	205
7.2	Fano-Bode Limits	206
7.3	Constant Q Circles	207
7.4	Stepped-Impedance Transmission Line Transformer	209
7.5	Tapered Matching Transformers	217
7.6	Matching a Series RC load	225
7.7	Broadband Matching to Reactive Loads	231
7.8	Summary	234
7.9	References	235
7.10	Exercises	235

7.1 Introduction

This chapter presents techniques for developing broadband matching networks. Sometimes these are akin to cascaded two-port matching networks. The general concept that works most of the time is to gradually step from an initial impedance to a final impedance. Design of broadband matching networks should also be done with the understanding that many RF systems will have multiple matching networks and so the maximum passband transmission loss of an individual matching network needs to be a fraction of a decibel so that when multiple networks are cascaded the insertion loss at the overall band edges will accumulate to equal the desired limit on loss. It is common to use a 1 dB insertion loss threshold to define bandwidth so the individual matching networks may need to have a bandwidth defined by a loss that is much less with insertion loss thresholds as low as 0.1 dB often used.

Bandwidth is limited by energy storage and Section 7.2 introduces the Fano-Bode limits which are theoretical limits of what can be achieved in matching given reactive loads. It is not possible to exceed the Fano-Bode limits on bandwidth. Section 7.3 introduces the constant Q circles plotted on Smith charts to provide a visual guide for the design of broadband matching networks. The next three sections describe three types of broadband matching networks. The first, in Section 7.4, describes the stepped-impedance transmission line transformer which is a generalization of the quarter-wave transformer. Section 7.5 describes tapered transmission-line

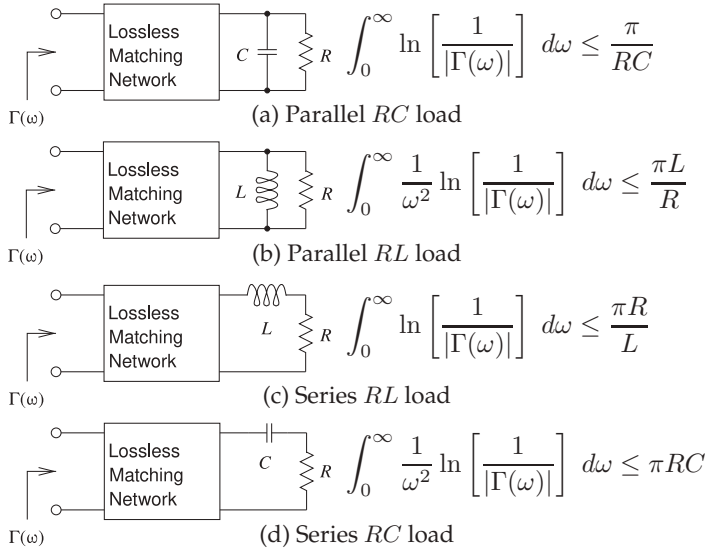


Figure 7-1: Fano-Bode limits for circuits with reactive loads.

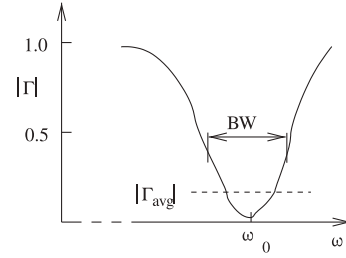


Figure 7-2: Response looking into matching network used in defining nonintegral Fano-Bode criteria. The bandwidth of the passband (low Γ , is BW).

transformers which are generalizations of stepped impedance broadband matching networks. An approach to broadband matching to reactive loads is described in Section 7.7.

7.2 Fano-Bode Limits

A complex load having energy storage elements limits the bandwidth of the match achieved by a matching network. Theoretical limits addressing the bandwidth and the quality of the match were developed by Fano [1, 2] based on earlier work by Bode [3]. These theoretical limits are known as the Fano-Bode criteria or the Fano-Bode limits. The limits for simple loads are shown in Figure 7-1. More general loads are treated by Fano [1]. The Fano-Bode criteria are used to justify the broad assertion that the more reactive energy stored in a load, the narrower the bandwidth of a match.

The Fano-Bode criteria include the term $1/|\Gamma(\omega)|$, which is the inverse of the magnitude of the reflection coefficient looking into the matching network, as shown in Figure 7-1. A matching network provides matching over a radian bandwidth BW, and outside the matching frequency band the magnitude of the reflection coefficient approaches 1. Introducing Γ_{avg} as the average absolute value of $\Gamma(\omega)$ within the passband, and with $f_0 = \omega_0/(2\pi)$ as the center frequency of the match (see Figure 7-2), then the four Fano-Bode criteria shown in Figure 7-1 can be written as

$$\text{Parallel RC load:} \quad \frac{\text{BW}}{\omega_0} \ln \left(\frac{1}{\Gamma_{\text{avg}}} \right) \leq \frac{\pi}{R(\omega_0 C)} \quad (7.1)$$

$$\text{Parallel RL load:} \quad \frac{\text{BW}}{\omega_0} \ln \left(\frac{1}{\Gamma_{\text{avg}}} \right) \leq \frac{\pi(\omega_0 L)}{R} \quad (7.2)$$

$$\text{Series RL load:} \quad \frac{\text{BW}}{\omega_0} \ln \left(\frac{1}{\Gamma_{\text{avg}}} \right) \leq \frac{\pi R}{(\omega_0 L)} \quad (7.3)$$

$$\text{Series RC load:} \quad \frac{\text{BW}}{\omega_0} \ln \left(\frac{1}{\Gamma_{\text{avg}}} \right) \leq \pi R(\omega_0 C). \quad (7.4)$$

In terms of reactance and susceptance these can be written as

$$\begin{array}{ll} \text{Parallel load:} & \text{Series load:} \\ \frac{BW}{\omega_0} \ln \left(\frac{1}{\Gamma_{\text{avg}}} \right) \leq \frac{\pi G}{|B|} & \frac{BW}{\omega_0} \ln \left(\frac{1}{\Gamma_{\text{avg}}} \right) \leq \frac{\pi R}{|X|}, \end{array} \quad (7.5) \quad (7.6)$$

where $G = 1/R$ is the conductance of the load, B is the load susceptance, and X is the load reactance. BW/ω_0 is the fractional bandwidth of the matching network. Equations (7.5) and (7.6) indicate that the greater the proportion of energy stored reactively in the load compared to the power dissipated in the load, the smaller the fractional bandwidth (BW/ω_0) for the same average in-band reflection coefficient Γ_{avg} .

Equations (7.5) and (7.6) can be simplified one step further:

$$\frac{BW}{\omega_0} \ln \left(\frac{1}{\Gamma_{\text{avg}}} \right) \leq \frac{\pi}{Q}, \quad (7.7)$$

where Q is that of the load. Several general results can be drawn from Equation (7.7) as follows:

1. If the load stores any reactive energy, so that the Q of the load is nonzero, the in-band reflection coefficient looking into the matching network cannot be zero across the passband.
2. The higher the Q of the load, the narrower the bandwidth of the match for the same average in-band reflection coefficient.
3. The higher the Q of the load, the more difficult it will be to design the matching network to achieve a specified matching bandwidth.
4. A match over all frequencies is only possible if the Q of the load is zero; that is, if the load is resistive. In this case a resistive load could be matched to a resistive source by using a magnetic transformer. Using a matching network with lumped L and C components will result in a match over a finite bandwidth. However, with more than two L and C elements the bandwidth of the match can be increased.
5. Multielement matching networks are required to maximize the matching network bandwidth and minimize the in-band reflection coefficient. The matching network design becomes more difficult as the Q of the load increases.

7.3 Constant Q Circles

One strategy for wideband matching is based on the concept of matching to an intermediate resistance that is the geometric mean of the source and load impedances. This concept was introduced in Section 6.6 and can be generalized to intermediate impedances and can be represented on a Smith chart using constant Q as shown in Figure 7-3. If the load and source impedances, R_L and R_S , are resistive, then the normalizing resistance (R_v) of the Smith chart should (although it is not necessary) be chosen as the geometric mean of the source and load resistance (i.e., $R_v = \sqrt{R_L R_S}$). To maintain a specific circuit Q , and hence bandwidth, the locus of impedances in the design must stay within or touch, the corresponding constant Q circle.

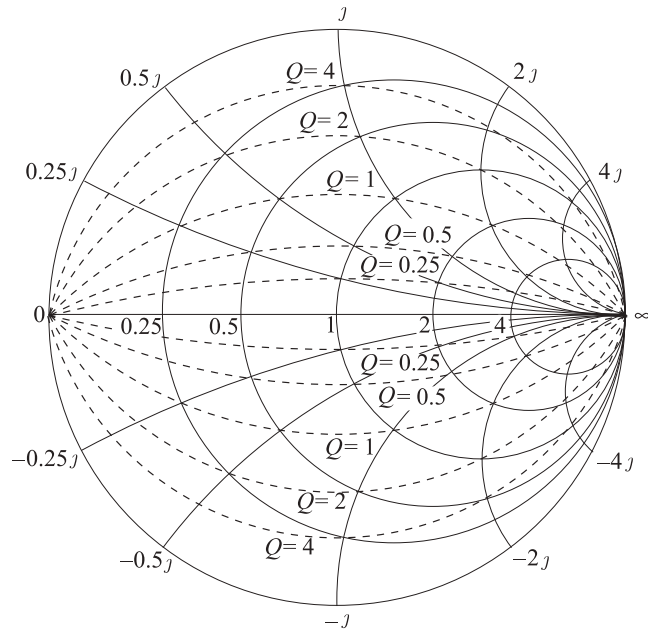


Figure 7-3: Impedance Smith chart with constant Q circles.

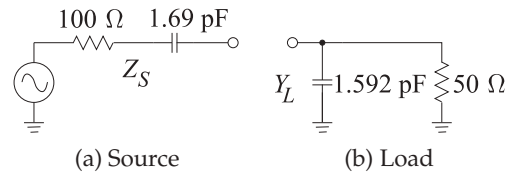


Figure 7-4: Matching problem in Example 7.1.

EXAMPLE 7.1

Broadband Matching Using Constant Q Circles

Design a broadband matching network at 1 GHz for the situation shown in Figure 7-4.

Solution:

$Z_S = 100 - j94.25 \, \Omega$, $Y_L = 0.02 + j0.01 \, \text{S}$, and $Z_L = 40.0 - j20.0 \, \Omega$. Normalizing these to $100 \, \Omega$ results in $z_S = 1 - j0.9425$, $y_L = 2 + j1$, and $z_L = 0.400 - j0.200$. Also the Q of the source, $Q_S = 0.9425$ and the Q of the load is $Q_L = 0.500$. The matching design puts a network in front of z_L to present an impedance z_S^* to the source. These values are plotted in Figure 7-5. The design objective is to maintain maximum bandwidth and this is done by staying inside the $Q = 0.9425$ circle, where the Q is the larger of the source and load Q s.

Design can proceed by moving back from the load toward the source, or from the source to the load. Most commonly the perspective used is moving back from the load. Then the load z_L is transformed to z_S^* . Maximum bandwidth is approximately achieved if the matching stages do not exceed the maximum Q of the load or of the source. So the Q of the stages cannot exceed 0.9425. An appropriate matching concept is shown in Figure 7-6. The locus is $B \rightarrow C \rightarrow D \rightarrow E \rightarrow F \rightarrow G \rightarrow A$. The matching network is therefore of the form shown in Figure 7-7. The rest of the design is extraction of numerical values, but the difficult part of the design has been done.

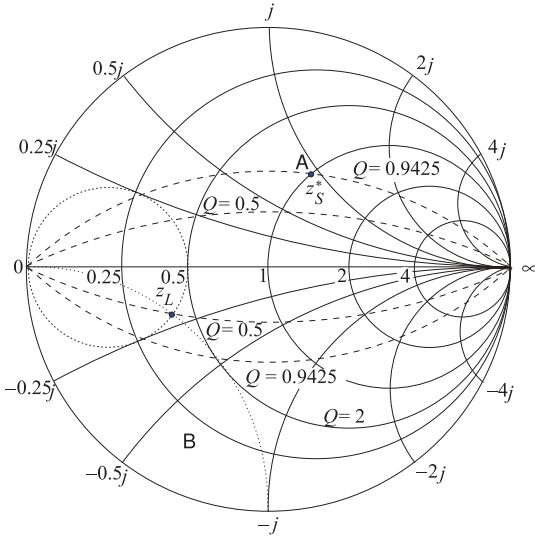


Figure 7-5: Impedance Smith chart indicating the matching problem in Example 7.1 with load and source plotted and their constant Q circles. The normalization impedance is $100\ \Omega$.

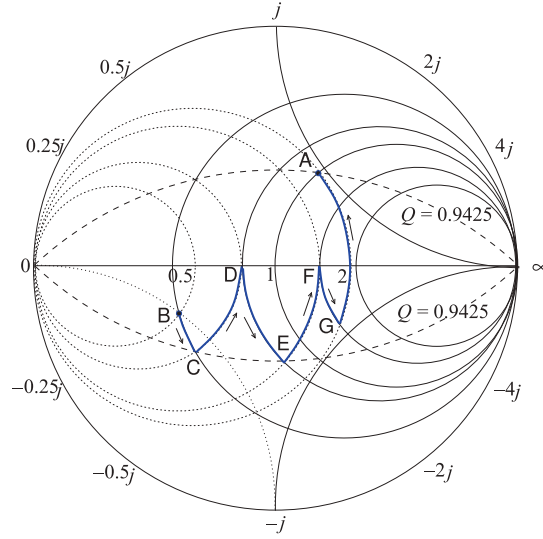


Figure 7-6: Outline of matching concept in Example 7.1.

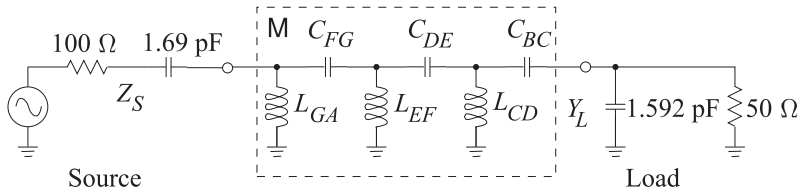


Figure 7-7: Matching network M in Example 7.1.

7.4 Stepped-Impedance Transmission Line Transformer

The wideband matching techniques described in this section use multiple quarter-wavelength-long transmission line sections with the lines having characteristic impedances which are stepped from the source impedance to the load impedance. They are conceptual extensions of the quarter-wave transformer and differ by how the characteristic impedances of the sections are chosen. The methods strictly are applicable to resistive source and load impedances yet achieve reasonably wideband matches with moderately reactive source and load impedances.

7.4.1 Quarter-Wave Transformer using Geometric Means

Design here uses multiple quarter-wave long transmission lines the characteristic impedances of which are chosen as geometric means of the source and load impedances. The procedure is described in the next example.

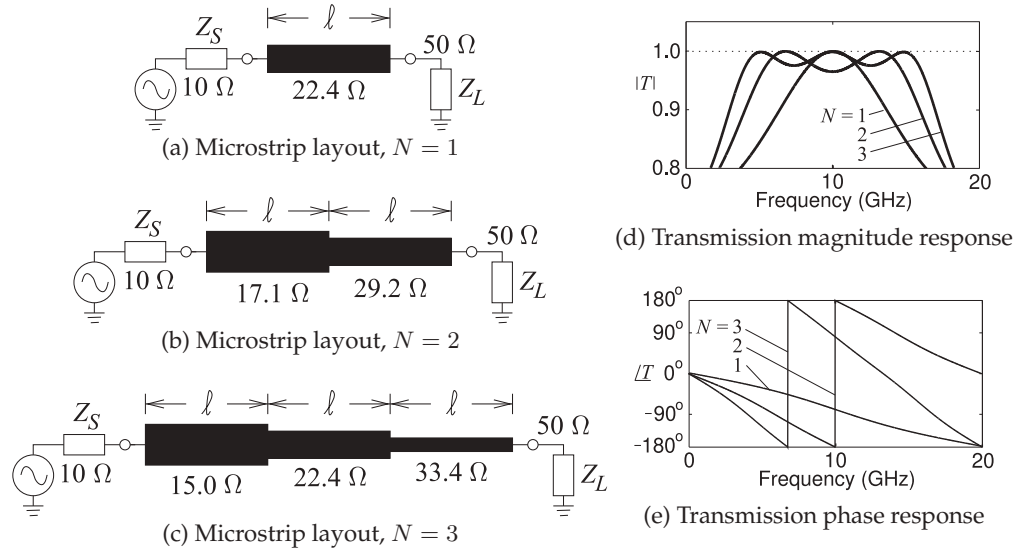


Figure 7-8: Transmission line transformer designed in Example 7.2. Each section is of length $\ell = \lambda_g/4 = 2.83$ mm where λ_g is the midband wavelength (at 10 GHz).

EXAMPLE 7.2

Multisection Quarter-Wave Transmission Line Transformer

Design one-, two, and three-section quarter-wave transformers in microstrip to connect a power amplifier with an output impedance of $10\ \Omega$ to a $50\ \Omega$ cable.

Solution:

The parameters are $Z_S = 10\ \Omega$ and $Z_L = 50\ \Omega$. The characteristic impedance of a single, $N = 1$, quarter-wave transformer is $Z_{01} = \sqrt{Z_S Z_L} = 22.36\ \Omega$.

With a two-section, $N = 2$, quarter-wave transformer (using geometric means)

$$Z_{01} = \sqrt[3]{Z_S^2 Z_L} = 17.10\ \Omega \quad Z_{02} = \sqrt[3]{Z_S Z_L^2} = 29.24\ \Omega.$$

With a three-section, $N = 3$, quarter-wave stepped-impedance transformer

$$Z_{01} = \sqrt{Z_S Z_{02}} = 14.95\ \Omega \quad Z_{02} = \sqrt{Z_S Z_L} = 22.36\ \Omega \quad Z_{03} = \sqrt{Z_{02} Z_L} = 33.44\ \Omega. \quad (7.8)$$

The microstrip layouts are shown in Figure 7-8 where each section is a quarter-wavelength long at mid band. The simulated transmission characteristics of the design realized at 10 GHz (on alumina, $\epsilon_r = 10$, and attenuation of 1.87 dB/m are shown in Figure 7-8(d and e).

7.4.2 Design Based on the Theory of Small Reflections

Another design method for choosing the characteristic impedances of cascaded lines is based on the theory of small reflections [4, 5]. The reflection coefficients at each boundary in Figure 7-9 are defined as

$$\Gamma_0 = \frac{Z_{01} - Z_S}{Z_{01} + Z_S} \quad \Gamma_n = \frac{Z_{n+1} - Z_n}{Z_{n+1} + Z_n} \quad \Gamma_N = \frac{Z_L - Z_{0N}}{Z_L + Z_{0N}}. \quad (7.9)$$

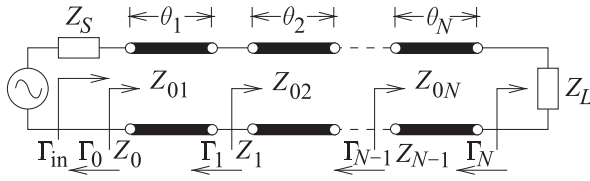


Figure 7-9: Stepped-impedance transmission line transformer with the n th section having characteristic impedance Z_{0n} and electrical length θ_n . Γ_n is the reflection coefficient, and Z_n the impedance, considering only the $(n + 1)$ th line.

As these are small reflections (since Z_{0n} changes gradually) the theory of small reflections (described in Section 2.6.5 of [6]) can be invoked and so, using Equation ((2.201) of [6]), the total reflection coefficient seen from the source Z_S is

$$\Gamma_{\text{in}} \approx \Gamma_0 + e^{-2j\theta_1} (\Gamma_1 + e^{-2j\theta_2} (\Gamma_2 + \dots e^{-2j\theta_N} \Gamma_N)). \quad (7.10)$$

It is now necessary to make a design choice. It has been found that a multisection transformer that provides a good broadband match at both the source and load has symmetrical reflection coefficients, i.e. $\Gamma_n = \Gamma_{N-n}$ [5]. Another design choice is that the electrical lengths of the sections are the same, i.e. $\theta_n = \theta$. Then Equation (7.10) becomes

$$\Gamma_{\text{in}} = \Gamma_0 + \Gamma_1 e^{-2j\theta_1} + \Gamma_2 e^{-4j\theta_2} + \dots + \Gamma_N e^{-2jN\theta_N} \quad (7.11)$$

$$\begin{aligned} &= \Gamma_0 [1 + e^{-2jN\theta}] + \Gamma_1 [e^{-2j\theta} + e^{-2j(N-1)\theta}] + \dots \\ &= e^{-jN\theta} \left\{ \Gamma_0 [e^{jN\theta} + e^{-jN\theta}] + \Gamma_1 [e^{j(N-2)\theta} + e^{-j(N-2)\theta}] + \dots \right\} \\ &= 2e^{-jN\theta} \{ \Gamma_0 \cos(N\theta) + \Gamma_1 \cos[(N-2)\theta] + \dots \} \end{aligned} \quad (7.12)$$

using the trigonometric identity $\cos x = \frac{1}{2}(e^{jx} + e^{-jx})$ (and this is where symmetry is used). The last term in Equation (7.12) is $\frac{1}{2}\Gamma_{N/2}$ if N is even and $\Gamma_{(N-1)/2} \cos \theta$ if N is odd. The design variables here are the reflection coefficients at each line boundary (from which the characteristic impedances of the lines can be found) and the mid-band electrical length θ_0 .

The general design approach is to assume a functional form for $\Gamma_{\text{in}}(\theta)$ and then to derive the Γ_n s that result in that functional form. $\Gamma_{\text{in}}(\theta)$ will now be used to indicate that Γ_{in} is a function of θ and hence of frequency. Also the mid-band electrical length θ_0 is set to $\pi/2$ corresponding to the sections being a quarter-wavelength long. This may seem arbitrary but it has been shown to be optimum [7] (for maximum bandwidth). The final design step is to derive the characteristic impedances of the line sections. Using Equation (7.9)

$$Z_{0N} = Z_L \left(\frac{1 - \Gamma_N}{1 + \Gamma_N} \right) \quad \text{and} \quad Z_{0n} = Z_{0(n+1)} \left(\frac{1 - \Gamma_n}{1 + \Gamma_n} \right). \quad (7.13)$$

7.4.3 Maximally Flat Stepped Impedance Transformer

The design objective here is to set the first N derivatives of Γ_{in} at midband to zero. This results in a very smooth response and that is what is desired in some situations. If the following assignment is made

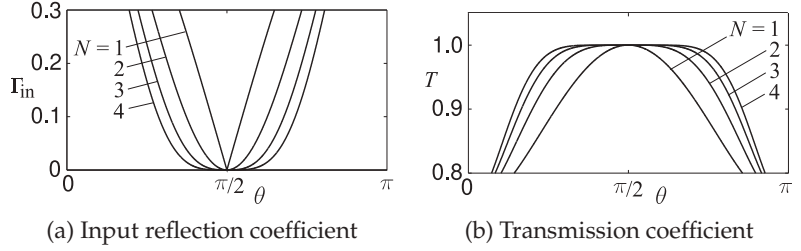
$$|\Gamma_{\text{in}}(\theta)| \propto |\cos(\theta)|^N \quad (7.14)$$

then $d^n |\Gamma_{\text{in}}(\theta)| / d\theta^n = 0$ at $\theta = \pi/2 = \theta_0$ for $n = 0, 1, \dots, (N - 1)$. An assignment that results in this is the binomial expansion

$$\Gamma_{\text{in}}(\theta) = A (1 + e^{-2j\theta})^N = \sum_{n=0}^N \binom{N}{n} e^{-2jn\theta} \quad (7.15)$$

Figure 7-10:

Characteristics of order $N = 1, 2, 3$ and 4 maximally flat stepped-impedance transformers with an impedance mismatch $\delta_z = \max(Z_L/Z_S, Z_S/Z_L) = 2$.



where (since N and n are integers)

$$\binom{N}{n} = \frac{N!}{(N-n)!n!} \quad (7.16)$$

is the binomial coefficient. Equating Equations (7.11) and (7.15)

$$\Gamma_n = A \binom{N}{n}. \quad (7.17)$$

To find A consider zero frequency. Then $\theta = 0$ and the transformer has no effect and Γ_{in} is just the mismatch of the source and load impedances and Equation (7.15) becomes

$$\Gamma_{in}(0) = A2^N = \frac{Z_L - Z_S}{Z_L + Z_S} \quad \text{so that} \quad A = 2^{-N} \left(\frac{Z_L - Z_S}{Z_L + Z_S} \right). \quad (7.18)$$

$$\text{Thus} \quad \Gamma_n(\theta) = 2^{-N} \left(\frac{Z_L - Z_S}{Z_L + Z_S} \right) \binom{N}{n} \quad (7.19)$$

and Z_{0n} comes from Equation (7.13) with the design accuracy determined by the approximation of a small discontinuity at each transmission line boundary.

The reflection Γ_{in} and transmission T characteristics of maximally flat stepped-impedance transformers are shown in Figure 7-10 for various orders. As with all lossless two-ports $|T| = \sqrt{1 - |\Gamma_{in}|^2}$. It can be seen that the bandwidth increases with increasing order and the transmission is remarkably flat.

EXAMPLE 7.3

Maximally Flat Multisection Transmission Line Transformer

Design a three-section maximally flat stepped-impedance transformer in microstrip to connect a $Z_S = 5 \Omega$ source to a $Z_L = 50 \Omega$ load.

Solution:

The design will have three transmission lines of different characteristic impedance and each section will be a quarter-wavelength long at mid band. Now $N = 3$ so from Equation (7.19)

$$\Gamma_n = 2^{-N} \left(\frac{Z_L - Z_S}{Z_L + Z_S} \right) \binom{N}{n} = 2^{-3} \left(\frac{50 - 5}{50 + 5} \right) \binom{3}{n} = \frac{45}{8 \cdot 55} \binom{3}{n}. \quad (7.20)$$

$$\Gamma_3 = 0.1023 \frac{3!}{0!3!} = \frac{1}{16} \frac{3 \cdot 2 \cdot 1}{1 \cdot 3 \cdot 2 \cdot 1} = 0.1023, \quad \Gamma_2 = 0.3068, \quad \Gamma_1 = 0.3068, \quad \Gamma_0 = 0.1023$$

resulting in (a sanity check is the expectation that $Z_L > Z_{03} > Z_{02} \dots$)

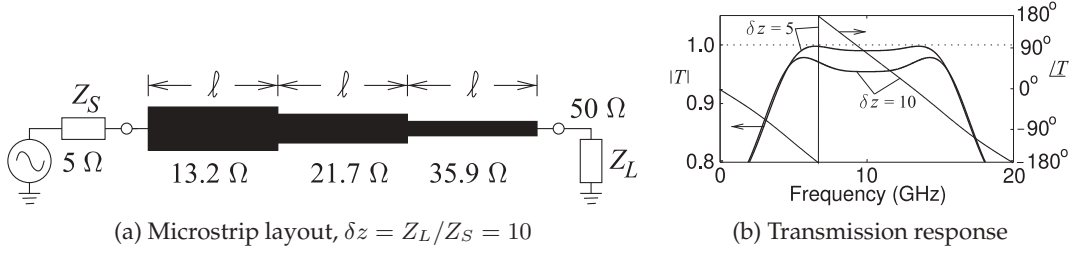


Figure 7-11: Maximally flat transmission line transformer designed in Example 7.3. At 10 GHz each section is of length $\ell = \lambda_g/4 = 2.83$ mm where λ_g is the midband wavelength.

$$Z_{03} = 50 \frac{1 - 0.1023}{1 + 0.1023} \Omega = 40.72 \Omega, \quad Z_{02} = 21.60 \Omega, \quad Z_{01} = 11.46 \Omega, \quad \text{and} \quad Z'_S = 9.333 \Omega$$

where Z'_S is ideally (the complex conjugate of) the original Z_S but is actually significantly different. This is because the design is based on the theory of small reflections and so multiple reflections at the transmission line boundaries were not considered. As a further investigation, and noting that each section is a quarter-wavelength long at midband, another estimate for Z_S , call this Z''_S , is found using Equation ((2.132)) of [6],

$$Z_2 = Z_{03}^2/Z_L = 33.16 \Omega, \quad Z_1 = Z_{02}^2/Z_2 = 14.07 \Omega, \quad Z''_S = Z_{01}^2/Z_1 = 9.334 \Omega.$$

The microstrip layout is shown in Figure 7-11(a). Simulation of the design realized at 10 GHz (on alumina, $\epsilon_r = 10$, a 2.83 mm section length, and a line attenuation of 1.87 dB/m for an overall attenuation of 0.016 dB) results in the transmission characteristics identified by $\delta z = Z_L/Z_S = 10$ in Figure 7-11(b). The final design does not have the ideal maximally flat transmission characteristics and this is due to deficiencies in the small reflection assumption. Final design requires a small amount of optimization as the synthesized design has a maximum in-band insertion loss of 0.4 dB ($T = 0.953$).

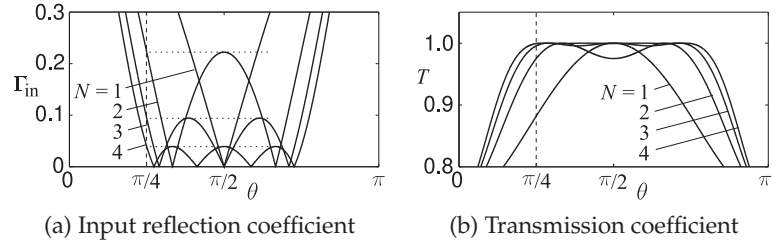
Repeating the design with $Z_S = 10 \Omega$ and $Z_L = 50 \Omega$ results in $\Gamma_0 = \Gamma_3 = 0.08333$, $\Gamma_1 = \Gamma_2 = 0.2500$, $Z_{01} = 15.23 \Omega$, $Z_{02} = 25.38 \Omega$, $Z_{03} = 42.31 \Omega$, and $Z'_S = Z''_S = 12.89 \Omega$. The transmission characteristics are identified by $\delta z = Z_L/Z_S = 5$ in Figure 7-11(b). The minimum in-band transmission coefficient is 0.990 for a maximum insertion loss of 0.091 dB. Thus design accuracy improves for a lower impedance transformation ratio.

7.4.4 Stepped Impedance Transformer With Chebyshev Response

Expressing the input reflection coefficient Γ_{in} of a stepped-impedance transformer in terms of a Chebyshev polynomial results in a good match in-band that rapidly transitions outside the passband. Compared to the maximally flat transformer a much better match can be obtained for the same number of line sections if the resulting ripples in the passband can be tolerated. With reference to Equation (7.10), the design choice is

$$\begin{aligned} \Gamma_{in}(\theta) &= \Gamma_0 + e^{-2j\theta} (\Gamma_1 + e^{-2j\theta} (\Gamma_2 + \cdots e^{-2j\theta} \Gamma_N)) \\ &= Ae^{-jN\theta} T_N(\cos \theta / \cos \theta_m). \end{aligned} \quad (7.21)$$

Figure 7-12: Characteristics of order $N = 1, 2, 3$ and 4 Chebyshev stepped-impedance transformers with impedance mismatch $\delta_z = \max(Z_L/Z_S, Z_S/Z_L) = 2$ and $\theta_m = \pi/4$. The transmission ripple cannot be seen for $N \geq 3$.



where T_N is the N th order Chebyshev polynomial of the first kind (as described in Section 1.A.10 of [6]). In Equation (7.21) θ_m defines the passband of the transformer as being between $\theta_m \leq \theta \leq (\pi - \theta_m)$ and in the passband $|\Gamma_{in}(\theta)| \leq \Gamma_m$ and at $\theta = \theta_m$ and $\theta = (\pi - \theta_m)$ (the edges of the passband)

$$|\Gamma_{in}(\theta_m)| = |\Gamma_{in}(\pi - \theta_m)| = \Gamma_m = |AT_N(\cos \theta_m / \cos \theta_m)| = |AT_N(1)|. \quad (7.22)$$

$$\text{Since } |T_N(1)| = 1 \quad A = \Gamma_m \quad (7.23)$$

To proceed another expression is needed for A so that Γ_m , N , and θ_m (and thus bandwidth) can be related. This is obtained by considering the mismatch at zero frequency, that is when $\theta = 0$:

$$\Gamma_{in}(0) = \left| \frac{Z_L - Z_S}{Z_L + Z_S} \right| = AT_N(\sec \theta_m). \quad (7.24)$$

(where $\sec \theta_m = 1 / \cos \theta_m$) and so

$$A = \left| \frac{Z_L - Z_S}{Z_L + Z_S} \right| \frac{1}{T_N(\sec \theta_m)}. \quad (7.25)$$

Substituting for A in Equation (7.21) and using Equation (7.10) results in

$$\begin{aligned} e^{jN\theta} \Gamma_{in}(\theta) &= AT_N(\cos \theta / \cos \theta_m) = \left(\frac{Z_L - Z_S}{Z_L + Z_S} \right) \frac{T_N(\cos \theta / \cos \theta_m)}{T_N(\sec \theta_m)} \\ &= 2 \{ \Gamma_0 \cos(N\theta) + \Gamma_1 \cos[(N-2)\theta] + \dots \}. \end{aligned} \quad (7.26)$$

The expansion of $T_N(\cos \theta / \cos \theta_m)$ is given in Equation ((1.198)) of [6] and has terms in $\cos(m\theta)$ and so design (which requires Γ_m) proceeds by equating terms in Equation (7.26) having the same $\cos(m\theta)$ for $m = 1, \dots, N$. This will be illustrated in an example.

The reflection Γ_{in} and transmission T characteristics of Chebyshev stepped-impedance transformers are shown in Figure 7-12 for orders from one to four for $\theta_m = \pi/4$ (this indicates a 100% bandwidth). It is seen that the maximum inband Γ_{in} reduces with increasing order. So with a Chebyshev response there is a trade-off between passband ripple and bandwidth.

An expression for bandwidth of the match will now be developed. Equating Equations (7.23) and (7.25)

$$T_N(\sec \theta_m) = \frac{1}{\Gamma_m} \left| \frac{Z_L - Z_S}{Z_L + Z_S} \right| \quad (7.27)$$

Using the identity

$$T_N(\sec \theta_m) = \cosh(N \cosh^{-1}(\sec \theta_m)) = \frac{1}{\Gamma_m} \left| \frac{Z_L - Z_S}{Z_L + Z_S} \right| \quad (7.28)$$

Table 7-1: Relationship of order N , fractional bandwidth, impedance ratio $\delta z = \max(Z_L/Z_S, Z_S/Z_L)$, and reflection coefficient ripple Γ_m for a Chebyshev stepped-impedance transformer. A transmission ripple of 0.1 dB has $\Gamma_m = 0.151$. (For example, a two-section ($N = 2$) transformer has a 95.4% bandwidth with $\delta_z = 3.0$.)

$N =$	1	1	1	2	2	2	3	3	3	4	4	4	5	5	5
$\Gamma_m =$	0.05	0.1	0.151	0.05	0.1	0.151	0.05	0.1	0.151	0.05	0.1	0.151	0.05	0.1	0.151
δz	Fractional bandwidth, $\Delta f/f_0$														
1.0	∞	∞	∞	∞	∞	∞	∞	∞	∞	∞	∞	∞	∞	∞	∞
1.2	0.741	∞	∞	1.275	∞	∞	1.502	∞	∞	1.622	∞	∞	1.696	∞	∞
1.3	0.501	1.112	∞	1.069	1.526	∞	1.346	1.680	∞	1.500	1.759	∞	1.596	1.807	∞
1.4	0.388	0.819	1.441	0.951	1.333	1.714	1.252	1.544	1.808	1.425	1.655	1.856	1.534	1.722	1.885
1.6	0.278	0.571	0.907	0.814	1.134	1.395	1.137	1.396	1.588	1.330	1.540	1.689	1.455	1.629	1.750
1.8	0.224	0.455	0.708	0.735	1.024	1.250	1.066	1.310	1.483	1.271	1.471	1.607	1.405	1.573	1.684
2.0	0.192	0.388	0.598	0.683	0.951	1.158	1.018	1.252	1.415	1.229	1.424	1.554	1.369	1.534	1.641
2.5	0.149	0.300	0.458	0.604	0.844	1.026	0.943	1.162	1.313	1.164	1.351	1.607	1.313	1.472	1.574
3.0	0.128	0.256	0.390	0.561	0.784	0.954	0.900	1.110	1.254	1.125	1.307	1.426	1.280	1.436	1.535
4.0	0.106	0.213	0.324	0.513	0.718	0.874	0.850	1.051	1.188	1.081	1.257	1.372	1.241	1.393	1.490
6.0	0.085	0.179	0.271	0.471	0.660	0.804	0.805	0.997	1.128	1.040	1.211	1.322	1.204	1.354	1.449
8.0	0.082	0.164	0.249	0.452	0.634	0.772	0.784	0.971	1.100	1.020	1.189	1.299	1.187	1.335	1.429
10	0.078	0.156	0.236	0.441	0.618	0.754	0.772	0.957	1.083	1.009	1.176	1.285	1.176	1.323	1.417

and so
$$\theta_m = \sec^{-1} \left\{ \cosh \left[\frac{1}{N} \cosh^{-1} \left(\frac{1}{\Gamma_m} \left| \frac{Z_L - Z_S}{Z_L + Z_S} \right| \right) \right] \right\}. \quad (7.29)$$

The fractional bandwidth can be obtained by noting that θ and thus θ_m are proportional to frequency f . That is, $f = k\theta$. At the passband center frequency f_0 , $\theta = \pi/2$ and so $k = 2f_0/\pi$. Thus if f_m is the frequency at the lower band edge, $f_m = k\theta_m = 2f_0\theta_m/\pi$. Then the fractional bandwidth (with the passband defined by when $|\Gamma_{in}| \leq \Gamma_m$) is

$$\frac{\Delta f}{f_0} = \frac{2(f_0 - f_m)}{f_0} = 2 - \frac{4\theta_m}{\pi}. \quad (7.30)$$

Thus Equations (7.29) and (7.30) relate the fractional bandwidth, the maximum passband reflection coefficient Γ_m , the impedance mismatch $\delta z = \max(Z_L/Z_S, Z_S/Z_L)$, and the Chebyshev order, N . Table 7-1 enables the required transformer order to be selected for a specified bandwidth and impedance mismatch.

EXAMPLE 7.4

Chebyshev Multisection Transmission Line Transformer

Design a 100% bandwidth three-section Chebyshev stepped-impedance transformer in microstrip to connect a power amplifier with an output impedance of 10Ω to a 50Ω cable.

Solution:

The design parameters are $N = 3$, $Z_S = 10 \Omega$, and $Z_L = 50 \Omega$. From Equation (7.30) the fractional bandwidth $\Delta f/f_0 = 1 = 2 - (4\theta_m)/\pi$ so that $\theta_m = \pi/4$. Then, with $\sec \theta_m = 1/\cos \theta_m = 1/\cos(\pi/4) = \sqrt{2}$ and $T_3(\sqrt{2}) = 7.071$ (from Equation ((1.193) of [6])), Equation (7.25) yields

$$\Gamma_m = A = \left(\frac{Z_L - Z_S}{Z_L + Z_S} \right) \frac{1}{T_3(\sec \theta_m)} = \left(\frac{50 - 10}{50 + 10} \right) \frac{1}{7.071} = 0.09428. \quad (7.31)$$

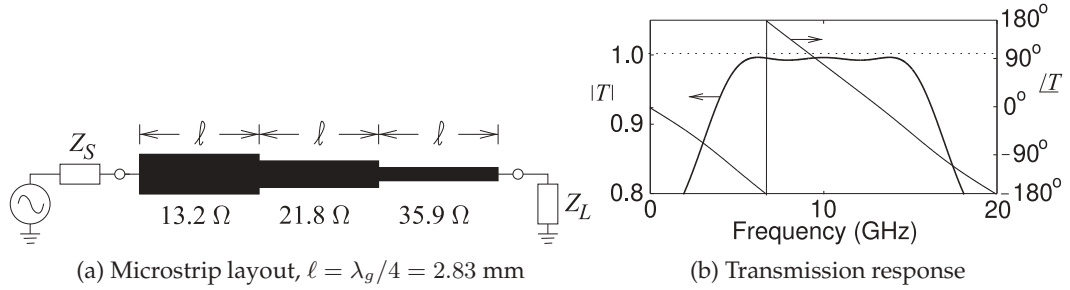


Figure 7-13: Chebyshev transformer of Example 7.4. (λ_g is the midband wavelength.)

Using Equation (7.26) and the Chebyshev expansion for T_3 this leads to

$$\begin{aligned} AT_3(\cos \theta / \cos \theta_m) &= A \{ \sec^3 \theta_m [\cos(3\theta) + 3 \cos \theta] - 3 \sec \theta_m \cos \theta \} \\ &= 2 [\Gamma_0 \cos(3\theta) + \Gamma_1 \cos(\theta)]. \end{aligned} \quad (7.32)$$

Thus after equating like terms in $\cos(m\theta)$ (noting that $\Gamma_n = \Gamma_{(N-n)}$ since symmetry is required)

$$\begin{aligned} \Gamma_0 = \Gamma_3 &= \frac{1}{2} A \sec^3 \theta_m = \frac{1}{2} 0.09428 \cdot (\sqrt{2})^3 = 0.1333 \\ \Gamma_1 = \Gamma_2 &= \frac{3}{2} A [\sec^3 \theta_m - \sec \theta_m] = \frac{3}{2} 0.09428 \cdot [(\sqrt{2})^3 - \sqrt{2}] = 0.2000 \end{aligned} \quad (7.33)$$

Then the characteristic impedances of the three line sections are (using Equation (7.13))

$$Z_{01} = 13.19 \, \Omega, \quad Z_{02} = 21.78 \, \Omega, \quad \text{and} \quad Z_{03} = 35.94 \, \Omega \quad (7.34)$$

and each section is a quarter-wavelength long at midband. The microstrip layout is shown in Figure 7-13(a). The simulated transmission characteristics of the design realized at 10 GHz (on alumina, $\epsilon_r = 10$, section lengths of 2.83 mm, and an attenuation of 1.87 dB/m (for an overall attenuation of 0.016 dB) are shown in Figure 7-13(b). The expected lossless ripple (from $T = \sqrt{1 - \Gamma_m^2} = 0.9955 = -0.039$ dB) is 0.039 dB. The simulated minimum insertion loss is 0.024 dB and the maximum in-band insertion loss is 0.057 dB for a passband ripple of 0.033 dB (line loss is known to reduce ripple).

7.4.5 Stepped Impedance Transformer Design

The multisection stepped-impedance transformers change the characteristic impedances of the section between the source and load resistances but do so in steps. It is possible to achieve a similar result by continuously tapering the characteristic impedance of the transmission line taper or, equivalently, tapering the width of microstrip line as shown in Figure 7-14.

7.4.6 Summary

The multisection impedance transformer design described in this section is based on transmission line sections each a quarter-wavelength long at the center frequency of the match. It is tempting to think that a better result could be obtained by having sections of various lengths. However it has been shown that optimum matching transformer designs are of the quarter-wave

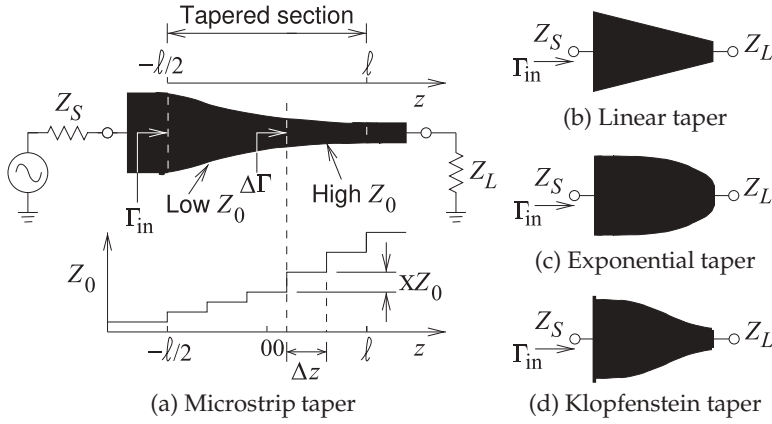


Figure 7-14: Tapered impedance transformers with length ℓ . The width of the microstrip line is approximately inversely proportional to the characteristic impedance of the line. (Here $Z_L > Z_S$ and both Z_L and Z_S are resistive.)

Chebyshev type and only minimum enhancement is possible [7].

7.5 Tapered Matching Transformers

Tapered impedance transformers match an impedance Z_S to an impedance Z_L using a transmission line having a characteristic impedance Z_0 that gradually and monotonically varies from Z_S to Z_L along the length of the line, see Figure 7-14. This figure references a microstrip line but the key aspect is the gradual change in characteristic impedance that applies to any transmission line. The central design problem is how to choose the function $Z_0(z)$. If the length of the line, ℓ here, is not constrained then the Klopfenstein taper [8, 9] is regarded as the optimum approach for design of the taper and will be discussed after first reviewing approaches used when the length of the line is constrained. Note that both Z_L and Z_S are resistive.

7.5.1 Small Reflection Theory and Tapered Lines

In this section the theory behind the synthesis of a taper is developed beginning with the theory of small reflections. The reflection at point z on the line for a taper segment of length Δz is (refer to Figure 7-14(a))

$$\Delta\Gamma = \frac{(Z_0(z) + \Delta Z) - Z_0(z)}{(Z_0(z) + \Delta Z) + Z_0(z)} = \frac{\Delta Z}{2Z_0(z) + \Delta Z} \approx \frac{\Delta Z}{2Z_0(z)}, \quad (7.35)$$

where $Z_0(z)$ is the characteristic impedance of the taper at z and ΔZ is the change of $Z_0(z)$ from one side of the taper segment to the other. In the limit as $\Delta Z \rightarrow 0$, ΔZ is replaced by dZ and $\Delta\Gamma$ is replaced by $d\Gamma$ so that Equation (7.35) becomes (and putting in differential operator form)

$$d\Gamma = \frac{dZ_0}{2Z_0(z)} \rightarrow \frac{d\Gamma}{dz} = \frac{1}{2Z_0(z)} \frac{dZ_0}{dz}. \quad (7.36)$$

The next step is to refer all of the small reflections, $\Delta\Gamma$, to the beginning of the taper at $z = -\ell/2$. The theory of small reflections is that these small reflections, accounting for the electrical lengths from the start of the taper to each taper segment, can be summed, see Equation (7.10). This is the same as saying that the small reflection from one taper segment is not affected by its own reflection from another taper segment. Noting that the electrical length

from the beginning of the taper to a taper segment at z is $\theta = \beta(\ell/2 + z)$, the reflection at the input of the tapered line is found as

$$\Gamma_{\text{in}}(\ell) = \int_{z=-\ell/2}^{z=\ell/2} e^{-2j(\ell/2+\beta z)} d\Gamma \quad (7.37)$$

$$= \frac{1}{2} e^{-j\beta\ell} \int_{-\ell/2}^{\ell/2} \frac{e^{-2j\beta z}}{Z_0(z)} \frac{dZ_0(z)}{dz} dz, \quad (7.38)$$

where Γ_{in} is shown explicitly as a function of the length of the taper. So the design problem becomes choosing the characteristic impedance function, $Z_0(z)$ to provide the desired input reflection coefficient Γ_{in} . This is difficult to achieve with the form of Equation (7.38). The problem can be simplified by noting that (and introducing Z_1 as a normalizing impedance so that the argument of \ln is dimensionless)

$$\begin{aligned} \frac{\ln(Z_0(z)/Z_1)}{dz} &= \frac{Z_1}{Z_0(z)} \frac{d(Z_0(z)/Z_1)}{dz} = \frac{Z_1}{Z_0(z)} \frac{1}{Z_1} \frac{d(Z_0(z)/Z_1)}{dz} \\ &= \frac{1}{Z_0(z)} \frac{d(Z_0(z)/Z_1)}{dz}, \end{aligned} \quad (7.39)$$

and so, making it clear that $d\Gamma$ varies along the taper,

$$d\Gamma(z) = \frac{1}{2} \frac{d(Z_0(z)/Z_1)}{dz} dz. \quad (7.40)$$

Thus after assuming the form of $Z_0(z)$, the incremental reflection coefficient $d\Gamma$ is obtained using Equation (7.37). Alternatively (after integrating Equation (7.40)) a form for Γ_{in} can be assumed and $d\Gamma(z)$ determined and then $Z_0(z)$. This will become clearer below when specific tapers are considered.

7.5.2 Linear taper

In the linear tapered line design $Z_0(z)$ varies linearly from the source impedance Z_S to Z_L :

$$Z_0(z) = Z_S + (Z_L - Z_S)z/\ell. \quad (7.41)$$

This is often approximated in microstrip by a linear taper of the width of the microstrip line as shown in Figure 7-14(b). A simple expression for the input reflection coefficient is not available and so must be found from simulation. This is the simplest taper and the taper performs better the greater its electrical length (i.e. at higher frequencies or longer physical length). The performance of the linear taper is compared to other tapers later.

7.5.3 Exponential taper

The exponential taper has an exponential taper of the line's characteristic impedance. Setting

$$Z_0(z) = Z_x e^{az} \quad \text{with} \quad a = \frac{1}{\ell} \ln(Z_L/Z_S) \quad \text{and} \quad Z_x = Z_S e^{-a\ell/2} \quad (7.42)$$

results in the input reflection coefficient, derived using Equation (7.38),

$$\Gamma_{\text{in}}(\ell) = \frac{1}{2} Z_x e^{-j\beta\ell} \int_{-\ell/2}^{\ell/2} e^{-2j\beta z} \frac{d \ln(e^{az})}{dz} dz = \frac{1}{2} \ln(Z_L/Z_S) \frac{\sin(\beta\ell)}{\beta\ell}. \quad (7.43)$$

So Γ_{in} has a sinc function characteristic with the variations of Γ_{in} reducing as the taper becomes longer. The main problem with this taper comes from the abrupt impedance discontinuity at the Z_L end of the taper. This taper will not be considered further as the Klopfenstein taper considered next has much better performance.

7.5.4 Klopfenstein taper

The Klopfenstein taper [8, 9] results in a specified reflection coefficient ripple (and thus transmission ripple) above a minimum passband frequency. It is believed to achieve the minimum taper length over a passband defined by the maximum allowable reflection coefficient mismatch, Γ_m , (and so minimum transmission loss) in the passband. The linear taper and most other tapers used in matching [10, 11] assume the form of a taper's characteristic impedance profile and the broadband reflection and transmission characteristics are whatever results. In contrast the Klopfenstein taper derives the required impedance profile for a source and load impedance mismatch ratio (Z_L/Z_S) and Γ_m .

Klopfenstein [8] showed that the input reflection coefficient of the taper could be expressed as the limiting form of a high-order Chebyshev polynomial. Thus the Klopfenstein taper has the passband ripples that occur with Chebyshev-based multi-section impedance transformers and Chebyshev filters. The maximum magnitude of the reflection coefficient in the passband is determined by the line length. The appropriate characteristic impedance is computed from [8, 9]

$$\begin{aligned} \ln Z_0(z) = & \ln \left(\sqrt{Z_S Z_L} \right) + \ln \left(\sqrt{Z_L/Z_S} \right) \cdot (\cosh A)^{-1} \\ & \times \left[A^2 \phi(2z/\ell, A) + U\left(z - \frac{1}{2}\ell\right) + U\left(z + \frac{1}{2}\ell\right) - 1 \right] \end{aligned} \quad (7.44)$$

where $U(x)$ is the unit step function so that $U(x) = 0$ for $x < 0$ and $U(x) = 1$ for $x \geq 0$.

The maximum reflection coefficient amplitude $\Gamma_m = \rho_0 / \cosh A$ where $\rho_0 = (Z_L - Z_S)/(Z_L + Z_S)$ is the reflection coefficient when the load and source are directly connected. Klopfenstein found that this introduced a small error attributed to the limitation of the small reflection assumption. He determined that a better estimate is $\rho_0 = \frac{1}{2} \ln(Z_L/Z_S)$. Thus

$$A = \cosh^{-1} [\ln(Z_L/Z_S)/\Gamma_m]. \quad (7.45)$$

That is, Γ_m , the maximum reflection coefficient in the passband, and the mismatch, Z_L/Z_S , determines A . Substituting Equation (7.45) in Equation (7.44) yields

$$\begin{aligned} \ln Z_0(z) = & \ln \left(\sqrt{Z_S Z_L} \right) + \ln \left(\sqrt{Z_L/Z_S} \right) \Gamma_m \frac{(Z_L + Z_S)}{(Z_L - Z_S)} \\ & \times \left[A^2 \phi(2z/\ell, A) + U\left(z - \frac{1}{2}\ell\right) + U\left(z + \frac{1}{2}\ell\right) - 1 \right] \end{aligned} \quad (7.46)$$

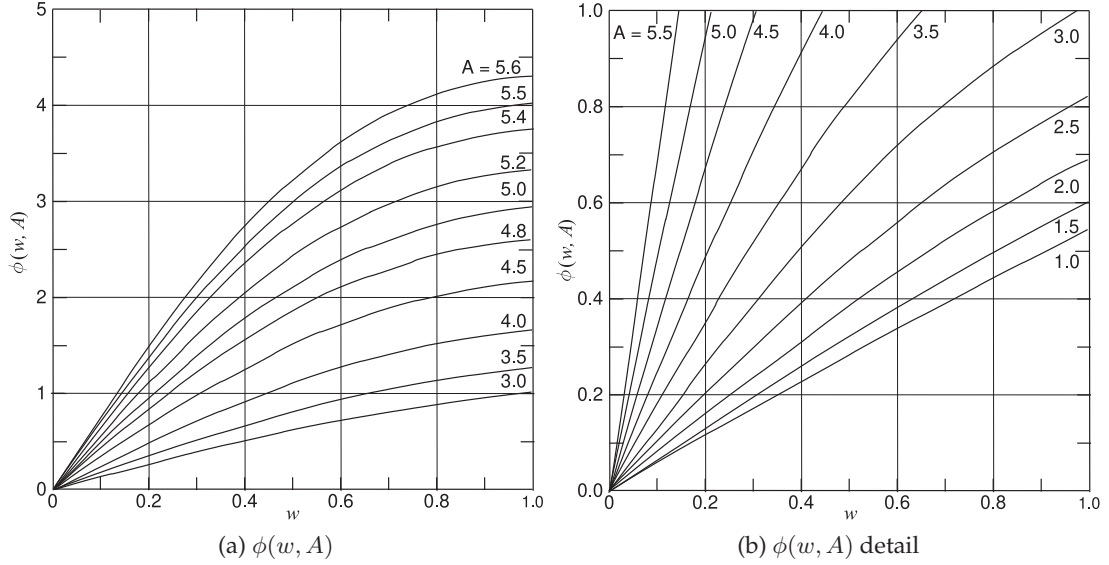


Figure 7-15: Klopfenstein taper function $\phi(w, A)$ used in designing a taper segment. The taper has length ℓ , z is the coordinate at the center of a taper segment, the center of the taper is at $z = 0$, and $\phi(-w, A) = -\phi(w, A)$, $w = 2z/\ell$.

and the function $\phi(w, A)$ is computed as [12]

$$\phi(w, A) = \sum_{k=0}^{\infty} a_k b_k \quad (7.47)$$

(summation up to $k = 20$ is sufficient) with the recursion formulas

$$a_0 = 1, \quad a_k = \frac{A^2}{4k(k+1)} a_{k-1}; \quad b_0 = \frac{1}{2}w, \quad b_k = \frac{\frac{1}{2}w(1-w^2)^k + 2kb_{k-1}}{2k+1}. \quad (7.48)$$

The results are shown in Figure 7-15.

It is interesting to derive the characteristic impedance at the center of the taper. At the center of the taper, $z = 0$, $\phi(0, A) = 0$ and Equation (7.44) becomes

$$\ln Z_0(0) = \frac{1}{2} \ln(Z_S Z_L), \quad \text{that is,} \quad Z_0(0) = \sqrt{Z_S Z_L}, \quad (7.49)$$

which is the geometric mean of the source and load resistances.

The Klopfenstein taper trades off line length ℓ , minimum passband frequency f_{\min} , and maximum passband reflection coefficient Γ_m . The passband of the taper is all frequencies above f_{\min} . This is a remarkable result with the line length being considerably less than that of a linear taper. The limitation is that with such a short line the reflections along the line cannot always be considered to be small so that it is often necessary to increase the line length slightly above the length derived from this synthesis procedure.

7.5.5 Simplified Klopfenstein taper

The simplified form of the Klopfenstein taper is obtained by noting that the acceptable value for the maximum in-band reflection coefficient Γ_m will

w	Exact $Z_0(w)/Z_S$	Simplified $Z_0(w)/Z_S$	Error
-1.0	1.163	1.177	1.23%
-0.8	1.326	1.344	1.32%
-0.6	1.577	1.597	1.26%
-0.4	1.944	1.964	1.04%
-0.2	2.460	2.476	0.64%
0.0	3.162	3.162	0%
0.2	4.065	4.039	0.64%
0.4	5.145	5.092	1.03%
0.6	6.214	6.262	1.25%
0.8	7.539	7.440	1.31%
1.0	8.520	8.542	1.12%

Table 7-2: Comparison of Z_0 of the exact and simplified Klopfenstein tapers (using Equation (7.46) with Equations (7.47) and (7.50) respectively) for a maximum passband transmission loss $T_m = 0.1$ dB and $Z_L/Z_S = 10$ ($\Gamma_m = 0.151$ and $A = 2.72$.) Errors are less for larger T_m and smaller Z_L/Z_S :

For $Z_L/Z_S = 20$, $T_m = 0.1$ dB, the max. error is 2.78%.

For $Z_L/Z_S = 20$, $T_m = 0.2$ dB, the max. error is 1.49%.

For $Z_L/Z_S = 10$, $T_m = 0.1$ dB, the max. error is 1.33%.

For $Z_L/Z_S = 10$, $T_m = 0.2$ dB, the max. error is 0.66%.

For $Z_L/Z_S = 5$, $T_m = 0.1$ dB, the max. error is 0.44%.

For $Z_L/Z_S = 5$, $T_m = 0.2$ dB, the max. error is 0.21%.

typically be small and for a maximum transmission loss of between 0.1 dB and 1 dB (corresponding to $\Gamma_m = 0.151$ and $\Gamma_m = 0.454$ respectively) and maximum $Z_L/Z_S = 10$. Then the maximum value of A is 2.72 and this is when the simplified Klopfenstein taper will have the most error. So retaining only the first three terms in Equation (7.47), $\phi(w, A)$ can be approximated as

$$\phi(w, A) = a_0 b_0 + a_1 b_1 + a_2 b_2 \quad (7.50)$$

and used in Equation (7.46). A comparison of the calculated impedances for a relatively high transmission loss of 1 dB (0.1 dB is more typical) and a large impedance mismatch $Z_L/Z_S = 10$ is given in Table 7-2. The maximum error of 1.33% is comparable to the characteristic impedance error of fabricated transmission lines. So for practical purpose the simplified approach can be used to design the Klopfenstein taper.

EXAMPLE 7.5

Design of a Klopfenstein Taper

Design a microstrip Klopfenstein taper to match a $Z_S = 10 \Omega$ source to a $Z_L = 50 \Omega$ load. The maximum transmission ripple is to be 0.1 dB and the minimum passband frequency is 8 GHz. The substrate has a thickness $h = 0.635 \mu\text{m}$, and relative permittivity $\epsilon_r = 10.0$.

Solution:

First determine the maximum reflection coefficient Γ_m in the passband. The minimum transmission in the passband is $T = 10^{0.1/20}$ and $\Gamma_m = \sqrt{1 - T^2} = 0.151$. Since $Z_L/Z_S = 5$ it is seen from Table 7-2 that the simplified Klopfenstein taper can be used with a maximum error of 1.33%. Using Equation (7.45) the required electrical length of the taper at 8 GHz is

$$A = \cosh^{-1} [\ln(Z_L/Z_S)/\Gamma_m] = \cosh^{-1} [\ln(50/5)/0.151] = 2.720.$$

A taper with ten segments is chosen and in the table below the normalized length $w' = 2z/\ell$ is used to distinguish the parameter from the microstrip width w . The microstrip parameters were obtained by interpolating Table 3-3 of [6]. \bar{Z}_0 and $\bar{\epsilon}_e$ are the average characteristic impedance and effective permittivity of a segment, a linear taper, extending from the width on the previous line to that on the same line. The electrical length of each segment is $\beta(\Delta\ell) = A/10 = 0.272$ radians so that the physical length of a segment $\ell = 0.272\lambda_{8\text{GHz}}/(2\pi\sqrt{\bar{\epsilon}_e})$ where $\lambda_{8\text{GHz}} = 3.745$ cm is the free-space wavelength at 8 GHz.

Segment	w'	$\phi(w', A)$	$Z_0 (\Omega)$	$u = h/w$	w (mm)	$\bar{Z}_0 (\Omega)$	$\bar{\epsilon}_e$	$\Delta\ell$ (μm)
	-1.0	-0.774	11.68	8.28				
1	-0.8	-0.661	12.84	7.38		12.2	8.35	
2	-0.6	-0.521	14.44	6.39		14.1	8.19	
3	-0.4	-0.360	16.52	5.40		16.0	8.05	
4	-0.2	-0.184	19.16	4.45		17.8	7.93	
5	0	0	22.36	3.62		20.8	7.75	
6	0.2	0.184	26.10	2.90		24.7	7.54	
7	0.4	0.360	30.26	2.33		28.7	7.35	
8	0.6	0.521	34.63	1.88		32.9	7.18	
9	0.8	0.661	38.93	1.54		37.3	7.03	
10	1.0	0.774	42.83	1.29		41.4	6.90	

As well at $w = (-1.0 - 1/\infty)$ $Z_0 = 510.03 \Omega$ and at $w = (1.0 + 1/\infty)$ $Z_0 = 49.81 \Omega$ matching the source and load impedances respectively and thus there is a step discontinuity at both ends, a characteristic of the Klopfenstein taper.

7.5.6 Comparison of Transmission Line Impedance Transformers

In this section the four main impedance transformers are compared: the linear taper, the Klopfenstein taper, the quarter-wave transformer and the two-section quarter-wave transformer. These transformers are lengths of nonuniform transmission line with a characteristic impedance that varies along the length of the line, i.e. $Z_0 = Z_0(z)$ where z is the position along the line of total length ℓ . The N -section quarter-wave transformer has step changes in $Z_0(z)$ at $n\lambda/4$ where $n = 1, 2, \dots, N$ but practically $N = 1$ or 2 is the limit usually considered as much better performance can be obtained with the Klopfenstein taper with a length typically between $\lambda/4$ and $\lambda/2$.

Figure 7-16 compares the performance of the tapers for $Z_S = 25 \Omega$ and $Z_L = 50 \Omega$ but the results are applicable in general for $Z_L/Z_S = 2$. Figure 7-16(a) shows the Z_0 profile for the transmission line transformers and where the length of the linear taper has been chosen to provide comparable passband responses defined as where the transmission loss is less than 0.1 dB corresponding to a maximum reflection coefficient $\Gamma_m = 0.151$ and a minimum transmission factor $T = 0.989$. The reflection coefficient response is shown in Figure 7-16(b). First consider the responses of the quarter-wave transformers. Both provide an ideal match at the passband center frequency $f_0 = 10$ GHz and this repeats at odd multiples of f_0 as a $3\lambda/4$ -long line is electrically identical to a $\lambda/4$ -long line. The linear taper, chosen here as $\lambda_m/2$ long where λ_m is the guide wavelength at f_0 , has a reflection coefficient mismatch that reduces as frequency increases as then the line becomes electrically longer.

The Klopfenstein taper for $\Gamma_m = 0.151$ and $Z_L/Z_S = 2$ has $A = 1.1103$ so that the passband of the Klopfenstein taper extends indefinitely above an electrical length of 1.1103 radians which defines the physical length of the line for a chosen minimum passband frequency f_{\min} . The design choice here is $f_{\min} = 0.532f_0$ so that f_{\min} was comparable to that of the two-section quarter-wave transformer. Then the electrical line length required is $0.87\lambda_m/2$. That is, a slightly shorter Klopfenstein taper has the same minimum passband frequency as a two-section quarter-wave transformer.

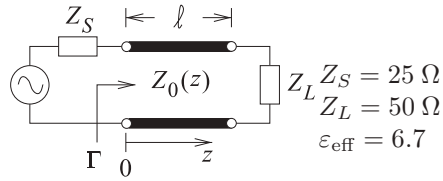
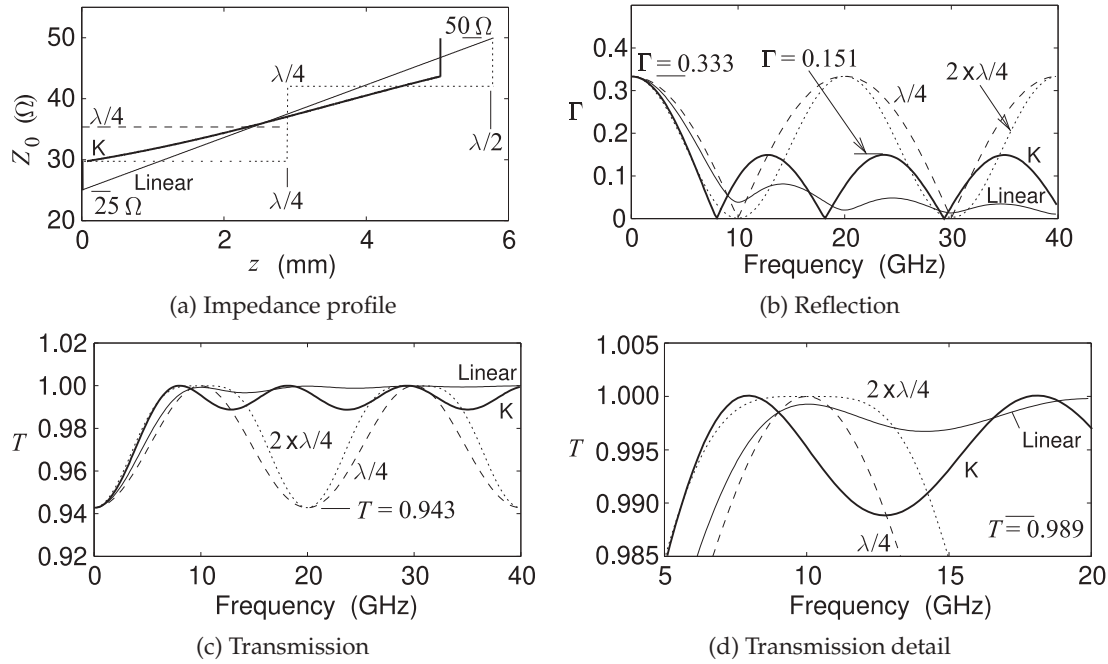


Figure 7-16: Characteristics of simulated transmission line transformers. Midband wavelength $\lambda_m = 11.58$ mm at $f_0 = 10$ GHz. Linear: Linear taper, $\ell = \lambda_m/2$. $\lambda/4$: $\lambda/4$ transformer, $\ell = \lambda_m/4$. $2 \times \lambda/4$: two-section $\lambda/4$ transformer, $\ell = \lambda_m/2$. K: Klopfenstein taper, $\ell = 3.88$ mm $= 0.335\lambda_m$.

The Klopfenstein taper has the distinct advantage that the passband extends indefinitely above f_{\min} whereas one-stage and multi-stage quarter-wave transformers have a finite bandwidth.

The previous paragraph considered matching when $Z_L/Z_S = 2$. A similar comparison is shown in Figure 7-17 for a much higher source and load impedance discontinuity with $Z_S = 5 \Omega$ and $Z_L = 50 \Omega$ and the results are applicable in general for $Z_L/Z_S = 10$. Figure 7-17(a) shows the Z_0 profile for the transmission line transformers and where the length of the linear taper has been chosen to provide comparable passband responses defined as where the transmission loss is less than 0.1 dB (corresponding to a maximum reflection coefficient magnitude of 0.151). The reflection coefficient response is shown in Figure 7-17(b). First consider the responses of the single- and two-section quarter-wave transformers. Both provide an ideal match at the passband center frequency $f_0 = 10$ GHz and repeating at odd multiples of f_0 . Again the passband defined by the two-section quarter-wave transformer is used to determine the length of the linear and Klopfenstein tapers resulting in the linear taper being $3\lambda_m$ long and the Klopfenstein taper being $0.595\lambda_m$ long, slightly longer than the two-section quarter-wave transformer. The linear taper, chosen here to be $\lambda_m/2$ long where λ_m is the guide wavelength at f_0 , has a reflection coefficient mismatch that reduces as frequency increases

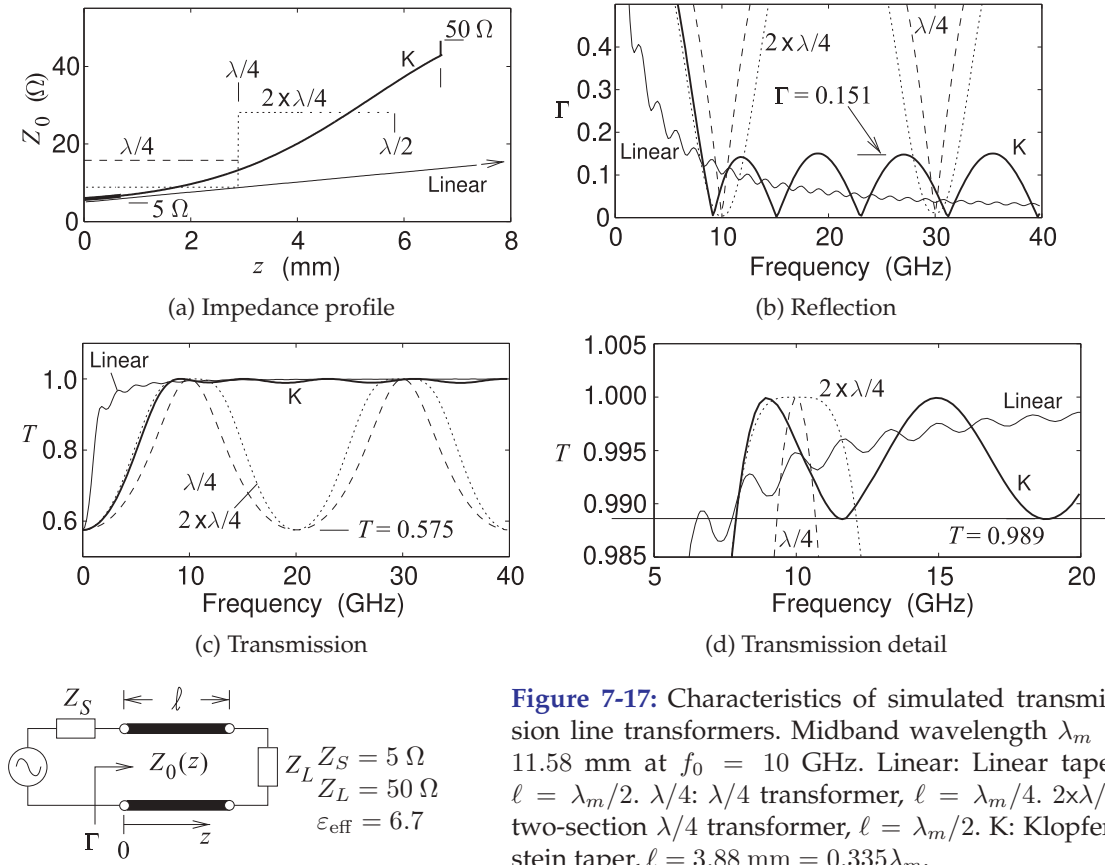


Figure 7-17: Characteristics of simulated transmission line transformers. Midband wavelength $\lambda_m = 11.58$ mm at $f_0 = 10$ GHz. Linear: Linear taper, $\ell = \lambda_m/2$. $\lambda/4$: $\lambda/4$ transformer, $\ell = \lambda_m/4$. $2 \times \lambda/4$: two-section $\lambda/4$ transformer, $\ell = \lambda_m/2$. K: Klopfenstein taper, $\ell = 3.88$ mm $= 0.335\lambda_m$.

Table 7-3: Comparison of passbands of the four transmission line impedance transformers considered in Section 7.5.6 with λ_m being the guide wavelength at 10 GHz. The lengths of the tapers were chosen to have the same minimum passband frequency as the two-section quarter-wave transformer.

$Z_L/Z_S = 2$	ℓ	Passband	Bandwidth
Linear taper	$0.5\lambda_m$	>6.53 GHz	
$\lambda/4$	$0.25\lambda_m$	7.16–11.84 GHz	50%
$2 \times \lambda/4$	$0.5\lambda_m$	5.43–14.57 GHz	91%
Klopfenstein taper	$0.335\lambda_m$	>5.43 GHz	
$Z_L/Z_S = 10$			
Linear taper	$3\lambda_m$	>7.72 GHz	
$\lambda/4$	$0.25\lambda_m$	9.32–10.69 GHz	14%
$2 \times \lambda/4$	$0.5\lambda_m$	7.87–12.12 GHz	42%
Klopfenstein taper	$0.595\lambda_m$	>7.87 GHz	
exponential taper	$1.68\lambda_m$	>7.87 GHz	

as the line becomes electrically longer.

The Klopfenstein taper for $\Gamma_m = 0.151$ and $Z_L/Z_S = 10$ has $A = 2.720$ so that the passband of the Klopfenstein taper extends indefinitely above an electrical length of 2.720 radians and so choosing the minimum passband frequency f_{\min} determines the physical length of the line.

The 0.1 dB passbands of the transmission line transformers are compared in Table 7-3. The two-section quarter-wave transformer and the Klopfenstein transformer have comparable performance near the center frequency of the design with the choice being made on whether it is more important to have

good transmission properties indefinitely above f_{\min} or to provide some frequency selectivity by having a poorer match at the second harmonic frequency of the center match frequency, here f_0 .

7.5.7 Summary

The transmission line transformers considered in this section match resistive source and load impedances. However these impedance transformers provide guidance for design strategies when the source and load include reactances. When the source and load are resistances then the clear choice for a transmission-line-based impedance transformer is the Klopfenstein tape.

With a reactive load the challenge is achieving broadband match since of course the reactance of the load and/or load will vary with frequency and so impose an overall bandwidth constraint. Design of the matching network needs to take into account the frequency characteristic of the load.

Different loads will have different frequency characteristics and hence variations in the type of matching network required. Four basic loads that are commonly encountered in microwave engineering and to which matching is required include the series RC model of the input of a FET transistor with a series reactance that is inversely proportional to frequency; the series LR model encountered in bonding to the input of a device where the inductance comes from a bond wire and which has a series reactance that is proportional to frequency; and a parallel RC load encountered at the output of a transistor with a susceptance that reduces with frequency. These two-element models of sources and loads are simple and other parasitics may need to be included. At microwave frequencies the Q of the impedances encountered with active devices is typically in the range of 0.5 to 3, and source/load resistance mismatch typically ranges from 1.5 to 10. For example, high mismatches are encountered at the output of power amplifiers.

7.6 Matching a Series RC load

The matching network design described in this section is appropriate for a real source impedance and series RC load where the load resistance is less than the source resistance. Also a two-section quarter-wave impedance transformer will be considered as this has performance that is representative of what is reasonable to achieve using transmission-line based impedance transformers. Tapers are not considered here as their particular advantage of an indefinite passband when matching resistive source and load impedance disappears when the load (or source) is reactive.

Design Examples

Figure 7-18(a) presents the problem of matching to the input of a transistor which is modeled here as a capacitor in series with a resistive load. This is the typical model for the input of a FET.

With a two-section cascaded quarter-wave transformer an appropriate matching network is shown in Figure 7-18(b). This topology is based on the design concepts shown in Figures 7-18(c, d and e) where the single-frequency reflection coefficient loci with respect to increasing line length are shown. The overall concept is that line 3 rotates the load impedance to a resistance R_X and then R_X is matched to R_S using a two-section quarter-wave transformer,

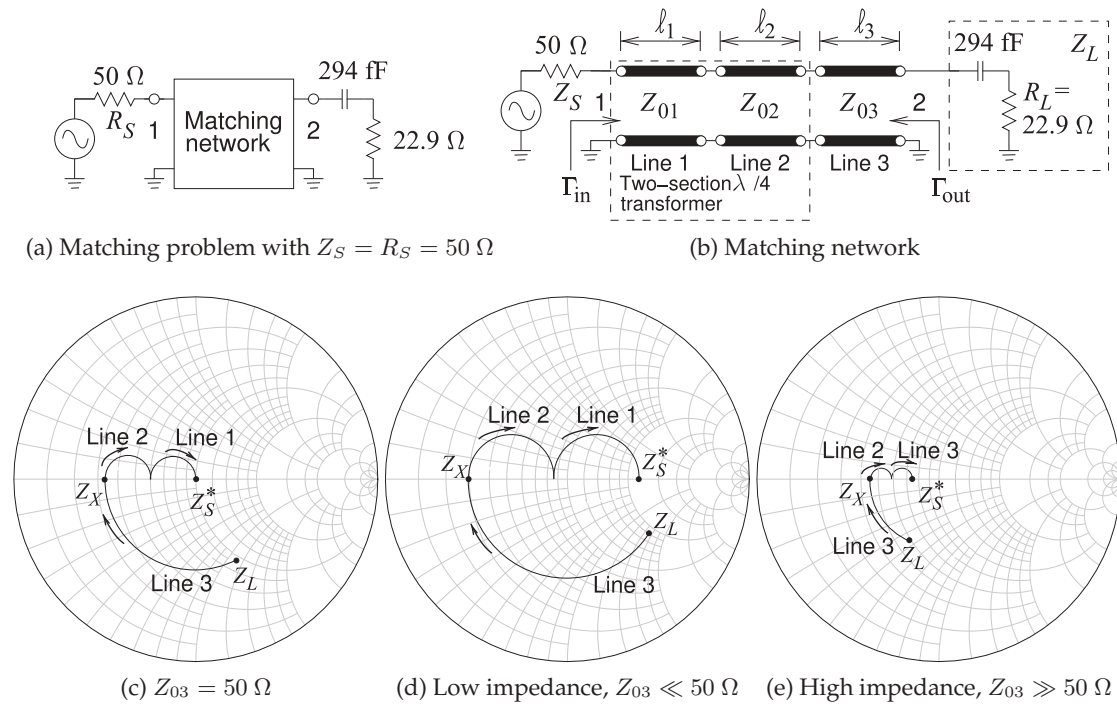


Figure 7-18: Matching problem of the case study of Section 7.6 using a two-section cascaded quarter-wave impedance transformer. The arrows in (c), (d), and (e) indicate increasing line length at 10 GHz. The Smith charts are normalized to Z_{03} and present three design concepts. (The choice of high Z_{03} is appropriate for $R_L < Z_S$ and a capacitor in the load.)

that is, lines 1 and 2.

At 10 GHz the 294 fF capacitor has a reactance of -54.13Ω and with the resistive part of the load the input of the transistor has a Q of 2.36. This is plotted on the 50Ω Smith chart in Figure 7-18(c). The design concept is that line 3 rotates the load Z_L to a purely resistive load of 10.0Ω . Then a $\lambda/4$ -long line, line 2, rotates the reflection coefficient to an intermediate impedance, and this is followed by line 1, another $\lambda/4$ -long line which takes the input impedance to 50Ω . Note that the electrical lengths of the lines are given by the angle subtended by the arcs and do not correspond to the drawn lengths of the arcs. Here the electrical length of line 1 is 50.0° and that of lines 2 and 3 are 90° .

Two alternative design concepts are shown in Figures 7-18(d and e). Figure 7-18(d) describes a low impedance ($Z_{03} \ll 50 \Omega$) design concept. If $Z_{03} = 20 \Omega$ then the electrical length of the line is 72.3° and the intermediate impedance $Z_X = 2.41 \Omega$. An alternative is to use a high characteristic impedance for line 3 as outlined in Figure 7-18(e). With $Z_{03} = 100 \Omega$ the electrical length of line 3 is 29.4° and $Z_X = 17.54 \Omega$. Of these three design concepts the third design concept with the highest Z_{03} is preferable on two accounts. One of these is that the electrical length of line 3 is the smallest, and since the electrical lengths of lines 1 and 2 are fixed (each is $\lambda/8$ long), this results in the lowest overall electrical line length. Secondly the intermediate resistance is closest

Z_{03} (Ω)	$\beta\ell_3$	Z_X (Ω)	Z_{02} (Ω)	Z_{01} (Ω)	0.1 dB Bandwidth (GHz)
10	81.1°	0.65	1.92	18.86	9.90–10.18 (0.28)
20	72.3°	2.41	5.14	23.4	9.76–10.25 (0.49)
30	64.1°	4.86	8.70	27.9	9.69–10.39 (0.70)
40	56.6°	7.50	9.62	31.1	9.62–10.46 (0.84)
50	50.0°	10.0	9.55	33.4	9.55–10.52 (0.97)
60	44.4°	12.2	17.3	35.1	9.54–10.53 (0.99)
70	39.6°	14.0	19.2	36.3	9.48–10.60 (1.11)
80	35.6°	15.4	20.7	37.3	9.48–10.60 (1.11)
90	32.3°	16.6	21.9	38.0	9.48–10.60 (1.11)
100	29.4°	17.5	22.8	38.5	9.48–10.60 (1.11)

Table 7-4: Matching network performance with different Z_{03} with electrical length $\beta\ell_3$. The minimum and maximum frequencies of the passband are when $T = 0.989$, i.e. when the transmission loss is 0.1 dB.

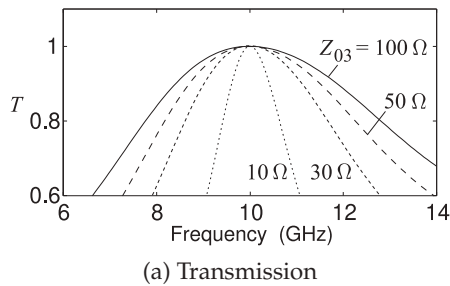
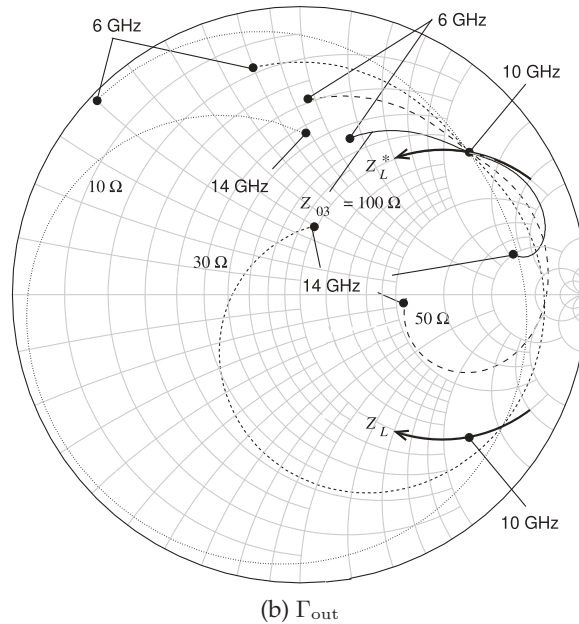


Figure 7-19: Characteristics of the matching network in Figure 7-18(b) for $Z_{03} = 10 \Omega, 30 \Omega, 50 \Omega$, and 100Ω . The Smith chart in (b) is normalized to 22.9Ω and show the frequency loci of Γ_{out} for four matching network designs for $Z_{03} = 10 \Omega, 30 \Omega, 50 \Omega$, and 100Ω . The Smith chart also shows the frequency locus of Z_L and Z_L^* . Note that Γ_{out} is equal to the reflection coefficient of Z_L^* at 10 GHz for all matching networks.



to the complex conjugate of the source impedance, Z_S^* , which of course is just Z_S here since the source is real.

Table 7-4 compares several trial designs with varying Z_{03} and it is apparent that the characteristic impedance of Z_{03} needs to be high. A maximum Z_{03} of 100Ω is typical of many transmission line technologies and especially of planar transmission lines like microstrip. Note that the maximum bandwidth is 11% which is considerably less than the approximately 90% bandwidth that could be obtained for a two-section quarter-wave transformer if the capacitance in the load was not present (see Table 7-3).

The transmission characteristics of the matching network designed using four values of Z_{03} ranging from 10Ω to 100Ω are shown in Figure 7-19(a). Examination of the Smith chart plot, Figure 7-19(b), reveals the fundamental problem in broadband matching of reactive loads to a resistive source impedance. First consider the frequency locus of the load Z_L which is seen to have a clockwise rotation on the Smith chart as is typical of non-resonant impedances. Matching requires that the impedance presented by

the network at port 2 be the complex conjugate of Z_L , i.e. Z_L^* . Z_L^* is seen to rotate in the counter-clockwise direction with increasing frequency. The frequency loci of the reflection coefficients, Γ_{out} , that are presented looking into port 2 of the matching network (in Figure 7-18(a)) for each of the four designs are also plotted in Figure 7-19(b). These all rotate in the clockwise direction so that it is only possible for these matching networks to present the desired impedance Z_L^* at a single frequency, here 10 GHz. The angular length of the Γ_{out} loci from 6 GHz to 14 GHz for the four designs differ. The line with $Z_{03} = 100 \Omega$ has the shortest Γ_{out} locus having the shortest total angular length (and hence shortest electrical and physical lengths). The passband responses of the various designs are shown in Figure 7-19(a) and the broadest passband response is obtained when $Z_{03} = 100 \Omega$ and this impedance is about the largest that could be tolerated for a planar line as otherwise the microstrip characteristic impedance is become close to the 377Ω free space and radiation (and this loss) from the microstrip line is starting to be significant.

7.6.1 Summary

The lessons learned from the design in this section can be generalized with the results shown in Table 7-5. While these results were obtained for a particular form of the load (a series RC load) they are a broad indication of

Table 7-5: Bandwidths achievable for various R_L/Z_S ratios and Q s using the two-section quarter-wave transformer of Figure 7-18(b) and $Z_{03} = 2Z_S$. The percentage bandwidth is calculated as 100 times the difference of the high and low frequencies of the passband divided by the ideal match frequency, f_0 . The notation >33 indicates that the passband is at all frequencies above $0.33f_0$ as for small impedance discontinuities and low Q , the two-section transformer is close to being a linear taper. Q is inversely proportion to frequency. Transmission losses of 0.1 dB, 0.2 dB, 0.5 dB, and 1.0 dB correspond to a maximum $|\Gamma_{\text{in}}|$ in the passband of $|\Gamma_m| = 0.151, 0.212, 0.330$, and 0.454 respectively. (The same bandwidths are obtained with inverted values of R_L/Z_S but requires a different design concept for the matching network.)

0.1 dB max. transmission loss, % bandwidth										
Z_L/Z_S	Q at f_0									
	0	0.25	0.5	0.75	1.0	1.5	2.0	2.5	3.0	
0.10	50	37	31	27	23	18	14	12	10	
0.25	59	47	38	31	26	19	14	11	9	
0.50	85	56	45	34	27	19	14	11	8	
0.75	∞	78	50	36	27	18	13	9	7	
1.00	∞	116	56	37	27	17	11	8	6	

0.5 dB max. transmission loss, % bandwidth										
Z_L/Z_S	Q at f_0									
	0	0.25	0.5	0.75	1.0	1.5	2.0	2.5	3.0	
0.10	66	58	52	46	42	34	29	24	21	
0.25	96	77	65	56	49	38	31	25	21	
0.50	187	108	82	66	55	40	30	24	19	
0.75	∞	>41	104	75	58	39	28	22	17	
1.00	∞	>33	150	83	60	37	26	19	14	

0.2 dB max. transmission loss, % bandwidth										
Z_L/Z_S	Q at f_0									
	0	0.25	0.5	0.75	1.0	1.5	2.0	2.5	3.0	
0.10	51	45	39	35	31	24	20	16	14	
0.25	73	59	49	41	34	26	20	16	14	
0.50	98	77	58	46	38	26	20	15	12	
0.75	∞	106	68	50	39	25	18	14	11	
1.00	∞	181	80	52	38	24	16	12	9	

1.0 dB max. transmission loss, % bandwidth										
Z_L/Z_S	Q at f_0									
	0	0.25	0.5	0.75	1.0	1.5	2.0	2.5	3.0	
0.10	82	72	64	58	53	45	38	33	29	
0.25	123	98	83	72	63	51	42	34	30	
0.50	∞	>38	114	88	74	55	42	34	27	
0.75	∞	>27	>47	172	82	55	40	31	24	
1.00	∞	>24	>43	160	88	53	37	27	21	

what can be achieved without exploiting resonance in the matching network. (Resonance is a technique to obtain improved results and is be considered in Section 7.7.) The performance metrics in Table 7-5 are much more realistic than the Fano-Bode limits which could require lossless networks of infinite complexity, and only consider the average passband reflection coefficient rather than the maximum in-band reflection coefficient.

For example, with a factor of 2 difference between Z_L and Z_S and with a Q of 1, the fractional bandwidth that can be readily achieved is 27%, 55%, 38%, and 74% for maximum passband losses of 0.1 dB, 0.2 dB, 0.5 dB, and 1 dB respectively. Since matching networks are not usually used for frequency selectivity (which is more appropriate for a filter), and since there will be multiple matching networks in a design, it is common to use a maximum transmission loss of 0.1 dB as a passband criterion.

7.6.2 Matching using Cascaded Transmission Lines and Constant Q Circles

The stepped-impedance transformer designs utilizing quarter-wavelength-long lines can be very long. In this section the design of a stepped-impedance transmission line transformer with shortened lines is considered. Design is conceptually derived from the quarter-wave transformer but design choices are made based on constant Q circles.

First consider the single-line matching problem shown in Figure 7-20(a). The normalized impedances are plotted on a Smith chart with constant Q circles in Figure 7-20(b). A detailed view is given in Figure 7-20(c) and this will be used to describe the design procedure. The normalizing reference impedance Z_0 is arbitrary and does not need to be related to the source or load impedance, or to the characteristic impedance of the line.

Figure 7-21(a) shows a quarter-wavelength-long transmission line matching a normalized load z_L to a normalized source impedance z_S with the arrow on the reflection coefficient locus indicating the direction of increasing line length. The arc subtends an angle of 180° corresponding to the line having an electrical length of 90° , i.e. it is $\lambda/4$ long. The maximum Q along the arc is near 0.6 indicating an approximate fractional bandwidth of $1/Q$ or 1.6.

Greater bandwidth of the match can be obtained by using more line sections and matching to an intermediate impedance. This situation is shown in Figure 7-21(b) where there are two quarter-wavelength-long transmission lines each matching to a normalized intermediate resistance $r_v = \sqrt{z_s z_L}$ since both z_s and z_L are resistances. The two arcs in the locus each are part of a circle whose center can be used to determine the characteristic impedance of each of the lines. As an approximation, the center of the circle containing the arc for transmission line n is C_n referenced to the impedance Z_0 and then $Z_{0n} \approx Z_0(1 + 2C_{0n})$ (see Section 4.5). (Of course we already know that each of the lines is a quarter-wave transformer so $Z_{01} = Z_0\sqrt{z_s r_v}$ and $Z_{02} = Z_0\sqrt{z_v r_L}$). The maximum Q set by the matching network is now 0.28 so the fractional bandwidth has increased to $1/0.28 = 3.57$. This process can be continued indefinitely. With a matching network with three quarter-wave lines, as shown in Figure 7-21(c) the maximum Q is further reduced and the fractional bandwidth increased.

The cascaded quarter-wave lines can reliably be used to obtain wide-bandwidth matching but the overall length of the network becomes quite

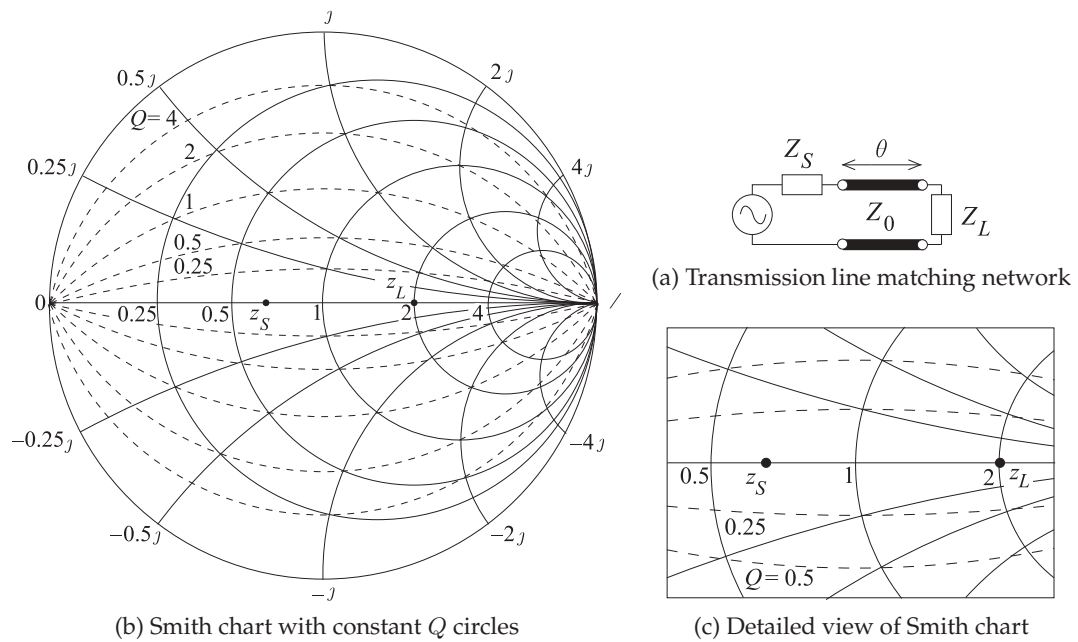


Figure 7-20: Transmission line matching a source impedance Z_S to a load impedance Z_L .

large. A more compact matching network with shorter overall line length can be obtained using lines that are shorter than $\lambda/4$. Such a network design is shown in Figure 7-21(d) with electrical lengths of each of the three lines being less than that of a quarter-wave line (each is about $\lambda/8$ long). The design problem then becomes one of determining the number of lines (or sections), determining the electrical lengths of the lines, the Θ s, and then the characteristic impedance of the lines.

A reasonably good estimate can be obtained using a Smith chart and the constant Q circles. Generally maximum bandwidth is obtained if no one point on the locus sets the maximum circuit Q . A better solution is when multiple arcs on the locus all touch the same Q line.

While the illustration used here has resistive load and source impedances the technique can be used with complex source and load impedances. The complicating factor is that if the source and/or load impedances have reactances, then the source and load impedances will vary with frequency. Still resistive matching provides a good initial point in a design and starting from here optimization in a microwave circuit simulator can be used to finalize a design. A good approach is to absorb the impedance variation with frequency into the matching network.

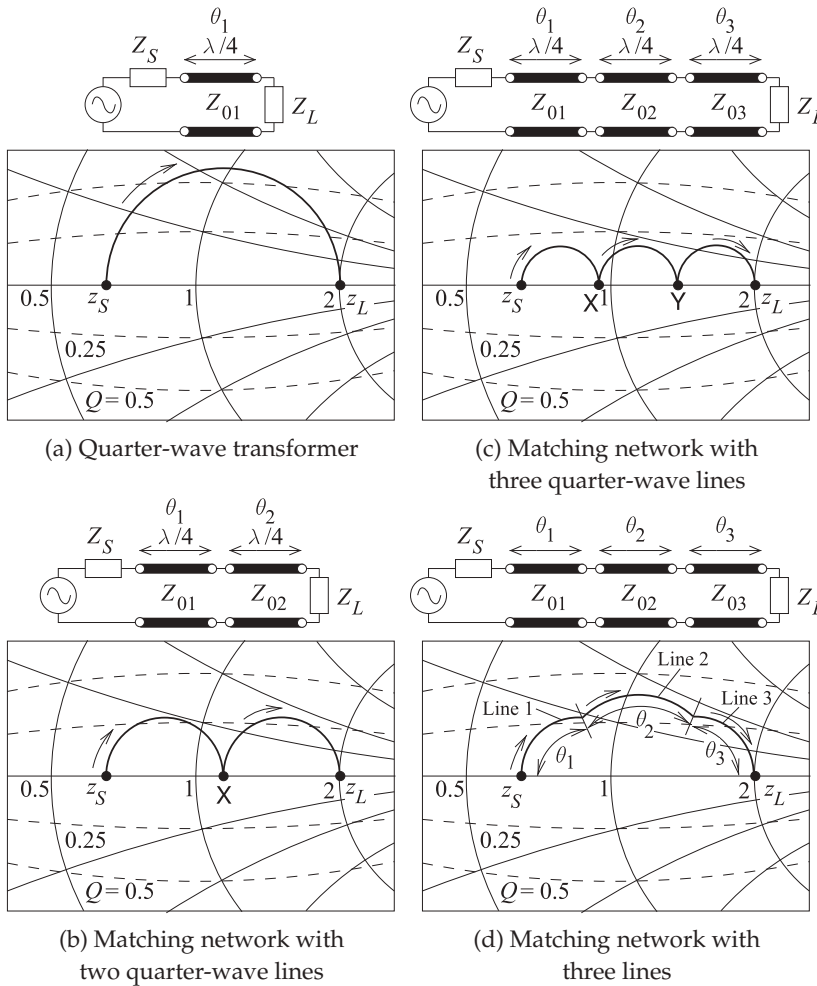


Figure 7-21: Broadband cascaded line matching networks. The arrows in the Smith chart locus indicate the direction with increasing line length.

7.7 Broadband Matching to Reactive Loads

Previous sections presented methods for broadband matching to resistive loads. Usually these techniques work quite well if the load is moderately reactive but this is not always the case. Inputs and outputs of transistors can have larger reactive parts than resistive parts. Broadband matching to such loads requires customization taking into account the frequency locus of the loads which nearly always rotates in the clockwise direction on a Smith chart so that the locus of the complex conjugate match rotates in the counter-clockwise direction. Circuits that achieve broadband match to these loads exploit resonance and as such have limited bandwidths so that half-octave matching is usually the most that can be achieved.

7.7.1 Broadband Matching to a Series RC Load

Consider matching to the input of a transistor. A transistor such as a FET has an input that can be modeled as a capacitor in series with a resistor as shown in Figure 7-22(a). At 10 GHz the 294 fF capacitor has a reactance of -54.06Ω so that the Q of the load is 2.36. The Fano-Bode limit, see Equation (7.7), indicates that the maximum fractional bandwidth that can be achieved

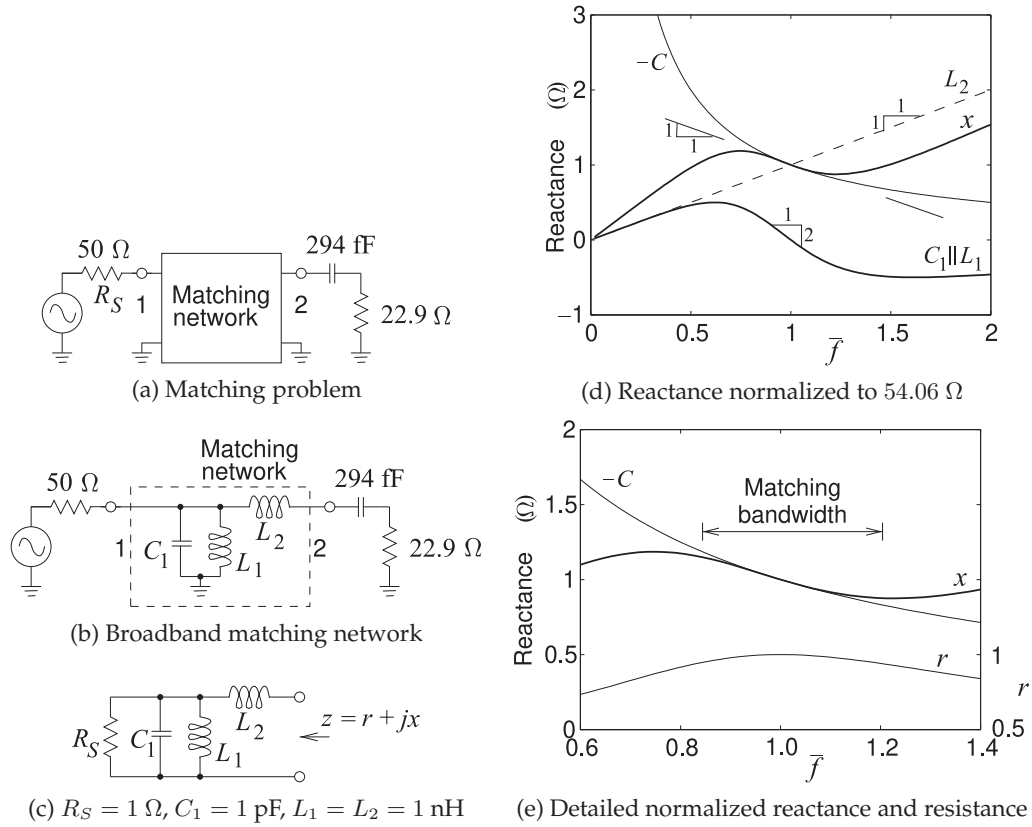


Figure 7-22: Broadband matching with normalized frequency \hat{f} in radians/s normalized to 10 GHz.

for an average reflection coefficient, Γ_{avg} , at Port 1 of 0.11 is 60%. This Γ_{avg} corresponds to an average transmission loss of 0.05 dB for a maximum transmission loss of approximately 0.1 dB in the bandwidth of the match. (Note that if the load was purely resistive, then $Q = 0$ and it is theoretically possible to achieve infinite bandwidth.)

Matching would be greatly simplified if the matching network presented a negative capacitor to the load. The reactance normalized to 54.06Ω versus frequency of the required negative capacitance (of capacitance -294 fF) is shown as the curve identified as $-C$ in Figure 7-22(d). At the normalized frequency $\hat{f} = 1$ (frequency normalized to 10 GHz) the slope of this curve is -1 . A circuit that approximates this over a moderate bandwidth is the broadband matching network shown in Figure 7-22(b). To see how this is achieved, consider the input impedance of the circuit in Figure 7-22(c). The reactance of the parallel LC subcircuit is shown in Figure 7-22(d) as the curve labeled $C_1 \parallel L_1$. At $\hat{f} = 1$ this reactance has a slope of -2 and adding a series inductor, L_2 , (having the reactance curve L_2 in Figure 7-22(d)) results in a reactance x , see Figure 7-22(d), which does have a slope of -1 at $\hat{f} = 1$. Thus the total reactance, x , closely matches the reactance of a negative capacitor over a limited, but still broad, bandwidth. The other part

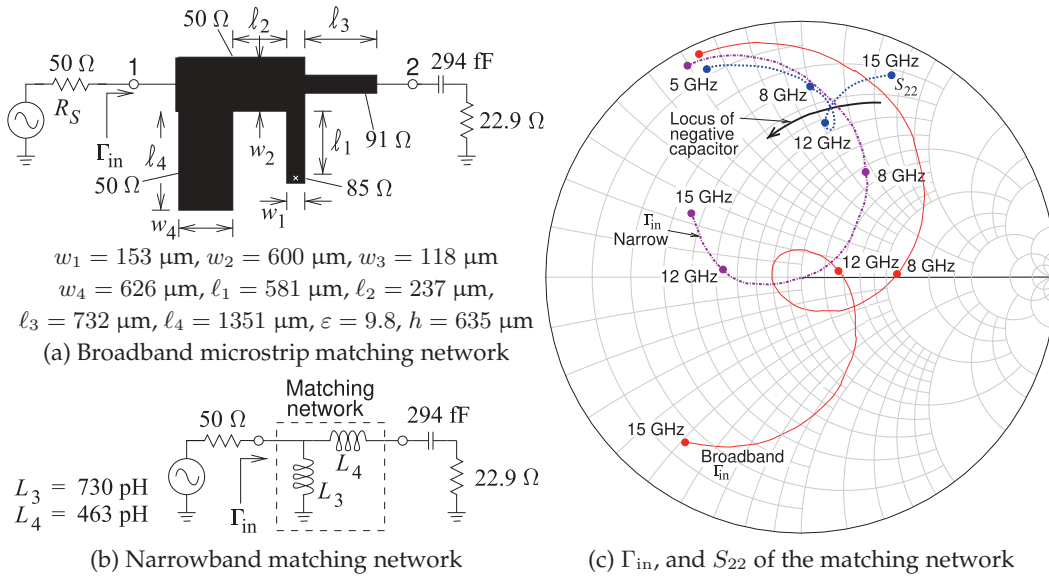


Figure 7-23: Broadband and narrowband matching networks with Γ_{in} of both networks and S_{22} of the broadband network shown with the locus of the ideal conjugate match (identified as the locus of negative capacitor). In (a) $\ell_1 = 0.048 \lambda$, $\ell_2 = 0.020 \lambda$, $\ell_3 = 0.060 \lambda$, and $\ell_4 = 0.117 \lambda$ at 10 GHz. In (b) a 50 Ω Smith chart is used.

of the matching problem is matching the source and load resistances and with appropriate choice of matching network values the resistance r (ideally 22.9 Ω normalized to 54.06 Ω) will be approximately constant in the matching region, see Figure 7-22(e).

A microstrip realization centered at 10 GHz of the broadband matching network concept is shown in Figure 7-23(a). At Port 1 is an open-circuited stub with a relatively short electrical length at 10 GHz and so presents the capacitance C_1 . This is followed by a short section of line that separates the two stubs and provides an extra degree of freedom to be used in matching the source and load resistances. Then follows a short shorted stub that implements L_1 . This is followed by a short high-impedance line which introduces the series inductance L_2 (see Section 2.4.5 of [6]). The performance of the matching network is shown in Figure 7-23(c) where it is compared to that of a narrowband matching network. The narrowband network, shown in Figure 7-23(b), is a conventional two-element matching network designed using the absorption method so that the 294 fF capacitor is absorbed into the network but still requires an additional inductance L_4 to compensate for the capacitance. The match of both the broadband and narrowband matching networks is ideal at 10 GHz. The Γ_{in} loci of the two networks are shown on a 50 Ω Smith chart in Figure 7-23(c).

The range of match for a maximum transmission loss of 0.1 dB is from 9.04 GHz to 11.53 GHz (a 2.49 GHz bandwidth) for the broadband network and 9.47 GHz to 10.62 GHz (a 1.15 GHz bandwidth) for the narrowband network. Using a 0.5 dB bandwidth criterion the bandwidth of the region of match for the broadband microstrip network is 8.13 GHz to 12.95 GHz

(a 4.82 GHz bandwidth) and the narrowband network has a passband from 8.54 GHz to 12.34 GHz (a 3.80 GHz bandwidth).

Also plotted in Figure 7-23(c) is S_{22} of the broadband microstrip network and from this the reason why a good match is achieved can be seen. Typically the reflection coefficient locus of simple networks rotates clockwise on the Smith chart with increasing frequency. For a small frequency range near the center match frequency S_{22} has a loop and effectively rotates in the counter-clockwise direction approximating the locus of a negative capacitor. Such a behavior is obtained in the lumped element version of the broadband network by the resonance of L_1 , C_1 , and L_2 . A very good match is therefore possible over a small frequency range. The good match is obtained over about half an octave (of frequency) and this is typically the best that can be achieved when matching to the inputs and outputs of microwave transistors. The microstrip broadband matching network has a finite length and width. Including the widths as well as the lengths of the lines, the broadband matching network has a width and length of 0.11λ , considerably less than that of a quarter-wave transformer used to match resistive source and load impedances when they are resistive but not when the load has a large reactance as here.

7.7.2 Summary

The broadband matching concept presented in this section is using resonance to present an impedance to a load or source that rotates in the counter-clockwise direction (with respect to frequency) on a Smith chart. This is achievable only over a moderate bandwidth and typically half-octave bandwidths are regarded as the limit of what can be achieved when matching to a load that is more reactive than resistive. There are techniques also that are sometimes able to achieve broader effective matches by incorporating the parasitic reactances of a device to be matched into a distributed transmission line.

7.8 Summary

This chapter presented design concepts for realizing matching networks with broad bandwidths. Matching a load and/or a source with a reactance presents a particular problem because reactive loads include energy storage elements and energy storage elements limit bandwidth. Theoretically, if negative capacitances and inductors could be realized then it would be possible to have infinite bandwidth matching of complex loads and/or sources provided that the elements of the matching network are lossless. Since negative capacitors and inductors cannot be realized, there will be a limit on matching bandwidth. The Fano-Body limits indicate the trade-off between the quality of the match in terms of the minimum reflection coefficient that can be achieved and the bandwidth of the match. While ideal magnetic transformers can achieve infinite matching of source and load resistors, actual magnetic transformers have self inductances and thus energy storage and so matching bandwidth is limited even with magnetic transformers.

All matching networks introduce energy storage elements. This includes capacitor, inductor, and transmission line elements, as well as magnetic

transformers. Thus design techniques are required that enable design trade-offs of the quality of a match and bandwidth. The constant Q circles on a Smith chart enable the maximum Q and hence fractional bandwidth, which is very approximately $1/Q$, of a matched to be controlled. As long as the locus of the input reflection coefficient of an evolving terminated matching network does not go outside a specific pair of equal-valued constant Q circles the bandwidth is constrained. This concept applies to loads and sources that are resistive only or include reactances. The stepped-impedance and tapered transmission-line matching networks presented enable broadband matching of source and load resistances but the concepts of gradual matching in stages to interim resistances levels can be extrapolated to matching general sources and loads.

The final concept of this chapter describes a topology for matching a reactive load, in particular a load comprising a resistor and a capacitor. This is what the input and output of a transistor looks like. The matching network described in Section 7.7 approximates a negative capacitor over a limited bandwidth and is one of the best such networks known and this matching network topology is commonly used in matching the input and output of transistors. Other broadband network topologies have been invented and these developments are tracked by microwave engineers involved in matching network design.

7.9 References

- [1] R. Fano, "Theoretical limitations on the broadband matching of arbitrary impedances," Massachusetts Institute of Technology, Research Laboratory of Electronics, Tech. Rep. 42, Jan. 1948.
- [2] —, "Theoretical limitations on the broadband matching of arbitrary impedances," *Journal of the Franklin Institute*, vol. 249, no. 1, pp. 57–83, Jan. 195, also see Feb. 1950, pp. 139–154.
- [3] H. Bode, *Network Analysis and Feedback Amplifier Design*. Van Nostrand, 1945.
- [4] R. Collin, "Theory and design of wide-band multisection quarter-wave transformers," *Proc. IRE*, vol. 43, no. 2, pp. 179–185, 1955.
- [5] L. Young, "Stepped-impedance transformers and filter prototypes," *IRE Trans. on Microwave Theory and Techniques*, vol. 10, no. 5, pp. 339–359, 1962.
- [6] M. Steer, *Microwave and RF Design, Transmission Lines*, 3rd ed. North Carolina State University, 2019.
- [7] J. W. Bandler, "Optimum noncommensurate stepped transmission-line transformers," *Electronics Letters*, vol. 4, no. 11, pp. 212–213, 1968.
- [8] R. Klopfenstein, "A transmission line taper of improved design," *Proc. IRE*, vol. 44, no. 1, pp. 31–35, 1956.
- [9] D. Kajfez and P. J. O, "Correction to "a transmission line taper of improved design"," *IEEE Trans. Microwave Theory and Techniques*, vol. 21, no. 5, pp. 364–364, 1973.
- [10] K. Lu, "An efficient method for analysis of arbitrary nonuniform transmission lines," *Microwave Theory and Techniques, IEEE Transactions on*, vol. 45, no. 1, pp. 9–14, 1997.
- [11] R. E. Collin, *Foundations for Microwave Engineering*. John Wiley & Sons, 2007.
- [12] M. A. Grossberg, "Extremely rapid computation of the klopfenstein impedance taper," *Proceedings of the IEEE*, vol. 56, no. 9, pp. 1629–1630, 1968.

7.10 Exercises

1. A load is modeled as a $50\ \Omega$ resistance in series with a reactance of $50\ \Omega$. This load is to be matched to a source with a Thevenin equivalent resistance of $50\ \Omega$. Use the Fano-Bode criteria to determine the upper limit on the matching network bandwidth when the average in-band reflection coefficient is $-10\ \text{dB}$.
2. A load is modeled as a $50\ \Omega$ resistance in series with a reactance of $50\ \Omega$. This load is to be

- matched to a source with a Thevenin equivalent resistance of $50\ \Omega$. Use the Fano-Bode criteria to determine the upper limit on the matching network bandwidth when the average in-band reflection coefficient is $-20\ \text{dB}$.
3. The output of a transistor amplifier operating at $1\ \text{GHz}$ is modeled as a $100\ \Omega$ resistor in parallel with a $10\ \text{pF}$ capacitor. The amplifier must drive the input of a $\lambda/2$ dipole antenna with an input resistance of $73\ \Omega$. To do this efficiently a matching network is required. Consider that the input resistance of the antenna is independent of frequency, and assume that the matching network is lossless. This is the same as assuming that its bandwidth is much greater than the bandwidth required. If the required fractional bandwidth of the matching network is 5% , and using the Fano-Bode criteria, determine the following:
 - (a) The lower limit on the average in-band reflection coefficient of the matching network.
 - (b) The upper limit on the average transmission coefficient of the matching network.
 4. Design a broadband matching network at $1\ \text{GHz}$ to match a source $Z_S = 80 + j50\ \Omega$ to a load with an impedance $Z_L = 60.0 + j20.0\ \Omega$. Maintain the maximum bandwidth possible with this source and load. [Parallels Example 7.1]
 5. Design a broadband matching network at $1\ \text{GHz}$ to match a source $Z_S = 45 + j10\ \Omega$ to a load with an impedance $Z_L = 50.0 + j80.0\ \Omega$. Maintain the maximum bandwidth possible with this source and load. [Parallels Example 7.1]
 6. Consider the problem of matching a source with a Thevenin equivalent impedance of $25\ \Omega$ to a load of admittance $0.035 + j0.035$.
 - (a) What is the minimum Q that can be achieved for the network, and what is the topology of the matching network that will yield the match with the widest bandwidth?
 - (b) Design the matching network with the widest bandwidth possible if the matching network can have at most four elements.
 7. Develop the electrical design of a three-section quarter-wave transformer to match a $50\ \Omega$ cable to an antenna with a $10\ \Omega$ input impedance. [Parallels Example 7.2]
 8. Design of a two-section quarter-wave transformer to match a $50\ \Omega$ cable to a $75\ \Omega$ cable. [Parallels Example 7.2]
 9. Develop the electrical design of a two-section quarter-wave transformer to match a $50\ \Omega$ cable to a $75\ \Omega$ cable. [Parallels Example 7.2]
 10. Develop the electrical design of a three-section maximally flat stepped-impedance transformer to match a source $Z_S = 20\ \Omega$ to a load $Z_L = 50\ \Omega$ load. [Parallels Example 7.3]
 11. Design a stepped impedance transmission line transformer with two transmission line sections to match a $50\ \Omega$ source to a load with an impedance of $25\ \Omega$. Design for a maximally flat response. [Parallels Example 7.3]
 12. Design a maximally flat four-section stepped impedance transmission line transformer matching a basestation amplifier with a $2\ \Omega$ output impedance to a $50\ \Omega$ cable. [Parallels Example 7.3]
 13. Develop the electrical design of a 100% bandwidth three-section Chebyshev stepped-impedance transformer in microstrip to connect a power amplifier with an output impedance of $2\ \Omega$ to a $50\ \Omega$ cable. [Parallels Example 7.4]
 14. Design a microstrip Klopfenstein taper to match a $Z_S = 15\ \Omega$ source to a $Z_L = 75\ \Omega$ load. The maximum transmission ripple is to be $0.5\ \text{dB}$ and the minimum passband frequency is $60\ \text{GHz}$. Only an electrical design is required but draw the microstrip layout. [Parallels Example 7.5]

7.10.1 Exercises by Section

[†]challenging, [‡]very challenging

§7.2 1, 2, 3

§7.4 7, 8, 9, 10, 11, 12, 13

§7.3 4, 5, 6

§7.5 14

7.10.2 Answers to Selected Exercises

A $41.36\ \text{meV}$

B $662.6\ \text{fJ}$

C $3.25\ \text{cm}$

Index

- S* parameters
 - generalized reciprocity, 25
 - normalized, 17
- ABCD parameters, 12, 14
 - reciprocity, 13
 - relationship to *S* parameters, 36
- absorption, 168
- ADC, 97
- admittance
 - parameters, 9
 - parameters, conversion to *S*, 29
- Amphenol precision connector, 99
- ANA, 89
- APC-7, 99
- attenuation, 38
 - intrinsic, 41
- attenuator, 124, 150
- balanced
 - circuit, 139
- balun, 139, 140, 144, 145
 - Marchand, 140
 - symbol, 140
- bend, 129
- Bode-Fano criterion, 206
- branch, 50
- branch-line hybrid, 150
- butterfly radial stub, 129
- calibration, 94, 99, 103, 104
 - critical length, 102
 - DTL, 104
 - error model, 98
 - 12-term, 98, 99, 104, 106
 - 16-term, 98
 - 6-term, 104
 - 8-term, 98
 - LRM, 105
 - LRRM, 104
 - one-port, 94
 - SOL, 95
 - SOLR, 104
 - SOLT, 104
 - standards, 94, 95
 - through reflect line, 99, 103
 - match, 104
 - through-line, 100
 - through-short-delay, 103
 - TL, 94, 100, 106
 - TRL, 94, 99, 103
 - TRM, 104
 - TSD, 103
 - two-port, 96
 - two-tier, 105
 - TxL, 99, 106
- capacitor
 - interdigitated, 119
 - MIM, 119
 - MOS, 119
 - on-chip, 119
- cascadable scattering parameters, 31
- cascading matrices, 101
- chain
 - scattering matrix, 32
- change of reference impedance, 77
- characteristic impedance
 - change, 77
 - from measurements, 109
 - Smith chart, 109
- Chireix combiner, 143
- coaxial
 - attenuator, 126
 - line
 - termination, 124
- coil, 134
- combiner, 148
 - Chireix, 143
 - hybrid, 148
 - Wilkinson, 141
- comparison loss, 41
- component
 - lumped-element, 121
- conjugate match, 15
- mismatch loss, 41
- connector
 - female, 99
 - male, 99
- constitutive relations, 162
- conversion
 - parameter
 - S*-*h*, 18
 - S*-*y*, 18
 - S*-*z*, 18
 - T*-*S*, 22
 - ABCD-*z*, 13
 - coupling coefficient, 134
 - CPW, 93
 - critical length, 102
 - crossover, 129
 - de-embedding, 96, 98
 - determining characteristic impedance, 109
 - device under test, 94, 98, 105
 - diagonal matrix, 26
 - dielectric resonator, 132
 - discontinuity, 128
 - microstrip, 128
 - distributed matching network, 183
 - divider
 - Wilkinson, 141
 - double
 - slug tuner, 184
 - stub matching, 185
 - stub tuner, 184
 - through line, 104
 - DTL, 104
 - DUT, 94, 98, 105
 - edge, 50
 - error model, *see* calibration
 - expanded Smith chart, 76
 - exponential taper, 218
 - Fano-Bode criterion, 206
 - fixturing, 100
 - four-port junction, 135
 - fractional bandwidth, 116
 - gap, 129
 - generalized
 - S* parameters, 23
 - reciprocity, 25
 - ground-signal-ground probe, 93
 - GSG probe, 93
 - H* parameters, 9
 - Hackborn, 98
 - half-angle transform, 130
 - hybrid, 135, 136, 148
 - 90°, 136
 - 180°, 136
 - branch-line, 150
 - combiner, 148, 149
 - lumped element, 152
 - lumped-distributed matching, 187
 - magnetic, 137
 - parameters, 9
 - power divider, 149
 - power splitter, 149
 - quadrature, 136
 - rat-race, 151, 152
 - ring, 151
 - IDC, 119
 - impedance
 - matching, 159
 - matrix, 28
 - normalization, 17
 - normalized, 31
 - parameters, 7
 - conversion to *S*, 28
 - reference, 17
 - transformer, 129
 - 4:1, 145
 - transforming network, 162
 - inductor
 - on-chip, 120
 - planar, 120
 - spiral, 120
 - insertion loss, 38
 - minimum, 41
 - interdigitated capacitor, 119
 - intrinsic attenuation, 41
 - Klopfenstein taper, 219
 - L matching network, 164
 - linear taper, 218
 - linearity, 6
 - loaded *Q*, 118
 - loop transmittance, 56
 - loss
 - insertion, 38
 - reflection, 37
 - return, 37
 - substitution, 38, 55
 - lossless

- two-port
 - S parameters, 21
 - scattering parameters, 21
- LRM, 105
- LRRM, 104
- LTCC
 - passive components, 150
 - planar inductor, 120
- lumped element, 119
 - hybrid, 152
- magnetic
 - circuit, 139
 - core, 133
 - flux
 - density, 133
 - transformer, 132
 - hybrid, 137
- Marchand balun, 140
- Mason's rule, 56, 57, 107
- matching, 159
 - complex conjugate, 160
 - double stub, 185
 - Fano-Bode criterion, 206
 - hybrid
 - lumped-distributed, 187
 - maximum power transfer, 160
 - network
 - absorption, 168
 - broadband, 177
 - complex load, 168
 - distributed, 183
 - L, 164
 - Pi network, 174
 - resonance, 168
 - T network, 177
 - three-element, 171, 173
 - two-element, 164, 167
 - reflectionless, 160
 - using stub, 185
 - wideband, 207
- matrix
 - diagonal, 26
 - unit, 26
- maximum
 - power transfer, 159
 - power transfer, 160
- measurement
 - calibration
 - through-line symmetry, 106
 - TL, 106
 - coplanar probes, 91, 92
 - leakage, 98
 - network analyzer, 91, 92
 - non-coaxial, 105
 - one-port, 94
 - planar, 106
 - scattering parameters, 89
 - two-tier, 105
 - TxL, 106
- metal
 - insulator-metal, 119
 - oxide-metal, 119
- MIC
 - passive components, 150
- microprobe, 90, 91
- microstrip, 129
 - attenuator, 126
 - bend, 129
 - crossover, 129
 - discontinuity, 128, 129
 - gap, 129
 - impedance transformer, 129
 - matched load, 124
 - notch, 129
 - quarter-wave impedance transformer, 129
 - radial stub, 129
 - step, 129
 - tapered line, 129
- MIM, 119
- MIM capacitor, 119
- minimum
 - insertion loss, 41
 - transducer loss, 41
- mismatch loss, 41
 - conjugate, 41
- MOM capacitor, 119
- multi-section
 - line transformer, 209
 - Chebyshev, 213
 - Constant Q, 229
 - maximally flat, 211
 - shortened, 229
- mutual inductance, 134
- N -port
 - lossless, 28
 - network, 22
 - passive, 28
- network
 - analysis, 5
 - analyzer, 89, 91, 92
 - automatic, 89
 - vector, 89
 - linear, 6
 - parameters, 7
 - cascading matrix, 101
 - passive, 6
 - reciprocal, 6
 - symmetrical, 6
 - two-port, 6
- node, 50
- normalization impedance, 17
- normalized S parameters, 17
- notch, 129
- on-chip
 - capacitor, 119
 - inductor, 120
 - spiral inductor, 120
- open, 127
- operator
 - real, 15
- pad, 124
- parallel
 - connection
 - two-port network, 11
 - reactive element, 164
- parameters
 - S to y , 29
 - S to z , 28
 - y to S , 29
 - z to S , 28
 - ABCD, 12
 - admittance, 9
 - to scattering, 29
 - hybrid, 9
 - impedance, 7
 - to scattering, 28
 - scattering, 14
 - to admittance, 29
 - to impedance, 28
- passive
 - components, 115
 - two-port
 - S parameters, 21
- passivity, 6
 - S parameters, 27
 - scattering parameters, 27
- Pennock, 104
- Pi network, 174
- planar
 - inductor, 120
- port definition, 6
- power
 - divider, 149
 - splitter, 149
 - waves, 23
 - root, 23
- probe
 - ground-signal-ground, 93
 - GSG, 93
- puck, 132
- Q , 115, 116
 - circles, Smith chart, 207
 - external, 118
 - loaded, 118
 - unloaded, 118
- Q_L , 118
- Q_U , 118
- Q_X , 118
- Q -factor
 - loaded, 118
- quadrature, 136
 - hybrid, 136
- quality factor, *see* Q
- quarter-wave transformer, 129
- \Re , 15
- radial stub, 129
- radio
 - frequency integrated circuit, 119, 120
- rat-race, 151, 152
- real part, 15
- reciprocal, 6
- reciprocity, 6
 - S parameters, 17
 - y parameters, 9
 - z parameters, 8
 - ABCD parameters, 13
 - generalized S parameters, 25
- rectangular cavity, 131
- reference
 - impedance, 16, 17
 - change, 77
 - resistance, 16
- reflection
 - coefficient, 14
 - graphical representation, 58
 - loss, 37
- resonant
 - circuit, 115, 116
 - frequency, 116
- resonator, 131
 - bandwidth, 118
 - dielectric, 132
- return loss, 37
- RFIC, 119, 120, 140
- root power wave, 23
- root power waves, 23
- S parameters, 14, 19, 58
 - cascadable form, 31
 - chain scattering parameters, 31
 - change in reference impedance, 26
 - conversion
 - to h , 18
 - to y , 18, 29
 - to z , 18, 28
 - to ABCD parameters, 36
 - conversion to

- y*, 30
- definition, 16
- derivation, 19
- generalized, 23, 26
- graphical representation, 58
- lossless, 28
- measurement, 89
- normalized, 26
- of common two-ports, 30
- of series element, 31
- of shunt element, 31
- of transmission line, 30
- passivity, 27
- polar plot, 58
- reference plane change, 35
- series element, 31
- SFG, 50
- shunt element, 19, 31
- signal flow graph, 50
- Smith chart, *see* Smith chart
- transmission line, 30
- two-port
 - lossless condition, 21
 - passive condition, 21
 - relationships, 35
- scattering parameters, 14, 19, 58
 - change in reference impedance, 26, 27
 - conversion
 - to ABCD parameters, 36
 - to admittance, 29
 - to impedance, 28
 - definition, 16
 - derivation, 19
 - generalized, 26
 - graphical representation, 58
 - measurement, 89
 - normalized, 26
 - of common two-ports, 30
 - of series element, 31
 - of shunt element, 31
 - of transmission line, 30
 - passivity, 27
 - polar plot, 58
 - reference plane change, 35
 - shunt element, 19
 - two-port
 - lossless condition, 21
 - two-port relationships, 35
- scattering transfer parameters, 21
- self-inductance, 134
- self-resonant frequency, 116
- series
 - connection
 - two-port network, 10
 - element, *S* parameters, 31
 - parallel connection, 11
 - reactive element, 162
- SFG, 49–52, 56, 57
 - S* parameters, 50
 - addition, 51
 - commutation, 51
 - in measurements, 97
 - loop transmittance, 56
 - manipulation, 50
 - Mason's rule, 56, 57
 - multiple loops, 52
 - multiplication, 51
 - path, 56
 - reduction, 50
 - self-loop, 52
 - simplification, 50
- shunt
 - element, *S* parameters, 19, 31
 - stub, 129
- Shurmer, 98
- signal flow graph, 49–52, 56
 - S* parameters, 50
 - addition, 51
 - commutation, 51
 - manipulation, 50
 - Mason's rule, 56
 - multiple loops, 52
 - multiplication, 51
 - reduction, 50
 - self-loop, 52
 - simplification, 50
- slide-screw slug tuner, 184
- SMA, 99
- Smith, 60
- Smith chart, 60, 61, 64, 65, 179
 - admittance chart, 76
 - determining
 - characteristic impedance, 109
 - expanded, 76
 - path length, 182
 - Q circles, 207
 - two-element matching, 179
- SOL calibration, 95
- SOLR, 104
- SOLT, 104
- spiral inductor, 120
- step, 129
- stepped impedance transformer, 209
 - Chebyshev, 213
 - Constant Q, 229
- maximally flat, 211
- shortened, 229
- stub, 64, 127, 129, 183
 - matching, 185
 - radial, 129
 - transformations, 130
 - tuner, 184
- subscript order, 8
- substitution loss, 38, 55
- surface
 - mount, 121
- symmetry, 6
- synthesizer, 89
- system
 - impedance, 16
 - change, 77
- T* parameters, 21
 - chain scattering matrix, 32
 - relationship to *S* parameters, 32
- T* network, 177
- taper, 209
- tapered
 - impedance transformer, 217
 - exponential, 218
 - Klopfenstein, 219
 - linear, 218
 - line, 129
- termination, 122, 124, 126
- thick-film passive components, 150
- three
 - element matching, 171
- through
 - line, 94, 100
 - reflect
 - line, 94, 99, 103
 - match, 104
 - short delay, 103
- TL, 106
 - calibration, 94
- transducer loss
 - minimum, 41
- transformer, 162
 - ideal, 162
 - inverting, 133
 - magnetic, 132, 133
 - multi-section line, 209
 - Chebyshev, 213
 - Constant Q, 229
 - maximally flat, 211
 - shortened, 229
- stepped impedance, 209
 - Chebyshev, 213
 - Constant Q, 229
 - maximally flat, 211
 - shortened, 229
- tapered line, 217
 - exponential, 218
 - Klopfenstein, 219
 - linear, 218
- transmission line, 143
 - balun, 145
- transmission line
 - S* parameters, 30
 - discontinuities, 128
 - impedance transformer, 129
 - stub, 127
 - tapered line, 129
 - transformer, 143
 - transformer, balun, 145
 - line transformer, 209
 - Chebyshev, 213
 - Constant Q, 229
 - exponential taper, 218
 - Klopfenstein taper, 219
 - linear taper, 218
 - maximally flat, 211
 - shortened, 229
 - taper, 209, 217
- TRL, 94, 99, 103
- TRM, 104
- TSD, 103
- tuner, 185
 - slide-screw slug, 184
 - slug, 184
 - stub, 184
- two-port network, 6
 - S* parameters
 - lossless condition, 21
 - calibration, 94, 96
 - input reflection, 18
 - insertion loss, 38
 - parallel connection, 11
 - parameter relationships, 35
 - passivity, 27
 - reflection loss, 37
 - return loss, 37
 - scattering parameters
 - lossless condition, 21
 - of common two-ports, 30
 - of series element, 31
 - of shunt element, 31
 - of transmission line, 30
 - passive condition, 21
 - series connection, 10
 - series-parallel connection, 11
 - two-tier measurements, 105
- TxL, 106
- U, 26

- unbalanced circuit, 139
- unit
 - matrix, 26
- unitary condition, 28
- unloaded Q , 118
- unterminating, 96, 98
- VNA, 89, 90, 96, 98
 - calibration, *see* calibration
- voltage
 - reflection coefficient, 16
- Wheeler, 120
- wideband matching, 207
- Wilkinson
 - combiner, 141
 - divider, 141
- \bar{y} , normalized, 31
- y parameters, 7, 9
 - conversion
 - to S , 29
- \bar{z} , normalized, 31
- z parameters, 7
 - conversion to S , 28

Microwave and RF Design: Networks presents the tools and techniques required to analyze and design microwave and RF circuits. Because of the finite speed of light, microwave circuits must be considered to be spatially distributed and so there is not a single ground. As such metrics that can be used to describe power flow are of most use. The topics covered include scattering parameters, signal flow graphs, and Smith charts. Acquiring expertise in these is the biggest barriers to a successful career in microwave and RF engineering. This book is suitable as both an undergraduate and graduate textbook, as well as a career-long reference book.

KEY FEATURES

- The third volume of a comprehensive series on microwave and RF design
- Open access ebook editions are hosted by NC State University Libraries at: <https://repository.lib.ncsu.edu/handle/1840.20/36776>
- 49 worked examples
- An average of 30 exercises per chapter
- Answers to selected exercises
- Detailed coverage of Smith charts and how they are used in design and in interpretation
- Extensive treatment of broadband matching
- A companion book, *Fundamentals of Microwave and RF Design*, is suitable as a comprehensive undergraduate textbook on microwave engineering

ABOUT THE AUTHOR

Michael Steer is the Lampe Distinguished Professor of Electrical and Computer Engineering at North Carolina State University. He received his B.E. and Ph.D. degrees in Electrical Engineering from the University of Queensland. He is a Fellow of the IEEE and is a former editor-in-chief of *IEEE Transactions on Microwave Theory and Techniques*. He has authored more than 500 publications including twelve books. In 2009 he received a US Army Medal, "The Commander's Award for Public Service." He received the 2010 Microwave Prize and the 2011 Distinguished Educator Award, both from the IEEE Microwave Theory and Techniques Society.

OTHER VOLUMES

Microwave and RF Design
Radio Systems
Volume 1
ISBN 978-1-4696-5690-8

Microwave and RF Design
Transmission Lines
Volume 2
ISBN 978-1-4696-5692-2

Microwave and RF Design
Modules
Volume 4
ISBN 978-1-4696-5696-0

Microwave and RF Design
Amplifiers and Oscillators
Volume 5
ISBN 978-1-4696-5698-4

ALSO BY THE AUTHOR

Fundamentals of Microwave
and RF Design
ISBN 978-1-4696-5688-5

Published by NC State University

Distributed by UNC Press

NC STATE
UNIVERSITY